MEASUREMENT AND METHODS OF ASSESSING THE IMPACT OF PREVALENT PARTICULATE MATTER SOURCES ON AIR QUALITY IN SOUTHERN CALIFORNIA

by

Harich Chandra Phuleria

A Dissertation Presented to the
FACULTY OF THE GRADUATE SCHOOL
UNIVERSITY OF SOUTHERN CALIFORNIA
In Partial Fulfillment of the
Requirements for the Degree
DOCTOR OF PHILOSOPHY
(ENVIRONMENTAL ENGINEERING)

May 2007

Dedication

To my father who showed me the path of patience, perseverance, and righteousness

Acknowledgements

During the development of my graduate studies in the University of Southern California several persons and institutions collaborated directly and indirectly with my research. Without their support and timely help it would not be possible for me to complete this work. That is the reason I want to dedicate these few words to recognize their support and contribution.

First and foremost, I would like to express my deepest gratitude to my advisor Constantinos Sioutas, who has become much more than a thesis advisor. His invaluable guidance and consistent support has enabled me to develop as an individual as well as a professional. Whether it were the thoughtful discussion concerning with the research or non-academic philosophical perspectives whiling sipping coffee outside, he has always been very enthusiastic, encouraging and open to share the ideas.

I also wish to thank the other members of my guidance committee, Dr Philip M. Fine, Dr. Dennis Phares, Dr. Massoud Pirbazari, and Dr. Nino Kuenzli for providing thoughtful suggestions on my research work as well as dissertation. I feel really fortunate to have had the opportunity to work with Dr Fine, who helped me time and again with his valuable suggestions and to-the-point advice in various research projects I have undertaken.

My sincere thanks to Bhabesh Chakrabarti and Michael Geller for their support in familiarizing me with the trivial but important details of the research work we undertook

together. I would also like to thank my colleagues Satya, Babu and Ning for their support and timely help when I needed it badly. I also wish to extend my thanks to Arantza and Meg for helping me during those all-day long organics extractions and hair-scratching GC-MS analysis. Heartiest thanks to Ajay, Subhash, Suresh, Biqin, Prasanna and Suraj for their moral support and stimulating conversations that made my stay so enjoyable and fun while on those gray days. Thank you all for listening to me.

I owe sincere thanks to all of the people associated with the Southern California Particle Center and Supersite for they continually provided support in both field and laboratory experiments and analyses. I would also like to acknowledge the United States Environmental Protection Agency and California Air Resources Board as the primary sponsors of all of this research.

In the end, I would like to mention my parents and my extended family, and my friends who have been an integral part of my being; whether it is my personal outlook or professional growth. They have not only been just observer but solid pillars of strength for whatsoever results I have produced. They are the reasons for my beliefs and convictions. Eeja, pitaji and mamiji, thank you from the bottom of my heart for your unconditional love and support.

Harish Chandra Phuleria
Los Angeles, CA

Table of Contents

List of Tables

List of Figures

Abbreviations

BAM	Beta Attenuation monitor
BaP	Benzo(a)perylene
BgP	Benzo(ghi)perylene
CA	California
CARB	California Air Resources Board
CHS	Children's Health Study
CMB	Chemical Mass Balance
CO	Carbon monoxide
Cor	Coronene
CPC	Condensation Particle Counter
CRCAES	Citrus Research Center and Agricultural Experiment Station
EC	Elemental Carbon
EF	Emission factor
ESP	Electrostatic precipitator
GCMS	Gas chromatography-Mass spectrometry
HDV	Heavy Duty Vehicles
LAB	Los Angeles Basin
LDV	Light Duty Vehicles
MOUDI	Micro Orifice Uniform Deposit Impactor
NAAQS	National Ambient Air Quality Standards
NMD	Number median diameter

NO	Nitrous oxide
NO_2	Nitric oxide
NO_x	Total nitrogen oxides species
O_3	Ozone
OC	Organic Carbon
PAH	Polycyclic Aromatic Hydrocarbons
PM	Particulate matter
PM_{10}	Particulate matter with aerodynamic diameters less than 10 μm
$PM_{2.5}$	Particulate matter with aerodynamic diameters less than 2.5 μm
PN	Particle Number
RFG	Reformulated gasoline
SA	Surface area
SCAQMD	South Coast Air Quality Monitoring District
SCPCS	Southern California Particle Center and Supersite
SD	Standard deviation
SE	Standard error
SMPS	Scanning Mobility Particle Sizer
SO_2	Sulfur dioxide
TC	Total Carbon
TEOM	Tapered Element Oscillation Microbalance
TIC	Total ion current
UCM	Unresolved complex mixture

UF	Ultrafine
USC	University of Southern California
USEPA	United States Environmental Protection Agency
VOC	Volatile organic compounds

Abstract

Recent focus of studies on health effects of ambient particulate matter (PM) have suggested particle chemical composition in addition to particle size, shape and number concentration responsible for the observed health outcomes. However, chemical composition and size distribution of the atmospheric particles can be strongly affected by the differences in ambient temperature, relative humidity, photochemical activity and source contributions. This thesis is intended to demonstrate the importance of characterizing predominant PM sources from an exposure perspective and develop methods of assessing their impact on air quality in Southern California. A study of particle number concentration and size distribution showed seasonal and spatial variability in Southern California. While contribution of local vehicular emissions was most evident in winter, effects of long-range transport of particles and photochemical particle formation were enhanced during warmer periods. Ship emissions are found to be dominant source of lower accumulation and ultrafine particles near ports. During the wildfires in October 2003 in Southern California, PM_{10} (particulate matter with aerodynamic diameter 10 μm and less) levels were found highly elevated, while ozone concentrations dropped during the fire episode and these fire-borne particles were found to effectively penetrate indoors. To characterize the emission profiles from on-road diesel and gasoline vehicle-fleets, size-segregated PM samples were collected inside the Caldecott tunnel in Orinda, CA and analyzed for vehicular organic tracers such as hopanes and steranes, and polycyclic aromatic hydrocarbons (PAHs). In a separate study, detailed information on the chemical characteristics of organic PM originating from a

pure gasoline and a diesel dominated mixed-traffic freeway is obtained. While hopanes and steranes, and high molecular weight PAHs levels are found comparable near these freeways, elemental carbon and lighter molecular weight PAHs are found much elevated near diesel dominated mixed-fleet freeway. Remarkably good agreement is observed between the roadside measurements and the emission factors calculated from the tunnel measurements especially for hopanes and steranes. Our results indicate that the fleet composition as well as atmospheric dilution has strong impact on the ambient concentrations of these organic tracers.

Chapter 1: Introduction

1.1 BACKGROUND

1.1.1 Particulate matter characteristics

Ambient particulate matter (PM) is a general term given to the atmospheric aerosols, where aerosol is a suspension of solid and/or liquid droplets in the atmosphere (Hinds, 1999). National Ambient Air Quality Standards (NAAQS) set primary and secondary standards for ambient PM to protect human health and to protect against adverse effects on plants, animals, visibility and public's enjoyment of life and property.

PM is a mixture of many different components with local and regional variation, e.g. anthropogenic or naturally emitted; primary or secondary particles; by source – e.g. combustion products and traffic or by physico-chemical properties such as solubility or acidity. For practical reasons under aspects of emission measurements, PM is characterized by particle size i.e. particle aerodynamic diameter (Figure 1.1).

PM_{10} is generally defined as all particles equal to and less than 10 μm in aerodynamic diameter. From the health point of view, particles larger than PM_{10} have a deposition of nearly 100% in the nose and deposition rate decreases with decreasing size below 10 μm (Hinds, 1999). Particles below aerodynamic diameter of 10 μm are therefore more important from the health perspective as they are inhalable. $PM_{2.5}$ is defined as the particles with an aerodynamic diameter of 2.5 μm or less and they are called fine PM. The particles in the range between $PM_{2.5}$ and PM_{10}- are termed as coarse mode particles. Particles with a diameter of less than about 0.1 μm are considered as the ultrafine particle

fraction (UFP) whereas the range between 0.1 to 2.5 µm is referred to as the accumulation mode (Ibald-Mulli et al., 2002).

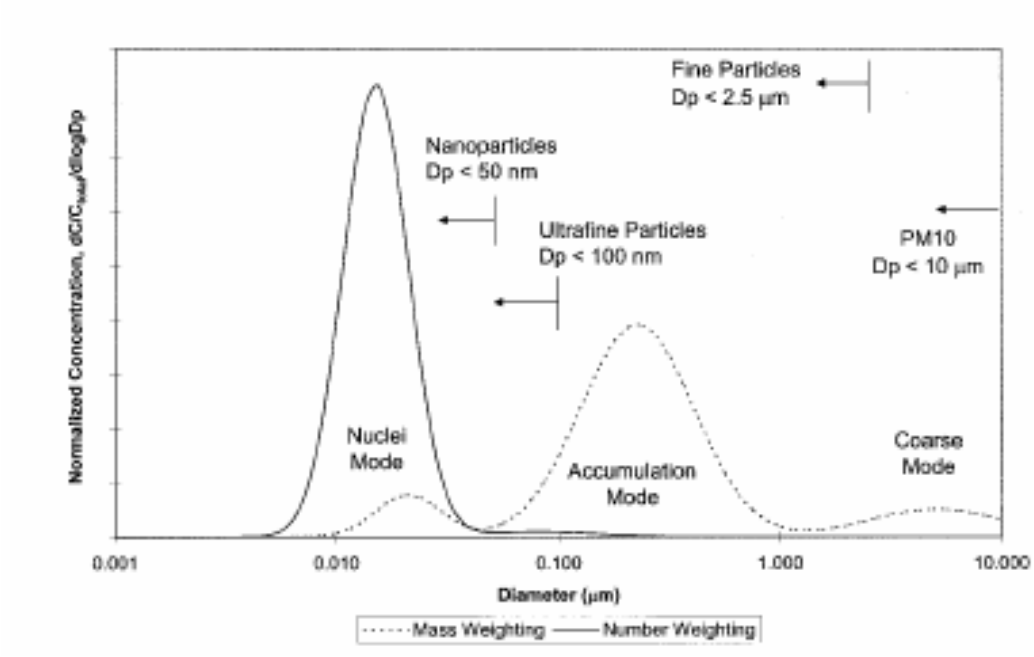

FIGURE 1.1: Typical particle size distribution by mass and number showing different size modes

PM can exist in liquid or in the solid phase and their size can vary from nanometer ranges (fresh emissions from vehicular exhausts) to as high as 100 µm (coarse particles). Based on experimental measurement of ambient PM size distribution, PM has been grouped into three size modes explained above. The number distribution is dominated by the presence of numerous smaller particles with aerodynamic diameters less than 0.1 µm, which are PM in the ultrafine mode, whereas the surface area is dominated by particles in the 0.1 to 0.5 µm size range. Two distinct modes are observed in the mass distribution, where the first fraction is the submicron mode typically referred to as accumulation mode, while the second mode is the coarse mode.

1.1.2 Sources of airborne particles

Two distinct processes can form PM in the atmosphere; it can be directly emitted into the atmosphere or formed indirectly by chemical reactions. The former process is called primary emissions, while the latter is called secondary formation. The relative importance of the primary and secondary PM is defined by the geographical location, precursor gas emissions, atmospheric chemistry and meteorology.

The smallest PM size range is the nuclei mode particles or the ultrafine particles and are formed either through direct emissions from the engine combustions or through gas-to-particle conversion mechanisms in the interface of tailpipe and atmosphere. Ultrafine particles are associated both with natural and anthropogenic sources (Kavouras et al., 1998; Whitby and Svendrup, 1980; Kotzick and Niessner, 1999). Ultrafine particle sizes change continuously due to phase transformation processes and this phenomenon becomes more enhanced as particle size decreases (Seinfeld et al., 1998). Diffusion is the predominant mechanism of their deposition and removal from atmosphere because of their small size. These particles also grow by condensation or coagulate with larger particles and as a result of which, the lifetime of ultrafine particles are very short

The next size range, the accumulation mode (0.1 to 2.5 μm), is the product of combustion, atmospheric reactions and the result of coagulation of smaller particles in the nuclei mode with these larger particles. Besides, condensation of gases onto pre-existing particles also contributes to the accumulation mode. The coagulation rate for particles in the nuclei size fraction with the larger particles in the accumulation range is generally

faster than the self-coagulation of the small particles, which is a result of high mobility of smaller particles combined with larger target area of the larger particles for coagulation. The accumulation mode represents a major fraction of aerosol by mass but only a small fraction of the number distribution. These particles are too small to settle down gravitationally and hence have a higher atmospheric residence time than the larger particles (coarse). The longer lifetime combined with visibility reduction resulting from scattering of solar radiation, cloud formation and health effects make them important for investigative studies.

The coarse mode consists of particles in 2.5 to 100 μm. They are usually generated by mechanical processes resulting from the disintegration of bulk solid material, or from natural sources like sea spray, natural erosion, volcanic explosion, and dust resuspension from wind. Coarse particles are relatively large and have a short lifetime of a few hours in the atmosphere, due to gravitational settling. Inhalable coarse particles are defined as those having diameter smaller than 10 μm. Chemically the composition of the coarse particles indicates their source and is dominated by inorganics and metals nevertheless significant amounts of organic compounds are also found to be associated with the dust particles (Boon et al, 1998).

1.2 AIRBORNE PM AND HEALTH EFFECTS

The health effects of particulate matter have been subjected to intense study in recent years. Exposure to airborne particulate matter has been associated with increase in mortality and hospital admission due to respiratory and cardiovascular diseases. These

effects have been found in short-term studies, which relate to day-to-day variations in PM concentrations and health and long term studies, whish have followed cohort of exposed individuals over time. While epidemiological studies indicate an association between adverse health effects and ambient fine particle concentrations in susceptible individuals, toxicological studies aim to identify mechanisms, which are causal for the gradual transition from the physiological status towards patho-physiological disease. Impressive progress has been made in recent years when objectives changed from classical tests like lung function, etc. to endpoints comprising of particle induced oxidative stress, cell signaling and activation, release of mediators initiating inflammatory processes not only in the respiratory tract but also in the cardio-vascular system. Particularly, the large surface area of ultrafine particles provides a unique interface for catalytic reactions of surface-located agents with biological targets like proteins, cells, etc.

Studies of health effects of particulate matter become complicated by the variable chemical composition and size, thus toxicity, of ambient particles. The potential for particulate matter to induce adverse health effects is related to particle size. Particles of 10 μm or less in aerodynamic diameter can be inhaled deep into the lungs where they can induce tissue damage and various adverse health effects. Particles larger than 10 μm in diameter are generally filtered out in the nasal passages, and do not enter the lungs to any great extent.

Numerous epidemiological and toxicological studies have found associations between measured PM mass and adverse health outcomes (Dockery et al., 1993; Linn et al., 2000;

Lippmann et al., 2003; Peters et al., 2001; Pope et al., 2002; Pope et al., 1995; Ritz et al., 2002; Samet et al., 2000). However, prevailing scientific opinion asserts that, when considering plausible biological mechanisms of injury, PM mass is probably only a surrogate measure of other physical or chemical properties of PM that are the actual cause of the observed health outcomes (NRC, 2004). Several studies have since attempted to link health effects or toxicity measurements with particle characteristics such as particle size, number concentration and chemical composition. For instance, ultrafine particles (with diameters less than about 100 nm) have been demonstrated to be more toxic and biologically active than larger particles (Li et al., 2003; Oberdorster, 2001). Other studies have found associations with PM chemical constituents and a summary is provided in table 1.1 (Biswas and Wu, 2005). In general, results from these studies have been inconsistent due to: a) the different health outcomes considered, b) the likelihood that health effects are induced by a combination of several physical or chemical properties of PM, c) the degree of association may be quite low despite being statistically significant, and d) the possibility of fortuitous associations given the limited sample sizes and the hundreds of measured particulate organic and elemental chemical species that may be the cause of the observed health effects.

It is worth mentioning that though greater association between ultrafine particles and associated health outcomes has been stressed recently, nevertheless it does not exclude the effect of the other two size fractions. In absence of definite mechanistic pathways associated with particle related health effects, associating a particular size fraction shall

be difficult to underline and would remain the area of focused research in the coming future.

TABLE 1.1: Health effects of PM (more pronouncedly ultrafine PM)

Category	Summary of Findings
Respiratory deposition	• Ultrafine particle s effectively deposit in all respiratory regions by diffusion • Dependence on age gender and activity • Different mathematical models developed • More effective for charged particles
Translocation	• Translocation occurs locally to interstitial sites in the respiratory tract and systematically to extrapulmonary organs • Also through olfactory pathway
Dermal uptake	• Insignificant penetration of TiO2 nanoparticles through the skin layer
Toxicity- TiO_2	• Ultrafine more reactive than larger per same mass basis • No special reactivity for TiO2 nanoparticles compared to larger particles • Different biological mechanism in different species • Ultrafine particles in sunscreen not penetrating the skin layer
Toxicity - Carbon	• Toxicity varies significantly depending on the type and structure of carbon • Effects due to iron in SWCNT that generate free radicals
Toxicity – Transition metals	• Generate free radicals through Fenton reaction • Acid coated on particles can also cause adverse health effects

(From Biswas and Wu, 2005)

1.3 RATIONALE OF THE CURRENT RESEARCH

The findings from both the toxicological and epidemiological studies further implicate the absolute need for a better understanding of PM characteristics in terms of their chemical composition, source emission profiles, variable spatial and temporal exposures and associated toxicological properties.

PM chemical composition of the atmospheric particles can vary with season, size and location. Differences in ambient temperature, relative humidity, photochemical activity, and source contributions are important parameters contributing to the differences in concentrations and size distributions of a particular chemical species (Neususs et al., 2002; Christoforou et al., 2000; Cass et al., 2000). Since particle chemistry and particle size most likely affect the toxicological potential of PM, knowledge of the seasonal and spatial variability of the size-resolved PM chemical composition is vital in understanding PM effects on health. This knowledge can also be utilized in the design of health studies that take advantage of this variability to examine the relative effects of different particle characteristics.

In addition, although state and federal environmental protection agencies keep regulating local as well as regional air quality, increasing population and hence increased direct pressure on resources would result in alleviated concentration of pollutants in ambient environments. Thus the regulators need to have a more comprehensive understanding of the seasonal, temporal and spatial variability in pollutant levels to avoid human exposure to the high concentration of these pollutants. Keeping that in mind, and with the

increasing evidence of associations of ultrafine particles and health impacts, a more complete representation of size-fractionated ultrafine chemical characteristic is attempted in this thesis across different seasons and locations in the Los Angeles basin.

Vehicles constitute a major source of particulate matter (PM) due to both direct emissions, via combustion and mechanical wear, and secondary formation, whereby organic and inorganic vapors undergo gas-to-particle conversions in the atmosphere (Shi et al., 1999). In Southern California most $PM_{2.5}$ originates from vehicular emissions. An attempt will be made in this thesis to determine the amount of particulate emissions produced by various vehicles types light-duty and heavy-duty Until now, none of the studies have examined the size segregated organic tracer emissions from on road vehicles and apportion the contribution from gasoline and diesel vehicles. In this study we attempted, for the first time, a thorough investigation of particulate phase organic tracer emissions from diesel and gasoline vehicles. Such information will add to the existing body of knowledge and to a better understanding of relative contribution of organic aerosol emissions from vehicles, which when combined with CMB models and other source data can provide the background information upon which long-term campaigns for population exposure assessments will be based.

1.4 THESIS OVERVIEW

The purpose of this research proposal is to demonstrate the importance of characterizing various airborne PM sources and develop methods of assessing their impact on air quality in particular in Southern California. Furthermore, the spatial and temporal variability in

various fractions of PM will be validated in order to emphasize and support more specific and rigorous nature of aerosol research.

In order to understand the crucial mechanistic link between airborne PM and PM constituents and associated health outcomes, characterization and contribution of various PM sources needs to be assessed. Understanding the definite character of source profiles under real-world conditions will further facilitate the air pollution mitigation efforts by state as well as federal environmental protection agencies. This thesis proposal comprised of five chapters with the first chapter being Introduction and brief account of aerosol science, establishing the desired motivation and need of such research presented in subsequent chapters.

Chapter two shall present the spatial and temporal variation of ambient PM and gaseous copollutants at various source, receptor and pristine sites in Southern California. The aim of this study is to assess the pollutant levels and PM characteristics such as size distributions at these sites affected by different sources. Further, this study affirms the localized nature of air quality in Southern California hence the differential PM exposure to the residents in these places. Also, studied is the impact of an one month harbor strike at Long Beach port on air quality and thus the impact of various PM sources targeting emissions from heavy duty diesel fleets transporting goods to and from the port. One of the important conclusions of this study was to highlight the impact of idling ship emissions during the strike and hence the dynamic nature of various activities and potent sources on Long Beach air quality.

In contrast to the very rigorous, planned and systematic study of air quality at different source and receptor sites in Southern California presented in chapter two, chapter three presents an "opportunistic" study of the impact of wildfires on air quality in Los Angeles Basin. We were fortunate to procure PM as well as gaseous copollutants data from few of the CHS sampling sites when the fire broke in late October 2003. The nature of generated aerosols from wildfires has been described and fire has been established as one of the major sources of lower accumulation mode particles. The impact on air quality is assessed and further ability of these fire-borne particles to penetrate indoors is outlined.

Shifting gears once again, in chapter four, organic aerosol emissions from real-world traffic on a roadway tunnel is studied. Size segregated emission factors of organic tracers of diesel and gasoline fleets such as PAHs, hopanes and steranes are calculated underlining the higher emissions from HDVs compared to LDVs. The real-world emission profile of steady state vehicle fleets would enable to apportion the contribution of HDVs and LDVs on freeway emissions and hence their potential as prevalent PM sources in urban areas.

Continuing further, in chapter five, organic aerosol emissions from real-world traffic is studied near freeway CA-110 (pure gasoline) as well as I-710 (20% HDV mix). Size segregated mass concentrations of organic tracers of diesel and gasoline fleets such as PAHs, hopanes and steranes are measured underlining the higher emissions from HDVs

compared to LDVs. The chemical profile of hopanes and steranes, and PAHs are compared with the one measured inside Caldecott tunnel for LDVs and HDVs. .

Finally chapter six ties together the work presented herein and future research directions are presented. The cohesiveness, of the topics outlined above and the ideas proposed there for future research, would become apparent as the characterization and application of emission profiles of vehicular and other sources would be applied on freeway emissions using CMB models.

1.5 Chapter 1: REFERENCES

Biswas P. and Wu Y. (**2005**) Nanoparticles and the environment. *Journal of the Air & Waste Management Association*, (6), 708-746.

Cass, G.R., L.A. Hughes, P. Bhave, M.J. Kleeman, J.O. Allen, and L.G. Salmon, (**2000**). The chemical composition of atmospheric ultrafine particles, *Philosophical Transactions of the Royal Society of London Series a-Mathematical Physical and Engineering Sciences*, 358 (1775), 2581-2592.

Christoforou, C.S., L.G. Salmon, M.P. Hannigan, P.A. Solomon, and G.R. Cass, (**2000**), Trends in fine particle concentration and chemical composition in Southern California, *Journal of the Air & Waste Management Association*, *50* (1), 43-53.

Dockery, D.W, Pope, C.A, Xu, X.P. Spengler, J.D., Ware Jh, Fay, M.E. Ferris, B.G., Speizer, F.E. (**1993**). An Association Between Air-Pollution and Mortality in 6 United-States Cities. *New England Journal of Medicine*.329 (24): 1753-1759.

Dockery, D.W. and Pope, C.A. (**1994**). Acute Respiratory Effects of Particulate Air-Pollution. *Annual Review of Public Health*.15: 107-132.

Donaldson, K. and MacNee, W. (**1998**). The Mechanism of Lung Injury Caused by PM_{10} *in Issues in Environmental Science and Technology*, Ed. R.E. Hester and R.M.Harrison, the Royal Society of Chemistry. 10:21-32.

EPA (**2003**). National Ambient Air Quality Standards (NAAQS). *http://www.epa.gov/air/criteria.html*

Ferin, J., Oberdorster, G., Soderholm, S.C. Gelein, R. (**1991**). Pulmonary Tissue Access of Ultrafine Particles. *Journal of Aerosol Medicine-Deposition Clearance and Effects in the Lung*.4(1):57-68.

Hinds, W.C. (**1999**). Properties, Behavior, and Measurement of Airborne Particles. Aerosol Technology, 2nd Ed. John Wiley & Sons Inc., New York.

Ibald-Mulli A, Wichmann HE, Kreyling W, Peters A. (**2002**). Epidemiological Evidence on Health Effects of Ultrafine Particles. *Journal of Aerosol Medicine.* 15 (2): 189-201.

Kavouras, I., Mihalopoulos, N., and Stephanou, E. (**1998**). Formulation of Atmospheric Particles from Organic Acids Produced by Forests. *Nature.* 395:683-686.

Kotzick, R. and Niessner, R. (**1997**). The Effects of Aging Processes on Critical Supersaturation Ratios of Ultrafine Carbon Aerosols. *Atmos. Environ.* 33:2669-2677.

Kunzli, N.; McConnell, R.; Bates, D.; Bastain, T.; Hricko, A.; Lurmann, F.; Avol, E.; Gilliland, F.; Peters, J. (**2003**). Breathless in Los Angeles: The exhausting search for clean air; *American Journal of Public Health,* 93, 1494-1499.

Li, N., C. Sioutas, A. Cho, D. Schmitz, C. Misra, J. Sempf, M.Y. Wang, T. Oberley, J. Froines, and A. Nel. (**2003**). Ultrafine particulate pollutants induce oxidative stress and mitochondrial damage, *Environmental Health Perspectives*, 111 (4), 455-460.

Misra, C.; Kim, S.; Shen, S.; Sioutas, C. (**2002**). A High Flow Rate, Very Low Pressure Drop Impactor for Inertial Separation of Ultrafine from Accumulation Mode Particles. *Journal of Aerosol Science.* 33:735-752.

Neususs, C., H. Wex, W. Birmili, A. Wiedensohler, C. Koziar, B. Busch, E. Bruggemann, T. Gnauk, M. Ebert, and D.S. Covert, (**2002**). Characterization and parameterization of atmospheric particle number-, mass-, and chemical-size distributions in central Europe during LACE 98 and MINT, *Journal of Geophysical Research-Atmospheres*, 107 (D21).

Oberdorster, G., Ferin, J., Gelein, R., Soderholm, S.C., Finkelstein, J. (**1992**). Role of the Alveolar Macrophage in Lung Injury - Studies with Ultrafine Particles. *Environmental Health Perspectives*. 97:193-199.

Peters, A., Dockery, D.W., Heinrich, J., Wichmann, E, (**1997**). Short term effects of particulate air pollution on respiratory morbidity in asthmatic children. *European Respiratory Journal***,** 10, 872-879.

Peters, A., Frohlich, M., Doring, A. (**2001**). Particulate Air Pollution is Associated with an Acute Phase Response in Men-Results from the MONICA-Augsburg Study. *Eur. Heart J.* 22 (14):1198-1204

Peters, A., Varrier, R.L., Schwartz, J., Gold, D.R., Mittleman, M., Baliff, J., Oh, J.A., Allen, G., Monahan, K. and Dockery, D.W. (**2000**). Air Pollution and Incidence of Cardiac Arrythmia. *Epidemiol.* 11:11-17.

Peters, A., Wichmann, H.E. (**1997**). Respiratory Effects are Associated with the Number of Ultrafine Particles. *American Journal of Respiratory and Critical Care Medicine*.155 (4): 1376-1383.

Pope, C.A., Dockery, D.W. and Schwartz, J. (**1995**). Review of Epidemiological Evidence of Health Effects of Particulate Air Pollution. *Inhalation Toxicology*. 7:1-18.

Pope, C.A., Verrier, R.L., Lovett, E.G., Larson, A.C., Raizenne, M.E., Kanner, R.E., Schwartz, J., Villegas, M., Gold, D.R. and Dockery, D.W. (**1999**). Heart Rate Variability Associated with Particulate Air Pollution. *Amer. Heart. J.* 138:890-899.

Schwartz J.and Dockery, D.W. (**1992**).Increased Mortality in Philadelphia Associated with Daily Air-Pollution Concentrations. *American Review of Respiratory Disease.*145 (3): 600-604.

Seinfeld, C. and Pandis, S. (**1998**). Atmospheric Chemistry and Physics. John Wiley & Sons Inc., New York.

Whitby, K.T. and Svendrup, G.M. (**1980**). California Aerosols: Their Physical and Chemical Characteristics. *Env. Health Perspectives*.10: 477.

Chapter 2: Seasonal and Spatial Trends in Particle Number Concentrations and Size Distributions at the Children's Health Study Sites in Southern California*

*Singh M.; Phuleria H.C; Bowers K. and Sioutas C. Seasonal and spatial trends in particle number concentrations and size distributions at the Children's Health Study sites in Southern California, *Journal of Exposure Analysis and Environmental Epidemiology,* 16: 3-18, 2006.

2.1 Chapter 2: ABSTRACT

Continuous measurements of particle number, particle mass (PM_{10}) and gaseous co-pollutants (NO_x, CO and O_3) were obtained at eight sites (urban, suburban and remote) in Southern California during years 2002 and 2003 in support of University of Southern California Children's Health Study. We report the spatial and temporal variation of particle numbers and size distributions within these sites. Higher average total particle number concentrations are found in winter (November to February), compared to summer (July to September) and spring (March to June) in all urban sites. Contribution of local vehicular emissions is most evident in cooler months, whereas effects of long-range transport of particles are enhanced during warmer periods. The particle size profile is most represented by a combination of the spatial effects, e.g. sources, atmospheric processes and meteorological conditions prevalent at each location. Afternoon periods in the warmer months are characterized by elevated number concentrations that either coincide or follow a peak in ozone concentrations, suggesting the formation of new particles by photochemistry. Results show no meaningful correlation between particle number and mass, indicating that mass based standards may not be effective in controlling ultrafine particles. The study of the impact of the Union worker's strike at port of Long Beach in October 2002 revealed statistically significant increase in particle

number concentrations in the 60-200 nm range ($p<0.001$), which are indicative of contributions of emissions from the idling ships at the port.

2.2 Chapter 2: INTRODUCTION

A number of observational studies have demonstrated acute and chronic effects of ambient particles on human health (Dockery and Pope 1994; Zanobetti et al. 2000; Pope, 2000). To this date, however, there appears to be heterogeneity in particulate matter (PM) concentrations and PM-associated health effects between locations within an urban setting, which raises considerable uncertainties as to whether PM mass, number, size, bulk or surface chemistry are the appropriate metrics associated with PM toxicity. For example, recent studies have shown that atmospheric ultrafine particles (with physical diameter < 100 nm) have the potential for eliciting adverse health effect (Oberdörster and Utell, 2002; Li et al., 2003; Li et al., 2004; Xia et al., 2004). Recent epidemiological studies by Peters et al. (1997), have demonstrated a higher association between health effects and exposures to ultrafine particles compared to accumulation mode or coarse particles.

In the complex environment of an urban atmosphere, there is great variability in the number and type of sources of particles as well as in the diurnal and seasonal patterns of their emission strengths, all of which affect human exposure. As one of many sources contributing to urban air pollution in general, the combustion of fossil fuel in motor vehicles is one of the major primary emission sources of ultrafine particles in urban atmospheres, especially in the developed nations. (Shi et al., 1999; Cyrys et al., 2003).

Recent studies have shown a dramatic decrease of ultrafine number concentrations with increasing distance from busy freeways in Los Angeles, thereby demonstrating that vehicular pollution is a major source of ultrafine particles and that high number concentrations can be a localized phenomenon, on scales of 100-300 meters (Zhu et al., 2002a,b). In addition to their direct emission in the atmosphere, particles may be formed as a result of photochemical reactions from gaseous precursors, including particulate sulfate formed from precursor sulfur dioxide, and secondary organic aerosols, formed from oxidation of aromatic hydrocarbons (Derwent et al., 2000). The secondary aerosol formation is largely governed by meteorological factors (Mäkelä et al., 1997, Kim et al., 2002). The high degree of temporal variability of the meteorological parameters such as degree of solar radiation, atmospheric mixing depth, humidity, and temperature - all contribute to the temporal variation in particulate number concentrations at a location. Understanding how the number concentrations of particles change as a function of particle size, time of the day, location and season may help characterize the sources of these emissions as well as refine human exposure parameters used in epidemiological studies that attempt to link particulate levels and health effects they induce.

Due to recent health concerns, particle size distributions and number concentrations in several cities have been measured. Some recent continental sampling campaigns that measured size distributions include the Pittsburgh Air Quality Study (Stanier et al., 2004), the Atlanta PM Supersite program (Woo et al., 2001), and sampling campaigns in Los Angeles (Kim et al., 2002; Fine et al., 2004), Northern Europe (Ruuskanen et al., 2001), Tennessee (Cheng and Tanner, 2002), Brisbane, Australia (Morawska et al.,

2002), the UK (Harrison et al., 2000), Estonia and Finland (Kikas et al., 1996) and Central Europe (Birmili et al., 2001). Most of these studies were conducted in urban areas in which the vast majority of ultrafine PM originate from primary sources (Morawska et al., 1998; Harrison et al., 2000; Woo et al., 2001), thus their diurnal profiles match those of local vehicular sources. The majority of these studies were also intensive in nature, conducted for a period ranging from a few weeks to a few months.

Shi et al. (2001) measured temporally resolved number concentrations to examine periods of nucleation events. Lawless et al. (2001) used the near continuous data obtained from a Scanning Mobility Particle Sizer and an optical particle counter to distinguish between primary and secondary contributions to $PM_{2.5}$ in Fresno, CA. These studies were intensive in nature, focusing on one specific location and for a limited time period. The spatial aerosol characteristics at different locations of a city have also been examined. Kim et al. (2002) identified periods of photochemistry and long-range advection as sources of ultrafine PM at two sites in Los Angeles Basin in addition to local vehicular emissions. Fine et al. (2004) inferred sources of ultrafine particles at two different locations in the eastern portion of Los Angeles Basin. Buzorius et al. (1999) measured aerosol characteristics at a series of sites in Helsinki, Finland in order to investigate the transport of aerosol traveling from source sites to receptor sites. Ruuskanen et al. (2001) conducted monitoring in three different European cities using continuous monitors to describe differences among the sites as well as diurnal variations of particle mass and number concentrations. Little information has been reported on the seasonal patterns of size distributions due to the lack of long-term monitoring. Stanier et al. (2004) measured

aerosol size distributions at one location in Pittsburgh for an entire year, providing one of the first data sets in Northern United States from which seasonal patterns can be described.

The work presented in this paper is intended to provide more comprehensive information about spatial, seasonal as well as diurnal variations of atmospheric particle numbers and size distributions (14-700 nm) within Southern California. This paper utilizes the data set generated in support of the University of Southern California (USC) Children's Health Study (CHS). The CHS, which began in 1993, is one of the largest investigations of the long-term consequences of air pollution on the respiratory health of children. The main goal of CHS is to identify chronic effects of ambient pollutants in Southern California by performing cross-sectional and longitudinal studies in school children in several communities with varying exposures to particulate matter, ozone, and acid vapors. In this paper we present ambient particle number characteristics measured at eight sites classified as urban (source and receptor) and remote (suburban/ mountainous) sites in Southern California during the years 2002 and 2003. The particle number concentration data is supported by gaseous co-pollutants data to help differentiate (mostly) ultrafine particle sources and formation mechanisms at each site as well as their prevalence over different times of day and different seasons.

2.3 Chapter 2: METHODS

Concentrations of carbon monoxide (CO), ozone (O_3), total nitrogen oxide species (NO_x), mass of particulate matter with aerodynamic diameters less than 10 μm (PM_{10}) and total

particle numbers (PN) were continuously measured in several locations in Southern California as a part of the University of Southern California Children's Health Study, supported by the South Coast Air Quality Management District (SCAQMD) and the California Air Resources Board (CARB). Size resolved sub-micrometer particle numbers (14-700 nm) were measured under an additional contract from the CARB and SCAQMD. Continuous data were collected concurrently throughout the calendar years 2002 and 2003. Eight sites were examined in this study, six within the Los Angeles Basin (LAB): Long Beach, Mira Loma, Upland, Riverside, Lake Arrowhead and USC; and two sites at other areas of Southern California: Alpine and Lancaster (as shown in Figure 2.1). Selection of the sampling sites, discussed in greater detail by Künzli et al. (2003), was made on the basis of their location within the LAB and the presumed contrasting air quality (hence exposure) regimes in terms of PM and gaseous co-pollutants, which have differentially affected children's health.

2.3.1 Sampling Sites

Los Angeles is a unique air basin because it epitomizes a distinct air quality problem in terms of particle composition, source mix, and meteorology. Unlike other metropolitan areas, the unique morphology and climate of Los Angeles create major differences in PM characteristics and composition within the basin. During the past twenty years, growth in both the population and the density of emission sources has been greatest in the central and eastern portions of the LAB. Nevertheless, primary emissions of VOC, NOx and PM are still dominated by the western, or coastal, portion of the region, which contains the greatest concentration of both mobile and stationary emission sources. Overall the

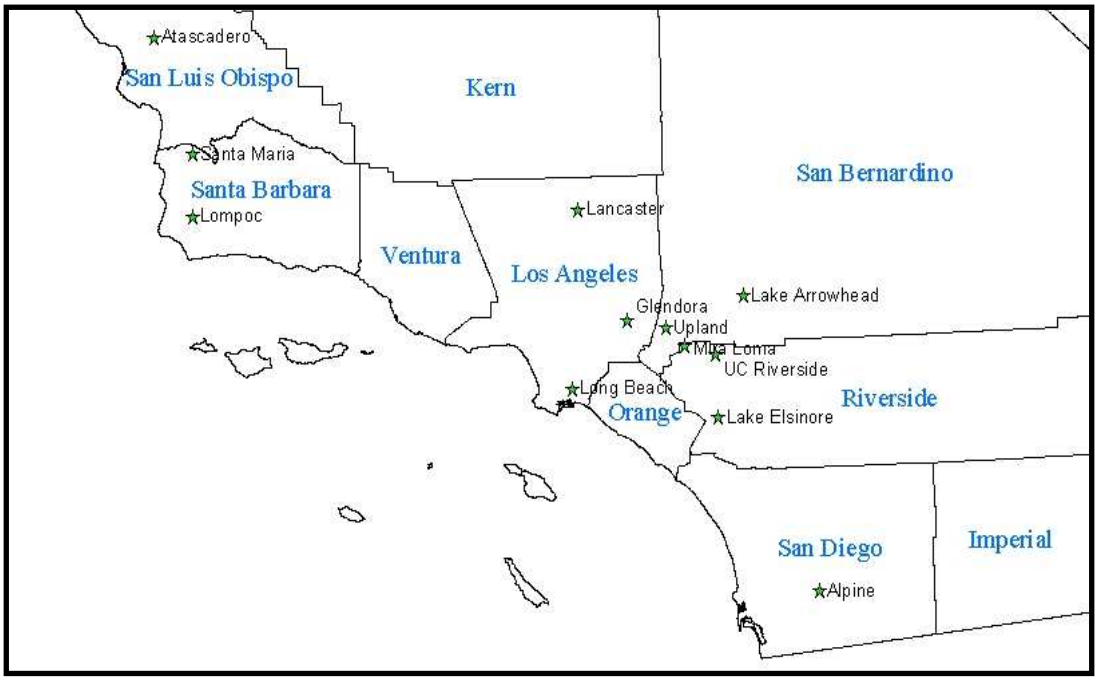

FIGURE 2.1: Locations of sampling sites in Southern California

highest ambient concentrations occur in the coastal areas for primary pollutants such as CO and NO_2, and in downwind inland valleys for secondary pollutants such as ozone and fine particulate matter. Thus, it remains appropriate to view the western/coastal portion of the LAB as a source region and the inland valleys of the central and eastern basin as receptor areas.

The winter period in the LAB is characterized by surface temperature inversions in the coastal region and generally weak on-shore flow. Hence the highest ambient levels of primary pollutants such as CO and NO_2 are generally observed in the coastal region during the winter months. In contrast, the "summer/fall" period is characterized by strong temperature inversions aloft, and by strong onshore flow and interior-mountain up-

slope flow, which together produce rapid transport of primary pollutants from the coastal region to the interior valleys. Combined with high actinic radiation in the summer, these conditions produce elevated concentrations of a wide spectrum of secondary air pollutants, including ozone and fine PM, in the central and eastern areas of the Basin in the summer. In addition, offshore flow under Santa Ana conditions can trap large quantities of pollution over the coastal regions of the LAB. Particles thus undergo transformations as they move along a wind trajectory from "source" to "receptor" sites in the basin. As a result, significant differences occur in the chemical composition and size distribution of PM in the LAB because of a wide range of sources, meteorological conditions, atmospheric chemistry, and temporal factors.

Located near a busy surface street, the Long Beach station is about 0.5 km northeast of freeway I-405 and approximately 1.5 km east of freeway I-710. The Long Beach station is mostly downwind of these two freeways as well as the Long Beach port which is situated approximately 7 km south of the sampling station. The Upland site is located in a residential area inside a community trailer park about 100 m from San Bernardino road, and is within 2 km (mostly downwind i.e., north-east) of the freeway 210. The Mira Loma site (about 80 km east of downtown Los Angeles) is located in a building on the Jurupa Valley High School campus, directly southeast of the intersection of freeways 60 and 15. It is surrounded by several major warehouse facilities with frequent heavy-duty diesel truck traffic (Sardar et al., 2004; Na et al., 2004) and near several major cattle feeding operations. The sampling location at Riverside is within the Citrus Research Center and Agricultural Experiment Station (CRCAES), a part of the University of

California, Riverside. It is about 20 km southeast of the Mira Loma site and is situated upwind of surrounding freeways and major roads (Phuleria et al., 2004). The desert site of Lancaster is located in the office of Mojave desert AQMD and is approximately 2 km away from the nearest freeway 14. The Lake Arrowhead monitoring station is located in the rim of World High School near highway 18, at an elevation of about 1700 m. It is a purely serene mountainous site with very few local emission sources, but heavily impacted by transported, aged air pollutants. The sampling site at USC is located near downtown Los Angeles, just 100 m downwind of freeway 110. The Alpine station is a remote suburban to rural site located approximately 50 km east of downtown San Diego (approximately 200 km southeast of downtown Los Angeles).

Fresh emissions from vehicular and industrial sources primarily make Long Beach a "source" site, which is at a relatively western location in the LAB and has an urban surrounding. USC, also, has an urban surrounding and is considered a "source" site. It represents an urban mix of industrial, vehicular and construction sources. Riverside, Upland and Mira Loma and Lake Arrowhead are designated "receptor" sites where the aerosol is composed of advected, aged and photochemically processed air mass from the central Los Angeles Area. The time for air masses to transport from source to receptor sites can vary from a few hours to more than a day (Sardar et al, 2004). It should be noted here that the designation of these sites as "receptors" by no means precludes the impact of local traffic sources, as it will be discussed later in this paper.

2.3.2 Instrumentation

The concentrations of CO were measured near-continuously by means of a Thermo Environmental Inc. Model 48C trace level CO monitor. A continuous Chemiluminescence Analyzer (Monitor Labs Model 8840) was used for the measurement of concentrations of NO_x, while O_3 concentrations were monitored using a UV photometer (Dasibi Model 1003 AH). Total particle number concentrations (greater than about 10 nm in diameter) were measured continuously by a Condensation Particle Counter (CPC, Model 3022/A, TSI Incorporated, St. Paul, MN) set at a flow rate of 1.5 L min^{-1}. In addition to the continuous data described above, efforts were made to monitor the number-based particle size distributions in each site for 1-3 months duration during a warmer and a cooler period. Accordingly, three Scanning Mobility Particle Sizers (SMPS, Model 3936, TSI Incorporated, St. Paul, MN) were deployed by rotation at each site during selected time periods, as shown in Table 1, to measure the size distribution of sub-micrometer aerosols (14-700 nm) using an electrical mobility detection technique. In this configuration, the CPC flow rate was maintained at 0.3 L min^{-1} (with the sheath flow of the SMPS set at 3 L min^{-1}), and size- segregated particle number concentrations were recorded. The CPC total count data were excluded for the months when the CPC was in the SMPS configuration (Table 2.1; Figure 2.2). Continuous particle number and gaseous co-pollutant concentrations were averaged over 1-hour and 24-hour intervals for the subsequent analysis.

TABLE 2.1: Sampling periods during which SMPS-CPC configuration was employed at various sampling sites

Site no	Site name	Sampling periods
1	Long Beach	Nov '02; Aug-Sep '03
2	Mira Loma	Jan-Feb '02; Jun '02
3	UC Riverside	Nov '02; Mar-Apr '02
4	USC	Dec '02 - Jan '03; Sep '03
5	Upland	Aug to Oct '03; Nov, '03 - Jan '04
6	Alpine	Apr-May '03; Dec '03 - Jan '04
7	Lancaster	Jun-Jul '03
8	Lake Arrowhead	Jul-Aug '02

Hourly PM_{10} mass concentrations in each site were measured by low temperature Differential Tapered Element Oscillating Microbalance monitors (low temperature TEOM 1400A, R&P Inc., Albany, NY). Jacques et al. (2004) have described the design and performance evaluation of this monitor in greater detail. Briefly, the system consists of a size-selective PM_{10} inlet, followed by a Nafion® dryer that reduces the relative humidity of the sample aerosol to 50% or less. Downstream from the Nafion dryer and ahead of the TEOM sensor is an electrostatic precipitator (ESP) to alternately remove particles from the sample stream or allow the particle laden sample stream to continue to the sensor. The ESP is alternately switched on and off, for equal time periods of about 10 minutes. Unlike a standard TEOM monitor, which collects samples and reports mass concentration continuously, the differential TEOM monitor only collects mass on the TEOM sample filter during half of the measurement time of the monitor, the period where the ESP is turned off (typically 5 minutes). During the other half of the operation, the ESP is energized and only the affects of the sampled gases and any evaporation of previously collected sample are measured by the TEOM sample filter. The change in the

collection filter mass obtained while collecting particle-free ambient air provides an internal reference, for the mass change sensed while collecting ambient particulate. Thus, the Differential TEOM directly measures ambient PM mass concentrations while accounting for collection artifacts, including loss of semivolatile aerosols, adsorption of organic vapors and temperature changes. The study by Jacques et al. (2004) showed that the time averaged TEOM PM_{10} mass concentrations agreed within ± 10% with those of collocated Federal Reference Methods (FRM).

The Quality Control and Quality Assurance procedures used in the study to assure accurate and unbiased measurements were performed in accordance with Southern California Particle Center and Supersite (SCPCS) Quality Assurance Project Plan (QAPP). The SCPCS QAPP incorporates all of the elements required by the U.S. EPA for air monitoring programs.

2.4 Chapter 2: RESULTS AND DISCUSSION

The section describing our results is divided into the following parts: Seasonal and spatial trends; Diurnal trends; Relation between PM mass, PM surface area and PM numbers; and Long Beach October 2002 strike analysis. The latter part is an "opportunistic" study focusing on the impact of the union workers strike at the port of Long Beach on air quality.

2.4.1 Seasonal and Spatial Trends

Descriptive statistics (surface area and number median diameter) of the measured particle size distributions are included in Table 2.2. The number median diameter is defined as

the particle diameter that divides the number based frequency distribution of aerosol in half; fifty percent of the total aerosol number has particles with a larger diameter, and fifty percent of the total aerosol number has particles with a smaller diameter. Figure 2.2 shows monthly averaged total particle number concentrations measured using the CPC along with the monthly averaged minimum and maximum ambient temperatures, in the eight sites sampled during the calendar year 2003. The error bars indicate the standard

TABLE 2.2: Summary statistics showing average total particle surface area (SA) and number median diameter (NMD)

Site Name	Season	Period	Particle SA ($\mu m^2/cm^3$)		NMD (nm)	
			Grand avg.	SD	Grand avg.	SD
Long Beach	Winter	Nov '02	609.5	320.1	79.9	18.8
Long Beach	Summer	Aug-Sep '03	330.0	166.0	59.8	18.3
Mira Loma	Winter	Jan-Feb '02	674.5	418.5	65.2	19.4
Mira Loma	Spring	Jun '02	542.9	231.9	81.6	20.5
Riverside	Winter	Nov '02	290.3	255.2	47.7	16.6
Riverside	Spring	Mar-Apr '02	334.0	273.0	62.6	21.3
USC	Summer	Sep '03	437.4	331.7	45.9	11.2
USC	Winter	Dec '02 - Jan '03	329.4	210.4	45.4	14.2
Upland	Summer[1]	Aug-Sep-Oct '03	371.7	161.9	61.5	14.1
Upland	Winter	Nov-Dec '03 - Jan '04	473.7	300.6	56.6	13.6
Alpine	Spring	Apr-May '03	122.4	101.7	42.9	14.4
Alpine	Winter	Dec '03 - Jan '04	135.1	116.5	79.3	18.5
Lancaster	Spring	Jun-Jul '03	164.9	136.0	81.9	18.0
Lake Arrowhead	Summer	Jul-Aug '02	154.9	117.4	77.9	16.7

---

[1] The data corresponding to the October Fire in Southern California is excluded

and the sampling size. A key observation in Figure 2.2 is the higher average particle number concentrations in winter (November to February), compared to summer (July to September) and spring (March to June) in all of the urban sites, e.g., USC, Long Beach,

Riverside, Upland, Mira Loma and Lancaster. The total particle number concentrations at these sites were quite similar and ranged from 25,000-30,000 particles/cm^3 in winter months to 12,000-15,000 particles/cm^3 in summer/spring months. High number concentrations at the urban sites during winter are likely due to lower temperatures favoring particle formation by condensable organics freshly emitted from vehicles (Baltensperger et al., 2002; Ziemann et al., 2001; Shi and Harrison, 1999).

Figure 2.2 a

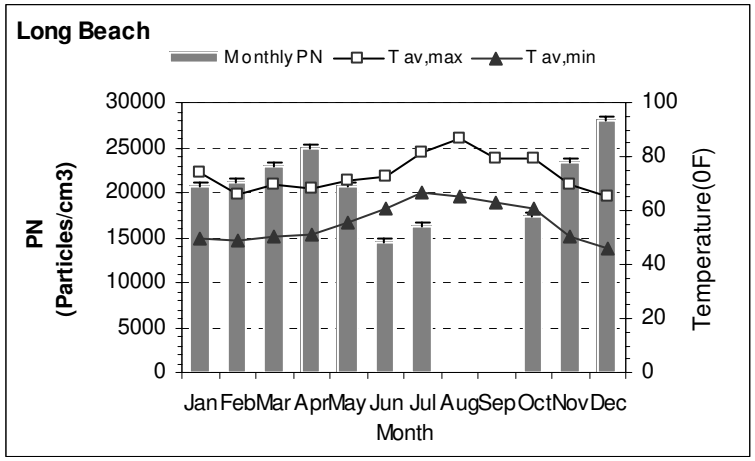

Figure 2.2 b

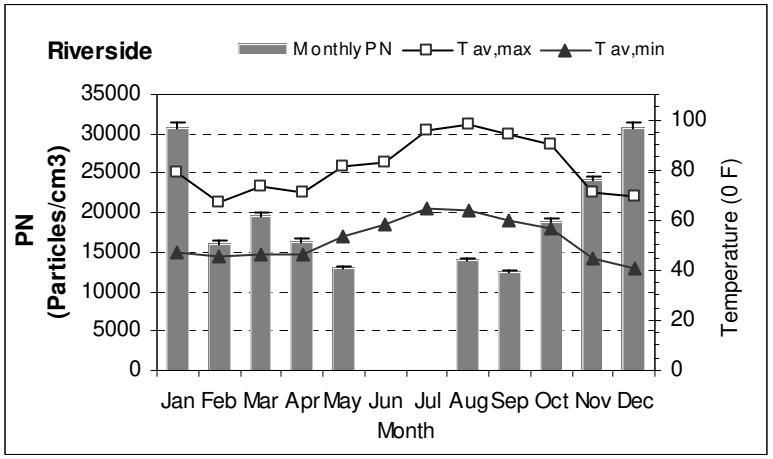

Figure 2.2 c

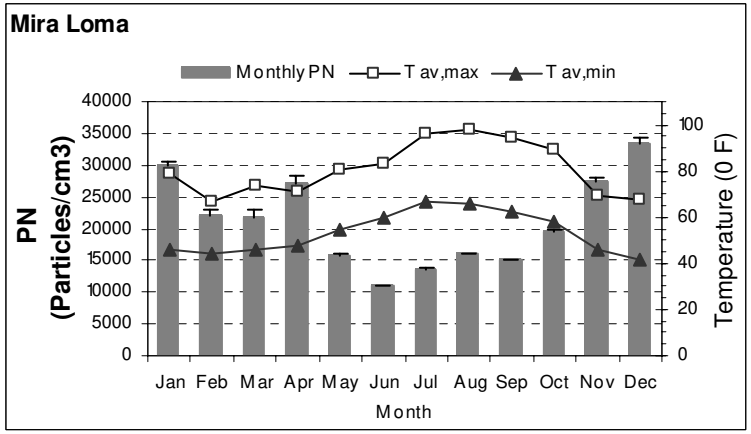

Figure 2.2 d

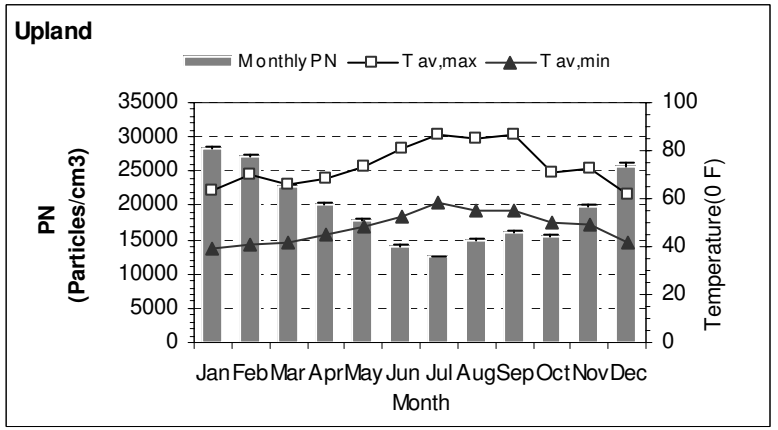

FIGURE 2.2: Monthly average particle number concentrations and ambient temperatures at a) Long Beach, b) Riverside, c) Mira Loma, d) Upland, e) Lancaster, f) Alpine, and g) Lake Arrowhead

FIGURE 2.2: Continued…

Figure 2.2 e

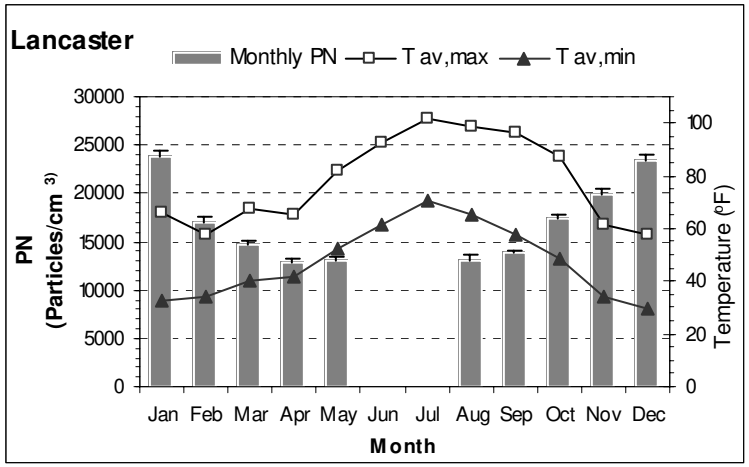

Figure 2.2 f

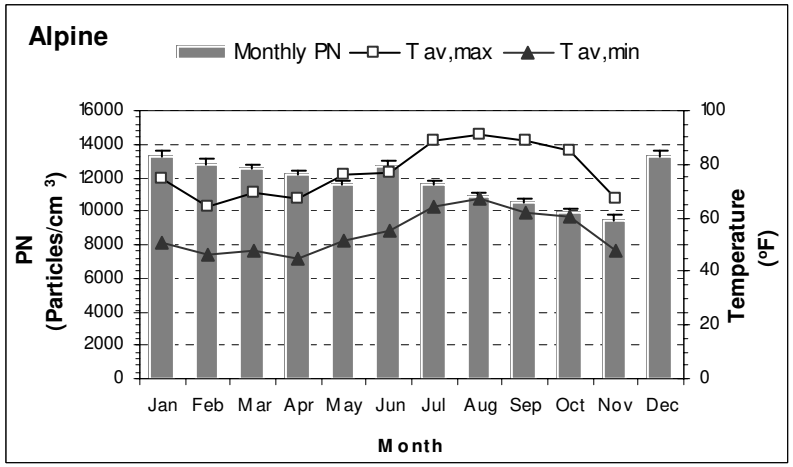

Figure 2.2 g

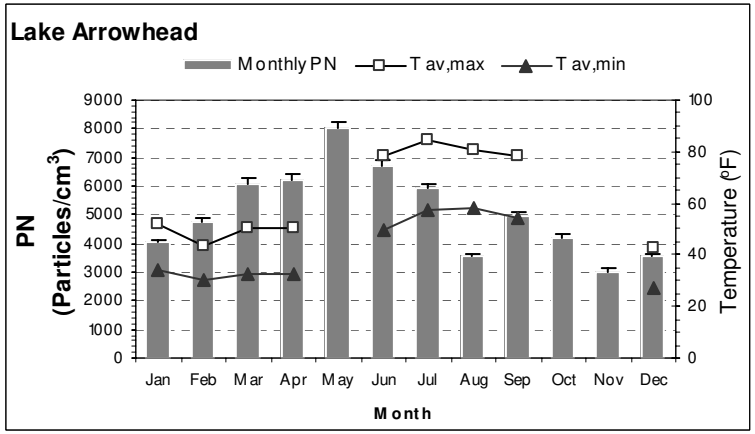

The lowest levels of particle number concentrations were observed at Lake Arrowhead, which is a remote mountainous site. The averaged particle concentrations at this site ranged from 6,000-8,000 particles/cm^3 in summer months and 3,000-5,000 particles/cm^3 in winter months (Figure 2.2g). The Lake Arrowhead sampling site is located at an elevation of 1700 m. The inversion layer is generally below the station location during morning and evening periods. As the day progresses, the warmer temperature cause the inversion layer to rise and subsequently the inversion layer passes the station elevation and the station is under the inversion layer. During summer months, as a consequence of the elevated mixing height the site is under the inversion layer for longer periods leading to higher number concentrations. Additionally, low atmospheric pressure and higher mid-day wind speed during summer favor long-range transport of the aerosol from the much more polluted upwind areas. Biogenic VOC emissions in the Lake Arrowhead region also possibly impact particle numbers in the summer months.

Particle counts at Alpine, although higher than those observed at Lake Arrowhead, are much lower than those observed in the urban sites, discussed earlier. This site is impacted by very few local traffic emissions and is largely a receptor site of the San Diego metropolitan area. On most summer days, an afternoon peak of particles of possibly secondary origin occurs several hours after the change of wind direction from easterly to westerly. Monthly averaged particle counts range between 9,000 - 13,000 particles/cm^3. A detailed discussion about the seasonal variations in particulate characteristics at Alpine is presented in a later section.

Figure 2.3 depicts the particle size distributions measured by the SMPS during different seasons at our sampling sites. Average number size distributions at USC in summer as well as winter are very similar and corroborate the hypothesis that this site is heavily influenced by fresh vehicular emissions. Particles in the 20 - 50 nm range, which could be attributed to traffic, are the most abundant at this site. Also, number concentrations of this size range increase during the winter period. USC has similar number median diameter during both seasons, an indication of the consistency of the sources (i.e., the traffic emissions from the nearby freeway I-110) affecting PM characteristics in that location.

Similar to USC, at Long Beach which is also a site highly impacted by vehicular emissions, the average particle number concentrations are higher in winter than summer for the particles > 40 nm. However, summer months witness an increase in particles <40 nm diameters. The size distribution in summer supports the hypothesis that this site may be influenced markedly by photochemically generated particles. Given that this site is situated close to the ocean, with the only major upwind sources being the port and the nearby freeway 710, both of which are quite proximal (i.e., within 7 km or less) to the site, the contribution of long range transport to particle numbers can be ruled out. The number median diameter of the aerosol is also lower in summer than in winter. Larger number median diameter in winter (79.9 nm) compared to summer (59.8 nm) may be due to high relative humidity in the winter months, which would contribute to growth of particles by condensation of water vapor in the air. It should be noted that the proximity

Figure 2.3 a

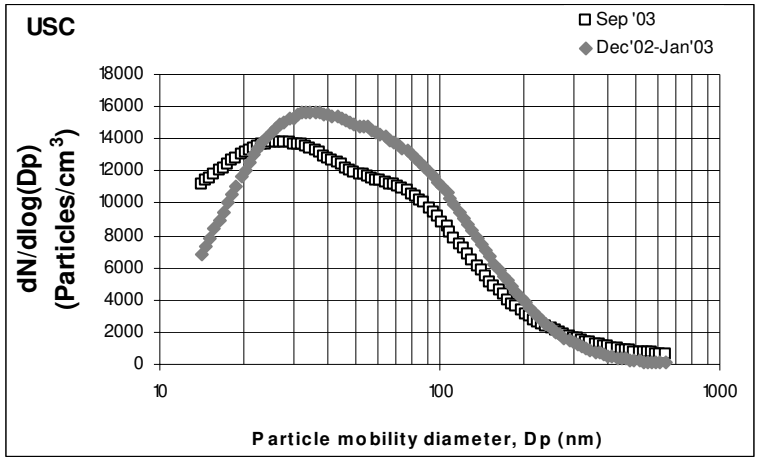

Figure 2.3 b

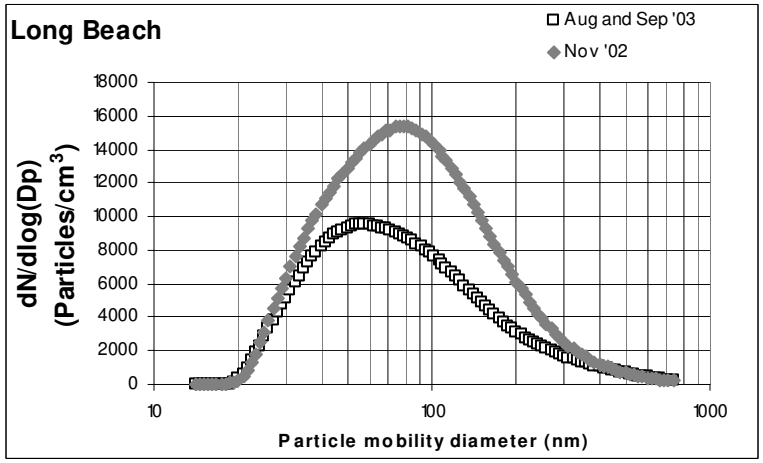

Figure 2.3 c

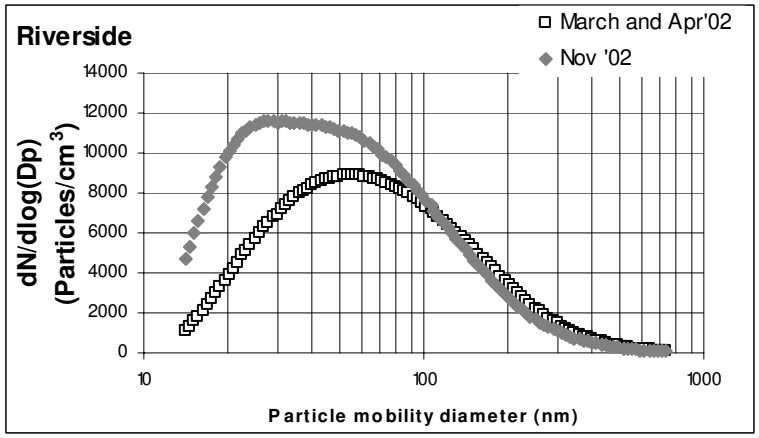

Figure 2.3 d

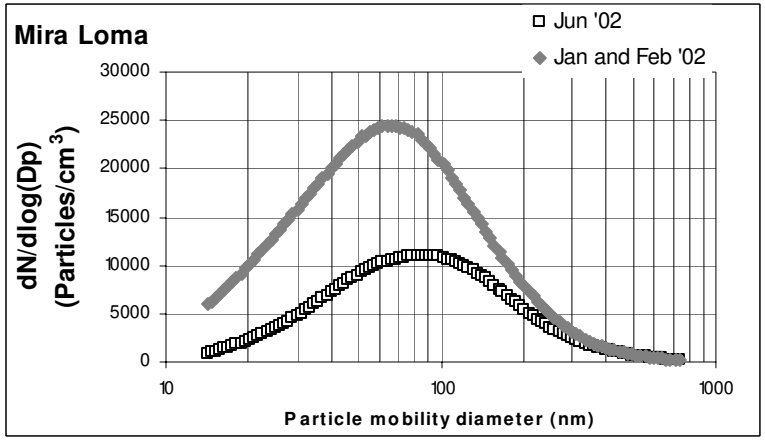

FIGURE 2.3: Average number size distributions in winter and summer/spring periods at a) USC, b) Long Beach, c) Riverside, d) Mira Loma, e) Upland, f) Lancaster, g) Alpine, and h) Lake Arrowhead

FIGURE 2.3: Continued…

Figure 2.3 e

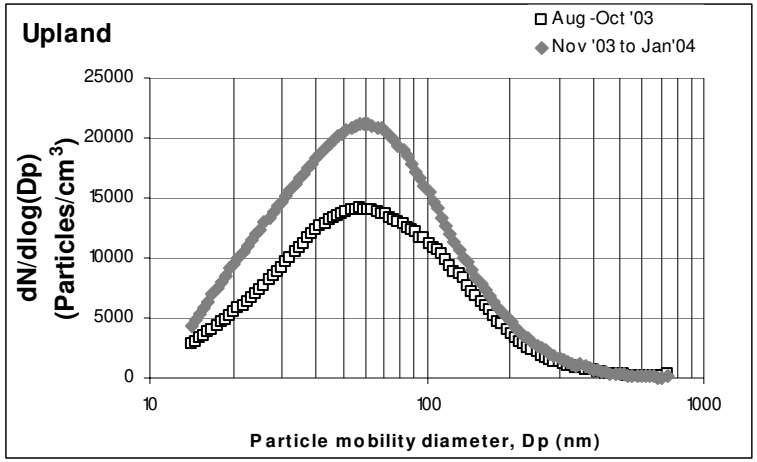

Figure 2.3 f

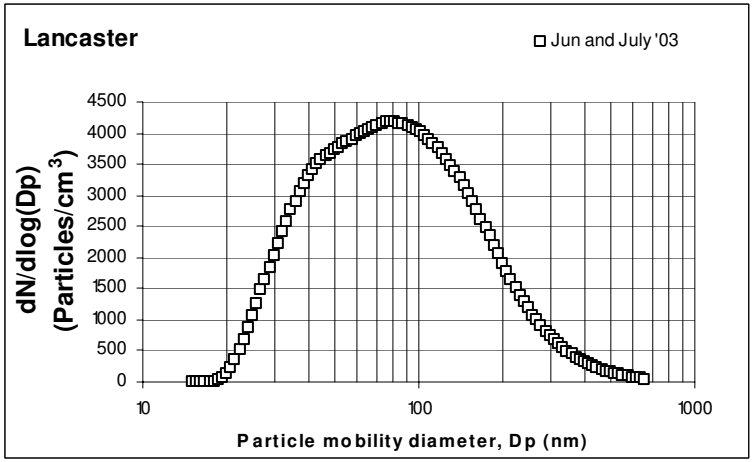

Figure 2.3 g

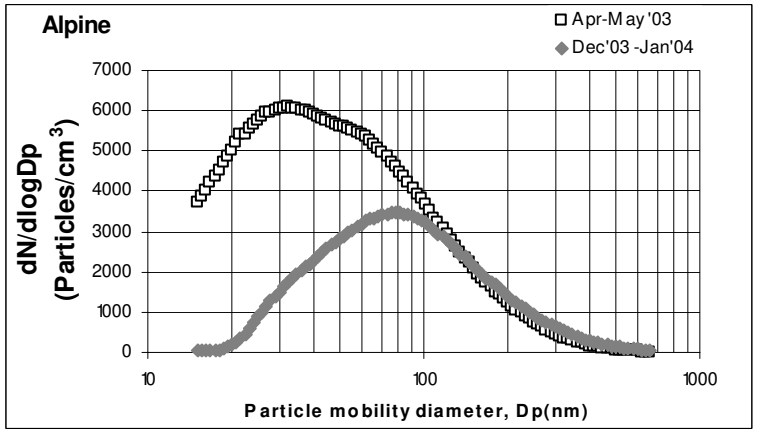

Figure 2.3 h

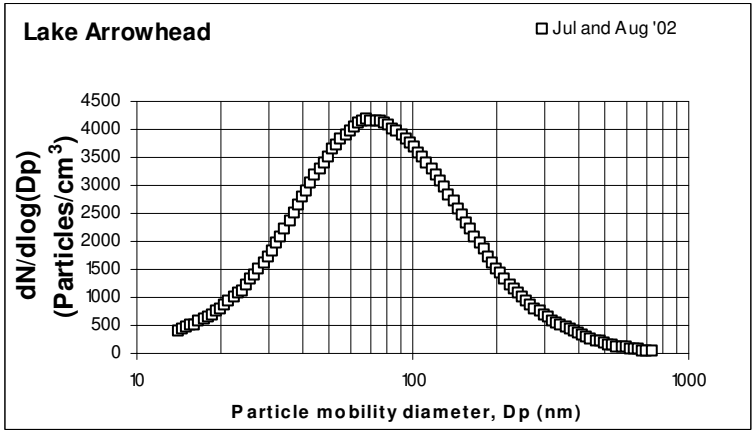

of that site to the ocean results in unusually higher relative humidity levels compared to the rest of the urban sites, with prolonged periods of nighttime and morning fog. The smaller summertime number median diameter could be due to the increased photochemical production of smaller particles, as observed by Kim et al. (2002) and Wehner and Wiedensohler (2003). During the first week of October, union workers at the port of Long Beach went on strike. A detailed analysis of the effect of this strike on particulate characteristics of Long Beach is discussed in later section of this paper.

Riverside, Mira Loma and Upland are receptor sites downwind of the high concentration of sources in the western part of LAB. In addition to the effect of few local emission sources, particle number concentration at these receptor areas is also influenced by aged, advected aerosol from the west, especially in summer season. The Upland station was directly impacted by Southern California wildfires during late October 2003 because of its location some 3.5 km downwind of one of the 13 fires during that period. The impact of this fire on aerosol characteristics is discussed in detail by Phuleria et al. (2004) and thus we do not present the analysis here. However, for our seasonal characteristics analysis, we have excluded the data from that period.

At Riverside, the particle number concentrations are higher in winter compared to spring for particles <100nm. It is interesting to observe that the particles >100 nm are slightly higher in the spring period. The increase in the peak median size in springtime may be due to the contribution of advected, thus aged aerosols, which are generally larger in

diameter (Zhang and Wexler, 2002), from the western polluted regions of the Los Angeles Basin.

The size distribution of aerosols also shows some seasonal variation at Mira Loma. In addition to a decrease in particle number concentrations, the number size distribution shifted towards larger sizes in summer compared to winter. Decrease in particle counts of all size ranges in summer reflects the effect of more dilution with elevated mixing height in warmer months. As in Riverside, the number median diameter of the aerosol in Mira Loma is larger in warmer season (Table 2.2). This may be the result of the increased wind speeds and onshore flow in the warmer months, leading to increased advection of pollutant air parcels from the western LAB. This advected aerosol is generally larger in diameter as noted earlier and would lead to larger number size distribution of the summer/spring aerosols.

At the suburban remote site Alpine, in contrast to all the receptor sites discussed above, the particle numbers <100 nm are markedly higher in spring than in winter (Figure 2.3g). The number median diameter also shifts from 79 nm in winter to 43 nm in spring (Table 2.2). This may be due to increased summertime advection and photochemical particle formation. The influence of summer advection and photochemical particle formation is supported by wind data, which indicates a change in wind direction from easterly (offshore) to westerly (onshore). The westerly winds would bring the aging air-mass from the San Diego metropolitan area to the station. The afternoon peak of aged and

photochemically-derived particles occurs several hours after the wind direction change, allowing time for the air mass to reach the station from San Diego.

Particle size distribution data is available for only summer months at Lancaster and Lake Arrowhead. Both sites display generally much lower number concentrations than the urban sites, as one would expect. The relatively large aerosol number median diameter of 82 and 78 nm at Lancaster and Lake Arrowhead, respectively, corroborate the absence of any major local sources, which would emit fresh hence smaller in size emitted PM.

2.4.2 Diurnal Trends

This section describes our observations of diurnal trends in particle numbers and gaseous copollutants, which, combined with the size distribution and number concentrations data, may provide insights into sources and possible formation mechanisms of particulate matter in each of these sites. Figures 2.4 through 2.9 display the diurnal variations of particle number (PN) and gaseous pollutants (O_3 and NO_x) concentrations averaged by time of day over the period that SMPS sampled at each of the sites. In these figures, particle sizes have been segregated into three ultrafine size ranges: 15-30nm, 30-60 nm and 60-100 nm.

The diurnal trends of PN in different size ranges and gaseous pollutants at USC and Long Beach during the winter sampling periods are shown in Figures 2.4a and 2.5a, respectively. As mentioned before, USC and Long Beach are close to vehicular sources

Figure 2.4a

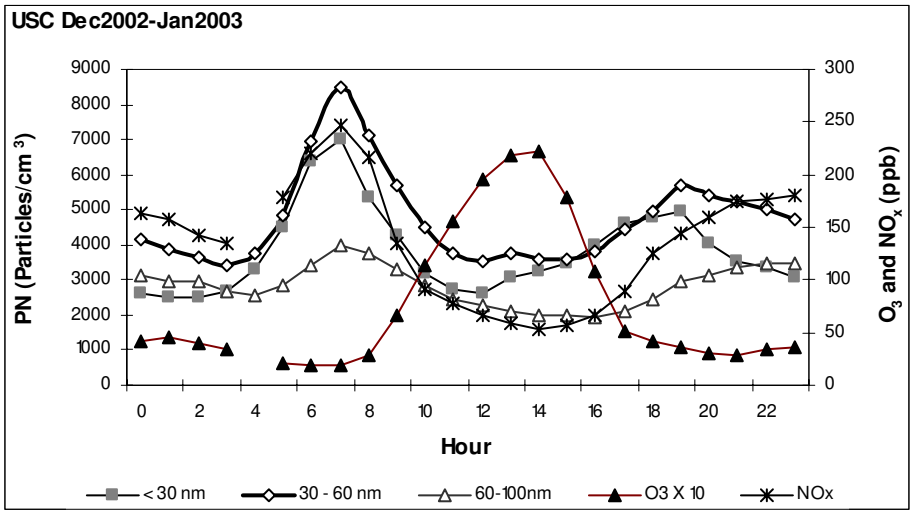

Figure 2.4b

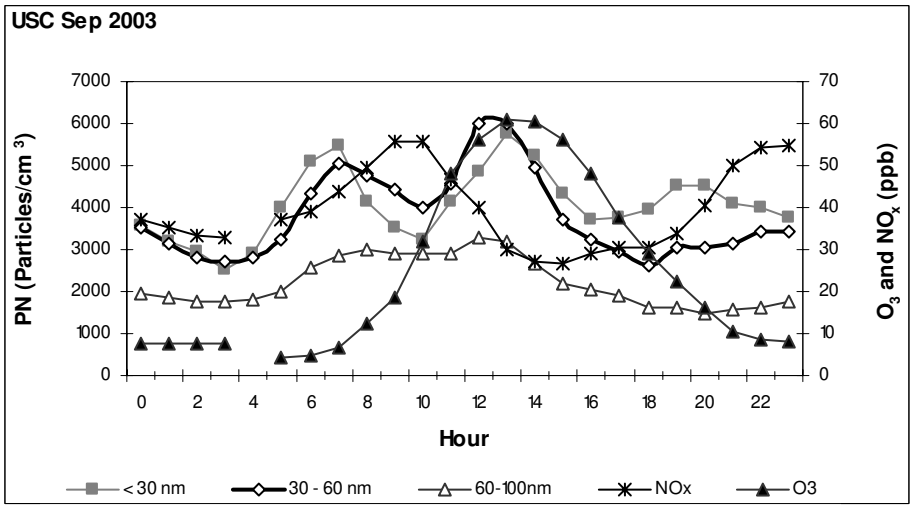

FIGURE 2.4: Diurnal trends of size-segregated particle number, O_3 and NO_x at USC during a) Dec 2002-Jan 2003 and b) Sep 2003

and traffic is expected to be primary source of these particles at these sites. The number concentrations have also been observed to be higher during winter months. The diurnal pattern of NO_x is very similar to diurnal patterns of particle number concentrations. The morning and evening peaks of these pollutants correspond to morning and evening

commutes, which suggests that local traffic is the major contributor to ultrafine PM at both these sites during winter.

Figure 2.5 a

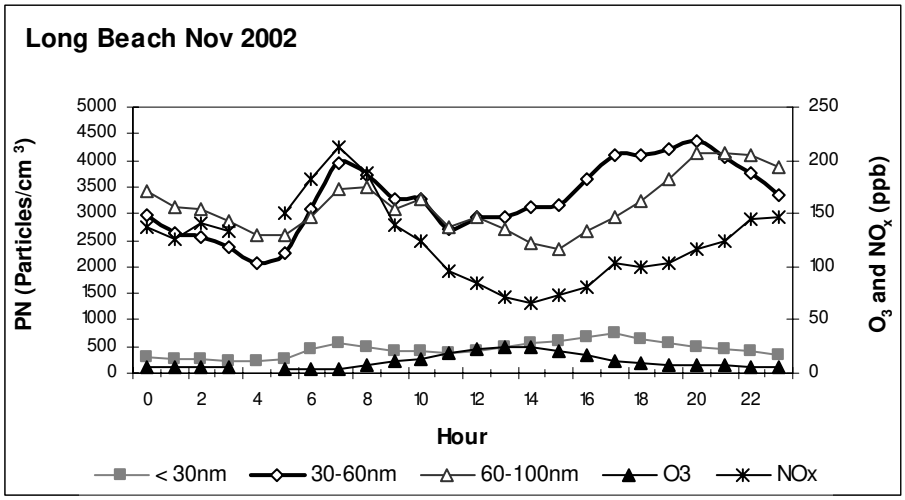

Figure 2.5 b

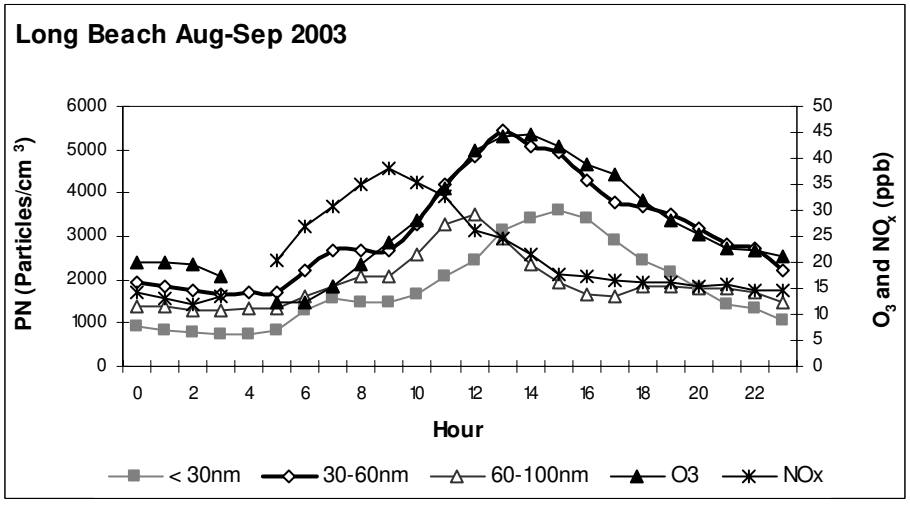

FIGURE 2.5: Diurnal trends of size-segregated particle number, O_3 and NO_x at Long Beach during a) Nov 2002 and b) Aug-Sep 2003

During summer months, secondary aerosol formation is favored and new ultrafine particles may form as a result of the condensation of low-volatility products of

Figure 2.6 a

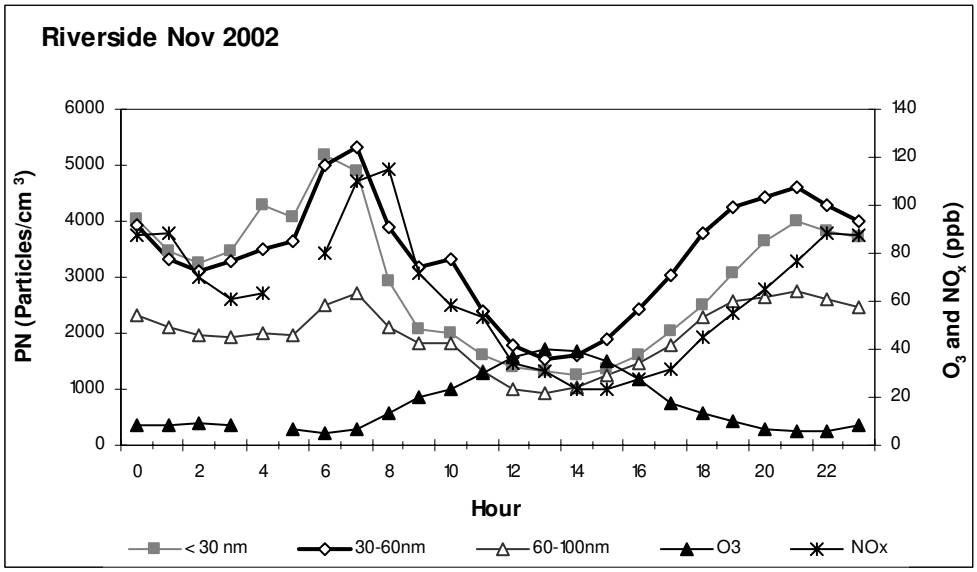

Figure 2.6 b

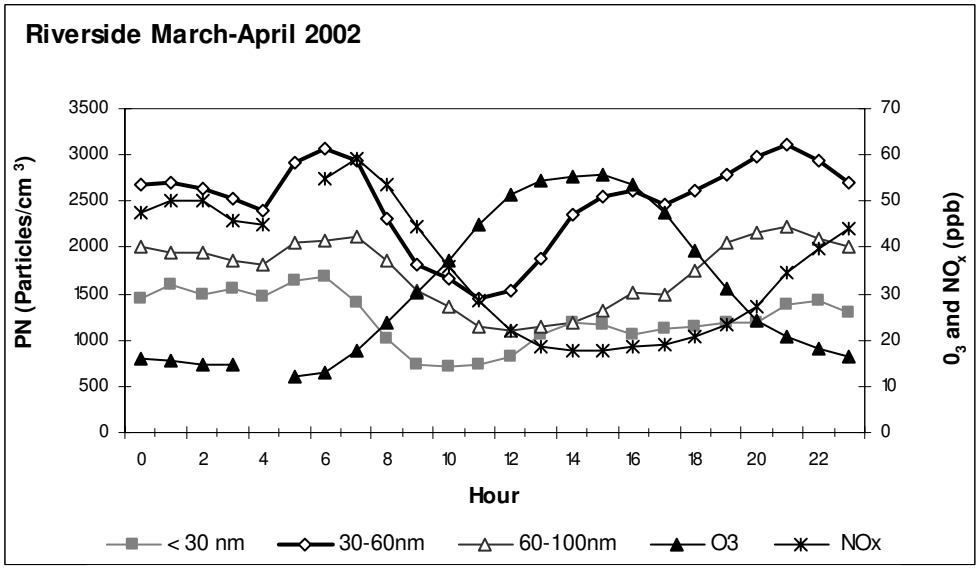

FIGURE 2.6: Diurnal trends of size-segregated particle number, O_3 and NO_x at Riverside during a) Nov 2002 and b) Mar-Apr 2002

photochemical reactions (largely organic compounds) onto stable, nanometer-size particles (O'Dowd et al 1999; Kim et al., 2002; Sardar et al., 2004). Secondary aerosol formation is the most likely explanation for the diurnal trends in PN during the summer

period at USC and Long Beach (Figures 2.4b and 2.5b, respectively) in which the peak particle concentrations during the afternoon period either coincide or slightly lag behind the peak in O_3 concentrations.

Figure 2.7 a

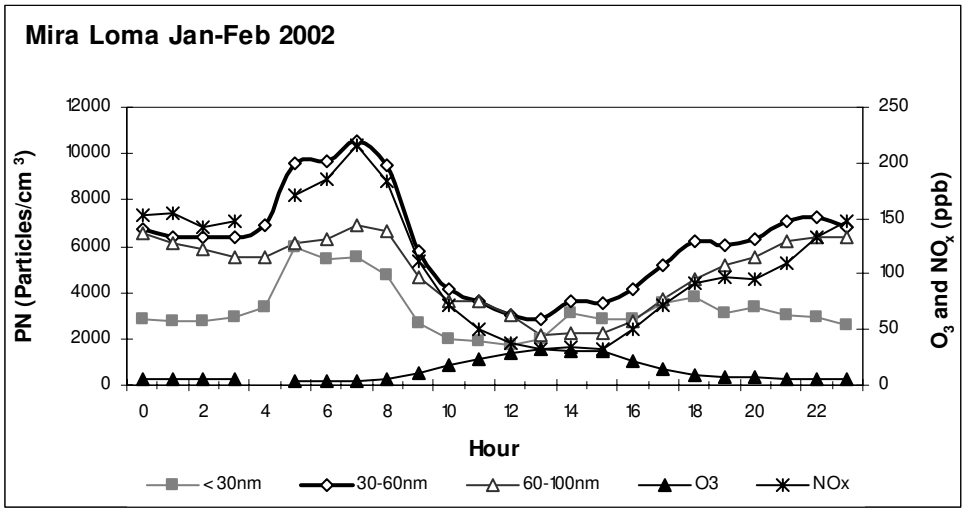

Figure 2.7 b

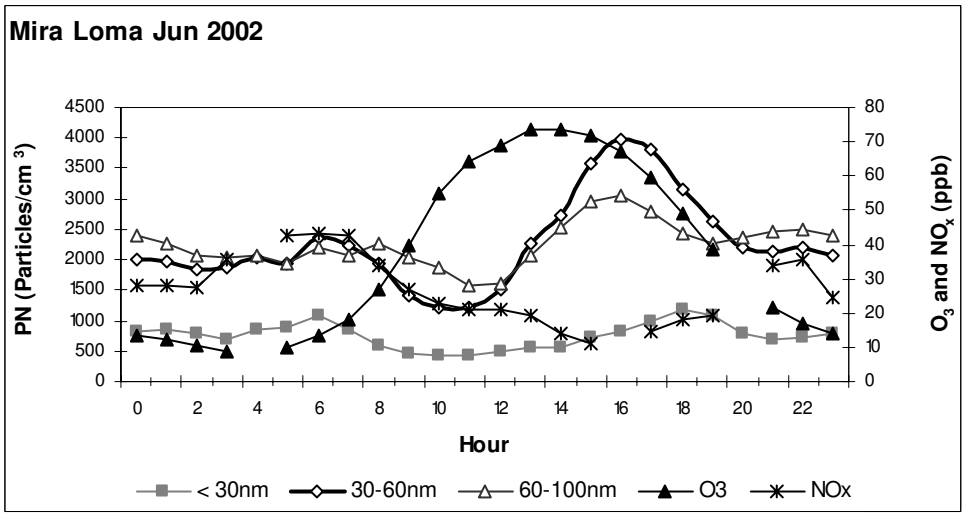

FIGURE 2.7: Diurnal trends of size-segregated particle number, O_3 and NO_x at Mira Loma during a) Jan-Feb 2002 and b) Jun 2002

Figures 2.6a and 2.7a show the diurnal trends of particle numbers as well as gaseous copollutants during winter period at Riverside and Mira Loma, respectively. Similar to the winter diurnal trends of the source sites, we notice a peak in number concentrations in the morning and another smaller peak in the evening across all particle size ranges. The diurnal pattern of NO_x is very similar to diurnal profile of number concentrations at both these sites, indicating once again a traffic origin for these particles during winter. Since particle number counts are high and wind speeds are generally low in the morning, the traffic sources are local and specific to the sampling locations. The higher number concentrations in morning, relative to evening rush hour levels, may be a result of the low mixing height during morning hours.

As the day progresses the temperature increases, causing the inversion height to rise. The lower number median diameter of aerosol during winter may also be explained by contribution from fresh emissions in winter. The diurnal patterns of particle number concentrations show an additional peak during the afternoon in spring and summer months at Riverside and Mira Loma, respectively (Figures 2.6b, 2.7b), similar to those observed during the summer in Long Beach and USC. This peak is either concurrent or slightly lagging the O_3 peak, as in the previous sites. We attribute this increase to secondary aerosol production by photochemical reactions, as discussed earlier, with the lag between the PN and O_3 peaks possibly being due to the time that is required for the newly formed particles to grow to a size that can be detected by the SMPS (i.e., >15 nm).

Figure 2.8 a

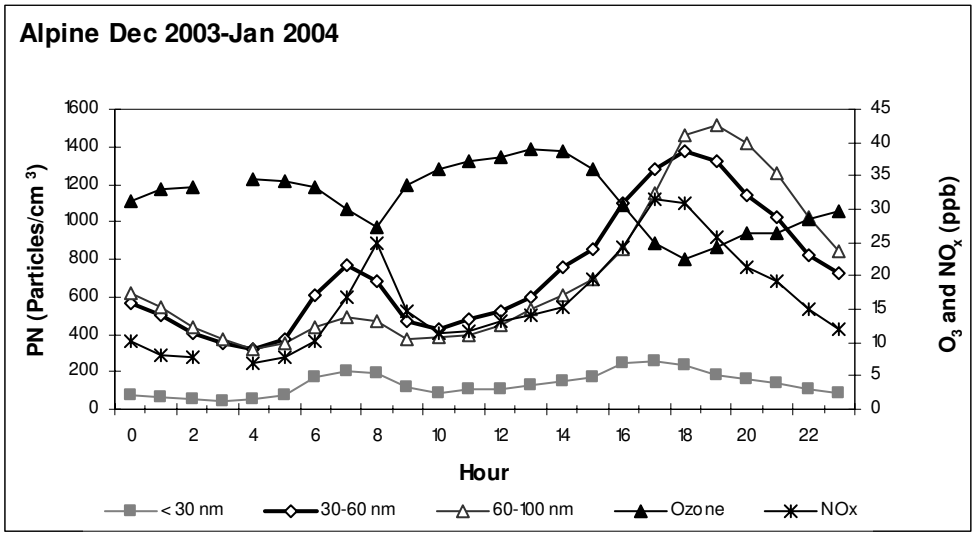

Figure 2.8 b

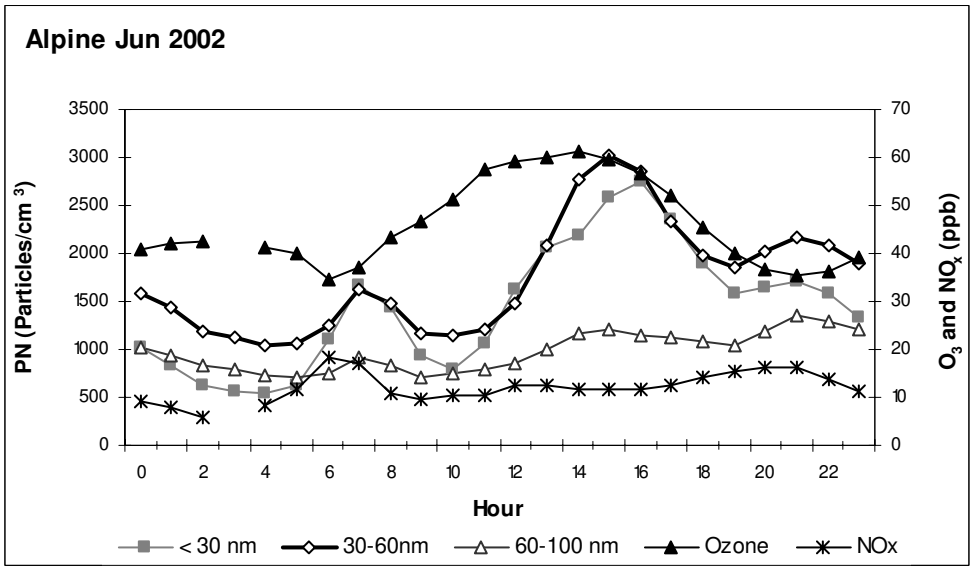

FIGURE 2.8: Diurnal trends of size-segregated particle number, O_3 and NO_x at Alpine during a) Dec 2003-Jan 2004 and b) Apr-May 2003

Similar diurnal patterns of particle counts for winter and summer to the LAB sites are observed at Alpine, depicted in Figure 2.8. During winter, higher numbers are observed in the morning, when the mixing height of the atmosphere is low. As the day progresses,

the temperature increases and mixing height rises, correspondingly the particle number concentrations drop due to dilution and dispersion, and they increase again in evening and night when the mixing height depresses. The diurnal trends of particle concentrations also track well those of NO_x. During the warmer period (April and May 2002), the diurnal profile of particulates displays a different trend. There is a surge in particle numbers in the afternoon, especially for particles below 60 nm, following a very similar pattern to the diurnal profile of O_3, which implies photochemical formation of these particles and air mass advection, as seen at the urban sites discussed earlier.

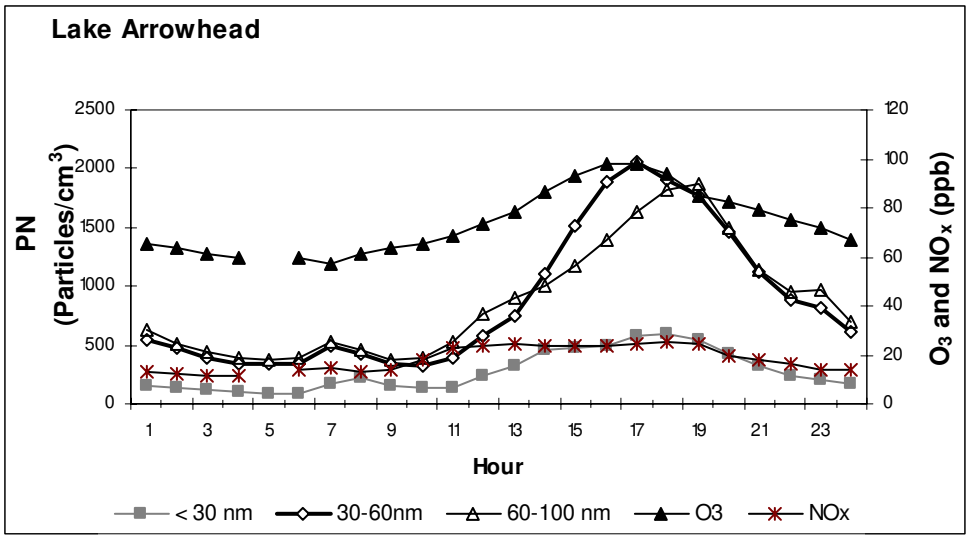

FIGURE 2.9: Diurnal trends of size-segregated particle number, O_3 and NO_x at Lake Arrowhead during Jul-Aug 2002

The diurnal profile of number concentrations and gaseous pollutant concentrations averaged by time of the day over two months (July-August 2002) of SMPS sampling in Lake Arrowhead is shown in Figure 2.9. The diurnal patterns of O_3 and NO_x are very similar to the diurnal patterns of particle number concentrations. All pollutant

concentrations increase during later part of the day. As discussed earlier, Lake Arrowhead is located at an elevation of approximately 1700 m with negligible local pollution sources. During early morning and night, the inversion layer is generally below the station location. As the day progresses, the warmer temperature cause the inversion layer to rise. Eventually, the station is under the inversion layer. In addition to the contribution of photochemical activity to the total particle numbers, the rise in particle numbers during that period is also a result of the increased vertical mixing and advection, which brings to the site aged and more polluted air parcels originating in the western parts of LAB. This is also supported by the unusual rise in NO_x concentrations in the middle of the day, also seen in Figure 2.9, which cannot be attributed to an increase in traffic or any other factors.

2.4.3 Correlations between PM Numbers, PM Surface Area and PM mass

Table 2.3 presents the Pearson correlation coefficient (R) between total particle number concentrations and total surface area concentrations calculated from the SMPS data assuming spherical particles. A moderate to high correlation (i.e., R=0.55-0.90) was observed between particle number and surface area concentrations for all sites in both sampling periods. This correlation was somewhat lower in the warmer period for all the sites in this study except Riverside and Long Beach. Strom et al. (2003) also found higher correlations between particle number and surface area in winter compared to summer. This finding is consistent with the hypothesis that the increased aerosol surface area acts as a deposition site for gaseous precursors to condense, thereby preventing new

TABLE 2.3: Pearson correlation coefficient (R) between total particle number concentration and total particle surface area concentration

Site name	Season	Period	Pearson correl. coeff.
Long Beach	Winter	Nov '02	0.76
Long Beach	Summer	Aug-Sep '03	0.80
Mira Loma	Winter	Jan-Feb '02	0.76
Mira Loma	Spring	Jun '02	0.53
Riverside	Winter	Nov '02	0.69
Riverside	Spring	Mar-Apr '02	0.69
USC	Winter	Dec '02 - Jan '03	0.65
USC	Summer	Sep '03	0.58
Upland	Winter	Nov-Dec '03 - Jan '04	0.74
Upland	Summer	Aug-Sep-Oct '03	0.68
Alpine	Winter	Dec '03 - Jan '04	0.90
Alpine	Spring	Apr-May '03	0.68
Lancaster	Spring	Jun-Jul '03	0.57
Lake Arrowhead	Summer	Jul-Aug '02	0.84

particle formation, as one would expect. The increased surface area may also act as a sink of ultrafine particles via heterogeneous coagulation.

The correlation of hourly and 24-hour averaged PM_{10} and particle number (PN) concentrations is shown in Table 2.4 for the different CHS sites. In general, the correlations were found to be weak-to-moderate (i.e., $R < 0.5$), except of the site in Alpine, where relatively strong correlations were observed in the springtime between both the hourly as well as 24-hour averaged concentrations. No particular trend in the hourly or 24-hour data between different seasons was observed that could be applied to all sites, as the relationship between the hourly and 24-hour PN and PM_{10} varied differentially from site-to-site and within seasons, as evident in the data shown in Table 2.4.

TABLE 2.4: Correlation coefficient (R) between total particle number concentration and PM_{10}

Site	Season	Period	Pearson correl. coeff.	
			Hourly avg.	Daily avg.
Long Beach	Winter	Nov '02	NA	NA
Long Beach	Summer	Aug-Sep '03	0.28	0.29
Mira Loma	Winter	Feb '02	0.38	0.31
Mira Loma	Spring	Jun '02	0.29	0.43
UC Riverside	Winter	Nov '02	-0.13	0.29
UC Riverside	Spring	Mar-Apr '02	0.46	0.53
USC	Winter	Dec '02 - Jan '03	0.14	0.49
USC	Summer	Sep '03	0.26	0.35
Upland	Winter	Nov-Dec '03 - Jan '04	0.47	0.20
Upland	Summer	Aug-Sep-Oct '03	0.19	-0.03
Alpine	Winter	Dec '03 - Jan '04	0.16	-0.02
Alpine	Spring	May '03	0.51	0.71
Lancaster	Spring	Jun-Jul '03	0.48	0.59
Lake Arrowhead	Summer	Jul-Aug '02	0.36	0.26

2.4.4 Long Beach October 2002 strike analysis

During the period of September 30 to October 9, 2002, union workers at the port of Long Beach, CA went on strike. The port which is located upwind to the sampling site is considered a major contributor to PM at Long Beach as a result of emissions from ships (Isakson et al., 2003), but perhaps more so because of the heavy-duty truck traffic associated with the port (Chow et al., 1994). It was interesting to determine whether significant changes in particle and co-pollutant characteristics were observed due to this strike. In order to understand the effects of this strike, we present the PM as well as co pollutant characteristics from pre-, during and post-strike periods in this section. Unfortunately, we do not have the SMPS data from September 25 to October 1, 2002,

due to calibration and maintenance performed on the instruments at that time, therefore PM characteristics for the pre-strike period are studied from September 16-24, 2002 and for the strike period from October 2-9, 2002.

Figure 2.10 a

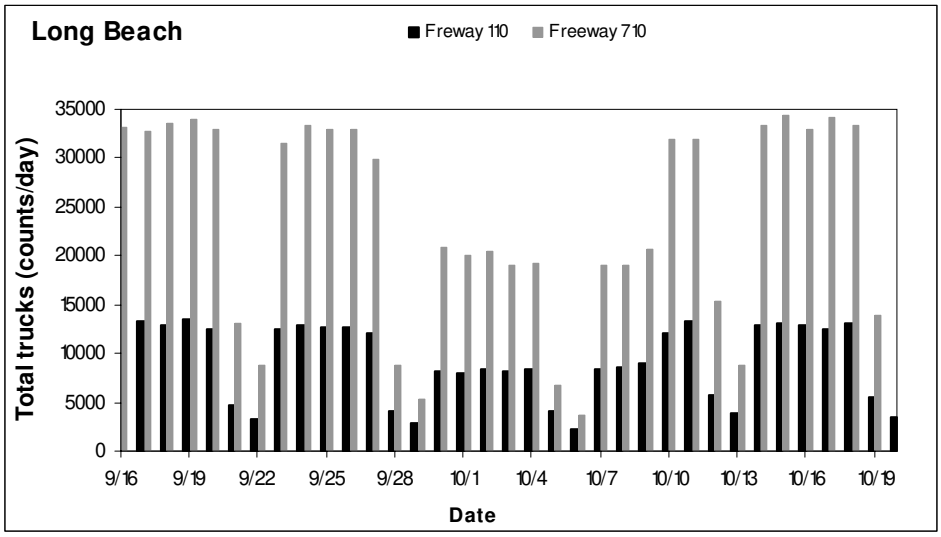

Figure 2.10 b

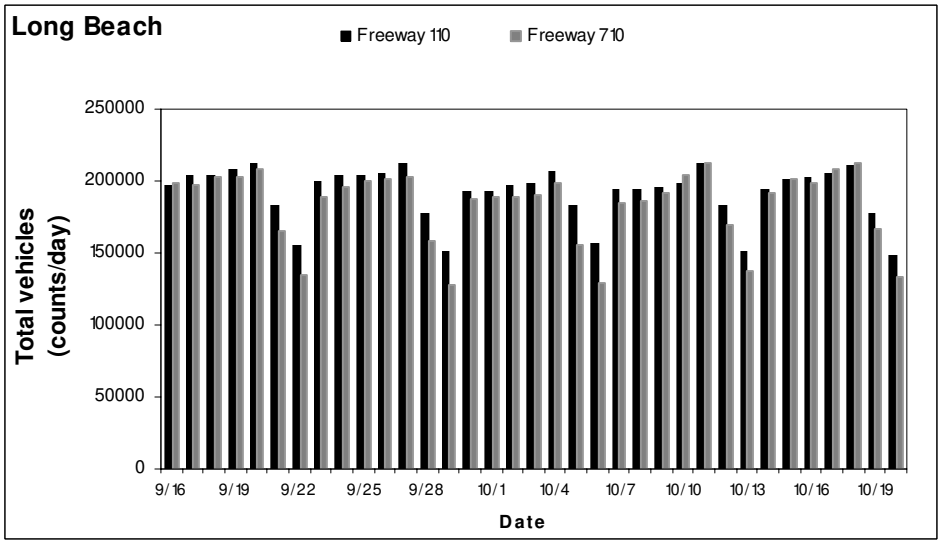

FIGURE 2.10: Daily traffic data for Freeways 710 and 410 before, during and after harbor strike at Long Beach a) total truck counts, and b) total vehicle counts

During the strike period, the following three major changes occurred that might have influenced air pollution in that area. First, there was a significant decrease in diesel truck traffic both on the nearby freeways 710 and 110 as well as local surface streets (Figure 2.10a). Second, about 200 ships were idling off the coast, immediately upwind of the Long Beach throughout the strike period (CNN, 2002). Third, there were significant changes in weather conditions during that period. While in September the weather in Long Beach was warm with the exception of the morning hours, it changed in early October (coincidentally with the strike) to cooler with mostly overcast days (Figure 2.11c). These weather conditions continued after the strike period. This change may be expected to increase particle concentration by enhancing formation by condensation, but to also particle size condensational growth of the formed particles.

Figure 2.11a shows the 24-hour averaged concentrations of particle number and PM_{10} during the strike and non-strike period. It should be noted here that since the CPC was used in conjunction with the SMPS, the total particle numbers shown in Figure 2.11a reflect the sum of the particle counts in each size bin of the SMPS and not those measured by the CPC alone. As other studies have indicated, this may underestimate quite substantially the total particle concentrations (Liu and Deshler, 2003).

The results of Figure 2.11a as well as our statistical analysis did not reveal any statistically significant impact of the strike on PN as well as PM_{10} concentrations

Figure 2.11 a

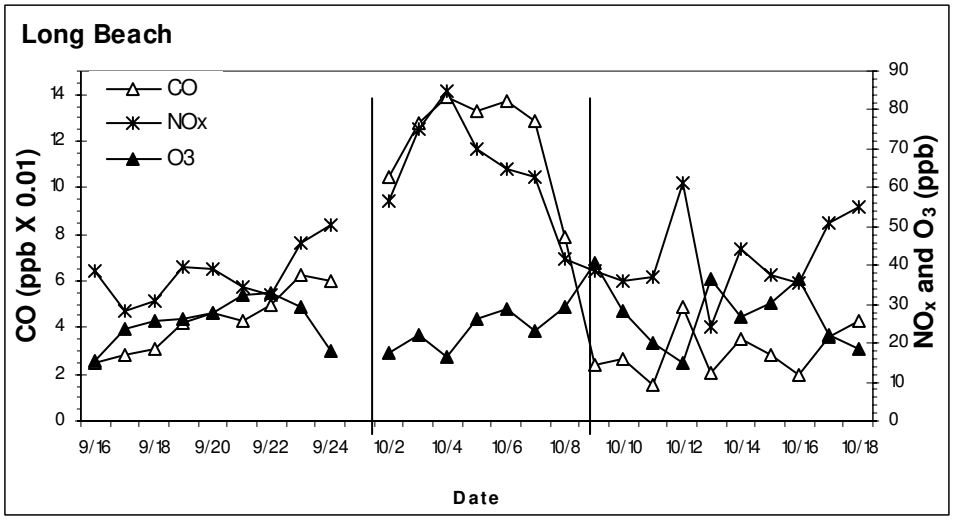

Figure 2.11 b

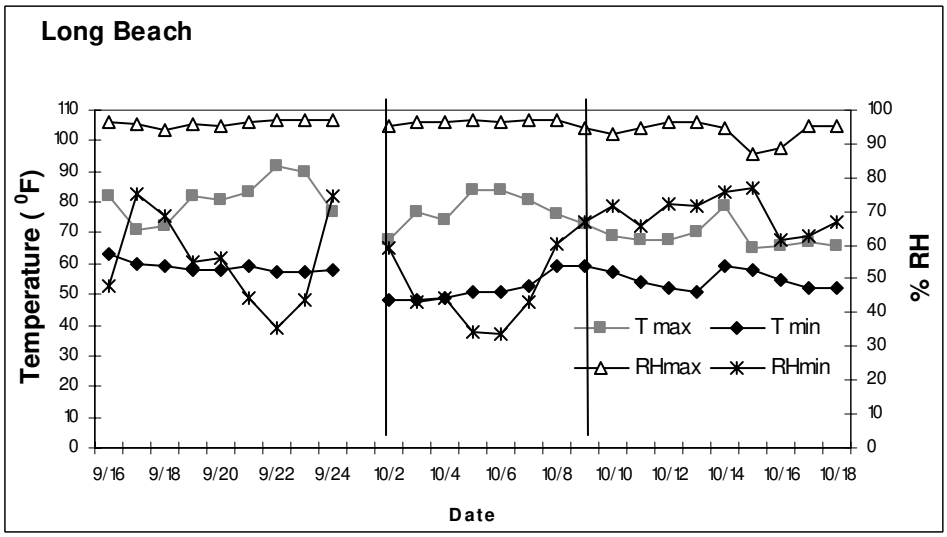

FIGURE 2.11: 24-hour averaged a) PN and PM_{10}, b) CO, NO_x, and O_3, and c) temperature and RH - before, during and after the port strike at Long Beach in Sep-Oct 2002

($p > 0.05$). The corresponding concentrations of gaseous co pollutants during the strike/non- strike period are presented in Figure 2.11b. There is a statistically significant increase in NO_x and CO concentrations during the strike compared to pre- as well as

FIGURE 2.11: Continued…

Figure 2.11 c

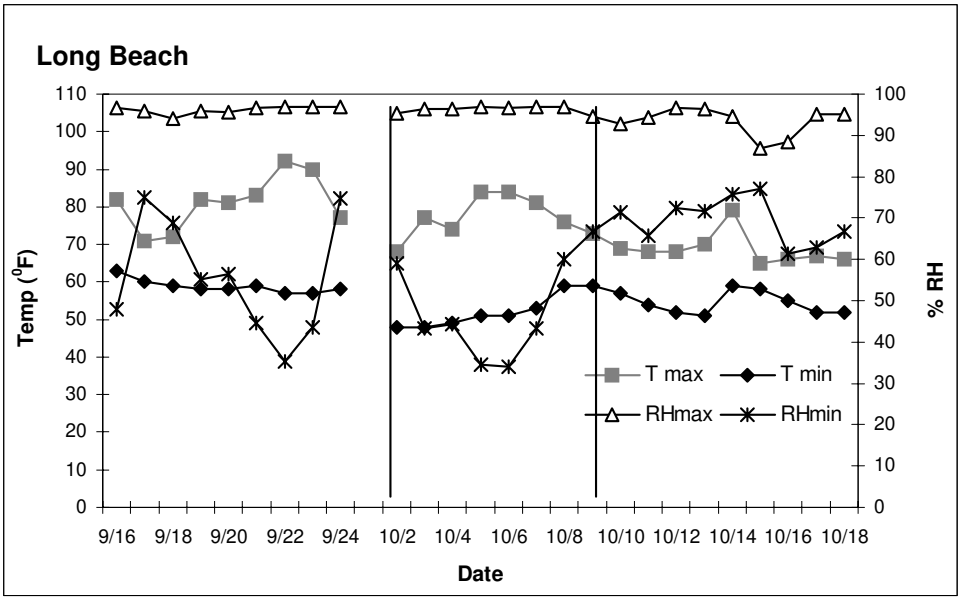

post-strike period ($p < 0.001$). High amounts of NO_x and CO emissions from ships have been observed in previous studies (Corbett and Fishback, 1997; Sinha et al., 2003; Cooper, 2003; Saxe and Larsen, 2004). These emissions have been reported to be more pronounced when the ships are at berth and idling (Cooper, 2003). We believe that the majority of the increase in CO levels must be attributed to emissions from the idling ships.

Emissions from diesel engines operating in ships contribute significantly to sub-micrometer range particles and typically have bimodal size distributions, with a dominant mode in the sub-40 nm and a weaker mode in the range of 70-100 nm (Isakson et al., 2003). The average size distributions of the particle number concentrations before, during

and after the strike are shown in Figure 2.12. Particle concentrations below 60 nm seem virtually unaffected by the strike. Even if a large number of these particles were emitted by ships, it is conceivable that a substantial fraction of them did not reach the sampling station due to coagulation, and-or volatilization processes that may have occurred during their transport. Particle numbers concentrations in the 60-200 nm range were, however, significantly elevated during the strike ($p < 0.001$), which may be indicative of the contributions of emissions from the idling ships. Also, the mode before and after the strike is smaller compared to the strike period, further supporting the argument for the larger-sized particles originating from ship emissions compared to those from heavy and light duty vehicles.

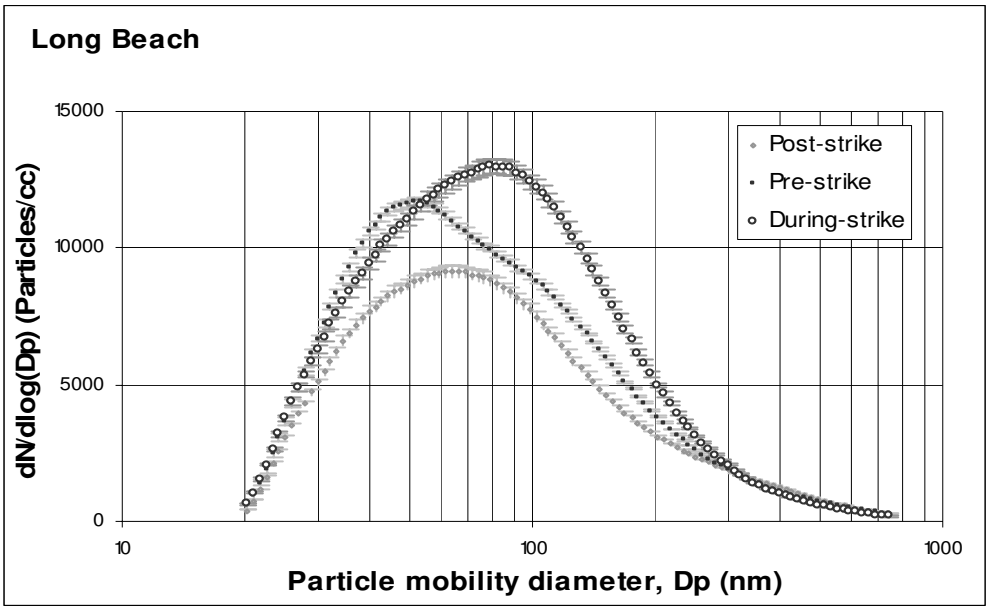

FIGURE 2.12: Average particle number size distribution before, during and after the port strike at Long Beach in Sep-Oct 2002

2.5 Chapter 2: SUMMARY AND CONCLUSION

Particle number concentrations and size distributions in complex urban environments can be seen to be highly variable on temporal scales, from diurnal to seasonal, and spatially, from local scale influences, such as distances from highways, to regional scale influences, such as long range transport across air basins. Seasonal difference in solar intensity, temperature, and relative humidity can also strongly influence the diurnal size profile.

In this study we see enhanced contribution of local emission sources during cooler months with stagnant meteorological conditions at all sites. During warmer months, effects of long-range dispersal of aerosol are observed most clearly at the easterly receptor sites of Riverside, Mira Loma and Lake Arrowhead. The increased wind speeds and onshore flow in the warmer months, lead to increased advection of pollutant parcels from the polluted western areas of the LAB (Fine et al., 2004). Additionally, dry and hot summer conditions would limit ultrafine particle growth to accumulation mode during transport (Kim et al., 2002).

In addition to the contribution of vehicular emissions to particle concentrations in Los Angeles, photochemical formation by secondary reactions in the atmosphere appears to be a major source of PM during the afternoon periods in the warmer months at all sites. Current studies by a number of groups have investigated and confirmed the photochemical formation of ultrafine particles in urban atmosphere. In addition to our

observations in Los Angeles, secondary particle formation events have been observed in urban areas, including Pittsburgh (Stanier et al., 2004), St. Louis (Shi and Qian, 2003), and Mexico City (Baumgardner et al., 2004). An excellent review of this topic is given by Kulmala et al. (2004). The actual formation mechanism of nanoparticles in the range of 1-3 nm remains largely unknown and has recently become the subject of intensive research in the field of atmospheric science. Current hypotheses on the composition of these fresh nuclei include the binary nucleation of water and sulfuric acid (Kulmala, 2002), ternary nucleation of ammonia-sulfuric acid-water (Weber et al., 1997), and ion-induced nucleation (Yu and Turco, 2001). There is also general consensus that the species responsible for further growth of these nanoparticles to the > 10 nm range are different than the nucleating species (Stanier et al., 2004). Our current understanding of atmospheric nanoparticle processes suggests that growth of these particles to larger sizes within the ultrafine PM mode occurs by condensation of low volatility organic species. These species are products of photochemical oxidation of volatile organic precursors on these pre-existing nuclei (O'Dowd et al., 1999; Kulmala et al., 2004). In fact, recent studies by Zhang et al. (2004) showed that nucleation rates of sulfuric acid are greatly increased in the presence of organic acids (including products of atmospheric photochemical reactions), by forming unusually stable organic-sulfuric acid complexes, thereby reducing the nucleation barrier of sulfuric acid.

It is interesting to note in our field measurements that summertime levels of ultrafine particles at source sites, such as long Beach and USC peaked in midday (i.e., noon to 1

pm), whereas ultrafine PM numbers peak slightly later (i.e., between 3-4 pm) in the inland receptor sites. A time delay in the peak concentrations observed at the receptor sites is possibly due to the transport time for polluted air masses to reach those sites. The correlation between particle number concentrations and PM_{10} has been widely studied and weak-to-moderate correlations have been generally observed between the two (Morawska et al., 1998; Woo et al., 2001; Noble et al., 2003; Fine et al., 2004; Sardar et al, 2004). Since the fine to ultrafine particle counts are dominated by very small particles and the PM_{10} mass is dominated by fewer, much larger particles, low correlation should be expected, especially in air masses dominated by fresher particles (either primary emission particles or freshly formed secondary particles). In our study, we also found weak-to-moderate correlations between PM_{10} and number concentrations with no particular seasonal trend. These findings are very important from a regulatory perspective because they imply that controlling ambient PM_{10} mass via national air quality standards may not necessarily reduce human exposure to ultrafine particles that dominate the particle counts and have recently been shown to have toxic effects (as discussed in the introductory part of the paper).

In conclusion, the results presented in this paper indicate that location and season significantly influence particle number and size distributions in locations within Southern California. Strong diurnal and seasonal patterns in number concentrations are evident as a direct effect of the sources, formation mechanisms, as well as meteorological conditions prevalent at each location during different times of the day and year. These results will

be used in the CHS as a first order indicator of not only human exposure, but also inhaled dose to ultrafine PM. They will also be used for the development and validation of predictive models for population exposure assessment to ultrafine PM in complex urban environments, such as that of the Los Angels Basin.

2.6 Chapter 2: REFERENCES

Baltensperger U., Streit N., Weingartner E., Nyeki S., Prevot A.S.H., Van Dingenen R., Virkkula A., Putaud J.P., Even A., ten Brink H., Blatter A., Neftel A., Gaggeler H.W. Urban and rural aerosol characterization of summer smog events during the PIPAPO field campaigne in Milan, Italy. *J Geophys Res.* **2002**.: 107 (D22): 8193-8204.

Baumgardner D., Raga G.B., and Muhlia A. Evidence for the formation of CCN by photochemical processes in Mexico City. *Atmos Environ* **2004**: 38(3): 357-367.

Birmili W., Wiedensolher A., Heintzenber J. and Lehmann K. Atmospheric particle number size distribution in central Europe: statistical relations to air masses and meteorology. *J Geophys Res* **2001**:106 (D23): 32005-32018.

Buzorius G., Hameri K., Pekkanen J. and Kulmala M. Spatial variation of Aerosol Number Concentration in Helinski City. *Atmos Environ* **1999**: 33: 553-565.

Cheng M.D. and Tanner R.L. Characterization of ultrafine and fine particles at a site near the Great Smoky Mountains. *Atmos Environ* **2002**: 36: 5795-5806.

Chow J.C., Watson J.G., Fujita E.M., Lu Z., Lawson D.R. and Ashbaugh L.L. Temporal and spatial variations of $PM_{2.5}$ and PM_{10} aerosol in the Southern California air quality study. *Atmos Environ* **1994**: 28 (12): 2061-2080.

CNN, Long Beach harbor strike, Internet, accessed August 24, **2004**, http://money.cnn.com/2002/10/08/news/ports_longshoremen

Cooper D.A. Exhaust emissions from ships at berth. *Atmos Environ* **2003**: 37: 3817-3830.

Corbett J.J. and Fischbeck P. Emissions from ships. *Science* **1997**: 278 (5339): 823-824.

Cyrys J., Stolzel M., Heinrich J., Kreyling W.G., Menzel N., Wittmaack K., Tuch T. and Wichmann H.E. Elemental composition and sources of fine and ultrafine ambient particles in Erfurt, Germany. *Sc Total Env* **2003**: 305: 143-156.

Derwent R.G., Davies T.J., Delaney M., Dollard G.J., Field R.A., Dumitrean P., Nason P.D., Jones B.M.R. and Pepler S.A. Analysis and interpretation of the continuous hourly monitoring data for 26 C_2–C_8 hydrocarbons at 12 United Kingdom sites during 1996. *Atmos Environ* **2000**: 34 (2): 297-312.

Dockery D.W. and Pope C.A. Acute respiratory effects of particulate air pollution. *Ann Rev of Pub Hlth* **1994**: 15: 107-132.

Fine P.M., Shen S. and Sioutas C. Inferring the sources of fine and ultrafine particulate matter at downwind receptor sites in the Los Angeles Basin using multiple continuous measurements. *Aerosol Sci Technol* **2004**: 18: 182-195.

Harrison R.M., Shi J.P., Xi S., Khan A., Mark D., Kinnersley R. and Yin J. Measurement of number mass and size distribution of particles in the atmosphere. *Phil Tran. R Soc Lond* 2000: 358: 2567-2580.Isakson J., Persson T.A. and Lindgren E.S. Identification and assessment of ship emissions and their effects in the harbor of Goteborg Sweden. *Atmos Environ* **2003**: 35: 3659-3666.

Jacques P.A., Ambs J.L., Grant W.L. and Sioutas C. Field evaluation of the differential TEOM monitor for continuous $PM_{2.5}$ mass concentrations. *Aerosol Sci Technol* **2004** (Suppl. 1): 38: 49-59.

Kikas U., Mirma A., Tamm E. and Raunemaa T. Statistical characteristics of aerosol in Baltic sea region. *J Geophys Res* **1996**: 101 (D14): 19319-19327.

Kim S., Shen S., Sioutas C., Zhu Y. F. and Hinds W. C. Size distribution and diurnal and seasonal trends of ultrafine particles in source and receptor sites of the Los Angeles Basin. *J Air Waste Manage Assoc* **2002**: 52: 297-307.

Kulmala M. How particles nucleate and grow. *Science.* **2002**: 302: 1000-1001

Kulmala M., Vehkamäki H., Petäjä T., Dal Maso M., Lauri A., Kerminen V.M., Birmili W. and McMurry P.H. Formation and growth rates of ultrafine atmospheric particles: a review of observations. *J Aerosol Sci* **2004**: 35: 143-176.

Künzli N., McConnell R., Bates D., Bastain T., Hricko A., Lurmann F., Avol E., Gilliland F. and Peters J. Breathless in Los Angeles: The exhausting search for clean air. *Am J Pub Hlth* **2003**: 93(9): 1494-1499.

Lawless P.A., Rodes C.E. and Evans G. Aerosol concentration during the 1999 Fresno exposure studies as functions of size season and meteorology. *Aerosol Sci Technol* **2001**: 34: 66-74.

Li N., Alam J., Eiguren A., Slaughter N., Wang X., Huang A., Wang M., Sioutas C. and Nel, A.E. Nrf2 is a Key Transcription Factor in Antioxidant Defense in Macrophages and Epithelial Cells: Protecting Against the Injurious Effects of Pro-oxidative Air Pollutants. *J Immunol* **2004**: 173 (5): 3467-3481.

Li N., Sioutas C., Froines J.R., Cho A., Misra C and Nel A., Ultrafine Particulate Pollutants Induce Oxidative Stress and Mitochondrial Damage. *Environ Health Persp* **2003**: 111 (4): 455-460.

Liu P.S.K. and Deshler T. Causes of concentration differences between a Scanning Mobility Particle Sizer and a Condensation Particle Counter. *Aerosol Sci Technol* **2003**: 37: 917-923.

Mäkelä J.M., Aalto P., Jokinen P., Pohja T., Nissinen A., Palmroth S., Markkanen T., Seitsonen K., Lihavainen H. and Kulmala M. Observations of ultrafine aerosol particle formation and growth in boreal forest. *Geophys Res Lett* **1997**: 24: 1219-1222.

Morawska L., Jayarantne E.R., Mengersen K. and Thomas S. Differences in airborne particle and gaseous concentrations in urban air between weekdays and weekends. *Atmos Environ* **2002**: 36: 4375-4383.

Morawska L., Bofinger N.D., Kocis L. and Nwankwoala A. Comprehensive characterization of aerosols in a subtropical urban atmosphere: particle size distribution and correlation with gaseous pollutants. *Atmos Environ* **1998**: 32 (14-15): 2467-2478.

Na K.S., Sawant A.A., Song C. and Cocker D.R. Primary and secondary carbonaceous species in the atmosphere of Western Riverside County, California. *Atmos Environ* **2004**: 38 (9): 1345-1355.

Noble C.A., Mukerjee S., Gonzales M., Rodes C.E., Lawless P.A., Natarajan S., Myers E.A., Norris G.A., Smith L., Ozkaynak H. and Neas L.M. Continuous measurement of fine and ultrafine particulate matter criteria pollutants and meteorological conditions in urban El Paso, Texas. *Atmos Environ* **2003**: 37: 827-840.

Oberdörster G. and Utell M.J. Ultrafine particles in the urban air: To the respiratory tract- and beyond? *Environ Health Persp* **2002**: 110 (8): A440-A441.

O'Dowd C., McFiggans G., Creasey D.J., Pirjola L., Hoell C., Smith M.H., Allan B.J., Plane J.M.C., Heard D.E., Lee J.D., Pilling M.J. and Kulmala M. On the photochemical production of new particles in the coastal boundary layer. *Geophys Res Lett* **1999**: 26 (12): 1707-1710.

Peters A., Wichmann H.E., Tuch T. and Heinrich J. Respiratory effects are associated with the number of ultrafine particles. *Amer J Resp Crit Care Med* **1997**: 155: 1376-1383.

Phuleria H.C., Fine P.M., Zhu Y. and Sioutas C. Characterization of Particulate Matter and co-pollutants during the fall 2003 Southern California fires. *J Geophy Res-Atmos* **2004** *(in press)*

Pope C.A. Review: epidemiological basis for particulate air pollution health standards. *Aerosol Sci Technol* **2000**: 32 (1): 4-14.

Ruuskanen J., Tuch. Th., Ten Brink H., Peters A., Khystov A., Mirme A., Kos G.P.A., Brunekreef B., Wichmann H.E., Buzorius G., Vallius M., Kreyling W.G. and Pekkanen J. Concentrations of ultrafine, fine and $PM_{2.5}$ particles in three European cities. *Atmos Environ* **2001**: 35: 3729-3738.

Sardar S.B., Fine P.M., Hoon A. and Sioutas C. Associations between particle number and gaseous copollutants concentrations in the Los Angeles Basin. *J Air Waste Manage Assoc* **2004** (*in press*).

Saxe H. and Larsen T. Air pollution from ships in three Danish ports. *Atmos Environ* **2004**: 38: 4057-4067.

Shi J.P. and Qian Y. Aerosol size distributions (3 nm to 3 um) measured at St. Louis Supersite (4/1/01-4/30/02) *M. S. Thesis Department of Mechanical Engineering University of Minnesota Minneapolis MN, 55455.* **2003**.

Shi J.P., Evans D.E., Khan A.A. and Harrison R.M. Sources and concentration of nanoparticles (<10 nm diameter) in the urban atmosphere. *Atmos Environ* **2001**: 35:1193-1202.

Shi J.P.; Khan A.A. and Harrison R.M. Measurements of ultrafine particle concentration and size distribution in the urban atmosphere. *Sci Total Environ* **1999**: 235: 51-64

Sinha P., Hobbs P.V., Yokelson R.J., Christian T.J., Kirchstetter T.W. and Bruintjes R. Emissions of trace gases and particles from two ships in the southern Atlantic Ocean. *Atmos Environ.* **2003**: 37: 2139-2148.

Stanier C.O., Khlystov A.Y. and Pandis S.N. Ambient aerosol size distributions and number concentrations measured during the Pittsburgh Air Quality Study (PAQS). *Atmos Environ.* **2004**: 38: 3275-3284.

Strom J., Umegard J., Torseth K., Tunved P., Hansson H.-C., Holmen K., Wismann V., Herber A. and Langlo G.K. One-year particle size distribution and aerosol chemical composition measurements at the Zeppelin Station, Svalbard, March 2000-March 2001. *Atmos Environ.* **2003**: 28: 1181-1190.

Weber R.J., Marti J.J., McMurry P.H., Eisle, F.L., Tanner D.J. and Jefferson A. Measurement of new particle formation and ultrafine particle growth rates at a clean continental site. *J Geophys Res* **1997**: 102 (D4): 4375-4385.

Wehner B., Wiedensohler A. A long-term measurement of submicrometer urban aerosols: statistical analysis for correlations with meteorological conditions and trace gases. *Atmos Chem Phys* **2003**: 3: 867-879.

Woo K.S., Chen D.R., Pui D.Y.H. and McMurry P.H. Measurement of Atlanta aerosol size distributions: observations of ultrafine particle events. *Aerosol Sci Technol* **2001**: 34: 75-87.

Xia T., Korge P., Weiss J.N., Li N., Venkatesen M.I., Sioutas C., and Nel A. Quinones and Aromatic Chemical Compounds in Particulate Matter (PM) Induce Mitochondrial Dysfunction: Implications for Ultrafine Particle Toxicity. *Environ. Health Persp.* **2004**: 112 (14): 1347-1359.

Yu F. and Turco R.P. From molecular clusters to nanoparticles: Role of ambient ionization in tropospheric aerosol formation. *J Geophys Res* **2001**: 106 (D5): 4797-4814.

Zanobetti A., Schwartz J. and Dockery D.W. Airborne particles are a risk factor for hospital admissions for heart and lung disease. *Environ. Health Persp.* **2000**: 108(11): 1071-1077.

Ziemann P., Tobias H.J., Beving D.E., Sakurai H., Zuk M., McMurry P.H., Zarling D. , Waytulonis R., Kittelson D.B. Chemical analysis of diesel engine nanoparticles using a nano-DMA/thermal desorption particle beam mass spectrometer. *Env. Sc. Technol.* **2001**: 35: 2233-2243

Zhang R., Suh I., Zhao J., Fortner E.C., Tie X., Molina L.T., and Molina M.J. Atmospheric new particle formation enhanced by organic acids. *Science* **2004**: 304: 1487-1490.

Zhang K.M. and Wexler A.S. A hypothesis for growth of fresh atmospheric nuclei. *J Geophys Res-Atmos* **2002**:107 (D21): 4577.

Zhu Y.F., Hinds W.C., Kim S., Shen S. and Sioutas C. Study of ultrafine particles near a major highway with heavy-duty diesel traffic. *Atmos Environ* **2002a**: 36: 4323-4335.

Zhu Y.F., Hinds W.C., Kim S. and Sioutas C. Concentration and size distribution of ultrafine particles near a major highway. *J. Air Waste Manage. Assoc.* **2002b**: 52: 1032-1042.

Chapter 3: Air Quality Impacts of the October 2003 Southern California Wildfires*

*Phuleria H.C.; Fine P.M.; Zhu Y.and Sioutas C. Air quality impact of October 2003 Southern California Wildfires, *Journal of Geophysical Research-Atmosphere* 10 (D7): Art. No. D07S08, 2005.

3.1 Chapter 3: ABSTRACT

In Southern California, dry summers followed by hot and dry westerly wind conditions contribute to the region's autumn fire season. In late October of 2003, 13 large Southern California wildfires burned more than 750,000 acres of land, destroyed over 3,500 structures, and displaced approximately 100,000 people. The fire episode was declared the deadliest and most devastating in more than a decade, and local media advised individuals to stay indoors to avoid exposure to excessive levels of PM, CO, VOCs, and ozone caused by the wildfires. This study examines the actual impact of these wildfires on air quality in urban Los Angeles using "opportunistic" data from other air pollution studies being conducted at the time of the fires. Measurements of pollutant gases (CO, NO_x, and ozone), particulate matter (PM), particle number concentrations (PN) and particle size distributions at several sampling locations in the LA basin before, during, and after the fire episode are presented. In general, the wildfires caused the greatest increases in PM_{10} levels (a factor of 3-4) and lesser increases in CO, NO, and PN (a factor of up to 2). NO_2 levels remained essentially unchanged and ozone concentrations dropped during the fire episode. Particle size distributions of air sampled downwind of the fires showed number modes at diameters between 100 and 200 nm, significantly larger than that of typical urban air. The particles in this size range were shown to

effectively penetrate indoors, raising questions about the effectiveness of staying indoors to avoid exposure to wildfire emissions.

3.2 Chapter 3: INTRODUCTION

Wildfires can produce substantial increases in the concentration of gaseous pollutants such as carbon monoxide (CO), nitrogen oxides (NO_x), ozone (O_3), and volatile organic compounds (VOCs) (Cheng et al., 1998; Crutzen and Andreae, 1990) as well as particulate matter (PM) (Dennis et al., 2002; Lighty et al., 2000). In recent years, there has been much interest in studying the impact of wildfires in elevating the concentrations of pollutants in the atmosphere. For instance, high CO concentrations that occurred episodically in the Southeastern United States during the summer of 1995 have been attributed to large forest fires in Canada (Wotawa and Trainer, 2000). In addition to regional and local impacts (Bravo et al., 2002) wildfires contribute significantly to global emissions of atmospheric trace gases including NO_x, CO, and CO_2 (Crutzen et al., 1979). Concerns arising from PM emissions from wildfires include acute health effects, direct and indirect climate forcing, and regional visibility (Bravo et al., 2002; LeCanut et al., 1996).

Emission inventories by the United States Environmental Protection Agency (US EPA) estimate that, for the calendar year 2001, wildfires in the U.S. emitted 7.1 million tons of CO, 0.98 million tons of VOCs, 0.60 million tons of $PM_{2.5}$, and 0.66 million tons of PM_{10} to the atmosphere (National Emissions Inventory – Air Pollutant Emissions Trends, Current Emission Trends Summaries, August 2003, U.S. Environmental Protection

Agency (USEPA), http://www.epa.gov/ttn/chief/trends/index.html). These amounts are significant, contributing 6%, 5%, 8% and 3% of the total CO, VOC, $PM_{2.5}$, and PM_{10} emissions to the atmosphere in the United States in 2001, respectively. These figures obviously vary from year-to-year with the degree of wildfire activity, and in the severe fire season of 2000, 18% of the total $PM_{2.5}$ emissions in the U.S. were estimated to originate from wildfires. Other emission inventories in specific areas have calculated significant NO_x emissions from wildfires as well (Dennis et al., 2002). Some systematic studies and source testing have been carried out for prescribed burns and controlled fires in North America (Einfeld et al., 1991; Radke et al., 1991; Woods et al., 1991). Other studies on wildfire emissions have taken advantage of existing pollution monitoring networks and other focused air pollution studies which happen to be sampling when a wildfire event occurs (Bravo et al., 2002; Brunke et al., 2001; Cheng et al., 1998; Goode et al., 2000). Such "opportunistic" studies can provide valuable information on wildfire pollutant emission rates and the impacts on air quality levels.

Dry summers, followed by conditions of hot and dry westerly winds (known as Santa Ana winds) contribute to Southern California's fire season in the autumn months. While the fire season usually starts around the middle of May, the exact date varies from year to year based on weather patterns and the moisture content, distribution, and amount of wild vegetation present. The fire season usually ends when cooler weather and precipitation conditions prevail. This usually occurs towards the end of October, but the fire season is occasionally extended well into January in some Southern California areas (California Department of Forestry and Fire Protection, Fire Statistics,

http://www.fire.ca.gov/MiscDocuments/FAQs.asp#13). The presence of thick and dry foliage and bushy chaparral adds to the fire danger in the fire season in Southern California. In general, pollution levels are observed to be high during fire events (Bravo et al., 2002). The Los Angeles basin is surrounded by high mountains on three sides, opening to the Pacific Ocean to the west and southwest. The topography and frequent temperature inversions lead to the accumulation of airborne pollutants, particularly in the eastern portion of the basin, due to the prevailing westerly sea breeze (Lu and Turco, 1996).

In late October of 2003, 13 large Southern California wildfires, ranging from Simi Valley in the North to San Diego 150 miles to the south, burned more than 750,000 acres of land, destroyed over 3,500 structures, including 2,700 homes, and displaced 100,000 people. Twenty human deaths were attributed to the wildfires. The cost of the damage has been estimated to be US$ 2 billion. The fires having the greatest effect on the air quality of the Los Angeles (LA) Basin included the Grand Prix and Old fires in San Bernardino County and the adjacent Padua fire in Los Angeles County. These fires were located to the northeast of central Los Angeles, with Santa Ana wind conditions, blowing towards the southwest, transporting emissions to the western portions of the Basin. The fuel was predominantly mixed chaparral, California sagebrush, annual grass and canyon live oak. Pine, perennial grass and other urban vegetation were also burned. The fires started around 23 October and had significant impacts on the air quality of the LA basin until 29 October, when the winds reversed direction and resumed their normal on-shore pattern (National Interagency Coordination Centre, 2003, Statistics and Summary,

http://www.nifc.gov/news/2003_statssumm/intro_summary.pdf). This fire episode was declared the deadliest and most devastating in more than a decade, and there was a significant level of worldwide press coverage. Local media advised individuals to stay indoors to avoid exposure to excessive levels of PM, CO, VOCs, and ozone caused by the wildfires. This motivated the following analysis that examines the actual impact of these wildfires on air quality and measured pollutant concentrations in urban Los Angeles. This paper presents measurements of pollutant gases (CO, NO_x, and ozone) as well as PM concentrations and characteristics at different sampling locations in the LA basin before, during, and after the October 2003 fire episode. In addition, the effect of fire on indoor particle concentrations and size distributions was also investigated. Since the fire episode could not be predicted, the current study took advantage of several pre-existing air pollution studies that were being conducted at the time of the wildfires. Given the "opportunistic" nature of these samples, the measurement techniques were not necessarily targeted for fire emissions, and not all of the data is complete in all sampling sites.

3.3 Chapter 3: METHODS

As part of the routine sampling of an ongoing study associated with the University of Southern California (USC) Children's Health Study (CHS), supported by the South Coast Air Quality Management District and the California Air Resources Board, concentrations of carbon monoxide (CO), ozone (O_3), nitrogen oxide (NO), nitrogen dioxide ($NO_{2,}$), particulate matter with aerodynamic diameters less than 10 μm (PM_{10}) and particle number (PN) are continuously measured in several locations in Southern California.

Continuous data were collected concurrently throughout the calendar year 2003, and five sites within the LA Basin impacted by the wildfires were examined in this study: Long Beach, Glendora, Mira Loma, Upland and Riverside (see Figure 3.1). The choice of these sampling sites was based on their location within the Los Angeles Basin, the availability of the data for the desired period, and the observed impacts of the Grand Prix, Old and Padua fires. Generally, these urban sites are the most polluted among the monitoring sites of the CHS.

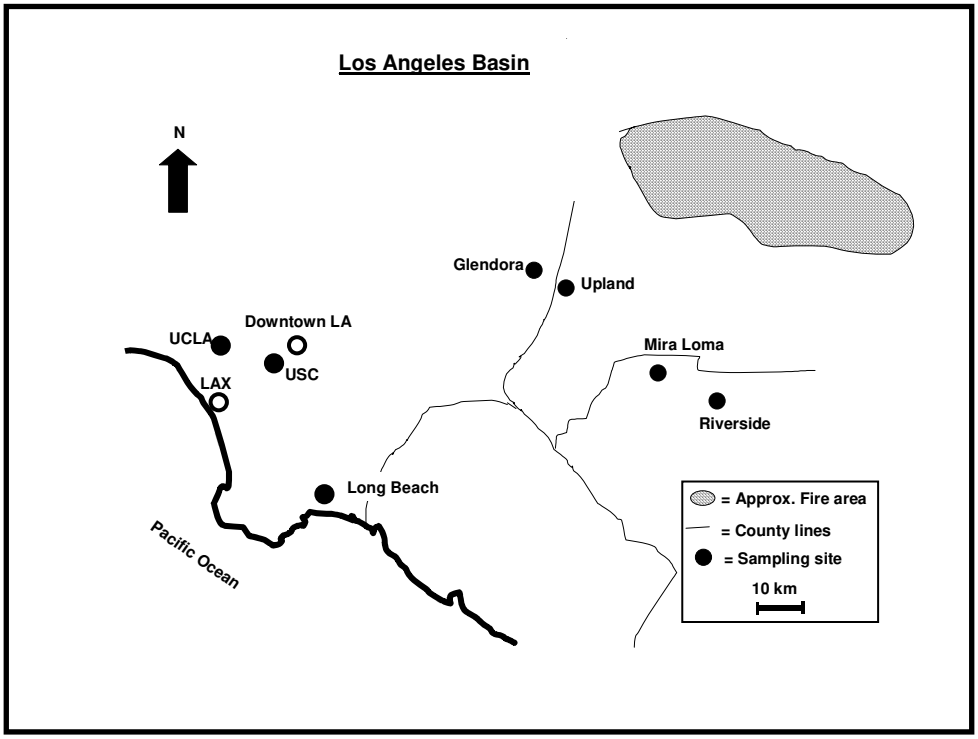

FIGURE 3.1: Map showing the fire area and the sampling sites in the Los Angeles basin.

Located near a busy surface street, the Long Beach station is about 1 km northeast of a major freeway. The Glendora station is located in a residential area nestled in the

foothills of the San Gabriel Mountains. It is at least 1 km away from major roadways and 3 km from the nearest freeway. The Upland site is also located in a residential area about 6 km downwind of the Glendora site, but is located within 1 km of the I-210 freeway. The Mira Loma site is located in a building on the Jurupa Valley High School campus. It is directly east of a major freeway interchange, is surrounded by several major warehouse facilities, and is located about 80 km east of downtown Los Angeles. The sampling location at Riverside is within the Citrus Research Center and Agricultural Experiment Station (CRCAES), a part of the University of California, Riverside. It is about 10 km southeast of the Mira Loma site and is situated upwind of surrounding freeways and major roads.

The concentrations of CO were measured near-continuously by means of a Thermo Environmental Inc. Model 48C trace level CO monitor. Concentrations of NO and NO_2 were measured with a Continuous Chemiluminescence Analyzer (Monitor Labs Model 8840), and O_3 concentrations were monitored using a UV photometer (Dasibi Model 1003 AH). Total particle number concentrations (greater than about 10 nm in diameter) were measured continuously by a Condensation Particle Counter (CPC, Model 3022/A, TSI Incorporated, St. Paul, MN) set at a flow rate of 1.5 L min^{-1}. At the Upland site, the CPC was connected to a Scanning Mobility Particle Sizer (SMPS, Model 3936, TSI Incorporated, St. Paul, MN), to measure the size distribution of submicrometer aerosols (15 - 750 nm) using an electrical mobility detection technique. In this configuration, the CPC flow rate was maintained at 0.3 L min^{-1} (with the sheath flow of the SMPS set at 3 L min^{-1}), and particle number counts were calculated from the SMPS size distributions.

Unfortunately, due to a brief power outage and limited site access resulting from the nearby fires, SMPS data was lost from the morning of 24 October to noon of the 29 October (the peak of the fire impact). However, the other monitors at this site continued to function properly in this time window. Continuous particle number and gaseous co-pollutant concentrations were averaged to form 1-hr and 24-hr average values for the subsequent analysis.

Hourly PM_{10} mass concentrations in each site were measured by a low temperature Differential Tapered Element Oscillating Microbalance monitor (low temperature TEOM 1400A, R&P Inc., Albany, NY). The design and performance evaluation of this monitor is described in greater detail by *Jaques et al.* [2004]. Briefly, the system consists of a size-selective PM_{10} inlet, followed by a Nafion® dryer that reduces the relative humidity of the sample aerosol to 50% or less. Downstream from the Nafion dryer and ahead of the TEOM sensor is an electrostatic precipitator (ESP) allowing for the removal of particles from the sample stream. The ESP is alternately switched on and off, for equal time periods of about 10 minutes. This dual sampling channel design makes it possible to account for effects such as volatilization of labile species, adsorption of organic vapors and changes in relative humidity and temperature, all of which affect the TEOM signal. The study by *Jaques et al.* [2004] showed that the time averaged TEOM PM_{10} mass concentrations agreed within ± 10% with those of collocated Federal Reference Methods (FRM).

In addition to the data collected at the CHS sites, semi-continuous $PM_{2.5}$ (fine) and ultrafine PM mass concentrations were measured at the Southern California Supersite located near downtown Los Angeles at the University of Southern California (USC). Two-hour PM mass concentration data was collected with a Beta Attenuation Monitor (BAM, Model 1020, Met One instruments, Inc., OR) (Chung et al., 2001). The BAM consisted of a size-selective inlet (2.5 μm for fine and 0.15 μm for ultrafine) (Chakrabarti et al., 2004), a filter tape, a beta radiation source, and a beta radiation detector. The difference in the transmission of beta radiation through the filter tape before and after a particulate sample has been collected, is measured and used to determine the mass of collected particulate matter. Continuous operation is achieved by automatic advancement of the filter tape between sampling periods.

Finally, in a concurrent but unrelated study, particle size distributions were measured indoors and outdoors of a two-bedroom apartment in the Westwood Village area near the University of California, Los Angeles. The residence is located about 100 m mostly downwind (east) of the I-405 freeway, a very busy traffic source. A Scanning Mobility Particle Sizer (SMPS 3936, TSI Inc., St. Paul., MN) was set up in a bedroom and sampled alternating indoor and outdoor size distributions on a 24-hr basis. The aerosol sampling flow rate of the SMPS was set to 1.5 L min^{-1} in order to measure particles as low as 6 nm as well as to minimize the diffusion losses of ultrafine particles during sampling. The maximum size detectable at these settings was 220 nm, and a scan time of 180 s was used. The sampling lines were kept the same length and as short as possible (1.5 m) for both indoor and outdoors samples. Measurements were made through a

switching manifold that alternately sampled indoor and outdoor air, each for 9-minute periods, in which three size distributions were taken in sequence. There were no known major indoor sources of aerosols in the residence for the period from 10 am to 7 pm, when the residents were at work and from 11 pm to 7 am when the residents were asleep in the other bedroom. The door of the sampling bedroom was always kept closed to minimize the influence of any other possible indoor activity. The residence was under natural ventilation with windows closed at all times during the sampling period. This study provided a unique opportunity to monitor infiltration of PM of outdoor origin into the indoor environment, and to estimate indoor exposures to PM from the wildfires.

3.4 Chapter 3: RESULTS AND DISCUSSION

Figures 3.2a-e present the 24-hour average concentrations of CO, NO, NO_2, O_3, PM_{10} and particle number (PN) before, during and after the October fire period in Southern California at the five CHS sampling sites examined in this study. A summary of the average concentrations of the pollutants before, during and after the fire is given in Table 3.1. As surmised from the news reports and the data, the period of fire influence was from the 23–29 October. Figure 3.2 clearly shows that the concentrations of all the pollutants drastically decreased on 30 October and then increased back to more typical levels by 4 or 5 November. The rapid decline is associated with the wind reversal on the afternoon of 29 October when an on-shore wind pattern replaced the Santa Ana conditions, followed by rainfall on 30 and 31 October. Figure 3.3a displays a satellite photo from NASA Earth Observatory on 28 October 2003 showing the extent of the fires and the prevailing wind direction during the peak of the fire episode. On 29 October, the

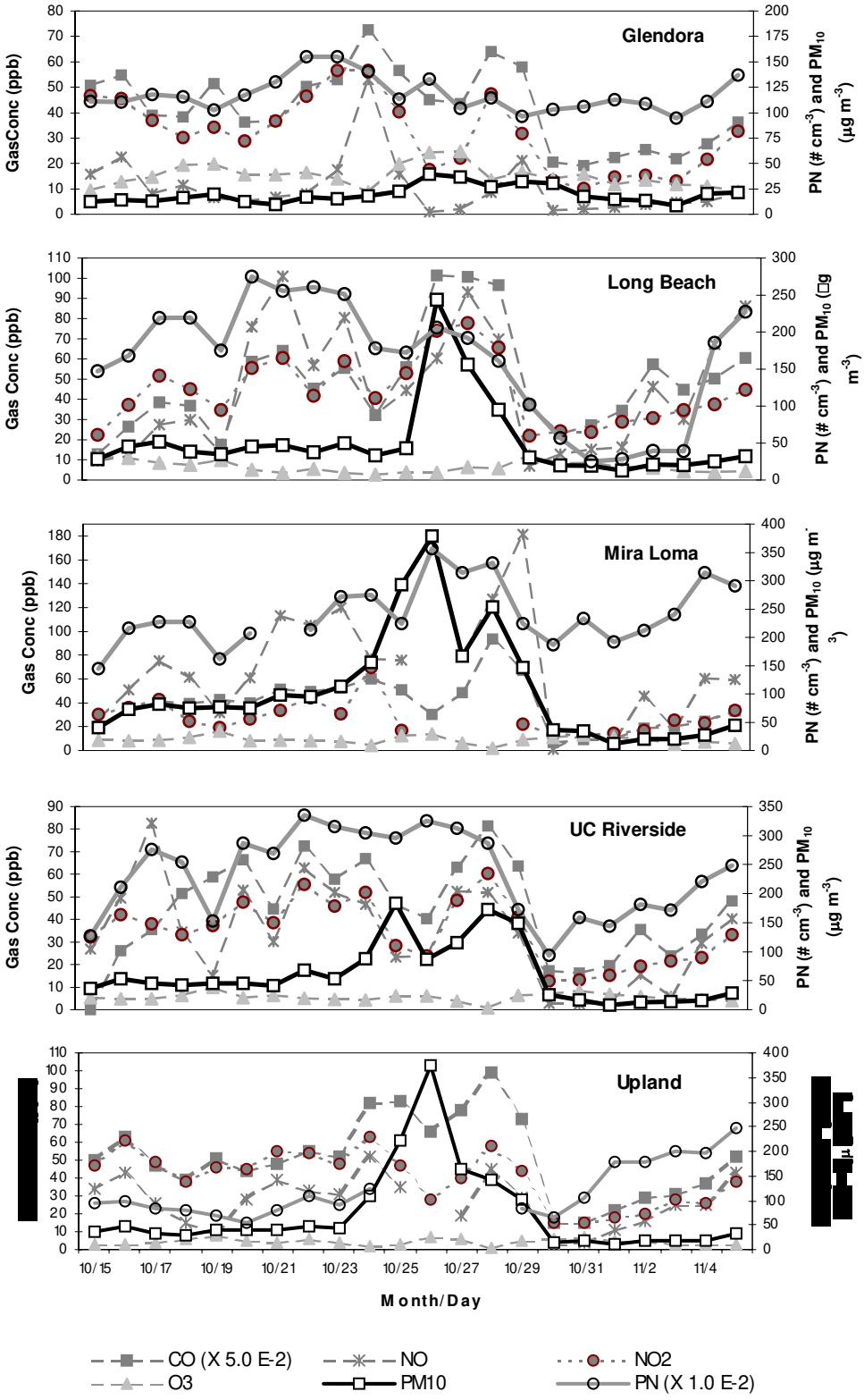

FIGURE 3.2: 24-hour averaged PM and gaseous pollutant concentrations during the study at a) Glendora, b) Long Beach, c) Mira Loma, d) UC Riverside and e) Upland

Figure3.3 a

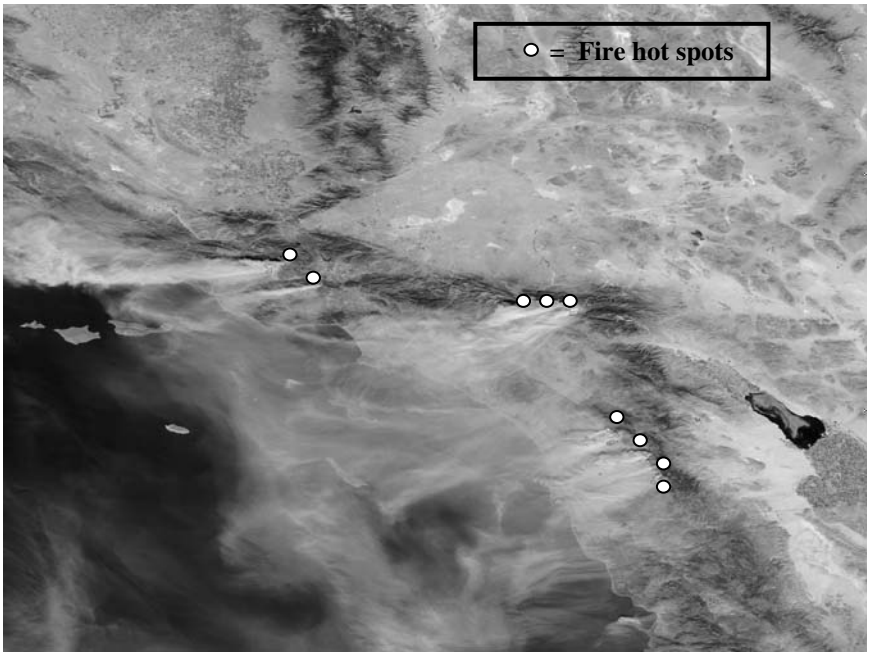

Figure 3.3 b

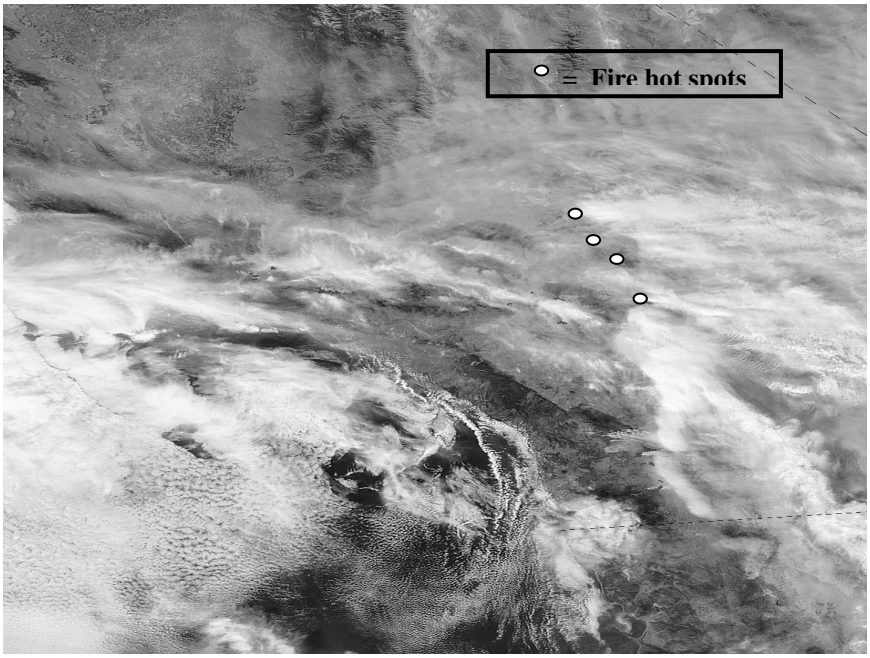

FIGURE 3.3: Satellite images from NASA earth observatory showing a) Southern California during the peak of the fire episode on October 28th, 2003, with the smoke plumes blowing west, and b) the same area after the wind reversal, on the afternoon of October 29th, 2003, with a visible marine layer and the smoke plumes blowing towards the east.

winds shifted to an on-shore pattern (Figure 3.3b) blowing fresh fire emissions towards the east away from the LA Basin. The fires continued to burn for many days after, but the cooler and wetter weather helped the firefighting effort and the fires were under control within another week.

TABLE 3.1: Average concentrations of pollutants with the standard deviation at the five CHS sites before, during and after the fire

	Average Concentration (± SD)					
	CO (ppm)	**NO (ppb)**	**NO_2 (ppb)**	**O_3 (ppb)**	**PM_{10} (μg m^{-3})**	**PN (particles cm^{-3})**
Pre Fire						
Glendora	9 ± 3	11 ± 16	37 ± 16	37 ± 21	12 ± 14	10400 ± 5500
Long Beach	6 ± 6	23 ± 49	47 ± 19	29 ± 18	33 ± 16	19300 ± 12400
Mira Loma	6 ± 4	45 ± 54	29 ± 14	25 ± 26	61 ± 35	16200 ± 8200
UC Riverside	8 ± 6	40 ± 29	33 ± 19	29 ± 29	47 ± 23	16200 ± 12100
Upland	10 ± 4	24 ± 28	44 ± 16	21 ± 23	39 ± 18	9000 ± 3700
During Fire						
Glendora	11 ± 5	**25 ± 30**	39 ± 28	44 ± 23	**27 ± 25**	12200 ± 6200
Long Beach	**14 ± 9**	**55 ± 68**	56 ± 24	**15 ± 16**	**93 ± 92**	18000 ± 8500
Mira Loma	**12 ± 8**	**105 ± 85**	39 ± 26	**17 ± 18**	**215 ± 171**	**28500± 14600**
UC Riverside	**12 ± 7**	**46 ± 36**	42 ± 22	**18 ± 21**	**121 ± 112**	**28800 ± 16100**
Upland	**15 ± 7**	**43 ± 34**	47 ± 24	**15 ± 16**	**165 ± 138**	Data not available
Post Fire						
Glendora	5 ± 2	5 ± 5	17 ± 11	31 ± 11	18 ± 29	11000 ± 6300
Long Beach	8 ± 6	39 ± 49	32 ± 11	16 ± 12	21 ± 10	8600 ± 9700
Mira Loma	4 ± 3	57 ± 45	20 ± 11	19 ± 15	28 ± 16	23900 ± 10700
UC Riverside	6 ± 4	14 ± 25	20 ± 10	23 ± 15	18 ± 10	17400± 11000
Upland	6 ± 4	21 ± 25	23 ± 12	17 ± 13	19 ± 10	16700 ± 8600

Data in bold indicate statistically significant difference between the pre- and during fire concentrations at p=0.05

The data summary in Table 3.1 indicates that with the exceptions of NO_2 and O_3, the concentrations of CO, NO, PM_{10} and PN during the fire event were significantly higher (at the p=0.05 level) than their respective values preceding the fire event. Statistical comparisons between during and post-fire concentrations was not conducted, because, as evident from the data in Table 3.1 and Figure 3.2, the unstable and wet weather

conditions during the week of 30 October to 5 November resulted in lower than average air pollutant concentrations. It is of particular note, however, that the most dramatic increase in the concentrations of any pollutant during the fire events was observed for the PM_{10} concentrations, which, with the exception of one site (Glendora), rose by almost three to four-fold in all sites during this period. While typical PM_{10} concentrations in Los Angeles are on the order of 50 $\mu g\ m^{-3}$ or less (Christoforou et al., 2000), levels rose to near or above 200 $\mu g\ m^{-3}$ at some sites during the fires. PM_{10} levels at Glendora did not rise to the same degree, possibly due to the site's location at the base of a canyon in the San Gabriel Mountains. The Santa Ana winds tend to blow down the mountain canyons, and there was little or no fire activity in or upwind of this particular canyon. Upland, on the other hand, was within 2-3 kilometers and directly downwind of extreme wildfire activity. The other three sites were all further downwind from the wildfires, but all sites experienced atypical PM_{10} levels. It is possible that the higher wind speeds during Santa Ana conditions increased re-suspended dust emissions that contributed to the elevated PM_{10} levels. This effect, if dominant, should be observed at all sites. However, the fact that Glendora PM_{10} levels remained within the "typical" range indicates that the impact of fire smoke plumes is the main cause of the elevated PM_{10} levels. Previously reported data during Santa Ana events without fires also demonstrate that such high levels of PM_{10} are not typically observed on a 24-hour basis (Geller et al., 2003, in press).

By contrast, the total particle number concentrations, also shown in Figure 3.2, did not exhibit the same extreme concentration increases during the fires. PN levels increased significantly only in Mira Loma and perhaps Riverside, and only by an approximate

factor of two. Even these higher levels of PN have been observed on occasion under typical, non-fire influenced, conditions in the LA Basin (Kim et al., 2002) No significant increase in PN was observed at Long Beach, and Glendora, the latter being minimally affected by the fires as discussed above. Due to the aforementioned power outage, PN data was not available at the closest site to the fires, Upland, during the wildfire period. Emissions testing of foliar fuels demonstrate that high particle number levels are emitted from these sources. However, given the observed high PM mass levels, and thus the increased PM surface area in the fire smoke plumes, it is conceivable that emitted smaller particles are scavenged by coagulation with larger particles in the smoke plume (Formenti et al., 2003). This process may occur over the few hours that it takes for the fire particles to reach our sampling sites. Many of the smaller particles, which make up the majority of particle number concentrations, may no longer exist as individual particles. Thus, PM mass levels remain high while PN levels are diminished. This hypothesis may explain why the largest PN increase was seen at Mira Loma and Riverside, both of which are much closer to the fire areas than the sites further downwind such as Long Beach.

Similar to particle number, CO concentrations at these sites were only modestly affected by the fires. With the exception of Glendora, the observed increases were statistically significant at the $p=0.05$ level, but the degree of increase was much less than that observed for PM_{10}. Mira Loma, Upland and Long Beach experienced CO around twice normal levels during the fire. As in the case of PN, CO concentrations in the area of Glendora appear to be unaffected by the fire events. The relatively low increase in CO

due to the fires can be explained by other, more significant sources of CO in Los Angeles. Emission factors from the USEPA and other studies (Barbosa et al., 1999; Pereira et al., 1999; Scholes et al., 1996) show that the ratio of CO mass to PM_{10} mass in wildfire emissions lies typically between 8-16. The same ratio for various motor vehicles under varying driving conditions is much higher, ranging from about 200 to over 2000 (Cadle et al., 2001; Chase et al., 2000). In urban areas dominated by vehicular sources, wildfires will thus affect ambient levels of CO to a lesser degree than the ambient levels of PM_{10}. A review of historical pollutant data during Santa Ana conditions without fire activity (9 February 2002 and 6 January 2003) shows that CO levels can diminish due to fewer CO sources upwind and increased basin ventilation. However, this effect is inconsistent, and varies greatly with sampling site and from event to event. Thus, no true "Santa Ana baseline" can be established for comparison purposes. For this reason, comparisons are limited to the "typical" conditions before the fire episode.

NO concentrations follow similar trends with those for CO and PN (i.e. they increase significantly in every location during the fire) but this increase is on the order of two-fold or less, hence smaller than the increase observed for PM_{10}. While the increase in NO concentrations during the fire event seems to be minor at the Riverside location, the nearby Mira Loma site shows more than double the NO levels relative to levels before the fire events. It is possible that Mira Loma may have been more directly downwind of fire areas than Riverside, which would explain this discrepancy. This is supported by the observed PM_{10} levels at these two sites, which also increased more dramatically in Mira Loma than in Riverside. Relative to NO, PN, and PM_{10}, the effect of fires was negligible

for NO_2 as the concentrations did not change significantly in any of the five sampling sites during the fire events. While some NO_2 is emitted directly from combustion processes, most of the NO_2 in urban air is formed in the atmosphere by the reaction of NO with ozone. Under normal conditions in Los Angeles, NO, and thus NO_2 levels are dominated by diesel vehicle emissions (Fujita et al., 2003). However, the NO increases observed during the fires were not accompanied by corresponding increases in NO_2 concentrations. Although no conclusive explanation can be determined from the current data, it is possible that the PM in the fire smoke blanketing the LA basin blocked incoming solar radiation and thus reduced photochemical activity in the atmosphere. This would result in lower ozone levels and thus, lower observed levels of NO_2. Increased concentrations of organic gases (VOCs) emitted by the fires may also play a role in the complex atmospheric chemistry of NO, NO_2, and ozone (Cheng et al., 1998). Interestingly, with the exception of Glendora, which experienced marginally (but not significant) increased O_3 concentrations during the fire episode; the concentrations of O_3 decreased by about 25-50% at all the other sites during the fire period. As mentioned above, the fire smoke covering the basin and the corresponding reduction in photochemical activity may be a possible explanation for this decrease in concentration.

The effect of the wind direction change can also be seen in the hourly concentrations of the measured pollutants in Upland as shown in Figures 3.4a and b. The high concentrations of PM_{10} at Upland can be clearly seen during the entire fire period, with the highest hourly concentration measured at 769 $\mu g\ m^{-3}$. On October 29th, at 12:00 P.M., the PM_{10} level was 153 $\mu g\ m^{-3}$ and within one hour it dropped to 65 $\mu g\ m^{-3}$. Within four

Figure 3.4 a

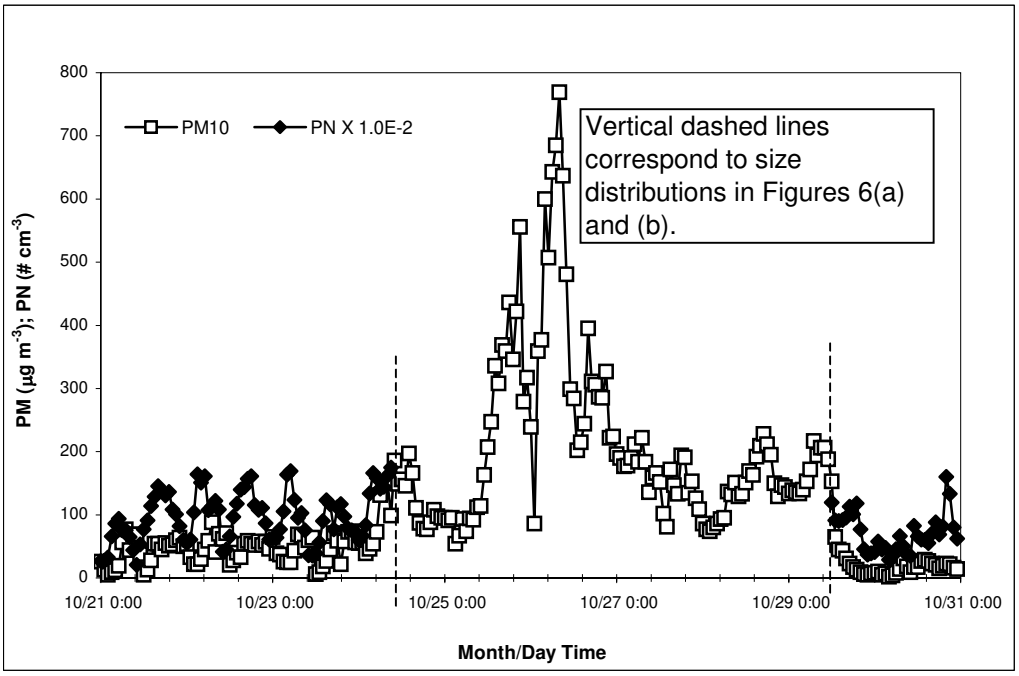

Figure 3.4 b

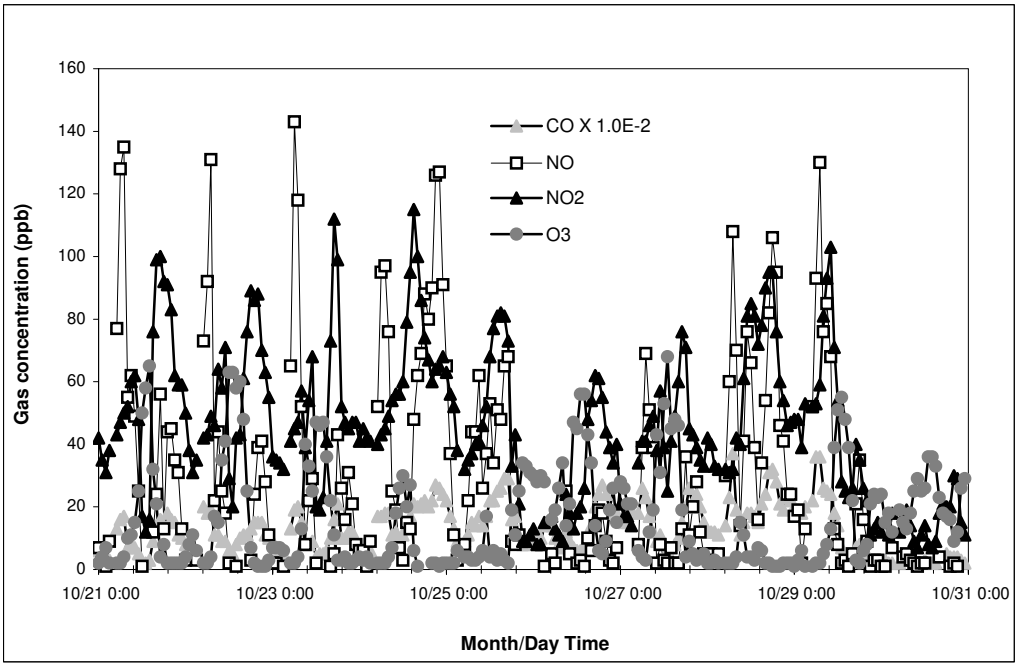

FIGURE 3.4: Hourly a) PM and b) gaseous pollutant concentrations at Upland

hours, PM_{10} concentrations dropped to below 20 μg m^{-3}. This marks the time of the wind reversal mentioned above. Unfortunately, hourly data of particle number concentrations in this time frame are not available due to the power outage. Similar to the 24-hr data, the hourly gaseous pollutant levels did not increase as much as the PM_{10} levels during the period of wildfire influence. However, with the exception of ozone, concentrations of all the gaseous pollutants dropped precipitously when the wind reversal occurred.

Semi-continuous ultrafine and fine ($PM_{2.5}$) particle mass concentration data support the argument that the atmospheric concentrations of smaller particles (measured above as PN), increased to a lesser extent than the larger particles. Figure 3.5 displays the 2-hour ultrafine and fine PM mass obtained from the BAM measurements at the USC site. The average ultrafine particle mass concentrations increased from an average value of 5.4 (±

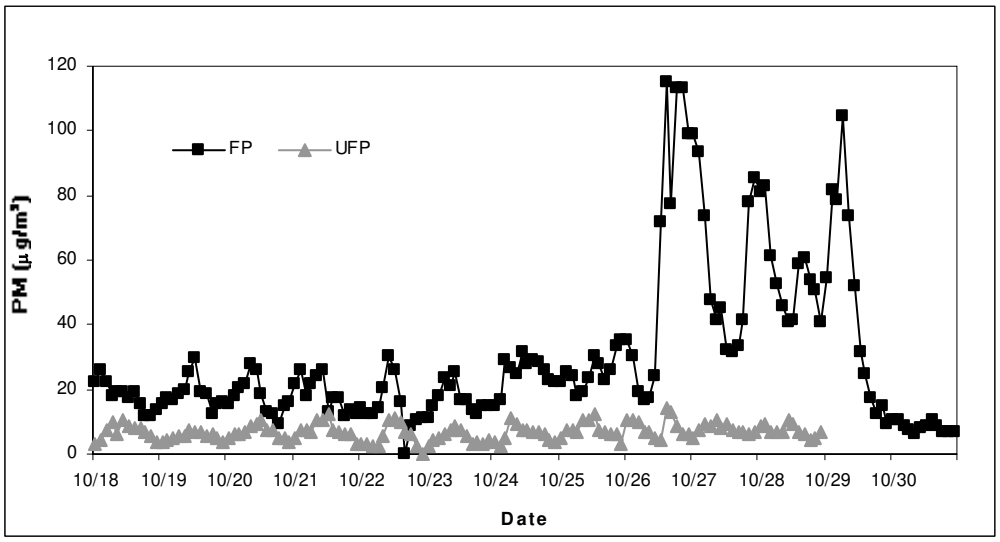

FIGURE 3.5 Two-hour averaged fine (FP) and ultrafine (UFP) particle mass concentrations at USC.

2.3) to 6.9 (± 2.7) μg m^{-3}. While this increase is statistically significant ($p<0.01$), it is still less dramatic than the obvious increase in $PM_{2.5}$ during the fire events. The average concentration of $PM_{2.5}$ more than doubled, from 19.1 (± 5.2) to 51.3 (± 26.1) μg m^{-3}.

The highest fine particle mass measured during the fire episode at USC was 115 μg m^{-3}. The wind reversal was marked by a steep reduction in fine particle mass midday on 29 October when the fine PM dropped from 105 μg m^{-3} in the morning to 25 μg m^{-3} by 2:00 P.M.

Figures 3.6a and b show the one-hour averaged particle size distribution at Upland corresponding to the times marked by vertical lines in Figure 3.4(a). Because of the loss of SMPS data for almost entire fire period, we have selected times just before (Figure 3.6a) and just after (Figure 3.6b) the power outage. The particle size distribution at a given hour (10 A.M and 12 P.M.) was averaged for different days before and after the fire, and compared to the same hour during the influence of the fires. It can be seen that the size distribution corresponding to the periods of fire influence significantly differs from those without the fire influence. The mode in the number-based particle size distribution spans from 100 to 300 nm and is indicative of the wildfire smoke.

Previous emissions testing have shown similarly large number modes in the particle size distributions from the burning of foliar fuels (Hays et al., 2002). Such large diameter number modes are not normally seen in urban locations (Kim et al. 2002) where particle

Figure 3.6 a

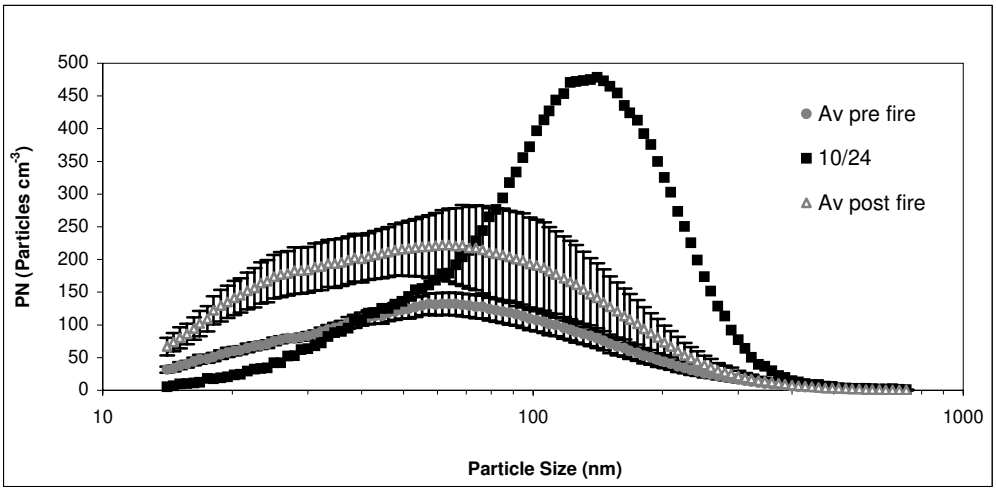

Figure 3.6 b

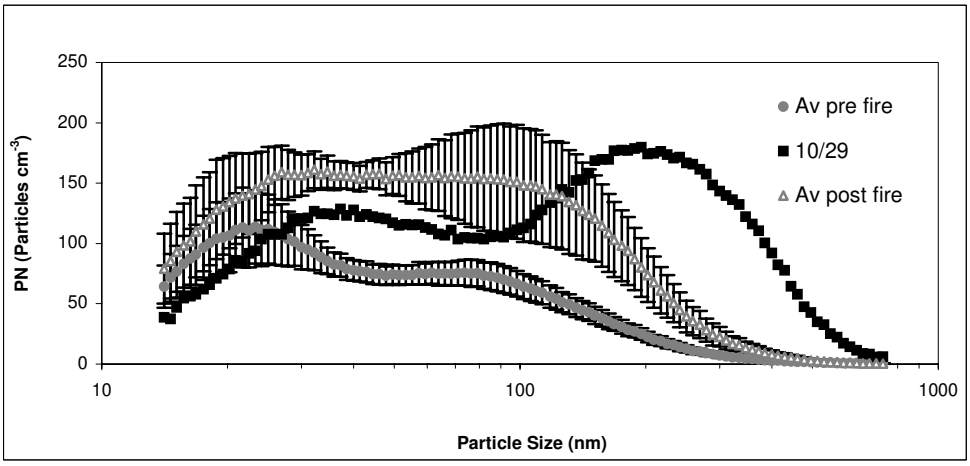

FIGURE 3.6: Particle size distributions at Upland a) at 10AM: before, 10/24/03, and after the fires; and b) at 12PM: before, 10/29/03, and after the fires.

number concentrations are dominated either by primary vehicular emissions or by nucleation processes (Woo et al., 2001). Since particle volume is proportional to the cube of the diameter, a modest increase in particle number concentrations in these larger size modes is sufficient to account for the larger increases observed for PM mass.

Indoor and outdoor particle number size distributions were also available from a concurrent study near UCLA in the western portion of the Los Angeles Basin. Figures 3.7a and b display ambient and corresponding indoor particle size distributions from 11 pm- midnight for different days during and after the fire events. This period was selected to minimize the influence of any possible indoor sources (i.e., cooking, cleaning) and outdoor traffic from the nearby freeway. The effect of the fires on indoor concentration is

Figure 3.7 a

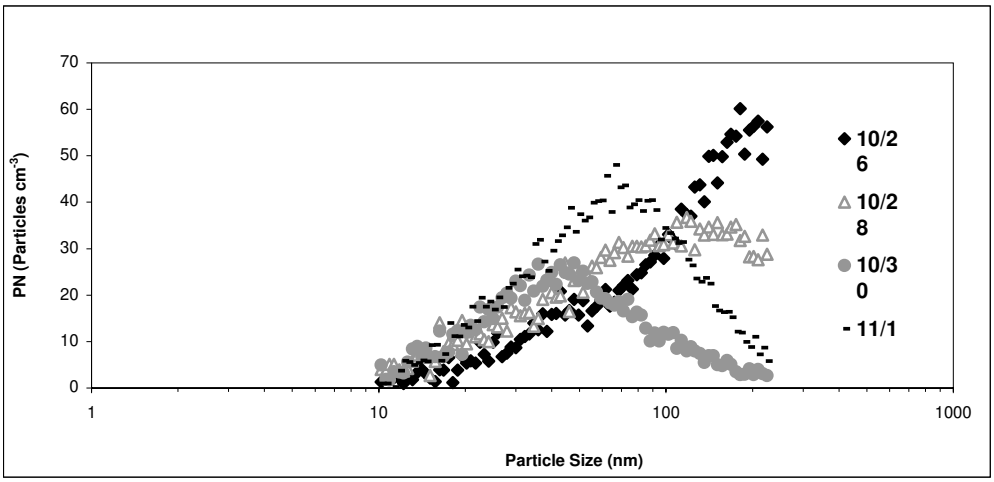

Figure 3.7 b

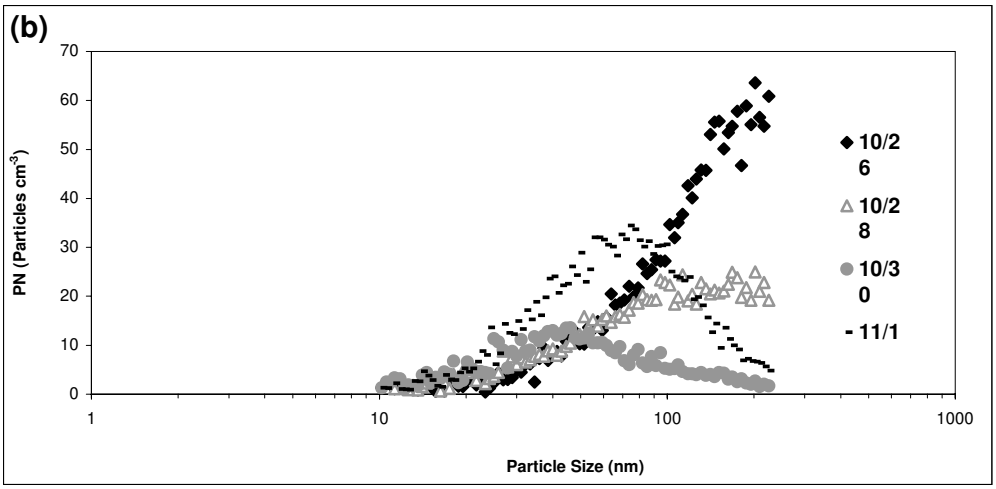

FIGURE 3.7: Particle size distributions on different days at 11PM in Westwood Village: a) Outdoor; and b) Indoor.

evident, with an aerosol mode diameter at about 200 nm on 26 and 28 October, and then a shift to a lower size range (between 50 to 70 nm) on 30 October and 1 November, respectively. Number concentrations both indoors and outdoors also decrease as we move away from the fire period. It is of interest to note that on 26 October (i.e., in the middle of the wildfire period), the indoor and outdoor size distributions are virtually identical in both number concentration and mode, which suggests that the majority of the outdoor aerosol infiltrated indoors with a penetration value close to 1. This is not a surprising result, considering that based on our measurements, the majority of the particles emitted from the fire are in the 100 – 300 nm range. This is also the range of maximum indoor penetration of outdoor aerosols and minimum indoor deposition rate (Allen et al., 2003; Long et al., 2001). As the mode in aerosol size distributions shifts to smaller sizes, the indoor concentrations are approximately 50 – 75% lower than outdoors, which is also consistent with the penetration values determined by Long et al., (2001) and Wallace and Howard-Reed, (2002) for the particles in the 40 – 80 nm range.

To put the above results in perspective, Figures 3.8a and b show the measured indoor and outdoor particle size distributions during the morning traffic commute period, from 6 A.M. to 7 A.M., while the wildfires were still active (27 October) and after the fire event (November 4). The outdoor size distribution on 27 October is characterized by one dominant mode at about 25 nm, which is associated with vehicular emissions (Zhu et al., 2002a; Zhu et al., 2002b), followed by a second mode at about 200 nm, which reflects the influence of the wildfires. The indoor size distribution for that date (Figure 3.8a) shows that the super-100 nm particles are virtually at identical concentrations with their

corresponding outdoor levels, whereas the concentrations of smaller particles indoors are substantially lower than those outdoors. Similar trends are also shown in Figure 8b, with the exception that the second mode in the 200 nm range observed during the fire period no longer exists in either the indoor or outdoor environment. The data plotted in Figures 3.8a and b indicates an average outdoor-to-indoor penetration ratio of about 0.15 to 0.20 for particles in the 20-50 nm range, which, as stated above, originate from nearby traffic

Figure 3.8 a

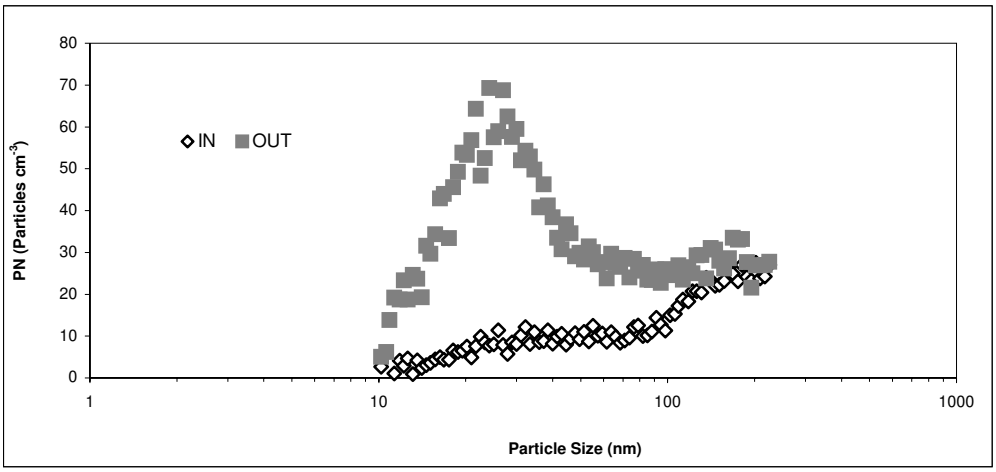

Figure 3.8 b

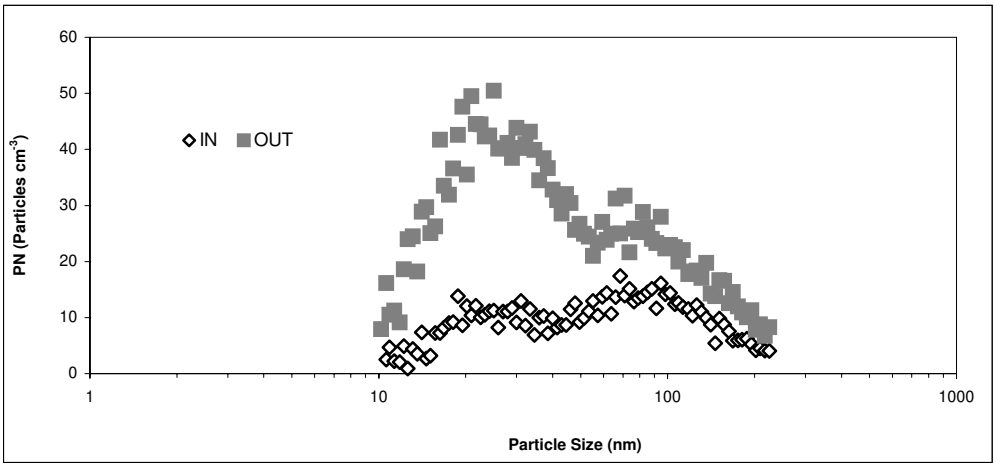

FIGURE 3.8: Indoor/Outdoor particle size distributions at 6AM in Westwood Village on a) 10/27/03; and b) 11/04/03

sources. This value is somewhat lower than the indoor penetration ratios reported by Long et al., (2001) and Wallace and Howard-Reed, (2002) for that size range, which normally range between 0.3 – 0.7, depending on home characteristics and air exchange rates. One possible explanation for the lower values observed in our study may be that, as shown in recent reports in the literature (Sakurai et al., 2003; Tobias et al., 2001), sub-50 nm particles from vehicular emissions consist of semi-volatile material, compared to the mostly non-volatile particles in the 50-100 nm range. Thus, after penetrating indoors, they may have completely evaporated or shrunk to sizes below about 6 nm, the lower size detection limit of the SMPS. It is unknown what source, size or composition of ambient PM is responsible for the observed health effects. But our results show that the prevailing advice during the fire episode for people to stay indoors may not be effective in reducing exposure to most of the particles emitted from wildfires.

3.5 Chapter3: SUMMARY AND CONCLUSIONS

Coincidental air pollution sampling campaigns proved valuable in determining the impacts of the October, 2003 wildfire episode on pollutant levels in the Los Angeles Basin. The greatest impact was observed on PM_{10} concentrations which increased by factors of three or four depending on location. CO and NO levels increased to a lesser extent (a factor of approximately two), most likely due to the different relative emission rates of these pollutants from wildfires compared to typical urban sources such as traffic. Particle number concentrations and NO_2 were essentially unchanged, except at the sites nearest the fires where PN levels almost doubled. Ozone levels during the fires were observed to be lower during the fires at some sites, a possible result of light scattering by

the smoke plume reducing photochemical activity levels. Particle number distributions downwind of the fires displayed number modes with diameters between 100 and 200 nm, larger than typical urban aerosol and explaining the larger increases in PM_{10} and $PM_{2.5}$ mass concentrations than that for ultrafine particle mass and particle number. These particles were also shown to penetrate effectively indoors, calling into question the prevailing advice to the public to remain inside to avoid exposure to harmful wildfire emissions.

3.6 Chapter 3: REFERENCES

Allen, R., T. Larson, L. Sheppard, L. Wallace, and L.J.S. Liu (**2003**), Use of real-time light scattering data to estimate the contribution of infiltrated and indoor-generated particles to indoor air, *Environmental Science & Technology*, *37* (16), 3484-3492.

Barbosa, P.M., D. Stroppiana, J.M. Gregoire, and J.M.C. Pereira (**1999**), An assessment of vegetation fire in Africa (1981-1991): Burned areas, burned biomass, and atmospheric emissions, *Global Biogeochemical Cycles*, *13* (4), 933-950.

Bravo, A.H., E.R. Sosa, A.P. Sanchez, P.M. Jaimes, and R.M.I. Saavedra (**2002**), Impact of wildfires on the air quality of Mexico City, 1992-1999, *Environmental Pollution*, *117* (2), 243-253.

Brunke, E.G., C. Labuschagne, and H.E. Scheel (**2001**), Trace gas variations at Cape Point, South Africa, during May 1997 following a regional biomass burning episode, *Atmospheric Environment*, *35* (4), 777-786.

Cadle, S.H., P. Mulawa, P. Groblicki, C. Laroo, R.A. Ragazzi, K. Nelson, G. Gallagher, and B. Zielinska (**2001**), In-use light-duty gasoline vehicle particulate matter emissions on three driving cycles, *Environmental Science & Technology*, *35* (1), 26-32.

Chakrabarti, B., M. Singh, and C. Sioutas (**2004**), Development of a continuous monitor for measuring the mass concentration of ultrafine PM, *Aerosol Science & Technology*, in press.

Chase, R.E., G.J. Duszkiewicz, T.E. Jensen, D. Lewis, E.J. Schlaps, A.T. Weibel, S. Cadle, and P. Mulawa (**2000**), Particle mass emission rates from current-technology, light-duty gasoline vehicles, *Journal of the Air & Waste Management Association*, *50* (6), 930-935.

Cheng, L., K.M. McDonald, R.P. Angle, and H.S. Sandhu (**1998**), Forest fire enhanced photochemical air pollution. A case study, *Atmospheric Environment*, *32* (4), 673-681.

Christoforou, C.S., L.G. Salmon, M.P. Hannigan, P.A. Solomon, and G.R. Cass (**2000**), Trends in fine particle concentration and chemical composition in Southern California, *Journal of the Air & Waste Management Association*, *50* (1), 43-53.

Chung, A., D. P. Y. Chang, M. J. Kleeman, K. D. Perry, T. A. Cahill, D. Dutcher, E. M. McDougall and K. Stroud (**2001**), Comparison of real time instruments used to monitor airborne particulate matter, *Journal of the Air & Waste Management Association*, *51* (1), 109-120.

Crutzen, P.J., and M.O. Andreae (**1990**), Biomass Burning in the Tropics - Impact on Atmospheric Chemistry and Biogeochemical Cycles, *Science*, *250* (4988), 1669-1678.

Crutzen, P.J., L.E. Heidt, J.P. Krasnec, W.H. Pollock, and W. Seiler (**1979**), Biomass Burning as a Source of Atmospheric Gases CO, H_2, N_2O, NO, CH_3Cl and COS, *Nature*, *282* (5736), 253-256.

Dennis, A., M. Fraser, S. Anderson, and D. Allen (**2002**), Air pollutant emissions associated with forest, grassland, and agricultural burning in Texas, *Atmospheric Environment*, *36* (23), 3779-3792.

Einfeld, W., D.E. Ward, and C.C. Hardy (**1991**), Effects of Fire Behaviour on Prescribed Fire Smoke Characteristics: A Case Study, *Global Biomass Burning: Atmospheric, Climatic, and Biospheric Implications*, edited by J. S. Levine, pp. 412-419, MIT Press, Cambridge, Mass.

Formenti, P., W. Elbert, W. Maenhaut, J. Haywood, S. Osborne, and M.O. Andreae (**2003**), Inorganic and carbonaceous aerosols during the Southern African Regional Science Initiative (SAFARI 2000) experiment: Chemical characteristics, physical properties, and emission data for smoke from African biomass burning, *Journal of Geophysical Research-Atmospheres*, *108* (D13), 8576.

Fujita, E.M., D.E. Campbell, B. Zielinska, J.C. Sagebiel, J.L. Bowen, W.S. Goliff, W.R. Stockwell, and D.R. Lawson (**2003**), Diurnal and weekday variations in the source contributions of ozone precursors in California's South Coast Air Basin, *Journal of the Air & Waste Management Association*, *53* (7), 844-863.

Geller M.D., P.M. Fine, and C. Sioutas (**2003**), The relationship between real-time and time-integrated coarse (2.5-10 mm) intermodal (1.0-2.5 mm) and fine particulate matter (<2.5 mm) in the Los Angeles basin, *Journal of the Air & Waste Management Association*, in press.

Goode, J.G., R.J. Yokelson, D.E. Ward, R.A. Susott, R.E. Babbitt, M.A. Davies, and W.M. Hao (**2000**), Measurements of excess O_3, CO_2, CO, CH_4, C_2H_4, C_2H_2, HCN, NO, NH_3, HCOOH, CH_3COOH, HCHO, and CH_3OH in 1997 Alaskan biomass burning plumes by airborne fourier transform infrared spectroscopy (AFTIR), *Journal of Geophysical Research-Atmospheres*, *105* (D17), 22147-22166.

Hays, M.D., C.D. Geron, K.J. Linna, N.D. Smith, and J.J. Schauer (**2002**), Speciation of gas-phase and fine particle emissions from burning of foliar fuels, *Environmental Science & Technology*, *36* (11), 2281-2295.

Jaques, P. A., J. L. Ambs, and C. Sioutas (**2004**), Field evaluation of the differential TEOM monitor for continuous $PM_{2.5}$ mass concentrations, *Aerosol Science & Technology*, in press.

Kim, S., S. Shen, C. Sioutas, Y.F. Zhu, and W.C. Hinds (**2002**), Size distribution and diurnal and seasonal trends of ultrafine particles in source and receptor sites of the Los Angeles basin, *Journal of the Air & Waste Management Association*, *52* (3), 297-307.

LeCanut, P., M.O. Andreae, G.W. Harris, F.G. Wienhold, and T. Zenker (**1996**), Airborne studies of emissions from savanna fires in southern Africa .1. Aerosol emissions measured with a laser optical particle counter, *Journal of Geophysical Research-Atmospheres*, *101* (D19), 23615-23630.

Lighty, J.S., M.V. John, and F.S. Adel (**2000**), Combustion aerosols: Factors governing their size and composition and implications to human health, *Journal of the Air & Waste Management Association*, *50*, 1565-1618.

Long, C.M., H.H. Suh, L. Kobzik, P.J. Catalano, Y.Y. Ning, and P. Koutrakis (**2001**), A pilot investigation of the relative toxicity of indoor and outdoor fine particles: In vitro effects of endotoxin and other particulate properties, *Environmental Health Perspectives*, *109* (10), 1019-1026.

Lu, R., and R.P. Turco (**1996**), Ozone distributions over the Los Angeles basin: Three-dimensional simulations with the SMOG model, *Atmospheric Environment*, *30* (24), 4155-4176.

Pereira, J.M.C., B.S. Pereira, P. Barbosa, D. Stroppiana, M.J.P. Vasconcelos, and J.M. Gregoire (**1999**), Satellite monitoring of fire in the EXPRESSO study area during the 1996 dry season experiment: Active fires, burnt area, and atmospheric emissions, *Journal of Geophysical Research-Atmospheres*, *104* (D23), 30701-30712.

Radke, L.F., D.A. Hegg, P.V. Hobbs, J.D. Nance, J.H. Lyons, K.K. Laursen, R.E. Weiss, P.J. Riggan, and D.E. Ward (**1991**), Particulate and Trace gas emissions from Large Biomass Fires in North America, *Global Biomass Burning: Atmospheric, Climatic, and Biospheric Implications*, edited by J. S Levine, pp. 209-224, MIT Press, Cambridge, Mass.

Sakurai, H., K. Park, P.H. McMurry, D.D. Zarling, D.B. Kittelson, and P.J. Ziemann (**2003**), Size-dependent mixing characteristics of volatile and nonvolatile components in diesel exhaust aerosols, *Environmental Science & Technology*, *37* (24), 5487-5495.

Scholes, R.J., D.E. Ward, and C.O. Justice (**1996**), Emissions of trace gases and aerosol particles due to vegetation burning in southern hemisphere Africa, *Journal of Geophysical Research-Atmospheres*, *101* (D19), 23677-23682.

Tobias, H.J., D.E. Beving, P.J. Ziemann, H. Sakurai, M. Zuk, P.H. McMurry, D. Zarling, R. Waytulonis, and D.B. Kittelson (**2001**), Chemical analysis of diesel engine nanoparticles using a nano-DMA/thermal desorption particle beam mass spectrometer, *Environmental Science & Technology*, *35* (11), 2233-2243.

Wallace, L., and C. Howard-Reed (**2002**), Continuous monitoring of ultrafine, fine, and coarse particles in a residence for 18 months in 1999-2000, *Journal of the Air & Waste Management Association*, *52* (7), 828-844.

Woo, K.S., D.R. Chen, D.Y.H. Pui, and P.H. McMurry (**2001**), Measurement of Atlanta aerosol size distributions: Observations of ultrafine particle events, *Aerosol Science and Technology*, *34* (1), 75-87.

Woods, D.C., R.L. Chaun, W.R. Cofer III, and J.S. Levine (**1991**), Aerosol Characterization in Smoke Plumes from a Wetland fire, *Global Biomass Burning: Atmospheric, Climatic, and Biospheric Implications*, *edited by J. S. Levine*, pp. 240-244, MIT Press, Cambridge, Mass.

Wotawa, G., and M. Trainer (**2000**), The influence of Canadian forest fires on pollutant concentrations in the United States, *Science*, *288* (5464), 324-328.

Zhu, Y.F., W.C. Hinds, S. Kim, S. Shen, and C. Sioutas (**2002a**), Study of ultrafine particles near a major highway with heavy-duty diesel traffic, *Atmospheric Environment*, *36* (27), 4323-4335.

Zhu, Y.F., W.C. Hinds, S. Kim, and C. Sioutas (**2002b**), Concentration and size distribution of ultrafine particles near a major highway, *Journal of the Air & Waste Management Association*, *52* (9), 1032-1042.

Chapter 4: Size-Resolved Emissions of Organic Tracers from Light- and Heavy-Duty Vehicles Measured in a California Roadway*

*Phuleria H.C.; Geller M.D.; Fine P.M. and Sioutas C. Size-resolved emissions of organic tracers from light- and heavy-duty vehicles measured in a California Roadway tunnel, *Environmental Science and Technology,* 40(13), 4109-4118, 2006

4.1 Chapter 4: ABSTRACT

Individual organic compounds found in particulate emissions from vehicles have proven useful in source apportionment of ambient particulate matter. Species of interest include the hopanes, originating in lube oil, and selected PAH generated via combustion. Most efforts to date have focused on emissions and apportionment PM_{10} or $PM_{2.5}$. However, examining how these compounds are segregated by particle size in both emissions and ambient samples will help efforts to apportion size-resolved PM, especially ultrafine particles which have been shown to be more potent toxicologically. To this end, high volume size-resolved (coarse, accumulation and ultrafine) PM samples were collected inside of the Caldecott tunnel in Orinda, CA to determine the relative emission factors for these compounds in different size ranges. Sampling occurred in two bores, one off-limits to heavy-duty diesel vehicles, which allows determination of the different emissions profiles for diesel and gasoline vehicles. Although tunnel measurements do not measure emissions over a full engine duty cycle, they do provide an average emissions profile over thousands of vehicles that can be considered characteristic of "freeway" emissions. Results include size-fractionated emission rates for hopanes, PAHs, elemental carbon, and other potential organic markers apportioned to diesel and gasoline vehicles. The results are compared to previously conducted $PM_{2.5}$ emissions testing using dynamometer facilities and other tunnel environments.

4.2 Chapter 4: INTRODUCTION

Motivated by the growing concern that human exposure to ultrafine particles poses a significant health hazard; characterization of particles emitted from gasoline and diesel engines has been the focus of many studies (Allaban et al., 2002; Geller et al., 2005; Lighty et al., 2000). Vehicular particulate emissions are of specific interest because of their ultrafine size and their potentially toxic components, such as polycyclic aromatic compounds (PAHs) and trace metallic elements. A number of health studies have demonstrated the adverse health effects of diesel exhaust particles (Mauderly, 1993; 1994; Weingartner et al., 1997).

The recent focus on the smaller vehicle-derived ultrafine particles has been due to their higher number and surface area relative to larger particles, their ability to penetrate cell membranes and to their increased toxicity on a per mass basis (Li et al., 2003; Xia et al., 2004). For example, Li et al. (2003) have shown that ultrafine particles (defined in this case as those having diameters less than about 180 nm) induce a higher degree of oxidative stress and cause more cell damage than an equivalent mass of fine particles (aerodynamic diameter <2.5 μm). Animal exposure studies have further corroborated increased adverse health outcomes from ultrafine airborne particles (Johnston et al., 2000; Kleinman et al., 2003; 2005; Oberdorster, 2001; Oberdorster et al., 2002).

Since ultrafine particle number and mass do not necessarily correlate with mass concentrations of larger particles (PM_{10} or $PM_{2.5}$) (Chakrabarti et al., 2004; Fine et al., 2004; Sardar et al., 2004), these more common measurements cannot be used for

information on ultrafine particle concentrations. Given the results of the recent health studies that may drive future regulatory strategies, it is essential that the sources of and the human exposure to vehicular ultrafine particle emissions are well understood (Janhall et al., 2004; Sioutas et al., 2005).

Several different approaches have been applied for examining vehicular emissions, including roadside measurements (Kuhn et al., 2005), on-road chase experiments (Canagaratna et al., 2004; Kittelson, 1998), laboratory dynamometer studies (Gross et al., 2005; Rogge et al., 1993; Schauer et al., 1999; 2002; Zielinska et al., 2004), and measurements inside of roadway tunnels (Geller et al., 2005; Allen et al., 2001; Chellam et al., 2005; Fraser et al., 1998; Kirchstetter et al., 1999; Marr et al., 1999; Miguel et al., 1998). Dynamometer and chase experiments are useful due to the ability of carefully control testing conditions. Emissions control technologies can be evaluated, and emissions differences over different driving conditions and cycles, including cold-start (Schauer et al., 2003), can be examined. However, the high cost and complexity of such tests limit the number of vehicles which can be assessed, and thus may not provide a good representation of the vehicle fleet composition on the road. Moreover, changing the dilution conditions in dynamometer testing is known to affect the measurements, especially for ultrafine particles (Mathis et al., 2004). Such studies may not account for particle aging effects, the mixing of emissions from different vehicles (Weingartner et al., 1997), and non-tailpipe emissions from tire wear, break wears, and re-suspended road dust (Allen et al., 2001).

An alternative to single vehicle emission measurements are roadway tunnel studies measuring the emissions from a large population of the on-road vehicle fleet mix under real-world, although very specific, driving conditions. Although the dilution, temperature, humidity and sunlight conditions inside a tunnel may differ from conditions outside tunnels, they more closely approximate real-world conditions than dynamometer tests. Roadside measurements will sample under actual ambient conditions, but are subject to wind and other environmental processes, which might vary the emissions and background conditions (Gross et al., 2005). Since air is directly sampled from inside the tunnel bore, very high concentrations are encountered and thus, practically all measurements can be attributed to vehicles (Kean et al., 2003). In tunnels with multiple bores that have traffic restrictions based on vehicle size, such as the Caldecott tunnel in California (Geller et al., 2005; Marr et al., 1999; Miguel et al., 1998), apportionment of emissions to vehicle or fuel type can be achieved (i.e. most heavy-duty vehicles (HDV) consume diesel fuel, while most passenger cars and other light-duty vehicles (LDV) are powered by gasoline) (Gross et al., 2005). The main limitation of tunnel measurements is that they measure emissions over the very specific driving conditions of the particular tunnel, missing cold-start and some transient effects. However, a highway tunnel can provide detailed emissions characterization under typical highway driving conditions, resulting in a real-world average highway source signature. The derived vehicular PM emission factors are important to assessing effects on human exposure and health (Dockery et al., 1993; Mazzoleni et al., 2004).

Several studies have measured individual organic compounds in atmospheric particulate matter (PM) samples. Using gas chromatography/mass spectrometry methods, hundreds of particle-phase individual compounds have been identified and quantified in ambient air (Fine et al., 2004; Fraser et al., 2003; Schauer et al., 1996; Schauer and Cass, 2000; Simoneit, 2002; Zheng et al., 2002). Usually, only between 10 and 20% of the total particulate organic compound mass can be quantified as individual organic species, but many of these compounds have been used to trace primary particle emissions via source apportionment techniques (Schauer et al., 1996; Schauer and Cass, 2000; Zheng et al., 2002). Accurate and up-to-date source profiles are essential for the successful application of these methods. Specific organic tracers of primary vehicular particle sources include hopanes and steranes. These species are found in the lubricating oils used by both gasoline and diesel powered motor vehicles and are thus found in the particulate emissions from both types of vehicles (Rogge et al., 1993; Schauer et al., 1996; Cass, 1998). High molecular weight PAHs have also been used as additional tracers for motor vehicle exhaust, although there are other combustion sources of PAH as well including wood combustion (Rogge et al., 1993; Cass, 1998; Fine et al., 2001). Miguel et al. (1998) reported that LDVs are a significant source of the higher molecular weight PAHs such as Benzo(ghi)perylene, while HDVs predominantly emit the lighter PAHs, such as fluoranthene and pyrene. Furthermore, diesel engines are known to have significantly higher elemental carbon (EC) emissions than gasoline-powered vehicles (Schauer et al., 1999; 1996; Schauer, 2003). It may be possible, therefore, that information on emissions of high and low molecular weight PAHs, hopanes, steranes, and EC from motor vehicles can be used to distinguish HDV and LDV contributions to ambient samples in chemical

mass balance source apportionment calculations (Fraser et al., 2003; McGaughey et al., 2004). Another potential vehicular marker is the so-called unresolved complex mixture (UCM) of hydrocarbons, which appears as an unresolved hump underlying identifiable compound peaks in typical GC/MS traces (Hays et al., 2004; Simoneit, 1984). The ion spectra of the UCM look very similar to that of typical motor oil (Schauer et al., 1999). To the extent that vehicle derived UCM can be accurately quantified in emission and ambient samples, it may serve as an additional indicator of vehicular particulate emissions.

A few previous studies have measured size-fractionated PAH, oxy-PAH, and organonitrates over 5-24 hour periods (Allen et al., 1996; 1997; 1998; Garnes et al., 2002). However, most ambient and emissions samples intended for organic speciation are not size-resolved, due to limitations in collecting sufficient particle mass for trace species analysis. A high-volume slit impactor developed by Misra et al. (2002) allows for separation of particles based on aerodynamic diameter with a cut-point of 0.18 μm and a flow rate of 450 lpm. The impactor, with a high volume after-filter, has been successfully deployed to collect separate ultrafine (<0.18 μm) and accumulation mode (0.18 – 2.5 μm) ambient samples in Los Angeles (Fine et al., 2004).

The current study was conducted within two bores of the Caldecott tunnel in Orinda, CA during August and September of 2004. The high-volume slit impactor was deployed to collect size-resolved PM (ultrafine and accumulation mode) for speciated organic analysis of vehicular emissions by GC/MS. The emissions characterization for bulk

species such as mass, elemental carbon (EC), organic carbon (OC) and trace elements, from this campaign has been reported previously (Geller et al., 2005). This work provides additional detailed information on organic tracers of real-world vehicular sources found in the two different PM size ranges. The first reported size-segregated emission factors for organic tracers, other than PAH, are calculated for both light-duty vehicles (LDV) and heavy-duty vehicles (HDV). Emission factor results for $PM_{2.5}$ are compared to previous tunnel and dynamometer studies. Combined with other source profiles, including that of vehicular cold-start emissions, the results of this study can be used in future chemical mass balance calculations to assess the relative contribution of PM sources to ambient samples.

4.3 Chapter 4: METHODS

4.3.1 Tunnel sampling

A detailed description of the tunnel environment, traffic characteristics and sampling procedure is described by Geller et al. (2005). Briefly, the 1.1-kilometer long Caldecott Tunnel in Orinda, CA includes three two-lane bores with a 4.2% incline from west to east (Geller et al., 2005; Allen et al., 2001; Kirchstetter et al., 1999a; 1999b). Bores 1 and 3 allow both light-duty vehicles (LDV) and heavy-duty vehicles (HDV), while bore 2 is restricted to LDV traffic only. Traffic flows from west-to-east in Bore 1, east-to-west in Bore 3, and the direction of traffic switches from westward in the morning to eastward in the afternoon and evening in Bore 2. Field sampling was conducted in the afternoon in Bores 1 and 2 for four days each. The sampling period occurred from approximately 12

PM to 6PM, when all traffic in the two bores traveled eastward, during August and September of 2004.

4.3.2 Traffic characterization

The traffic volume and vehicle characteristics in the tunnel during the sampling campaign are also described by Geller et al. (2005). Vehicle counts broken down by axle class are reported in Table 4.1. Although Bore 2 is legally restricted to light-duty traffic, some medium-duty diesels and an occasional heavy-duty three-axle vehicle passed through. The method for attributing 2-axle/6-tire vehicles to gasoline and diesel fuel is given in Geller et al. (2005). As a percentage of the total vehicles counts, diesel vehicles are an order of magnitude less prevalent in Bore 2 than in Bore 1. During the sampling campaign, heavy-duty vehicles comprised an average of 3.8% of the total vehicles in bore 1 and less than 0.4% of vehicles in bore 2.

TABLE 4.1. Traffic volume in the Caldecott tunnel

Bore	Date	Axle Class			% HD Diesel
		3+ axles	2-axle, 6 tire	2-axle, 4 tire	
2	8/23/2004	1	29	4041	0.38
	8/24/2004	3	38	4113	0.54
	8/25/2004	0	20	3982	0.25
	8/26/2004	0	28	4028	0.34
1	8/30/2004	49	102	3013	3.2
	8/31/2004	76	109	2482	4.9
	9/1/2004	65	88	2951	3.5
	9/2/2004	66	66	2741	3.4

4.3.3 Pollutant measurement and sample collection

Both gaseous and particulate pollutant concentrations in the tunnel bores were measured with various continuous and time-integrated instruments, approximately 50 m from the tunnel exit. Pollutant levels at the entrance were measured with an identical set of instrumentation located 50 m from the tunnel entrance. Since this location was also inside the tunnel, it is not a pure ambient background sample, considering that it includes roadway emissions from the first 50 m of the tunnel. Emission factors are calculated based on the difference in concentrations between exit and entrance samples over a known, fixed distance of roadway between sampling locations.

The primary sampling apparatus used for PM collection was a custom built, high-volume (450 lpm) sampler designed to separate and collect coarse ($Dp > 2.5$ μm), accumulation ($0.18 < Dp < 2.5$ μm) and ultrafine mode ($Dp < 0.18$ μm) aerosols. This sampler is described in greater detail by Misra et al. (2002). It allows collection of particles with aerodynamic diameters greater than about 180 nm onto quartz-fiber impaction strips. A preceding impaction stage with a 2.5 μm aerodynamic diameter collects coarse particles. Due to low concentrations of organic tracers in the coarse mode, no coarse data is presented here. Downstream of the ultrafine impactor, a commercially available 8 x 10 inch high-volume filter holder contains a Quartz-fiber filter (Pallflex® Tissuquartz™ 2500QAT-UP-8x10, Pall Corp.) to collect the ultrafine PM fraction. Field blanks for quartz filters contained negligible levels of the compounds quantified in this study. Quartz filters and substrates were pre-baked at 550°C for 12 hours and stored in baked aluminum foil prior to deployment (Geller at al., 2005; Fine et al., 2004).

4.3.4 Organic Speciation Analysis

Methods for the quantification of individual organic compounds in ambient particulate matter were based on the procedures initially developed by Mazurek et al. (1987) and advanced further by others (Fine et al., 2004; Schauer et al., 1999; 2002; Sheesley et al., 2003). The quartz filter samples from the high-volume sampler were cut into smaller portions and combined in an annealed glass jar with a Teflon-lined lid. Samples were then spiked with known amounts of isotope labeled internal standard compounds, including three deuterated PAH, two deuterated alkanoic acids, deuterated cholestane, deuterated cholesterol, and C^{13} labeled levoglucosan. Solvent extraction of all samples was performed with three successive 10-minute mild sonications in 50 mL of a 9:1 mixture of HPLC-grade dichloromethane and methanol. The 50 mL extracts from each sonication step were then combined and reduced in volume to approximately 10 mL by rotary evaporation at 35 ^{0}C under a slight vacuum. The remaining volume was filtered through a baked quartz-fiber filter in a filtration assembly consisting of only stainless steel and Teflon components. The samples were then reduced to approximately 1 mL under pure nitrogen evaporation before the samples were split into two separate fractions. One fraction was derivatized for organic acid analysis, the results of which are not presented here. The other fraction was further reduced to a specified volume ranging from 50 to 200 μL by evaporation under pure nitrogen. The final target volume was determined based on the amount of organic carbon mass in each sample (Fine et al., 2004; Fraser et al., 2003).

The underivatized samples were analyzed by auto-injection into a GC/MSD system (GC model 5890, MSD model 5973, Agilent). A 30 m x 0.25 mm DB-5MS capillary column (Agilent) was used with a 1 μL splitless injection. Along with the samples, a set of authentic quantification standard solutions were also injected and used to determine response factors for the compounds of interest. Overall, 100 compounds are included in this set of standard mixtures in known concentrations, including known amounts of the same isotope labeled compounds used to spike the samples. Each standard compound is assigned a response factor relative to one of the internal standards with a similar retention time and structure. Between one and three of the most prevalent ions in the spectrum for each compound were selected for peak integration. These response factors were then applied to the compounds identified in the sample extracts relative to the internal spike compounds. While some compounds are quantified based on the response of that compound in the standard mixtures, others for which matching standards were not available, are quantified using the response factors of compounds with similar structures and retention times. UCM quantification was based on the total ion current (TIC) response of standard alkanes with similar retention times. Analytical errors for these methods have been reported to be no more than 25% (Fine et al., 2004; Zheng et al., 2002; Sheesley et al., 2003).

4.3.5 Emission factors

Fuel-based emission factors relating total carbon emissions in the tunnel (primarily in the form of CO_2) to the carbon content of fuel are computed as described in detail by Kirchstetter et al. (1999a) and were applied in the previous paper from this sampling

campaign (Geller et al., 2005). Briefly, pollutant concentrations are expressed as mass emitted per unit mass of fuel burned by the following equation:

$$E_p = 10^3 \left(\frac{\Delta[P]}{\Delta[CO_2] + \Delta[CO]} \right) w_c \qquad \ldots(4.1)$$

where E_p is the emission factor (g emitted per kg fuel burned) for pollutant P, Δ[P] is the increase in the concentration of pollutant P ($\mu g/m^3$) above the tunnel entrance location, $\Delta[CO_2]$ and Δ[CO] are the increases in the concentrations of CO_2 and CO (μg of Carbon/m^3) above the tunnel entrance, and w_c is the weight fraction of carbon in the fuel (Geller et al., 2005; Kirchstetter et al.,1999a).

In order to derive HDV and LDV specific emission factors, Δ[P], $\Delta[CO_2]$, and Δ[CO] must be apportioned between HDV and LDV contributions. Ignoring the very low numbers of diesel vehicles in bore 2, $\Delta[P]_{LDV}$, $\Delta[CO_2]_{LDV}$, and $\Delta[CO]_{LDV}$ are assumed to be equal to the measured concentrations in bore 2. $\Delta[CO_2]_{HDV}$ is calculated based on fuel consumption rates, fuel densities, vehicle counts and w_c as described in Kirchstetter et al. (1999a). The calculation to determine the pollutants emitted by HDV essentially reduces to the following equation

$$\Delta[P]_{HDV} = \Delta[P]_{bore\ 1} - X\ \Delta[P]_{bore\ 2} \qquad \ldots(4.2)$$

which subtracts the LDV emissions as determined in bore 2 from those in bore 1. In the Kirchstetter et al. (1999a) method, which was applied here, the factor X is based on measured CO levels and vehicles counts, resulting in a value of 0.86 in our study.

Based on the above calculations, the main source of error for the HDV apportionment is the value of X and the uncertainty in the measured levels of species for which LDVs emit more than HDVs (when $\Delta[P]_{bore\ 1} \sim X\ \Delta[P]_{bore\ 2}$). The main source of error in LDV emissions estimates derives from the few diesel vehicles that passed through bore 2. Since the presence of diesel vehicles in bore 2 does not significantly affect the HDV emissions estimates (<10%), the calculated HDV emissions factors can be used to assess the impact of Bore 2 diesel vehicles on calculated LDV emission factors.

4.4 Chapter 4: RESULTS AND DISCUSSION

4.4.1 Tunnel concentrations

Table 4.2a and 4.2b presents the average mass concentrations and standard deviations of the measured species in Bore 2 and Bore 1 respectively at both the ends in the tunnel in the ultrafine and accumulation size modes. The measured concentrations of each organic species were found to be higher at the east end than the west end, confirming significant contributions from the vehicles in the tunnel. Most of the organic species were measured to be an order of magnitude higher in ultrafine mode than the accumulation mode; an expected result given the smaller sized primary particles emitted by vehicles. However, tunnel concentrations of particulate mass were about equivalent or at least of the same order of magnitude in both the size fractions. Tables 4.2a and 4.2b also indicate that Bore 1 concentrations of the organic species are significantly greater than the respective Bore 2 concentrations, showing the relatively higher contribution of HDVs in Bore 1 to emissions of these species.

TABLE 4.2a. Mean mass concentration in Bore 2 (in ng/m^3)

Species measured	Accumulation mode				Ultrafine mode			
	East		West		East		West	
	Mean	SD	Mean	SD	Mean	SD	Mean	SD
PM Mass*	16.970	2.241	7.743	1.829	8.633	0.965	2.573	0.626
EC*	0.688	0.337	0.095	0.089	8.147	0.609	2.049	0.528
Fluoranthene	0.115	0.033	0.032	0.008	0.763	0.120	0.220	0.048
Acephenanthrylene	0.014	0.003	0.003	0.001	0.118	0.009	0.021	0.006
Pyrene	0.168	0.051	0.043	0.009	1.157	0.201	0.333	0.079
Methyl substituted MW 202 PAH	0.128	0.113	0.029	0.025	1.132	0.705	0.279	0.254
Benzo(ghi)fluoranthene	0.121	0.040	0.021	0.014	1.042	0.241	0.236	0.105
Benz(a)anthracene	0.120	0.033	0.021	0.006	1.112	0.208	0.178	0.078
Chrysene/Triphenylene	0.142	0.047	0.029	0.008	1.243	0.283	0.236	0.098
Methyl substituted MW 228 PAH	0.075	0.064	0.018	0.014	0.820	0.305	0.117	0.106
Benzo(k)fluoranthene	0.097	0.019	0.014	0.003	0.987	0.347	0.133	0.038
Benzo(b)fluoranthene	0.128	0.035	0.023	0.005	1.259	0.357	0.180	0.055
Benzo(j)fluoranthene	0.016	0.002	0.002	0.001	0.243	0.079	0.017	0.006
Benzo(e)pyrene	0.114	0.026	0.019	0.003	1.176	0.362	0.170	0.056
Benzo(a)pyrene	0.089	0.011	0.012	0.003	1.281	0.370	0.125	0.028
Perylene	0.015	0.008	0.000	0.001	0.180	0.055	0.012	0.009
Indeno(cd)pyrene	0.077	0.020	0.013	0.004	0.978	0.320	0.115	0.031
Benzo(ghi)perylene	0.186	0.052	0.032	0.008	2.524	0.692	0.333	0.096
Indeno(cd)fluoranthene	0.023	0.007	0.004	0.001	0.324	0.111	0.037	0.012
Dibenz[a,h]anthracene	0.011	0.003	0.001	0.001	0.079	0.018	0.013	0.003
Coronene	0.070	0.024	0.015	0.004	1.337	0.227	0.127	0.042
22,29,30-trisnorhopane	0.072	0.040	0.020	0.001	0.487	0.108	0.131	0.042
22,29,30-trisnorneohopane	0.065	0.028	0.021	0.003	0.435	0.164	0.123	0.036

TABLE 4.2a Continued…

Species measured	Accumulation mode				Ultrafine mode			
	East		West		East		West	
	Mean	SD	Mean	SD	Mean	SD	Mean	SD
17a(H)-21b(H)-29-norhopane	0.163	0.091	0.049	0.004	1.141	0.294	0.259	0.067
18a(H)-29-norneohopane	0.037	0.019	0.010	0.007	0.252	0.052	0.059	0.014
17a(H)-21b(H)-hopane	0.147	0.068	0.045	0.013	1.112	0.270	0.257	0.054
17b(H),21a(H)-moretane	0.010	0.004	0.001	0.002	0.087	0.014	0.019	0.003
22S, 17a(H),21b(H)-homohopane	0.065	0.039	0.020	0.003	0.411	0.124	0.095	0.023
22R, 17a(H),21b(H)-homohopane	0.055	0.038	0.020	0.003	0.331	0.077	0.074	0.022
22S, 17a(H),21b(H)-bishomohopane	0.040	0.020	0.013	0.005	0.206	0.070	0.066	0.008
22R, 17a(H),21b(H)-bishomohopane	0.031	0.017	0.008	0.003	0.163	0.040	0.041	0.009
22S, 17a(H),21b(H)-trishomohopane	0.027	0.021	0.007	0.005	0.142	0.021	0.035	0.007
22R, 17a(H),21b(H)-trishomohopane	0.016	0.007	0.005	0.003	0.087	0.022	0.027	0.005
20R+S, abb-cholestane	0.013	0.005	0.012	0.002	0.085	0.016	0.031	0.012
20R, aaa-cholestane	0.073	0.036	0.026	0.005	0.450	0.103	0.148	0.056
20R+S, abb-ergostane	0.026	0.007	0.006	0.008	0.148	0.048	0.045	0.014
20R+S, abb-sitostane	0.107	0.054	0.029	0.019	0.619	0.163	0.146	0.045
UCM	793.386	452.601	217.609	18.094	4426.087	1169.775	1038.072	365.281

* expressed in $\mu g/m^3$

TABLE 4.2b. Mean mass concentration in Bore 1 (in ng/m^3)

Species measured	Accumulation mode				Ultrafine mode			
	East		West		East		West	
	Mean	SD	Mean	SD	Mean	SD	Mean	SD
PM Mass*	28.690	4.469	16.510	2.607	28.860	5.868	4.328	2.041
EC*	2.370	1.742	0.134	0.129	27.346	4.503	1.865	0.532
Fluoranthene	0.851	0.159	0.033	0.006	4.644	1.191	0.269	0.068
Acephenanthrylene	0.155	0.042	0.003	0.001	0.990	0.239	0.025	0.008
Pyrene	1.379	0.246	0.040	0.006	8.076	2.119	0.344	0.086
Methyl substituted MW 202 PAH	1.140	0.179	0.050	0.007	9.172	2.175	0.495	0.095
Benzo(ghi)fluoranthene	0.498	0.021	0.027	0.002	4.054	0.410	0.297	0.065
Benz(a)anthracene	0.352	0.017	0.018	0.002	3.223	0.494	0.181	0.032
Chrysene/Triphenylene	0.379	0.020	0.032	0.004	2.915	0.504	0.292	0.060
Methyl substituted MW 228 PAH	0.242	0.022	0.024	0.003	2.145	0.082	0.170	0.046
Benzo(k)fluoranthene	0.237	0.069	0.014	0.004	2.356	0.309	0.141	0.012
Benzo(b)fluoranthene	0.353	0.084	0.020	0.005	3.145	0.385	0.193	0.014
Benzo(j)fluoranthene	0.053	0.016	0.001	0.001	0.599	0.099	0.020	0.016
Benzo(e)pyrene	0.315	0.081	0.017	0.003	3.113	0.527	0.176	0.026
Benzo(a)pyrene	0.213	0.041	0.009	0.003	2.741	0.622	0.150	0.035
Perylene	0.054	0.051	0.000	0.000	0.495	0.042	0.012	0.014
Indeno(cd)pyrene	0.117	0.032	0.011	0.002	1.146	0.139	0.109	0.014
Benzo(ghi)perylene	0.329	0.049	0.027	0.003	3.825	0.789	0.299	0.045
Indeno(cd)fluoranthene	0.040	0.005	0.004	0.001	0.507	0.126	0.036	0.005
Dibenz[a,h]anthracene	0.020	0.023	0.001	0.001	0.105	0.010	0.017	0.004
Coronene	0.073	0.025	0.015	0.002	1.065	0.248	0.121	0.016
22,29,30-trisnorhopane	0.217	0.003	0.017	0.001	0.877	0.094	0.117	0.023

TABLE 4.2b Continued…

Species measured	Accumulation mode				Ultrafine mode			
	East		West		East		West	
	Mean	SD	Mean	SD	Mean	SD	Mean	SD
22,29,30-trisnorneohopane	0.185	0.023	0.022	0.002	0.784	0.052	0.130	0.020
17a(H)-21b(H)-29-norhopane	0.476	0.021	0.043	0.007	2.212	0.179	0.248	0.052
18a(H)-29-norneohopane	0.094	0.015	0.008	0.006	0.432	0.073	0.073	0.020
17a(H)-21b(H)-hopane	0.414	0.045	0.048	0.007	2.005	0.249	0.237	0.045
17b(H),21a(H)-moretane	0.019	0.013	0.002	0.002	0.140	0.024	0.018	0.012
22S, 17a(H),21b(H)-homohopane	0.176	0.021	0.023	0.001	0.775	0.132	0.096	0.015
22R, 17a(H),21b(H)-homohopane	0.144	0.018	0.017	0.001	0.685	0.138	0.075	0.008
22S, 17a(H),21b(H)-bishomohopane	0.114	0.026	0.013	0.003	0.468	0.113	0.058	0.015
22R, 17a(H),21b(H)-bishomohopane	0.091	0.025	0.011	0.002	0.318	0.059	0.036	0.005
22S, 17a(H),21b(H)-trishomohopane	0.061	0.005	0.010	0.003	0.293	0.051	0.004	0.009
22R, 17a(H),21b(H)-trishomohopane	0.042	0.008	0.008	0.002	0.156	0.076	0.006	0.012
20R+S, abb-cholestane	0.027	0.010	0.009	0.013	0.115	0.016	0.034	0.009
20R, aaa-cholestane	0.187	0.027	0.024	0.005	0.778	0.085	0.146	0.021
20R+S, abb-ergostane	0.071	0.021	0.006	0.007	0.235	0.024	0.041	0.029
20R+S, abb-sitostane	0.300	0.035	0.034	0.005	1.262	0.176	0.162	0.036
UCM	2521.784	200.072	195.182	48.166	10093.186	1230.612	1546.339	221.702

* expressed in $\mu g/m^3$

Table 4.3 shows the Pearson correlation coefficients between the measured mass concentrations of certain organic species and classes in both the size modes. The measurements made at the tunnel entrance can also be considered samples heavily influenced by traffic emissions. Therefore, all concentration data from individual days, from both bores and both ends of the tunnel, are included in the correlation calculations. The inter-species correlation among all the measured hopanes and steranes (Hop-Ster) is very high with a minimum r of 0.86 and an average r of 0.96 in the ultrafine mode (minimum r = 0.72, average r = 0.91 in the accumulation mode). Hence, the sum of the hopanes and steranes is used for comparison rather than individual species. Lower molecular weight polycyclic aromatic hydrocarbons (PAHs) and their methyl derivatives have been found to predominantly come from HDVs, while higher molecular weight PAHs such as Benzo(ghi)perylene (BgP) and Coronene (Cor) have been attributed to LDVs (Marr et al., 1999; Miguel et al., 1998; Gross et al., 2000). Based on these previous findings, we have grouped the PAHs based on their molecular weights in three groups; PAHs MW = 226+228 (sum of the PAHs with molecular weights 226 and 228); PAHs MW = 252 and PAHs MW ≥ 276. Coronene and Benzo(ghi)perylene are included individually since they have been proposed as indicators of LDV emissions. It should be noted that this grouping of individual species does not change the correlations significantly, since the species within each group are high correlated with one another.

In general elemental carbon (EC) is found to have good correlation with all the other parameters presented in the Table 4.3 in both the ultrafine and accumulation modes. The

TABLE 4.3. Pearson correlation coefficient between mass concentrations of various measured species in ultrafine and accumulation modes

	EC	PAH = 226+228 MW[1]	PAH = 252 MW[2]	BgP	Cor	PAH >= 276 MW[3]	Sum Hop-Ster[4]	UCM
Ultrafine mode								
EC	1.00							
PAH = 226+228 MW	0.98	1.00						
PAH = 252 MW	0.95	0.98	1.00					
BgP	0.84	0.91	0.96	1.00				
Cor	0.56	0.64	0.73	0.88	1.00			
PAH >= 276 MW	0.79	0.86	0.92	0.99	0.93	1.00		
Sum Hop-Ster	0.96	0.97	0.95	0.91	0.74	0.89	1.00	
UCM	0.96	0.99	0.99	0.94	0.70	0.90	0.96	1.00
Accumulation mode								
EC	1.00							
PAH = 226+228 MW	0.78	1.00						
PAH = 252 MW	0.83	0.97	1.00					
BgP	0.65	0.95	0.91	1.00				
Cor	0.36	0.72	0.64	0.87	1.00			
PAH >= 276 MW	0.59	0.92	0.88	1.00	0.90	1.00		
Sum Hop-Ster	0.76	0.99	0.96	0.94	0.73	0.91	1.00	
UCM	0.80	0.99	0.96	0.93	0.70	0.90	0.99	1.00

[1] Sum of Benzo(ghi)fluoranthene, Benz(a)anthracene and Chrysene/Triphenylene

[2] Sum of Benzo(k)fluoranthene,Benzo(b)fluoranthene,Benzo(j)fluoranthene,Benzo(e)pyrene,Benzo(a)pyrene and Perylene

[3] Sum of Indeno(cd)pyrene, Benzo(ghi)perylene, Indeno(cd)fluoranthene and Coronene

[4] Sum of Hopanes and Steranes

correlation is greater in the ultrafine mode than the accumulation mode, as EC and the other species are predominantly found in the ultrafine mode where non-vehicular background contributions are negligible. The lowest correlations with EC are found for the heavier PAHs. Diesel HDVs are known to emit much higher amounts of EC, while gasoline powered LDVs have been shown to emit relatively high amounts of heavier PAHs. The lower correlations can thus be attributed to two different sources of these species. Higher correlations between EC and the lighter PAHs are consistent with the previous work showing that HDVs emit relatively more light PAHs than LDVs.

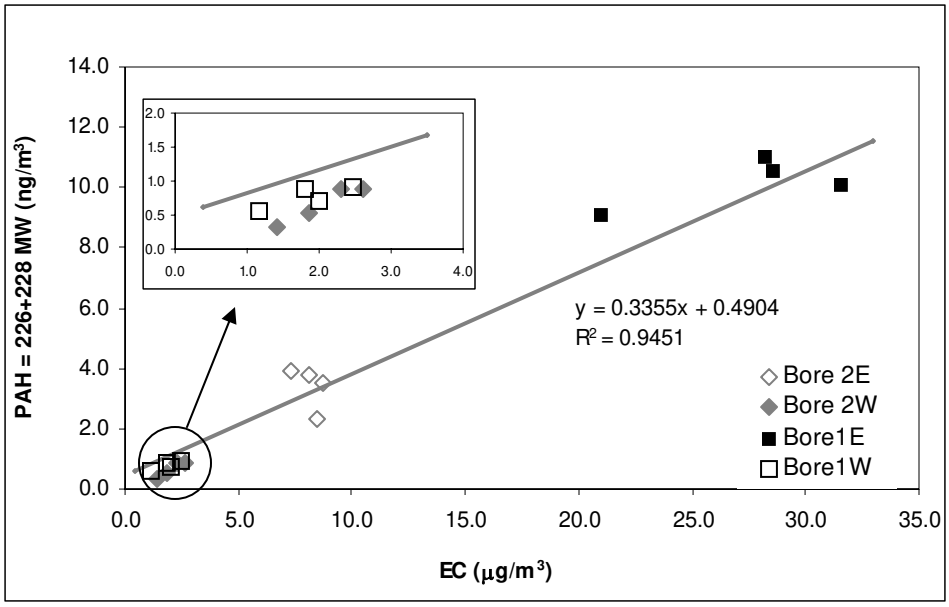

FIGURE 4.1 Correlation between mass concentrations of EC and Sum PAHs with MW 226 and 228 in ultrafine mode

Figure 4.1 further demonstrates the correlation between EC and lighter PAHs (MW = 226 + 228). It should be noted that the levels observed at the east end of Bore 2 are higher

Figure 4.2 a

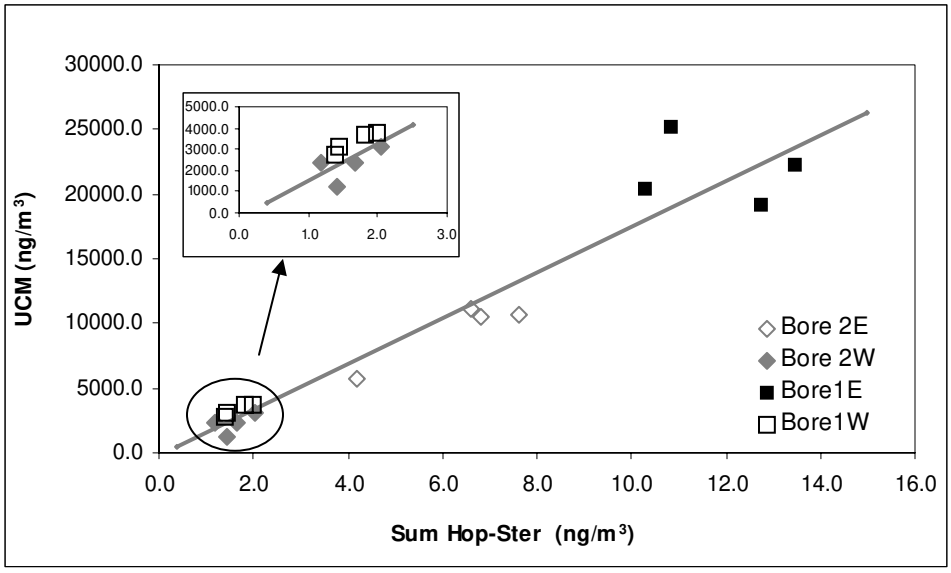

Figure 4.2 b

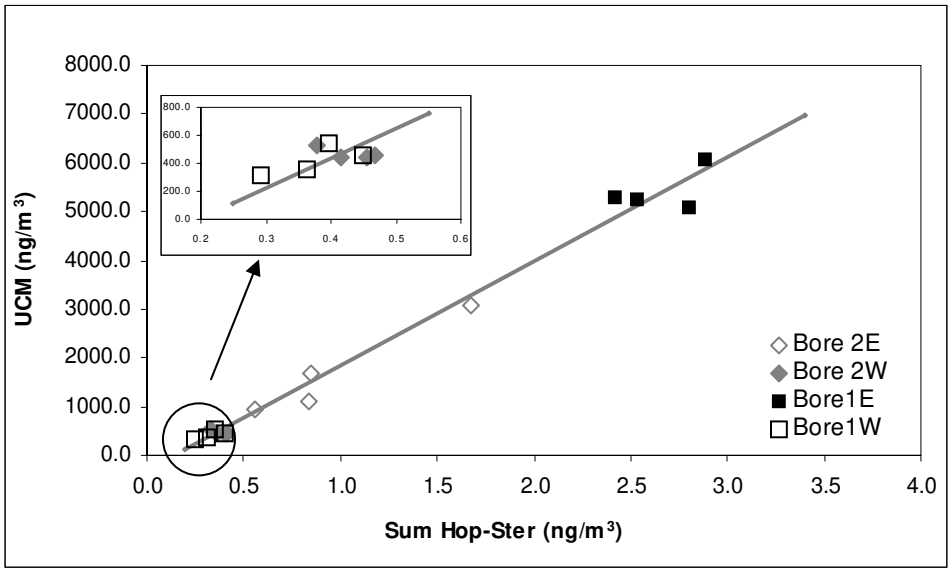

FIGURE 4.2 Correlation between mass concentrations of Sum Hop-Ster and UCM in a) ultrafine mode; b) accumulation mode

than those that can be attributed to the few (0.4%) diesel vehicles that passed through Bore 2. The EC and light PAH concentrations in Bore 2 are approximately 25% that of the Bore 1, but the HDV traffic in Bore 2 was 10% of that observed in Bore 1. Although

there was more traffic in Bore 2, the high EC and lighter PAH levels in bore 2 cannot be attributed completely to HDV. This may indicate that the fleet of gasoline vehicles also emits EC and lighter PAHs, albeit in lower amounts per vehicle, but with a similar ratio as that observed for HDV. It is possible that that the formation mechanisms of these two species are similar in both HDV and LDV engines. The west end concentrations depicted in the figure inset appear more enriched in EC than the east end, but they lie within the error of the best-fit linear regression parameters.

Both the unresolved complex mixture (UCM) and the hopanes and steranes derive from the same petroleum source (lubricating oil), and thus a very high correlation is observe between the two in both size ranges (Schauer et al., 1999; 2002), Figures 4.2a and 4.2b display the scatter-plots demonstrating this correlation in both size modes. Again, all daily data points from both bores and tunnel ends are included. The high correlation between UCM and the hopanes/steranes imply a similar origin (lubricating oil components), and suggest that the particulate emission processes responsible for these two potential tracers are the same in both HDV and LDV.

4.4.2 Size resolved emission factors

Table 4.4 presents the size resolved emission factors with standard deviations attributed to LDVs and HDVs for the measured organic markers. All of the emissions factors of the organic markers predominantly exist in ultrafine mode in both vehicle classes. Higher molecular weight PAHs such as BgP (9.63 ± 2.76mg/kg fuel burned) and Cor (5.32 ±

1.00 mg/kg fuel burned) are the most abundant species emitted from LDVs, along with medium weight Benzo(a)pyrene (BaP) (5.08 ± 1.56 mg/kg fuel burned) in the ultrafine mode. Similarly, in the accumulation mode, the highest emission factors from LDVs are found for BgP (0.68+-0.22 mg/kg fuel burned). Conversely, HDVs emit more of the lighter molecular weight PAHs (i.e. Fluoranthene, Pyrene, and methyl substituted Flu/Pyr) in both the ultrafine and accumulation size modes relative to the heavier PAHs. However high BgP emissions were also calculated in both modes from HDVs. Even though HDV PAH emission factors are generally larger than those for LDV, LDV emissions are enriched in heavier PAH relative to total emitted mass or total PAH emissions, while HDV emit more light PAH relative to total emissions. Comparison of these calculated emission factors to earlier studies measuring $PM_{2.5}$ emissions, is presented later in the text.

Hopanes and steranes are emitted from both types of vehicles, but the relative emission factors are higher for HDVs. The predominant species in both size modes and from both types of vehicles are 17a(H)-21b(H)-29-norhopane and 17a(H)-21b(H)-hopane. In general, the LDVs emission factors are an order of magnitude less than that of the HDVs for all the hopanes and steranes. UCM shows the same trends with size and vehicle type as hopanes and steranes, which is expected due their similar origins in lubricating oil.

TABLE 4.4 Emission factors (in mg/kg fuel burned) attributable to LDVs and HDVs in ultrafine and accumulation mode

Sample ID	LDV				HDV			
	Ultrafine		Accumulation		Ultrafine		Accumulation	
	Mean	SD	Mean	SD	Mean	SD	Mean	SD
Fluoranthene	2.39	0.43	0.37	0.13	114.90	33.16	21.93	4.50
Acephenanthrylene	0.43	0.05	0.05	0.01	25.91	6.93	4.18	1.23
Pyrene	3.63	0.68	0.55	0.20	206.47	60.03	36.23	7.10
Methyl substituted MW 202 PAH	3.75	2.34	0.44	0.40	233.54	61.53	29.52	5.10
Benzo(ghi)fluoranthene	3.55	0.78	0.44	0.14	89.99	11.04	11.32	0.55
Benz(a)anthracene	4.11	0.76	0.43	0.13	65.69	13.80	7.30	0.46
Chrysene/Triphenylene	4.43	1.03	0.50	0.19	51.52	15.64	7.33	0.52
Methyl substituted MW 228 PAH	3.09	0.95	0.25	0.22	40.19	3.00	4.94	0.61
Benzo(k)fluoranthene	3.75	1.40	0.36	0.09	43.41	9.37	4.47	1.95
Benzo(b)fluoranthene	4.75	1.35	0.46	0.15	59.34	11.17	7.11	2.34
Benzo(j)fluoranthene	0.99	0.34	0.06	0.00	11.29	3.27	1.17	0.44
Benzo(e)pyrene	4.42	1.40	0.41	0.11	60.80	15.28	6.36	2.29
Benzo(a)pyrene	5.08	1.56	0.34	0.04	46.76	18.55	4.04	1.13
Perylene	0.74	0.24	0.06	0.04	9.92	1.37	1.76	1.31
Indeno(cd)pyrene	3.79	1.36	0.28	0.09	8.52	4.20	1.49	0.87
Benzo(ghi)perylene	9.63	2.76	0.68	0.22	47.90	23.47	4.96	1.40
Indeno(cd)fluoranthene	1.26	0.44	0.08	0.03	6.53	3.67	0.59	0.15
Dibenz[a,h]anthracene	0.29	0.07	0.04	0.02	0.92	0.31	0.48	0.64
Coronene	5.32	1.00	0.24	0.09	5.74		0.68	0.38
22,29,30-trisnorhopane	1.56	0.36	0.23	0.17	13.27	2.46	4.53	0.13
22,29,30-trisnorneohopane	1.38	0.63	0.20	0.12	11.28	1.02	3.65	0.67
17a(H)-21b(H)-29-norhopane	3.87	1.07	0.50	0.39	35.33	4.00	9.82	0.46
18a(H)-29-norneohopane	0.85	0.20	0.12	0.06	5.63	1.86	1.81	0.47
17a(H)-21b(H)-hopane	3.76	1.06	0.45	0.26	30.21	6.15	8.15	1.18

TABLE 4.4 Continued…

Sample ID	LDV				HDV			
	Ultrafine		Accumulation		Ultrafine		Accumulation	
	Mean	SD	Mean	SD	Mean	SD	Mean	SD
17b(H),21a(H)-moretane	0.30	0.06	0.04	0.02	1.88	0.53	0.48	0.07
22S, 17a(H),21b(H)-homohopane	1.39	0.50	0.20	0.17	11.91	3.61	3.37	0.62
22R, 17a(H),21b(H)-homohopane	1.13	0.33	0.16	0.18	11.38	3.89	2.81	0.54
22S, 17a(H),21b(H)-bishomohopane	0.61	0.33	0.12	0.10	8.51	3.46	2.32	0.79
22R, 17a(H),21b(H)-bishomohopane	0.53	0.14	0.10	0.07	5.22	1.58	1.79	0.77
22S, 17a(H),21b(H)-trishomohopane	0.47	0.11	0.09	0.07	5.75	1.64	0.99	0.09
22R, 17a(H),21b(H)-trishomohopane	0.27	0.08	0.05	0.02	3.98	1.52	0.73	0.19
20R+S, abb-cholestane	0.24	0.10	0.01	0.01	1.02	0.47	0.44	0.23
20R, aaa-cholestane	1.33	0.36	0.21	0.14	10.89	1.99	3.58	0.78
20R+S, abb-ergostane	0.45	0.27	0.09	0.03	3.07	1.09	1.43	0.75
20R+S, abb-sitostane	2.08	0.56	0.34	0.20	20.33	4.67	5.83	0.96
UCM	14893.03	5365.50	2531.00	2036.95	165124.63	38365.16	53779.13	5552.17

Figure 4.3 shows the ratio of emission factors between HDV and LDV of the measured organic markers for both the size ranges. The HDV/LDV emission factor ratio of lighter PAHs (MW <= 216) is very high (60 to 90) as compared to the higher molecular weight ones (MW >= 276) (< 10) for both the size ranges. The results demonstrate that lower molecular weight PAHs are emitted in relatively higher amounts by HDVs than the higher molecular weight PAHs. While HDVs emit much more PM mass and PAHs overall, the distribution of the PAHs with molecular weight is very different between HDV and LDV. Such differences may prove useful in source apportionment calculations attempting to distinguish the contributions of diesel and gasoline vehicles to ambient samples. Hopanes, steranes and UCM are emitted from both LDVs and HDVs with similar species distributions. The relative emission factors between HDVs and LDVs lie in relatively narrow ranges, with ratios of 6-14 for the ultrafine mode and 12-21 for the accumulation mode. These ratios are more similar to the medium MW PAH than for the lighter or heavier PAHs. It can also be seen that this ratio is higher in all cases for the accumulation mode relative to the ultrafine mode, indicating HDV emissions are shifted to larger particle sizes than LDVs.

To further demonstrate the particle size partitioning for these organic species, Figure 4.4a and 4.4b present the correlation between the ultrafine and accumulation mode emission factors of PAHs and hopanes and steranes from LDVs and HDVs. The high correlations for HDV show that high emissions of particular species in one mode are accompanied by high emissions in the other mode, indicating similar size distributions for these species.

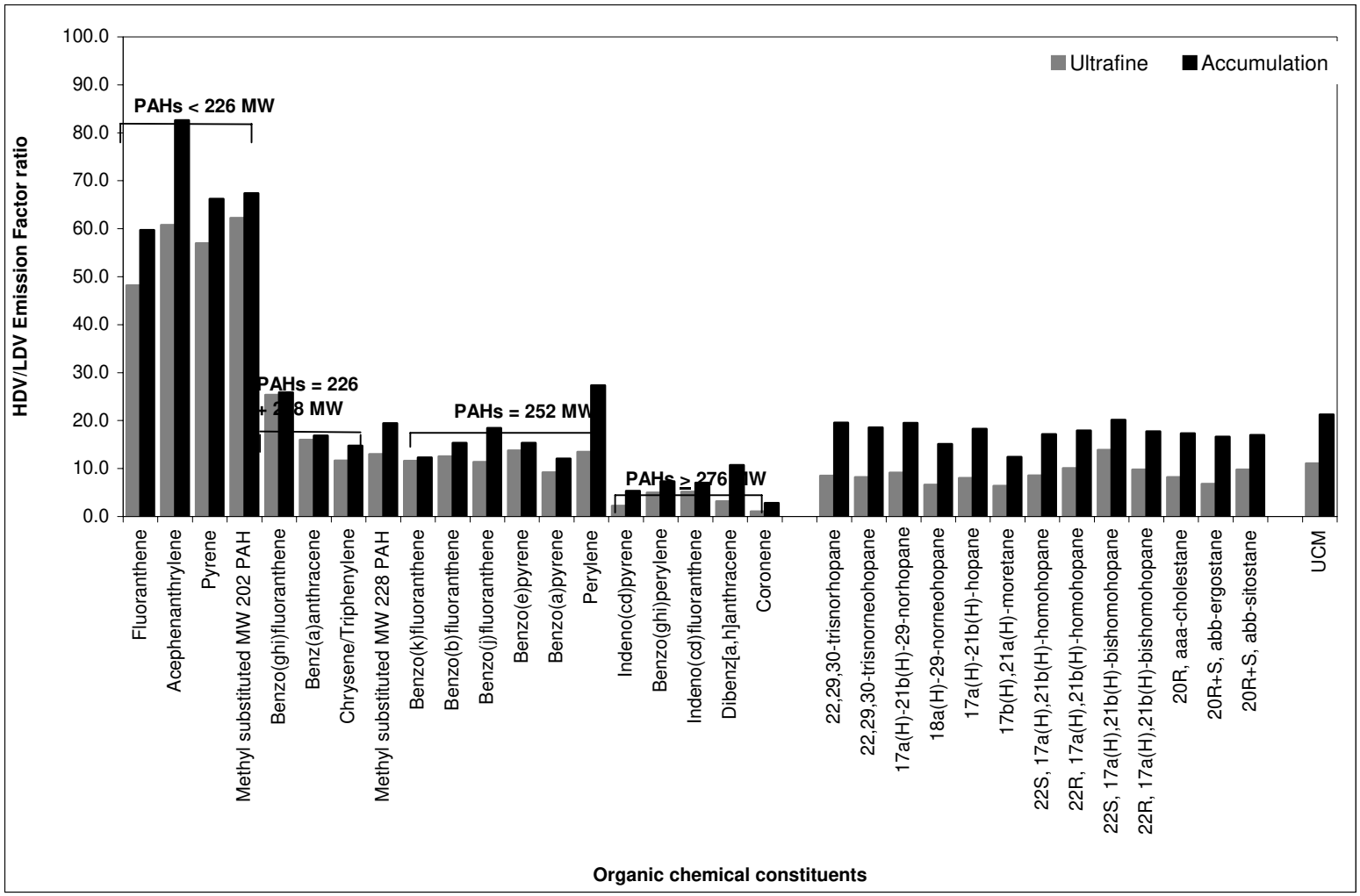

FIGURE 4.3 HDV/LDV emission factor ratios for the measured organics species

Figure 4.4 a

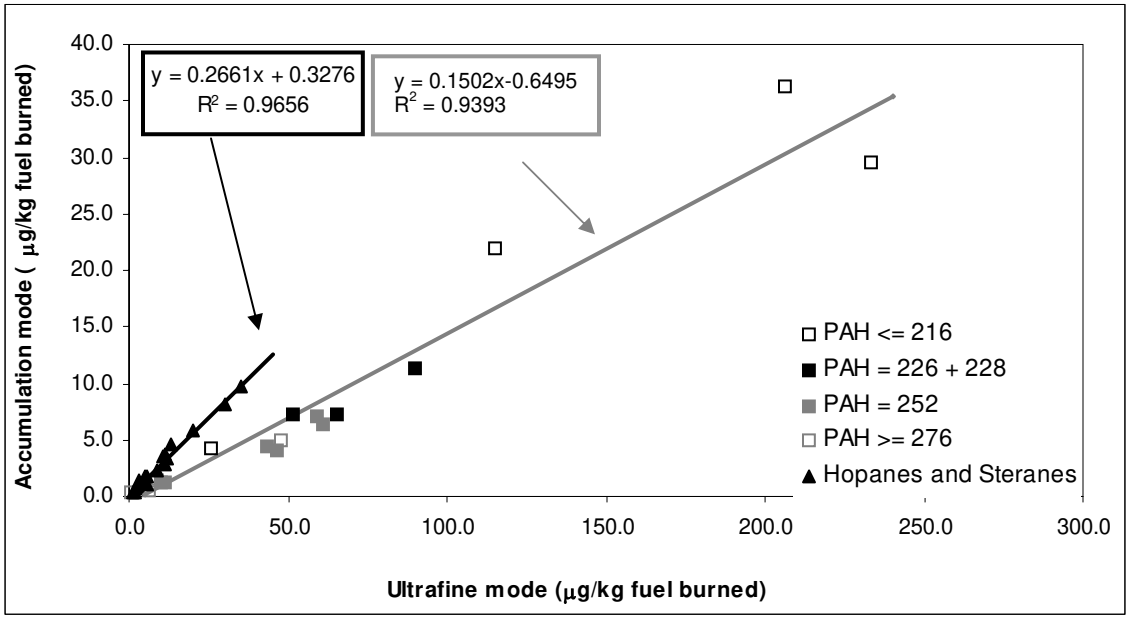

Figure 4.4 b

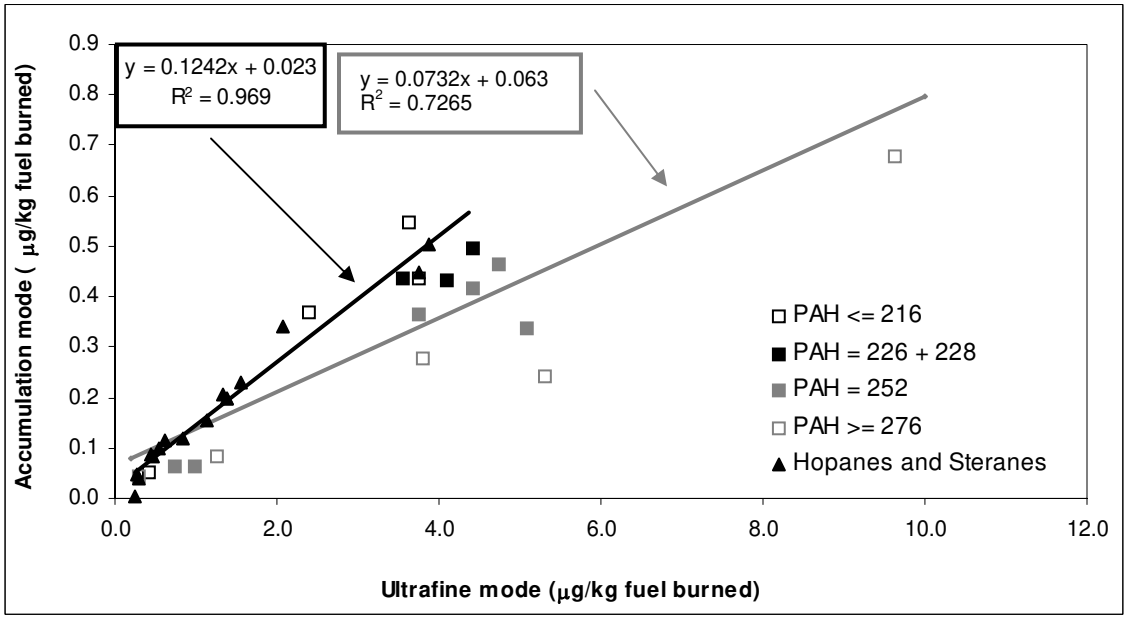

FIGURE 4.4 Correlation between ultrafine and accumulation mode PAHs, Hopanes and Steranes for a) HDVs; b) LDVs

The slopes less than unity show that most of the species are in the ultrafine mode, but the higher slope for the hopanes and steranes relative to the PAHs indicates that the size distribution of PAHs is shifted to smaller particle sizes than the size distribution of hopanes and steranes. Note also that the ratio of accumulation to ultrafine mode HDV emission factors for UCM is 0.33, closer to the hopanes/ steranes slope of 0.27 than the PAH slope of 0.15. For the LDVs, there is more scatter in the PAH emission factor size distributions, but the hopanes/steranes are again shifted to the larger particles relative to most PAHs.

In the case of HDVs, all the PAHs, regardless of molecular weight, are found to partition between ultrafine and accumulation modes in similar ways. But it is apparent in figure 4b that for LDVs, the lighter PAHs tend to be more associated with larger particles than the heavier PAH, suggesting that the volatility of a particular species affects its size distribution. This observation is in agreement with earlier reported studies that the more volatile PAH tend to partition into higher particle size fractions (Marr et al., 1999; Miguel et al., 1998). As suggested in Figure 4.4, all HDV emission factors result in higher slopes than LDVs, indicating that HDV emissions are shifted to larger sizes relative to LDV emissions. This is somewhat expected given the agglomerate nature of soot particles emitted from diesel engines which can have larger aerodynamic diameters than the nucleation mode gasoline emissions (Kittelson et al., 1998; Kleeman et al., 2000).

4.4.3 Comparison with other studies

Table 5.5a and 5.5b compare the LDV and HDV $PM_{2.5}$ emission factors from this study (accumulation plus ultrafine modes) to other earlier studies, including tunnel and chassis dynamometer studies. It is immediately evident that there are large differences in reported emission factors from various studies. Testing an individual vehicle, or even averaging over several vehicles, can lead to very different results than a tunnel study that includes an average over thousands of vehicles. Miguel et al. (1998) and Marr et al. (1999) have reported PAHs emissions from the Caldecott tunnel measured in 1996 and 1997 respectively. Miguel et al. (1998) have reported $PM_{1.3}$ emission factors for particulate PAHs and it can be seen that for the LDVs, there is a modest decrease in the PAHs emission factors between 1996 and the current 2004 study. This may be due to better control technologies, but is more likely due to the removal of older high-emitting vehicles from the on-road fleet during the seven years between the measurements.

Reformulated gasoline (RFG) was introduced in the San Francisco Bay Area in 1996, which resulted in significant reductions in overall pollutant emissions. Kirchstetter et al. (1999b) have attributed this reduction in pollutant emissions from vehicles to both fleet turnover and the introduction of RFG. The 1997 study by Marr et al. (1999) in the same tunnel also showed a slight reduction in PAHs emissions as compared to the previous 1996 study by Miguel et al. (1998). For HDVs, the lighter PAHs emissions were lower in this study as compared to both of the 1996 and 1997 studies. However, in both of these studies they did not attribute the higher molecular weight PAHs to HDVs, while we

TABLE 4.5a. Comparison of particle phase $PM_{2.5}$ emission factors (in mg/kg fuel burned) attributable to LDVs

Organic compounds	This study	Zielinska et al., 2004[1]		Schauer et al., 2002[3]		Rogge et al., 1993[4]		Marr et al., 1999[5]	Miguel et al., 1998[6]
		Cat.	Non-cat.[2]	Cat.	Non-cat.	Cat.	Non-cat.		
PAHs									
Fluoranthene	2.75	416.44	2759.67	0.78	1,711.71	22.52	543.92	8	10.3
Acephenanthrylene	0.48			0.14	650.90				
Pyrene	4.17	195.27	1568.46	0.87	2,443.69	28.15	349.10	9.00	13.80
Methyl substituted MW 202 PAH	4.19	356.24	5260.04		2,623.87	47.30	1203.83		
Benzo(ghi)fluoranthene	3.98			0.71	527.03	14.64	278.15		
Benz(a)anthracene	4.54	37.02	573.35	1.09	584.46	21.40	831.08	4.80	8.80
Chrysene/Triphenylene	4.92	54.38	828.15	2.32	586.71	42.79	628.38	7.00	8.60
Methyl substituted MW 228 PAH	3.34			2.73	1,159.91	38.29	1615.99		
Benzo(k)fluoranthene	4.12			0.93	368.24	22.52	458.33	2.50	3.00
Benzo(b)fluoranthene	5.21	23.17	476.63		420.05	32.66	426.80	7.60	8.10
Benzo(j)fluoranthene	1.06			0.10	17.12	6.08	67.57		
Benzo(e)pyrene	4.84	13.93	293.81	1.69	430.18	22.52	515.77		
Benzo(a)pyrene	5.42	12.74	328.91	0.24	461.71	21.40	489.86	6.40	8.30
Perylene	0.80			0.35		6.76	157.66		
Indeno(cd)pyrene	4.07	10.36	243.95	4.91	1,036.04	5.29	72.07		
Benzo(ghi)perylene	10.31	16.24	428.05			52.93	1637.39	18.00	20.70
Indeno(cd)fluoranthene	1.35					19.14	367.12	9.00	7.50
Dibenz[a,h]anthracene	0.34	2.10	47.00			3.72	93.47	16.20	1.30
Coronene	5.56	7.14	84.44		1,137.39	12.39	1177.93		
Hopanes and Steranes									
22,29,30-trisnorhopane	1.80	0.07	9.03		777.03				
22,29,30-trisnorneohopane	1.57	6.02	286.82	0.43	1,407.66	76.58	33.78		
17a(H)-21b(H)-29-norhopane	4.38	3.57	235.41	0.21	3,175.68	120.50	66.44		
17a(H)-21b(H)-hopane	4.21	0.14	22.40	0.37	3,614.86	204.95	101.35		
17b(H),21a(H)-moretane	0.34	0.21	39.05						

TABLE 4.5a Continued…

Organic compounds	This study	Zielinska et al., 2004[1]		Schauer et al., 2002[3]		Rogge et al., 1993[4]		Marr et al., 1999[5]	Miguel et al., 1998[6]
		Cat.	Non-cat.[2]	Cat.	Non-cat.	Cat.	Non-cat.		
22S, 17a(H),21b(H)-homohopane	1.59	1.19	116.04		2,916.67	93.47	34.91		
22R, 17a(H),21b(H)-homohopane	1.29	0.84	84.83			61.94	21.40		
22S, 17a(H),21b(H)-bishomohopane	0.73	0.49	65.44		2,207.21	52.93	16.89		
22R, 17a(H),21b(H)-bishomohopane	0.64	0.42	44.48			39.41	12.39		
22S, 17a(H),21b(H)-trishomohopane	0.56	0.28	49.87						
22R, 17a(H),21b(H)-trishomohopane	0.31	0.14	31.81						
20R+S, abb-cholestane	0.24	1.61	94.84		1,914.41	94.59	40.54		
20R, aaa-cholestane	1.53				1,340.09	104.73	45.05		
20R+S, abb-ergostane	0.54				1,565.32	88.96	46.17		
20R+S, abb-sitostane	2.42	1.19	92.70		1,531.53	128.38	60.81		

[1] Run on California unified driving cycle (UDC); 5 catalyst equiped vehicles (1993-1996 model year); 2 non-catalyst (1976 model year black emitter and 1990 model year white emitter)

[2] Average of black emitter and white emitter gasoline vehicles

[3] Run on cold-start FTP urban driving cycle; 9 catalyst equipped ith average model year 1990 (1981-1994) and 2 1970 model year non-catalyst vehicles

[4] Run on cold-start FTP urban driving cycle; 5 catalyst equipped vehicles (model year 1977-1983) and 6 non-catalyst (model year 1965-1976)

[5] 1997 data from Caldecott tunnel with %HD Diesel = 4.3

[6] 1996 data from Caldecott tunnel with %HDVs = 4.7

TABLE 4.5b. Comparison of particle phase $PM_{2.5}$ emission factors (in mg/kg fuel burned) attributable to HDVs and mixed tunnel fleets

Organic compounds	HDVs						Mixed tunnel fleet	
	This study	Zielinska et al., 2004[1]	Schauer et al., 1999[2]	Rogge et al., 1993[3]	Marr et al., 1999[4]	Miguel et al., 1998[5]	Chellam et al., 2005[6*]	Fraser et al., 1998[7*]
PAHs								
Fluoranthene	136.83	32.51	143.36	32.93	480.00	749.00	18.90	4.85
Acephenanthrylene	30.09		41.03					1.48
Pyrene	242.70	44.24	224.16	57.24	690.00	986.00	21.37	8.35
Methyl substituted MW 202 PAH	263.06	31.25	205.17	32.42				27.74
Benzo(ghi)fluoranthene	101.30		50.15	17.48				26.53
Benz(a)anthracene	72.99	2.76	19.66	9.12	140.00	180.00	5.62	28.14
Chrysene/Triphenylene	58.85	7.71	39.51	25.08	66.00	140.00	20.16	32.05
Methyl substituted MW 228 PAH	45.12		16.57	6.84				90.09
Benzo(k)fluoranthene	47.87			6.84	2.80	59.00	8.94	21.28
Benzo(b)fluoranthene	66.46	3.59		7.35	25.00	90.00	11.44	
Benzo(e)pyrene	67.16	2.08		6.59			13.56	29.22
Benzo(a)pyrene	50.80	6.79		3.29		126.00	5.32	24.64
Perylene	11.24			2.53			3.11	5.25
Indeno(cd)pyrene	10.01	0.91					5.32	41.21
Benzo(ghi)perylene	52.86	2.15		4.05			10.96	137.62
Indeno(cd)fluoranthene								14.00
Dibenz[a,h]anthracene	1.28	0.14					7.38	
Coronene	1.94	1.27						
Hopanes and Steranes								
22,29,30-trisnorhopane	17.80	8.66	2.51				15.99	24.24
22,29,30-trisnorneohopane	14.93	102.88	6.94	58.51			15.24	37.71
17a(H)-21b(H)-29-norhopane	45.15	5.61	28.62	100.30			45.05	73.53
18a(H)-29-norneohopane	7.44						11.05	21.01
17a(H)-21b(H)-hopane	38.36	7.23	28.88	238.60			53.98	110.42

TABLE 5.5b (Continued)

Organic compounds	HDVs						Mixed tunnel fleet	
	This study	Zielinska et al., 2004[1]	Schauer et al., 1999[2]	Rogge et al., 1993[3]	Marr et al., 1999[4]	Miguel et al., 1998[5]	Chellam et al., 2005[6*]	Fraser et al., 1998[7*]
17b(H),21a(H)-moretane	2.24	4.20						
22S, 17a(H),21b(H)-homohopane	15.29	48.65		96.25			18.34	46.73
22R, 17a(H),21b(H)-homohopane	14.18	33.17		97.01			14.96	31.38
22S, 17a(H),21b(H)-bishomohopane	10.84	49.99		57.50			10.89	29.36
22R, 17a(H),21b(H)-bishomohopane	7.01	31.52		40.53			8.11	18.85
22S, 17a(H),21b(H)-trishomohopane	6.74	14.66						
22R, 17a(H),21b(H)-trishomohopane	3.72	8.74						
20R+S, abb-cholestane	1.46	28.53	1.98	100.30				15.35
20R, aaa-cholestane	14.47		3.01	108.92				23.70
20R+S, abb-ergostane	4.50		7.98	109.93				30.03
20R+S, abb-sitostane	26.16	31.71	6.61	160.59				28.82
UCM	218903.76		104863.22					

[1] Run on California unified driving cycle (UDC); 4 diesel vehicles (model year 1991-2000)

[2] Run on hot-start FTP urban driving cycle; 2 medium duty diesel trucks

[3] 2 diesel trucks (1987 model year)

[4] 1997 data from Caldecott tunnel with %HDVs = 4.3

[5] 1996 data from Caldecott tunnel with %HDVs = 4.7

[6] 2000 Houston tunnel study; %HDVs = 3.4

[7] 1993 Los Angeles tunnel study with average 1986 model year vehicles; % HDVs = 2.7 and % non-catalyst vehicles = 3.6

[*] Tunnel study with mixed fleet, hence mixed fleet (LDV+HDV) emision factors are reported

attribute significant emissions of the higher PAHs to HDVs. Zielinska et al. (2004), also measured heavier PAH (Coronene and BgP in the emissions from diesel vehicles), and Rogge et al. (1993), also found BgP in diesel emissions.

The other tunnel studies are from Chellam et al. (2005) in a Houston tunnel and Fraser et al. (1998) in a Los Angeles tunnel. Both of these studies reported mixed fleet (LDVs + HDVs) emission factors for the organic markers. The PAH emission factors from the Houston tunnel are generally between our LDVs and HDVs emission factors, with the exception of Dibenz(a,h)anthracene, which had a higher emission factor from the Houston tunnel than that of what was attributed to HDVs here. However, the hopanes/steranes emissions in the Houston tunnel are very similar to our results for HDV from the Caldecott tunnel.

Differences may also be due to different vehicle types, fuel blends, tunnel characteristics, or average speeds. Also, the Houston tunnel study occurred at different times over different days whereas the current study sampled over the same time period every day. The Van Nuys tunnel study in 1993 by Fraser et al. (1998) shows higher levels of higher molecular weight PAHs emissions as well as higher hopanes/steranes emissions compared to our study. The lighter PAHs, however, are much less as compared to our HDVs contributions. Again, there are many possible reasons for these discrepancies, including higher numbers of older or non-catalytic cars, different vehicle driving conditions and fuel composition.

Shown in Table 5.5a are three chassis dynamometer studies done in 1993, 2002 and 2004 for LDVs. Compared to the Schauer et al. (2002) study, our LDV emission factor values fall in between the catalyst and non-catalyst emissions for all the measured species, as one would expect in a tunnel with mostly catalyst but some non-catalyst (or malfunctioning catalyst) vehicles as well. The higher catalyst emissions from Rogge et al. (1993) may be due to the pre-reformulation gasoline and possibly less advanced control technologies at the time of that study. Zielinska et al. (2004) fine PAHs emission factors for the catalyst-equipped vehicles are higher than the LDVs emission factor reported in this study. Since all of the dynamometer testing occurs over specified driving cycles, often including cold-start and multiple accelerations, it is not surprising that the emissions of certain species will be higher.

For the HDVs, the dynamometer studies by Zielinska et al. (2004), and Rogge et al. (1993) resulted in generally lower PAH emissions, whereas a few of the hopanes and steranes are significantly higher in theses previous studies. A similar study by Schauer et al. (1999), however, is very close to our results for the lighter PAHs and the hopanes and steranes, but no higher molecular weight PAHs were reported.

As stated earlier, the main source of error for the HDV apportionment is the value of X, which relates to the uncertainty in CO and CO_2 measurements, vehicle counts and the assumption that gasoline and diesel emit CO in similar amounts elative to fuel consumption. Also, the uncertainty in the measured levels of species for which LDVs

emit more than HDVs can induce additional error. For an estimated upper bound 15% total uncertainty in X the maximum error in the HDV emission factors across all species due to this calculation is less than 10%. The main source of error in LDV emissions estimates derives from the few diesel vehicles (less than 10% that of in bore 1) that passed through bore 2. The presence of diesel vehicles in bore 2 does not significantly affect the HDV emissions estimates which therefore can be used to assess the impact of Bore 2 diesel vehicles on calculated LDV emission factors. For the worst case of the lightest PAH emission factors, the diesel vehicles in bore 2 can add as much as 40% uncertainty to the LDV results in the ultrafine mode. For all the other organic species, the error introduced by this issue is generally less than 10%. Due to the extremely low counts of HDV in bore 2, and the uncertainty in the 2-axle/6-tire split assumptions, it is not feasible to correct LDV emissions factors based on our HDV data. The use of previously measured fuel economies, as well as the assumed classification of 2-axle/6-tire trucks as gasoline or diesel, can contribute to additional but minor uncertainties in the apportionment of emissions to LDVs and HDVs (Kirchstetter et al., 1999a).

4.5 Chapter 4: REFERENCES

Abu-Allaban, M.; Coulomb, W.; Gertler, A. W.; Gillies, Pierson, J. W. R.; Rogers, C. F.; Sagebiel, J. C.; Tarnay, L. Exhaust particle size distribution measurements at the Tuscarora mountain tunnel. *Aerosol Sci. Technol*. **2002**, *36*, 771 – 789.

Geller, M. D., Sardar, S. B., Phuleria H. C., Fine P. M.; Sioutas, C. Measurements of particle number and mass concentrations and size distributions in a tunnel environment *Environ. Sci. Technol.* **2005** (in press).

Li, N.; Sioutas, C.; Cho, A.; Schmitz, D.; Misra, C.; Sempf, J.; Wang, M. Y.; Oberley, T.; Froines, J.; Nel, A. Ultrafine particulate pollutants induce oxidative stress and mitochondrial damage. *Environ. Health Perspect.* **2003**, *111*(4), 455-460.

Lighty, J.B.; Veranth, J.M.; Sarofim, A.F. Combustion aerosols: Factors governing their size and composition and implications to human health. *J. Air Waste Manage. Assoc.* **2000**, *50*, 1565-1618.

Mauderly, J. L. Toxicological and epidemiological evidence for health risks from inhaled engine emissions. *Environ. Health Perspect.* **1994**, *102*, 165-171.

Mauderly, J. L. Toxicological approaches to complex mixtures. *Environ. Health Perspect.* **1993**, *101*, 155-165.

Weingartner, E.; Keller, C.; Stahel, W.A.; Burtscher, H.; Baltensperger, U. Aerosol emission in a road tunnel. *Atmos. Environ.* **1997**, *31*(3), 451-462.

Xia, T.; Korge, P.; Weiss, J. N.; Li, N.; Venkatesen, I. M.; Sioutas, C.; Nel A. Quinones and aromatic chemical compounds in particulate matter induce mitochondrial dysfunction: Implications for ultrafine particle toxicity. *Environ. Health Perspect.* **2004**, *112*(14), 1347 –1358.

Johnston, C. J.; Finkelstein, J. N.; Mercer, P.; Corson, N.; Gelein, R.; Oberdorster, G. Pulmonary Effects Induced by Ultrafine PTFE Particles. *Toxicol. Applied Pharmacol.* **2000**, *168*, 208-215.

Kleinman, M. T.; Sioutas, C.; Chang, M. C.; Boere, A. J. F.; Cassee, F. R. Ambient fine and coarse particle suppression of alveolar macrophage functions *Toxicol. Letters*, **2003**, *137*, 151-158.

Kleinman, M. T.; Hamade, A.; Meacher, D.; Oldham, M.; Sioutas, C.; Chakrabarti, L.; Stram, D.; Froines, J. R.; Cho, A. K. Inhalation of concentrated ambient particulate matter near a heavily trafficked road stimulates antigen-induced airway responses in mice. *J. Air Waste Manage. Assoc.* **2005**, *55*(9), 1277-1288.

Oberdorster, G. Pulmonary effects of inhaled ultrafine particles. *Int. Archives Occupat. Environ. Health.* **2001**, *74*, 1-8.

Oberdorster, G.; Sharp, Z.; Atudorei, V.; Elder, A.; Gelein, R.; Lunts, A.; Kreyling, W.; Cox, C. Extrapulmonary translocation of ultrafine carbon particles following whole-body inhalation exposure of rats. *J. Toxicol. Environ. Health-Part A.* **2002**, *65*, 1531-1543.

Chakrabarti, B.; Singh, M.; Sioutas, C. Development of a near-continuous monitor for measurement of the sub-150 nm PM mass concentration. *Aerosol Sci. Tech.* **2004**, *38*, 239-252.

Fine, P. M.; Chakrabarti, B.; Krudysz, M.; Schauer, J. J.; Sioutas, C. Diurnal variations of individual organic compound constituents of ultrafine and accumulation mode particulate matter in the Los Angeles Basin. *Environ. Sci. Technol.* **2004**, *38*, 1296-1304.

Sardar, S.B.; Fine, P. M.; Yoon, H.; Sioutas, C. Associations between particle number and gaseous co-pollutant concentrations in the Los Angeles Basin. *J. Air Waste Manage. Assoc.* **2004**, *54*, 992-1005.

Janhall, S.; Jonsson, A. M.; Molnar, P.; Svensson, E. A.; Hallquist, M. Size resolved traffic emission factors of submicrometer particles. *Atmos. Environ.* **2004**, *26*, 4331-4340.

Sioutas, C., Delfino, R. J.; Singh M. Exposure assessment for atmospheric ultrafine particles (UFPs) and implications in epidemiologic research. *Environ. Health Perspec*. **2005,** *113*, 947-955.

Kuhn, T.; Biswas, S.; Fine, P. M.; Geller, M.; Sioutas, C. Physical and chemical characteristics and volatility of PM in the proximity of a light-duty vehicle freeway. *Aerosol Sci Tech.* **2005**, *39*(4), 347 – 357.

Canagaratna, A.; Jayne, J.; Ghertner, D.; Herndon, S.; Shi, Q.; Jimenez, J.; Silva, P.; Williams, P.; Lanni, T.; Drewnick, F.; Demerjian, K.; Kolb, C.; Worsnop D. Chase studies of particulate emissions from in-use New York city vehicle. *Aerosol Sci. Technol.* **2004**, *38*, 555-573.

Kittelson, D. B., Engines and nanoparticles: A review. *J. Aerosol Sci*., **1998**, *29*, 575-588.

Gross, D.S.; Barron, A. R.; Sukovich, E. M.; Warren, B. S.; Jarvis, J. C.; Suess, D. T.; Prather, K. A. Stability of single particle tracers for differentiating between heavy- and light-duty vehicle emissions. *Atmos. Environ.* **2005**, *39*(16), 2889-2901.

Rogge W. F.; Hildemann, L. M.; Mazurek, M. A.; Cass, G. R.; Simoneit B. R. T. Sources of fine organic aerosol. 2. Noncatalyst and catalyst-equipped automobiles and heavy-duty diesel trucks. *Environ. Sci. Technol.* **1993**, *27*, 636-651.

Schauer, J. J.; Kleeman, M. J.; Cass, G. R.; Simoneit, B. R. T. Measurement of emissions from air pollution sources. 2. C_1 through C_{30} organic compounds from medium duty diesel trucks. *Environ. Sci. Technol.* **1999**, *33*, 1578-1587.

Schauer, J. J.; Kleeman, M. J.; Cass, G. R.; Simoneit, B. R. T. Measurement of emissions from air pollution sources. 5. C_1-C_{32} organic compounds from gasoline-powered motor vehicles. *Environ. Sci. Technol.* **2002**, *36*, 1169-1180.

Zielinska, B.; Sagebiel, J.; McDonald, J. D.; Whitney, K.; Lawson, D. R. Emission rates and comparative chemical composition from selected in-use diesel and gasoline-fueled vehicles. *J. Air Waste Manage. Assoc.* **2004**, *54*, 1138-1150.

Allen, J. O.; Mayo, P. R.; Hughes, L. S.; Salmon, L. G.; Cass, G. R. Emissions of size-segregated aerosols from on-road vehicles in the Caldecott tunnel. *Environ. Sci. Technol.* **2001**, *35*, 4189-4197.

Chellam, S.; Kulkarni, P.; Fraser, M. P. Emissions of organic compounds and trace metals in fine particulate matter from motor vehicles: A tunnel study in Houston, Texas. *J. Air Waste Mange. Assoc.* **2005**, *55*, 60-72.

Fraser, M. P.; Cass, G. R.; Simoneit, B. R. T. Gas-phase and particle-phase organic compounds emitted from motor vehicle traffic in a Los Angeles roadway tunnel. *Environ. Sci. Technol.* **1998**, *32*, 2051-2060.

Kirchstetter, T. W.; Harley, R. A.; Kreisberg, N. M.; Stolzenburg, M. R.; Hering, S. V. On-road measurement of fine particle and nitrogen oxide emissions from light- and heavy-duty motor vehicles. *Atmos. Environ.* **1999a**, *33*, 2955-2968.

Marr, L. C.; Kirchstetter, T. W.; Harley, R. A.; Miguel, A. H.; Hering, S. V.; Hammond, S. K. Characterization of polycyclic aromatic hydrocarbons in motor vehicle fuels and exhaust emissions. *Environ. Sci. Technol.* **1999**, *33*, 3091-3099.

Miguel, A. H.; Kirchstetter, T. W.; Harley, R. A.; Hering, S. V. On-road emissions of particulate polycyclic aromatic hydrocarbons and Black Carbon from gasoline and diesel vehicles. *Environ. Sci. Technol.* **1998**, *32*, 450-455.

Schauer, J. J.; Shafer, M.; Christensen, C.; Kittelson, D. B.; Johnson, J.; Watts, W. Impact of Cold-Cold Start Temperature on the Chemical Composition of PM Emissions from SI Vehicles. *13th CRC On-Road Vehicle Emissions Workshop*, San Diego, CA, April 7-9, **2003.**

Mathis, U.; Ristimäki, J.; Mohr, M.; Keskinen, J.; Ntziachristos, L.; Samaras, Z.; Mikkanen, P. Sampling conditions for the measurement of nucleation mode particles in the exhaust of a diesel vehicle. *Aerosol Sci. Technol.* **2004**, *38*(12), 1149 – 1160.

Kean, A. J.; Harley, R. A.; Kendall, G. R. Effects of vehicle speed and engine load on motor vehicle emissions. *Environ. Sci. Technol.* **2003**, *37*, 3739-3746.

Dockery, D. W.; Pope, C. A.; Xu, X. P.; Spengler, J. D.; Ware, J. H.; Fay, M. E.; Ferris, B. G.; Speizer, F. E. An association between air-pollution and mortality in 6 United-States cities. *New England J. Med.* **1993**, *329*, 1753-1759.

Mazzoleni, C.; Kuhns, H. D.; Moosmuller, H.; Keislar, R. E.; Barber, P. W.; Robinson, N. F.; Watson, J. G. On-road vehicle particulate matter and gaseous emission distributions in Las Vegas, Nevada, compared with other areas. *J. Air Waste Mange. Assoc.* **2004**, *54*(6), 711-726.

Fraser, M. P.; Cass, G. R.; Simoneit, B. R. T. Air quality model evaluation data for organics. 6. C_3–C_{24} organic acids. *Environ. Sci. Technol.* **2003**, *37*, 446-453.

Schauer, J. J.; Rogge, W. F.; Hildemann, L. M.; Mazurek, M. A.; Cass, G. R.; Simoneit, B. R. T. Source apportionment of airborne particulate matter using organic compounds as tracers. *Atmos. Environ.* **1996**, *30*, 3837-3855.

Schauer, J. J.; Cass, G. R. Source apportionment of wintertime gas-phase and particle-phase air pollutants using organic compounds as tracers. *Environ. Sci. Technol.* **2000**, *34*, 1821-1832.

Simoneit, B. R. T. Chemical characterization of sub-micron organic aerosols in the tropical trade winds of the Caribbean using gas chromatography-mass spectrometry. A*tmos. Environ.* **2002**, *36*, 5259-5263.

Zheng, M.; Cass, G. R.; Schauer, J. J.; Edgerton, E. S. Source apportionment of $PM_{2.5}$ in the Southeastern United States using solvent-extractable organic compounds as tracers. *Environ. Sci. Technol.* **2002**, *36*, 2361-2371.

Cass, G. R. Organic molecular tracers for particulate air pollution sources. *Trends in Anal. Chem.* **1998**, *17*(6), 356-366.

Fine, P. M.; Cass, G. R.; Simoneit, B. R. T. Chemical characterization of fine particle emissions from fireplace combustion of woods grown in the Northeastern United States. *Environ. Sci. Technol.* **2001**, *35*, 2665-2675.

Schauer, J. J. Evaluation of elemental carbon as a marker for diesel particulate matter. *J. Exposure Anal. Environ. Epidem.* **2003**, *13*, 443-453.

Fraser, M. P.; Buzcu, B.; Yue, Z. W.; McGaughey, G. R.; Desai, N. R.; Allen, D. T.; Seila, R. L.; Lonneman, W. A.; Harley, R. A. Separation of fine particulate matter emitted from gasoline and diesel vehicles using chemical mass balancing techniques. *Environ. Sci. Technol.* **2003,** *37*, 3904-3909.

McGaughey, G. R.; Desai, N. R.; Allen, D. T.; Seila, R. L.; Lonneman, W. A.; Fraser, M. P.; Harley, R. A.; Pollack, A. K.; Ivy, J. M.; Price, J. H. Analysis of motor vehicle emissions in a Houston tunnel during the Texas Air Quality Study 2000. *Atmos. Environ.* **2004**, *38*(20), 3363-3372.

Hays, M. D.; Smith, N. D.; Dong, Y. Nature of unresolved complex mixture in size-distributed emissions from residential wood combustion as measured by thermal desorption-gas chromatography-mass spectrometry. *J. Geophys. Res.*, **2004**, *109* (D16S04).

Simoneit, B. R. T. Organic-matter of the troposphere. 3. Characterization and sources of petroleum and pyrogenic residues in aerosols over the Western United States *Atmos. Environ.* **1984**, *18*(1), 51-67.

Allen, J. O.; Dookeran, K. M.; Smith, K. A.; Sarofim, A. F.; Taghizadeh, K.; Lafleur, A. L. Measurement of polycyclic aromatic hydrocarbons associated with size-segregated atmospheric aerosols in Massachusetts. *Environ. Sci. Technol.* **1996**, *30*, 1023-1031.

Allen, J. O.; Dookeran, N. M.; Taghizadeh, K.; Lafleur, A. L.; Smith, K. A.; Sarofim, A. F. Measurement of oxygenated polycyclic aromatic hydrocarbons associated with a size-segregated urban aerosol. *Environ. Sci. Technol.* **1997**, *31*, 2064-2070.

Allen, J. O.; Durant, J. L.; Dookeran, N. M.; Taghizadeh, K.; Plummer, E. F.; Lafleur, A. L.; Sarofim, A. F.; Smith, K. A. Measurement of $C_{24}H_{14}$ polycyclic aromatic hydrocarbons associated with a size-segregated urban aerosol. *Environ. Sci. Technol.* **1998**, *32*, 1928-1932.

Garnes, L. A.; Allen, D. T. Size distributions of organonitrates in ambient aerosol collected in Houston, Texas. *Aerosol Sci. Technol.* **2002**, *36*(10), 983-992.

Misra, C.; Kim, S.; Shen, S.; Sioutas, C. A high flow rate, very low pressure drop impactor for inertial separation of ultrafine from accumulation mode particles. *J. Aerosol Sc.* **2002**, *33*, 735-752.

Kirchstetter, T. W.; Singer, B. C.; Harley, R. A.; Kendall, G. R.; Traverse, M. Impact of California reformulated gasoline on motor vehicle emissions. I. Mass emission rates. *Environ. Sci. Technol.* **1999b**, *33*, 318-328.

Mazurek, M. A.; Simoneit, B. R. T.; Cass, G. R.; Gray, H. A. Quantitative high-resolution gas-chromatography and high-resolution gas-chromatography mass-spectrometry analyses of carbonaceous fine aerosol-particles. *Int. J. Environ. Anal. Chem.* **1987**, *29*, 119-139.

Sheesley, R. J.; Schauer, J. J.; Chowdhury, Z.; Cass, G. R.; Simoneit, B. R. T. Characterization of organic aerosols emitted from the combustion of biomass indigenous to South Asia. *J. Geophys. Res. - Atmos.* **2003**, *108*, No. 4285.

Fraser, M. P.; Yue, Z. W.; Buzcu, B. Source apportionment of fine particulate matter in Houston, TX, using organic molecular markers. *Atmos. Environ* **2003**, *37*(15), 2117-2123.

Gross, D. S.; Galli, M. E.; Silva, P. J.; Wood, S. H.; Liu, D.Y.; Prather, K. A. Single particle characterization of automobile and diesel truck emissions in the Caldecott tunnel *Aerosol Sci. Technol.* **2000**, *32*(2), 152-163.

Kleeman, M. J.; Schauer, J. J.; Cass, G. R. Size and composition distribution of fine particulate matter emitted from motor vehicles. *Environ. Sci. Technol.* **2000**, *34*, 1132-11

Chapter 5: Roadside measurements of size-segregated particulate organic compounds near gasoline and diesel-dominated freeways in Los Angeles, CA*

*Phuleria H.C; Sheesley R.; Fine P.M.; Schauer J.J; Sioutas C. Roadside measurements of size-segregated particulate organic compounds near gasoline and diesel-dominated freeways in Los Angeles, CA. Submitted for publication to *Atmospheric Environment*, January 2007.

5.1 Chapter 5: ABSTRACT

Individual organic compounds such as hopanes and steranes (originating in lube oil) and selected polycyclic aromatic compounds (PAHs) (generated via combustion) found in particulate emissions from vehicles have proven useful in source apportionment of ambient particulate matter. Detailed information on the size-segregated (ultrafine and accumulation mode) chemical characteristics of organic particulate matter during the winter season originating from a pure gasoline traffic freeway (CA-110), and a mixed fleet freeway with the highest fraction of heavy-duty diesel vehicles in the state of California (I-710) is reported in this study. Hopanes and steranes as well as high molecular weight PAHs such as benzo(ghi)perylene (BgP) and coronene levels are found comparable near these freeways, while elemental carbon (EC) and lighter molecular weight PAHs are found much elevated near I-710 compared to CA-110. The roadway organic speciation data presented here is compared with the emission factors measured in the Caldecott tunnel, Berkeley CA (Phuleria et al., 2006) for light duty vehicles (LDVs) and heavy-duty vehicles (HDVs). Very good agreement is observed between CA-110 measurements and LDV emission factors (EFs) as well as I-710 measurements and corresponding reconstructed EFs from Caldecott tunnel for hopanes and steranes as well as heavier PAHs such as BgP and coronene. Our results, therefore, suggest that the

emission factors for hopanes and steranes obtained in tunnel environments, where emissions are averaged over a large vehicle-fleet, enable reliable source apportionment of ambient particulate matter (PM), given the overall agreement between the roadway vs tunnel concentrations of these species.

5.2 Chapter 5: INTRODUCTION

Several epidemiological studies have shown positive associations between adverse health effects and fine particles (diameter < 2.5 μm) (Pope and Dockery, 2006; Schwartz et al., 2002) as well as ultrafine particles (with aerodynamic diameter <100 nm) (Peters et al., 1997). Although the causal mechanisms are still uncertain, particle characteristics such as particle chemistry, number and size have been linked to the associated health effects.

In urban environments, vehicular emissions are the major sources of ultrafine and fine particles (Schauer et al., 1996; Sternbeck et al., 2002), which are of particular interest because of their potentially toxic components, such as PAHs and trace metallic elements, their high number and surface area relative to larger particles, and their ability to penetrate cell membrane and alleviated cardiovascular responses (Nel et al., 2006). A number of health studies have demonstrated the adverse health effects of diesel exhaust particles (Diaz-Sanchez et al., 2003; Mauderly, 1994; Weingartner et al., 1997). Children living near freeways have been shown to have increased prevalence of asthma and symptoms of airway allergies (Brunekreef et al., 1997; Kleinman et al., 2005; McDonald et al., 2004).

Vehicular emissions have been examined using a number of different methods including roadside measurements (Biswas et al., 2006; Hitchins et al., 2000; Kuhn et al., 2005a; 2005b; Zhu et al., 2002a; 2002b; 2004), on-road chase experiments (Canagaratna et al., 2004; Kittelson, 1998), laboratory dynamometer studies (Cadle et al., 1997; Rogge et al., 1993; Schauer et al., 1999; 2002; Zielinska et al., 2004), and measurements inside of roadway tunnels (Chellam et al., 2005; Geller et al., 2005; Kirchstetter et al, 1999; Phuleria et al., 2006*)*. Emission measurements based on dynamometer and chase experiments offer the advantage of precise and controlled testing conditions, which enable the evaluation of emissions control technologies over different driving conditions and cycles, including cold-start (Schauer et al., 2003). However, these tests cannot capture the large variation in engine type, age of the vehicles and maintenance history due to the high cost and complexity of such tests, and thus may not provide a good representation of the in-use vehicle fleet on the road. Such studies may also not account for particle aging effects, the mixing of emissions from different vehicles (Weingartner et al., 1997), and non-tailpipe emissions from tire wear, break-wear, and re-suspended road dust (Allen et al., 2001).

More realistic estimates of vehicle emissions, under actual on-road driving conditions, are possible using air-quality measurements in highway tunnels and near-roadside measurements. Roadway tunnel studies measure the cumulative contribution of the emissions from a large population of the on-road vehicle fleet mix under real-world driving conditions, thus more closely approximate actual on-road emissions than dynamometer tests. Limitations of tunnel measurements include sampling only the

specific driving conditions of the tunnel (thus missing cold-start emissions), and under dilution, temperature, and humidity conditions that may differ from ambient. Similar to tunnel studies, roadside studies provide the opportunity for PM measurements under actual ambient conditions and a representative large vehicle fleet. They also can provide the real exposure to vehicular emissions near - or within the freeway environment where people spend a significant amount of time during commute.

Several studies have utilized gas chromatography-mass spectrometry (GC-MS) methods for identification and quantification of individual organic compounds in atmospheric particulate matter (PM) samples (Fine et al., 2004; Fraser et al., 1998; 1999; 2003a; Phuleria et al, 2006; Schauer et al., 1996; Simoneit, 2002; Venkataraman et al., 1994). Many of these compounds or combinations of compounds are unique to different primary PM sources and have been used to apportion ambient PM using chemical mass balance (CMB) methods (Fraser et al., 2003a; 2003b; Schauer et al., 1996; 2000). These methods rely on representative and up-to-date source profiles for successful application. Hopanes and steranes, which are found in the lubricating oils employed by both gasoline and diesel powered motor vehicles, have been frequently used as organic tracers of primary vehicular particle sources (Cass, 1998; Schauer et al., 1996). High molecular weight PAHs such as BgP have been reported as a tracer of gasoline-powered vehicles, while diesel vehicles predominantly emit the lighter PAHs (Miguel et al., 1998; Zielinska et al., 2004).

Assessment of the relative contributions of diesel and gasoline vehicles to the overall PM urban load in the United States remains an elusive scientific undertaking (Gertler, 2005). While some studies using organic molecular markers to trace emissions have attributed greater contribution to ambient PM from diesel vehicles (Fraser et al., 2003a; Schauer et al., 1996; Zheng et al., 2002), others incorporating cold-start and poorly maintained gasoline engine source profiles attribute larger contributions to gasoline vehicles. These inconsistencies in sources attribution emanate largely from the differences in source profile selection, seasonal differences in emissions and the time and place of the studies (Fraser et al., 2003a; Gertler, 2005). From a regulatory standpoint, it is very important to accurately segregate diesel and gasoline particulate emissions and thus, more representative and robust real-world source profiles for these classes of vehicles are desired.

The primary goal of this study is to provide detailed information on the chemical characteristics of organic PM originating from a pure gasoline traffic freeway, and a mixed fleet freeway with the highest fraction of heavy-duty diesel vehicles in the state of California. Size-resolved PM samples (ultrafine and accumulation mode) were collected, and speciated organic tracer concentrations were measured using GC-MS methods. A comparison is made between the roadway organic speciation data presented here with the emission factors measured in the Caldecott tunnel, Berkeley, CA for LDVs and HDVs, in order to validate their use in source apportionment models.

5.3 Chapter 5: METHODS

5.3.1. Sampling locations

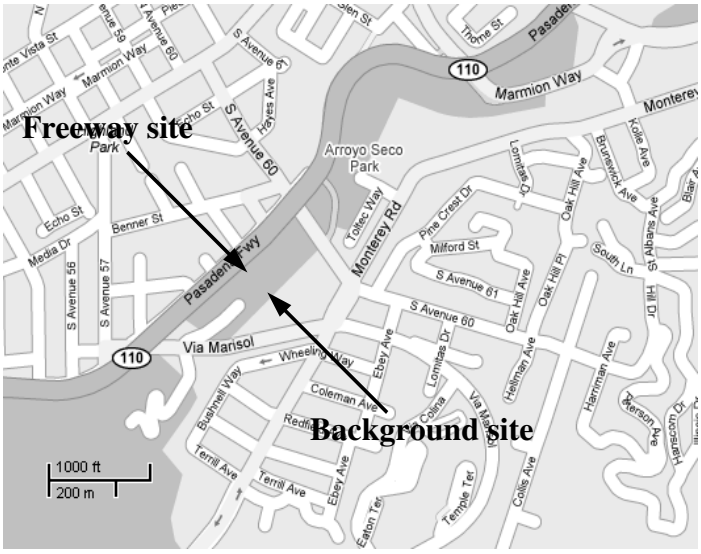

FIGURE 5.1a. Sampling locations near CA-110 Freeway

Field samples were collected near the CA-110 freeway as well as near the I-710 freeway in Los Angeles, CA. A detailed description of the CA-110 freeway environment, traffic characteristics and sampling procedure is described by Kuhn et al. (2005a). Briefly, measurements were conducted at the CA-110, between downtown Los Angeles and Pasadena, CA as shown in figure 5.1a. On this stretch of the freeway, only light-duty vehicles are permitted thus affording a unique opportunity of studying emissions from pure light-duty traffic under ambient conditions. The study took place in January 2005, from about 12 p.m. to 7 p.m. every day, capturing the evening rush-hour traffic. Samples were collected from two different sites, one of which was very close to the three northbound traffic lanes, at a distance of around 2.5 m from the edge of the freeway. The other site was chosen to characterize background aerosols at a greater distance to the freeway (~150 m).

Detailed description of the I-710 freeway measurements can be found elsewhere (Biswas et al., 2006; Ntziachristos et al., 2006) and only a brief description follows. The sampling location (see figure 5.1b) was directly adjacent to the roadway, at approximately 10 m from the centerline of the freeway, with no other immediate sources either upwind or downwind. Background measurements were conducted at Downey, CA, a location 1.6

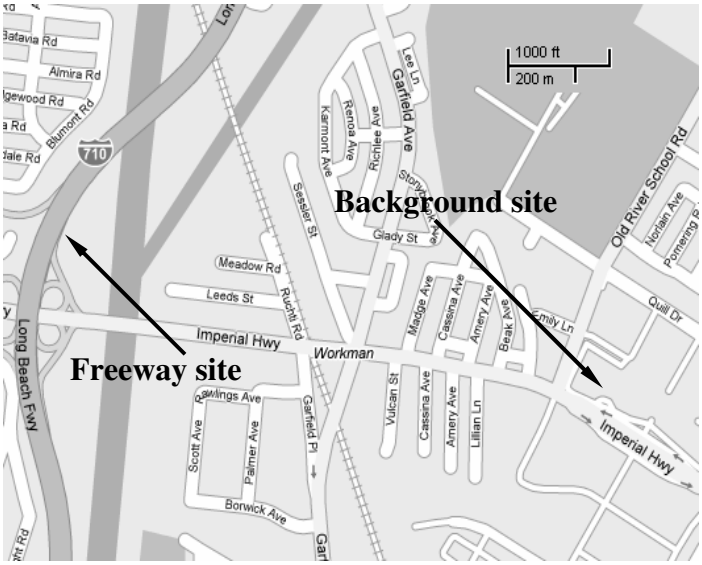

FIGURE 5.1b. Sampling locations near I-710 Freeway

km southeast (hence downwind) of the freeway, at the facilities of Rancho Los Amigos Rehabilitation Center. The sampling campaign took place during February and March of 2006, and from 11am -7 pm each day, similar to the CA-110 measurements.

5.3.2. Traffic characterization

Traffic volume and average speed data in each freeway were obtained from the California Department of Transportation. Manual and videotaped counts were also taken for one

minute out of every five minutes during selected sampling intervals. Estimates for counts broken down by vehicle type were done by analyzing the videotapes and counting the number of axles per vehicle. The average traffic density on the CA-110 freeway was about 4,500-5,400 vehicles per hour. Traffic speed was fairly constant during the day and, even during evening rush hour no significant slowing of traffic was observed (Kuhn et al., 2005a). The traffic volume and vehicle characteristics on the I-710 freeway during the sampling campaign are described by Ntziachristos et al. (2006). Heavy-duty vehicles comprised an average of 17 % of the total vehicles on the I-710. Total traffic counts on this freeway are also very high, with approximately 10,000-11,000 vehicles per hour passing the sampling location.

5.3.3. Pollutant measurement and sample collection

Gaseous and particulate pollutant concentrations near the freeways were measured with various continuous and time-integrated instruments. PM collection was accomplished with a custom built, high-volume (450 lpm) sampler designed to separate and collect coarse ($Dp > 2.5$ μm), accumulation ($0.18 < Dp < 2.5$ μm) and ultrafine mode ($Dp < 0.18$ μm) aerosols (Misra et al., 2002). The sampler collects particles with aerodynamic diameters greater than about 0.18 μm onto quartz-fiber impaction strips. A preceding impaction stage with a 2.5 μm aerodynamic diameter cut-point removes coarse particles. Downstream of the ultrafine impactor, an 8 x 10 inch high-volume filter holder containing Quartz-fiber filters (Pallflex® Tissuquartz™ 2500QAT-UP-8x10, Pall Corp.) is used to collect the ultrafine PM fraction. Field blanks for quartz filters contained negligible levels of the compounds quantified in this study. Quartz filters and substrates

were pre-baked at 550 ^{o}C for 8 hours and stored in baked aluminum foil prior to deployment (Phuleria et al., 2006). For gravimetric measurements, two micro-orifice uniform deposit impactors (MOUDI, MSP, Inc., Minneapolis, MN) sampled concurrently at 30 lpm at the freeway and background sites. 4.7 cm PTFE filters were used as impaction substrates for coarse and accumulation mode PM, and a 3.7 cm PTFE filter was used to collect ultrafine PM. Similar to high volume sampler, the MOUDI was used to collect coarse ($10 < Dp < 2.5$ μm), accumulation ($2.5 < Dp < 0.18$ μm) and ultrafine ($Dp < 0.18$ μm) size particles.

5.3.4. Organic Speciation Analysis

Methods for the quantification of individual organic compounds in ambient particulate matter were based on earlier established solvent extraction methods (Schauer et al., 1999; 2002; Sheesley et al., 2003). Procedures for sample extraction and molecular quantification for the organic tracers is described in detail elsewhere (Phuleria et al., 2006) and only a brief summary is presented here. The quartz filter samples from the high-volume sampler were spiked with known amounts of isotope labeled internal standard compounds, including three deuterated PAHs, two deuterated alkanoic acids, deuterated cholestane, deuterated cholesterol, and C^{13} labeled levoglucosan. Samples were extracted in dichloromethane and methanol and were combined and reduced in volume to approximately 1 mL by rotary evaporation followed by pure nitrogen evaporation. One fraction of the extracts was derivatized for organic acid analysis, the results of which are not presented here. The other fraction was further reduced to a specified volume ranging from 50 to 200 μL by evaporation under pure nitrogen. The

final target volume was determined based on the amount of organic carbon mass in each sample (Phuleria et al., 2006).

The underivatized samples were analyzed by auto-injection into a GC/MSD system (GC model 5890, MSD model 5973, Agilent). A 30 m x 0.25 mm DB-5MS capillary column (Agilent) was used with a splitless injection. Along with the samples, a set of authentic quantification standard solutions were also injected and used to determine response factors for the compounds of interest. While some compounds are quantified based on the response of a matching compound in the standard mixtures, others for which matching standards were not available are quantified using the response factors of compounds with similar structures and retention times. Analytical errors for these methods have been reported to be no more than 25% (Fine et al., 2004; Sheesley et al., 2003).

5.4. Chapter 5: RESULTS AND DISCUSSION

5.4.1. Mean measured organic species concentrations

The ambient concentrations of each organic species at the CA-110 were found to be higher near the freeway site compared the background site (Table 5.1a). However, the difference is not very significant (i.e., on the order of 20-30%) for most of the chemical species, PM mass, and EC (Table 5.2), indicating a significant impact of freeway emissions at the distant site. The traffic impact on that site is also manifested by the somewhat higher CO_2 concentrations measured during our study (427 ± 44 ppm) compared to typical background CO_2 levels of 375-380 ppm (Ntziachristos et al., 2006).

The relatively similar levels for these PM species are in contrast to the influence of freeways on nearby sites based on particle numbers as well as gaseous co pollutants such as CO, NO_x that originate from traffic sources (Zhu et al., 2002a; 2002b; 2004). Given the

TABLE 5.1a. Mean mass concentration (in ng/m^3) of the organic tracers measured near CA-110 Freeway

Organic Species	Ultrafine mode				Accumulation mode			
	Freeway		Background		Freeway		Background	
	Mean	SD	Mean	SD	Mean	SD	Mean	SD
PAHs								
Pyrene	0.328	0.103	0.238	0.126	0.058	0.024	0.048	0.006
Benzo(ghi)fluoranthene	0.171	0.030	0.141	0.075	0.037	0.018	0.028	0.004
Benz(a)anthracene	0.108	0.068	0.096	0.070	0.029	0.020	0.017	0.003
Chrysene	0.220	0.071	0.181	0.108	0.047	0.023	0.036	0.010
Benzo(k)fluoranthene	0.149	0.078	0.125	0.090	0.035	0.013	0.025	0.008
Benzo(b)fluoranthene	0.211	0.095	0.183	0.133	0.044	0.017	0.035	0.009
Benzo(j)fluoranthene	0.016	0.021	0.019	0.019	0.005	0.004	0.004	0.001
Benzo(e)pyrene	0.210	0.087	0.179	0.121	0.046	0.016	0.035	0.010
Benzo(a)pyrene	0.172	0.128	0.159	0.132	0.043	0.017	0.034	0.011
Perylene	0.032	0.026	0.029	0.024	0.008	0.003	0.006	0.002
Indeno(cd)pyrene	0.163	0.111	0.145	0.116	0.038	0.014	0.032	0.009
Benzo(ghi)perylene	0.454	0.306	0.412	0.331	0.084	0.030	0.074	0.023
Indeno(cd)fluoranthene	0.046	0.038	0.047	0.043	0.011	0.004	0.010	0.003
Dibenz(ah)anthracene	0.013	0.011	0.012	0.010	0.004	0.001	0.004	0.001
Coronene	0.275	0.195	0.271	0.230	0.047	0.020	0.045	0.017
Hopanes and Steranes								
22,29,30-Trisnorhopane	0.373	0.117	0.295	0.192	0.046	0.018	0.040	0.016
22,29,30-Trisnorneohopane	0.488	0.130	0.362	0.229	0.054	0.016	0.044	0.019
17α(H)-21α(H)-30-Norhopane	1.201	0.505	0.951	0.725	0.151	0.059	0.129	0.046
18α(H)-29-Norneohopane	0.335	0.159	0.246	0.201	0.037	0.016	0.027	0.009
17α(H)-21β(H)-Hopane	1.767	0.983	1.362	1.137	0.186	0.078	0.148	0.064
22S-Homohopane	0.536	0.249	0.401	0.327	0.069	0.031	0.056	0.021
22R-Homohopane	0.474	0.238	0.366	0.311	0.066	0.030	0.054	0.026
22S-Bishomohopane	0.282	0.116	0.230	0.172	0.044	0.020	0.037	0.015
22R-Bishomohopane	0.254	0.138	0.196	0.156	0.034	0.014	0.026	0.012
22S-Trishomohopane	0.208	0.072	0.171	0.127	0.041	0.021	0.029	0.014
22R-Trishomohopane	0.132	0.069	0.099	0.078	0.022	0.013	0.018	0.006
20(R+S), $\alpha\beta\beta$-Cholestane	0.072	0.023	0.056	0.034	0.017	0.005	0.014	0.007
20R, $\alpha\alpha\alpha$-Cholestane	0.387	0.151	0.294	0.179	0.080	0.028	0.074	0.038
20(R+S), $\alpha\beta\beta$-Ergostane	0.102	0.044	0.102	0.065	0.025	0.009	0.024	0.011
20(R+S), $\alpha\beta\beta$-Sitostane	0.484	0.198	0.385	0.292	0.114	0.044	0.090	0.036

TABLE 5.1b. Mean mass concentration (in ng/m^3) of the organic tracers measured near I-710 Freeway

Organic species	Ultrafine mode				Accumulation mode			
	Freeway		Background		Freeway		Background	
	Mean	SD	Mean	SD	Mean	SD	Mean	SD
PAHs								
Pyrene	0.590	0.201	0.041	0.020	0.025	0.009	0.010	0.004
Benzo(ghi)fluoranthene	0.446	0.184	0.060	0.028	0.035	0.014	0.021	0.006
Benz(a)anthracene	0.307	0.138	0.011	0.001	0.011	0.002	0.010	0.004
Chrysene	0.264	0.123	0.057	0.028	0.030	0.014	0.015	0.010
Benzo(k)fluoranthene	0.126	0.067	0.032	0.017	0.012	0.002	0.015	0.011
Benzo(b)fluoranthene	0.194	0.062	0.078	0.016	0.051	0.020	0.039	0.011
Benzo(j)fluoranthene	0.062	0.004	ND		ND		ND	
Benzo(e)pyrene	0.250	0.108	0.075	0.022	0.037	0.014	0.031	0.015
Benzo(a)pyrene	0.147	0.085	0.057	0.025	0.024	0.010	0.029	0.010
Perylene	0.044	NA	ND		ND		ND	
Indeno(cd)pyrene	0.233	0.098	0.088	0.023	ND		ND	
Benzo(ghi)perylene	0.531	0.198	0.190	0.064	0.020	0.008	0.030	0.011
Indeno(cd)fluoranthene	NR		NR		NR		NR	
Dibenz(ah)anthracene	ND		ND		ND		ND	
Coronene	0.292	0.115	0.111	0.030	0.009	NA	0.018	0.007
Hopanes and Steranes								
22,29,30-Trisnorhopane	0.257	0.098	0.062	0.028	0.025	0.012	0.014	NA
22,29,30-Trisnorneohopane	NR		NR		NR		NR	
17α(H)-21α(H)-30-Norhopane	0.614	0.249	0.157	0.057	0.086	0.014	0.048	0.008
18α(H)-29-Norneohopane	NR		NR		NR		NR	
17α(H)-21β(H)-Hopane	0.434	0.215	0.111	0.044	0.058	0.016	0.037	0.004
22S-Homohopane	0.192	0.103	0.049	0.023	0.030	0.005	0.018	0.005
22R-Homohopane	0.159	0.096	0.049	0.023	0.025	0.013	0.015	0.007
22S-Bishomohopane	0.139	0.088	0.048	NA	0.009	NA	0.014	NA
22R-Bishomohopane	0.073	0.020	0.019	NA	0.019	NA	0.009	NA
22S-Trishomohopane	NR		NR		NR		NR	
22R-Trishomohopane	NR		NR		NR		NR	
20(R+S), $\alpha\beta\beta$-Cholestane *	0.282	0.106	0.095	0.028	0.026	0.015	0.023	NA
20R, $\alpha\alpha\alpha$-Cholestane	0.250	0.122	0.081	0.045	0.029	0.020	0.026	NA
20(R+S), $\alpha\beta\beta$-Ergostane *	0.330	0.192	0.036	0.009	0.023	NA	ND	
20(R+S), $\alpha\beta\beta$-Sitostane *	0.376	0.229	0.080	0.087	0.055	0.030	0.040	NA

ND = Not detected; NR = Not reported; NA = Not applicable
* R and S isomers measured separately and summed together

smaller sized primary particles emitted by vehicles, most of the organic species were measured to be an order of magnitude higher in ultrafine than the accumulation mode.

The dominant PAHs near the CA-110 freeway are BgP, coronene and pyrene. 17α(H)-21β(H)-29-norhopane and 17α(H)-21β(H)-hopane are the pre-dominant hopanes in both size modes and at both sites. Similar to PAHs, hopanes and steranes are measured in comparable amounts at freeway and background sites near CA-110 in both size modes (Figure 5.2a-b). Unlike the CA-110, the concentrations of EC and several organic species are substantially higher at the proximal site of the I-710 freeway compared to the urban background site (Figure 5.3b; Table 5.2), possibly a result of the longer distance to that background site (~1.6 km downwind of the freeway) compared to the background site at the CA-110. The CO_2 level in the urban background site is also close to its typical background levels (Table 5.2).

TABLE 5.2. Mean concentrations of the meteorological and bulk-chemical parameters measured near CA-110 and I-710 Freeway

Parameters	CA-110				I-710			
	Freeway		Background		Freeway		Background	
	Mean	SD	Mean	SD	Mean	SD	Mean	SD
CO_2 (ppm)	476	39	427	44	430	28	383	10
T (^{0}C)	21.6	3.0	21.3	3.4	18.9	2.9	18.0	2.2
RH (%)	50.7	14.2	50.1	15.3	46.0	11.8	45.3	7.0
$PM_{2.5}$ (μg/m^3)	20.0	11.2	15.7	5.6	15.4	5.1	12.0	6.0
$EC_{2.5}$ (μg/m^3)	1.8	1.2	1.4	0.9	3.3	0.6	0.7	0.3
$OC_{2.5}$ (μg/m^3)	14.9	5.2	11.4	6.6	6.9	1.8	5.4	1.6

Lighter PAHs are an order of magnitude higher near the freeway site, while heavier PAHs, such as BgP and coronene as well as hopanes and steranes are about 3-4 times higher near I-710 freeway site compared to background measurements for ultrafine PM. The accumulation mode PM concentrations are comparable at both locations, and account

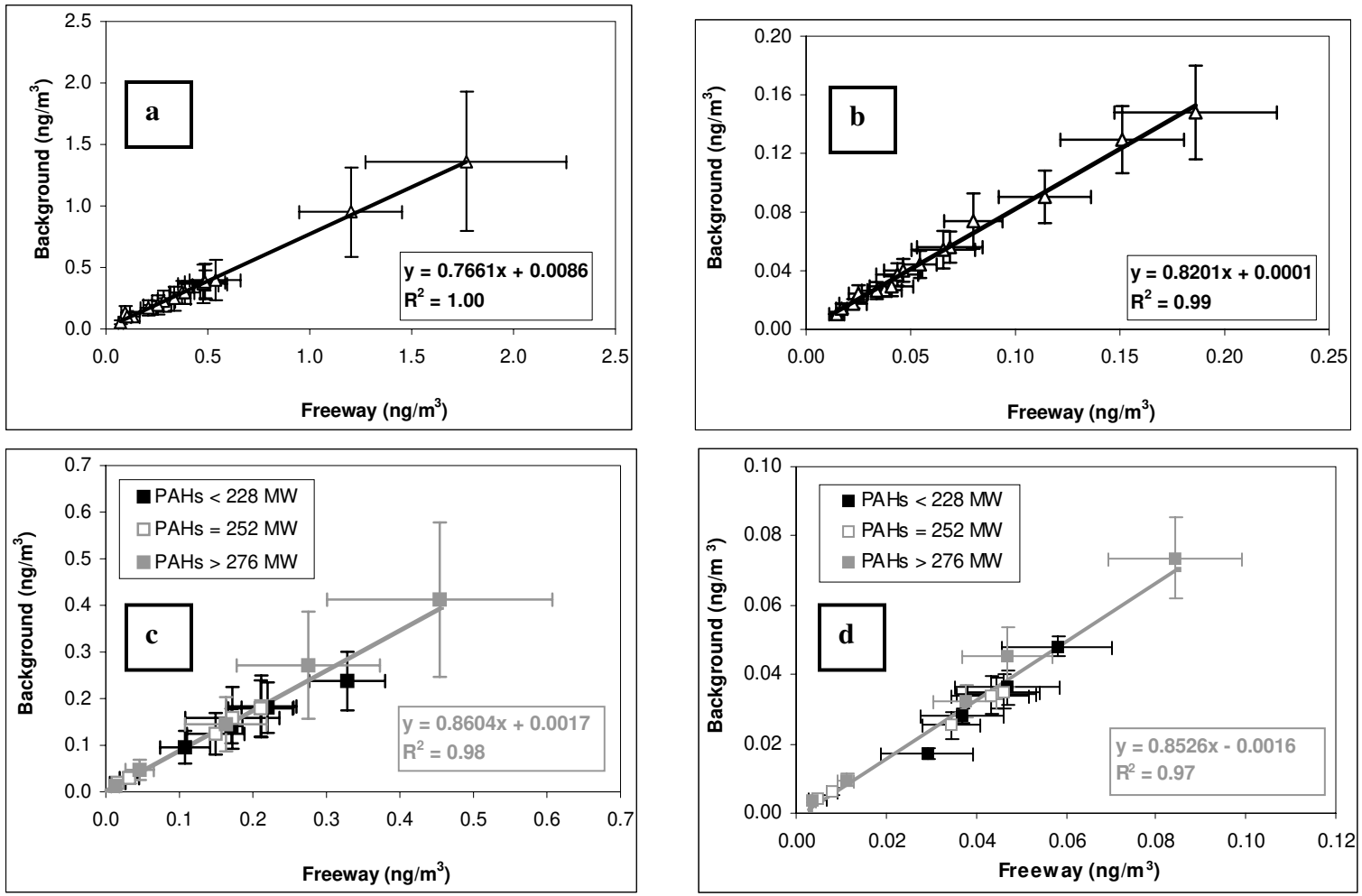

Figure 5.2 Correlation of organic species between freeway and background sites near CA-110 in a) ultrafine size mode for hopanes and steranes; b) accumulation size mode for hopanes and steranes; c) ultrafine size mode for PAHs; and d) accumulation size mode for PAHs. Uncertainty in the measurements is presented in terms of standard error (SE).

on average for 10% or less of the total $PM_{2.5}$ concentrations of these organic species. Pyrene, benzo(ghi)fluoranthene, benzo(a)anthracene, BgP and coronene are the predominant PAHs near the freeway. Benzo(b)fluoranthene has the highest concentrations in the accumulation mode at the freeway as well as background sites. Hopanes and steranes are about 3-4 times higher at the freeway than the background site for most species in ultrafine size mode (Figure 5.2a); however, similar levels are observed in the accumulation mode between the two sites (Figure 5.2b).

Figures 5.2a-d illustrate the impact of CA-110 freeway emissions to the background site. The very high correlation (~ 1) and slopes (~0.8) of the plotted linear regressions suggest that emissions from gasoline vehicles on CA-110 are the predominant and possibly the single source of PAHs and hopanes and steranes at a distance 150 m away from the freeway. Also the mass of the organics tracers is dominated by the ultrafine mode (90%) at both the sites.

Similarly, Figures 5.3a-d present the correlations between the concentrations of PAHs and hopane and steranes in different PM size mode at the I-710 freeway and background sites. Unlike the case of the CA-110, we find a lower linear regression slope between the proximal and distant sites for these species. High correlation, but smaller slope for hopanes and steranes, indicates that background site is influenced by the freeway emissions, but to a lower degree, as a result of higher atmospheric dilution, given its distance from the freeway. The ultrafine mode concentrations of PAHs and hopanes-

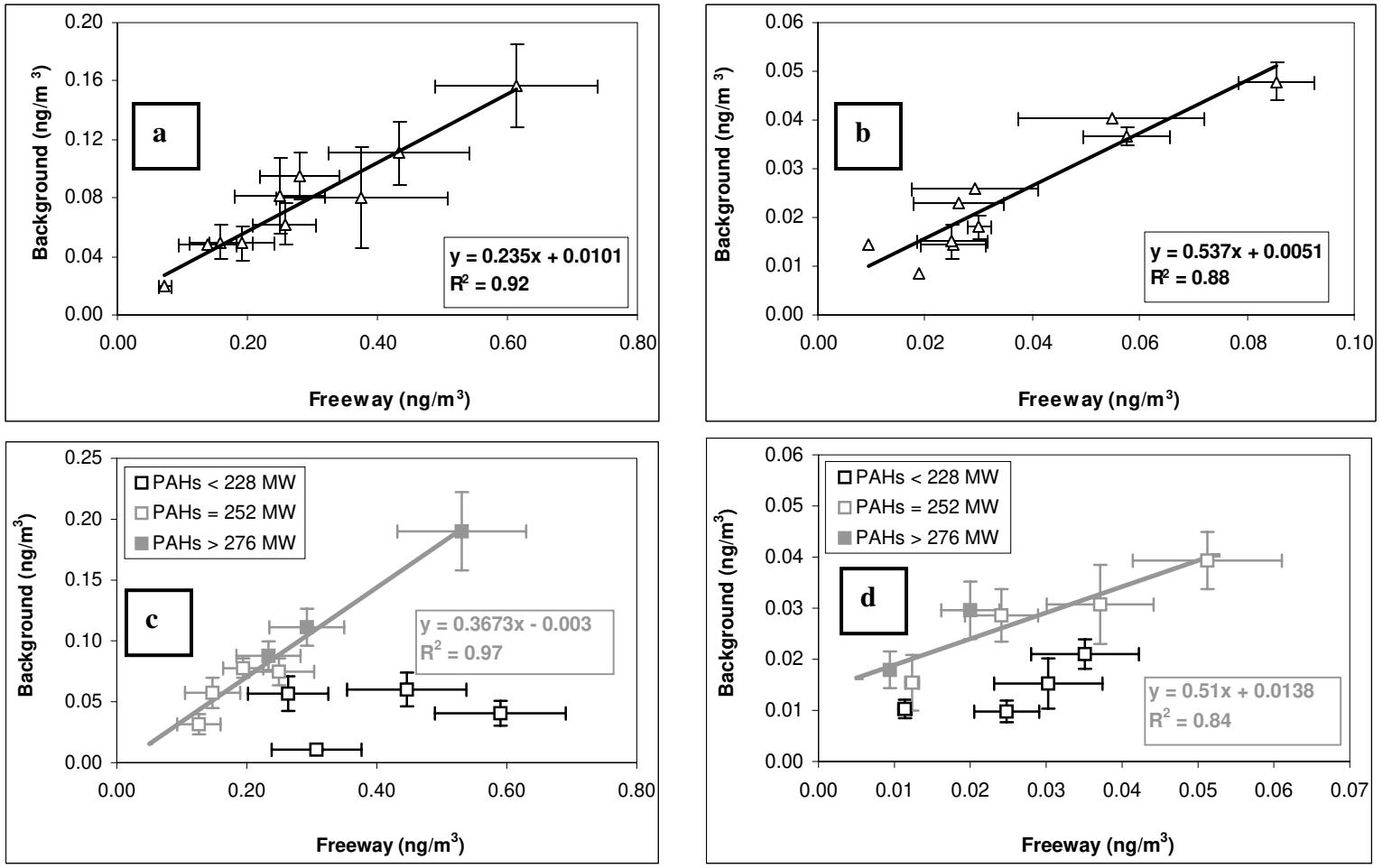

Figure 5.3 Correlation of organic species between freeway and background sites near I-710 in a) ultrafine size mode for hopanes and steranes; b) accumulation size mode for hopanes and steranes; c) ultrafine size mode for PAHs; and d) accumulation size mode for PAHs. Uncertainty in the measurements is presented in terms of SE. Also, the correlation coefficient for PAHs is calculated for PAHs $\geq$ 252 MW only (Figure c and d).

steranes are roughly 0.25-0.37 those of the freeway site, and about 50% lower that those of the freeway site in the accumulation mode. The degree of correlation and linear regression slopes between the freeway and background sites for both ultrafine and accumulation PM mode are quite similar between higher MW PAHs and hopanes-steranes, whereas the degree of correlation decreases for the more volatile, lighter PAHs. This finding is consistent with previous experimental (Biswas et al., 2006; Kuhn et al., 2005a; 2005b) and theoretical (Zhang et al., 2005) studies on the fate of semi-volatile labile species emitted from vehicles as they move away from the freeway, indicating a greater decrease in concentration with distance from the freeway due to evaporative losses in addition to atmospheric dilution.

5.4.2. Comparison of CA-110 and I-710 measurements

Direct comparison in the PAH and hopanes- steranes levels at CA-110 and I-710 freeway sites reveals that higher concentrations are observed near the CA-110. While HDVs generally emit one order of magnitude higher hopanes and steranes than LDVs (excluding poor maintenance high emitters and non-cat gasoline driven vehicles) (Phuleria et al; 2006; Schauer et al., 2002; Zielinska et al., 2004), the higher levels at CA-110 (which is a pure gasoline freeway) may be due to lower atmospheric dilution and high background influence compared to I-710. CO_2 concentrations, which have been used as a measure of atmospheric dilution ratio (Ntziachristos et al., 2006), are quite similar at the I-710 freeway site and the CA-110 background site, and substantially higher at the CA-110 freeway site, suggesting significantly higher atmospheric dilution during the

field experiments at the I-710 (Table 2). While CO_2 levels are starkly different in these two studies, temperature and relative humidity are similar between these measurements. Based on the above discussion, a direct comparison of the measurements near these two freeways may not be appropriate without taking into account the higher atmospheric dilution conditions during the measurements at I-710. In order to account for the different background sources and different degrees of atmospheric dilution, the concentrations of hopanes-steranes and PAHs at the freeway sites were adjusted by subtracting the background and normalized according to equation (5.1)

$$\text{Normalized Pollutant concentration} = (P_{FW} - P_{BG}) / (CO_{2\,FW} - CO_{2\,BG}) \qquad \ldots(5.1)$$

where, P_{FW} and P_{BG} are the organic species concentration measured at freeway and background sites and $CO_{2\ FW}$ and $CO_{2\ BG}$ are the corresponding CO_2 concentrations measured at the freeway and background sites respectively. Assuming insignificant CO levels, this normalization effectively provides a roadway emission rate per unit of fuel.

These normalized concentrations (or pseudo-emission rates) are shown in Figures 5.4a and 5.4b. Similar normalized concentrations for hopanes and steranes can be observed for CA-110 and I-710 freeways (Figure 5.4a), especially given the uncertainty in the measurements. This implies that even at the I-710, with a HDV fraction of about 20%, the overall levels of hopanes and steranes are dominated by gasoline vehicles. Heavy MW PAHs also have similar normalized concentrations on these freeways (Figure 5.4b).

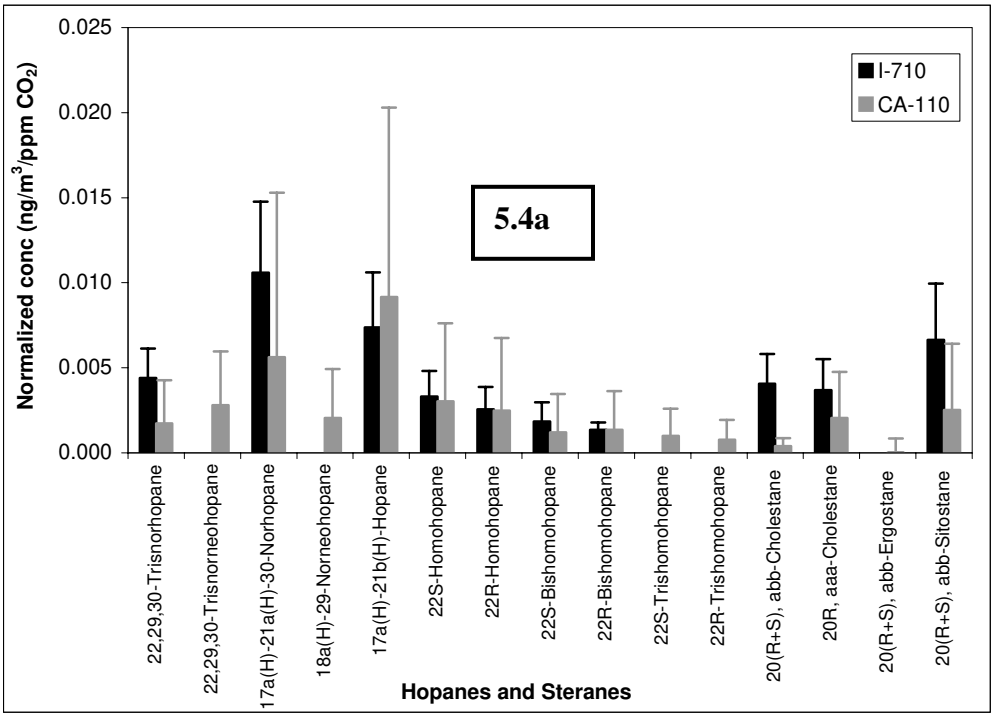

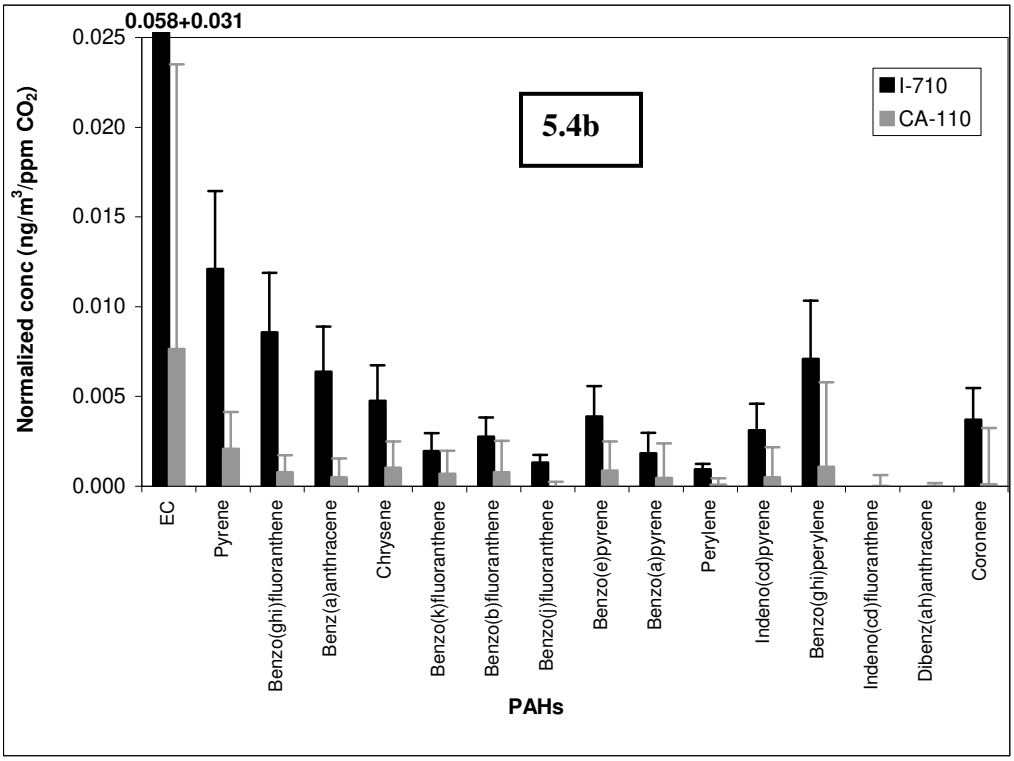

Figure 5.4 Comparison of measured - a) hopanes and steranes (normalized to ΔCO_2); and b) PAHs and EC (normalized to ΔCO_2) - between CA-110 and I-710 in $PM_{2.5}$ size mode. Error bars represent SE.

As the levels of species at the background site were comparable to the freeway site in CA-110 (Table 5.1a), subtracting them resulted in larger uncertainty. The difference in the absolute levels of these PAHs, however, is not as striking, possibly because heavy molecular weight PAHs are shown to be emitted more in creep and transient driving modes (Shah et al., 2005) as well as cold start conditions (Cadle et al., 1999; Schauer et al., 2003), compared to the cruise driving conditions of our study at both I-710 and CA-110. In contrast to hopanes- steranes and heavy PAHs, the emission of EC and lighter PAHs are dominated by diesel-powered vehicles (Figure 5.4b), implying a significantly higher contribution of diesel vehicles to the ambient concentrations of these species.

5.4.3. Chemical profiles of organic markers

The concentrations of vehicular molecular markers measured in this study are compared with the emission factors measured in a similar study conducted at the Caldecott roadway tunnel in Berkeley, CA (Phuleria et al., 2006). Size-segregated, fuel-based emission factors (EFs) were calculated for LDVs and HDVs using exactly the same sampling system for PM collection as that in the present study. Since this study has focused on organic molecular markers only, the chemical profiles of these organic markers are presented as a fraction of total carbon (TC) (in units of ng/μg TC). LDV emission factors (normalized to TC) from the Caldecott tunnel are compared with the pure gasoline vehicle emissions (normalized to TC) on the CA-110. For a similar comparison of the I-710 measurements, reconstructed EFs were obtained using equation 5.2:

$$EF_{Reconstructed} = 0.8 \times EF_{LDV} + 0.2 \times EF_{HDV} \quad \ldots(5.2)$$

where, $EF_{Rreconstructed}$ represented the expected mixed-fleet emission factor for the 20% HDV fraction on I-710 based on EF_{LDV} and EF_{HDV}, LDV and HDV emission factors measured in the Caldecott tunnel, respectively. The reconstructed EFs were calculated to account for the 20% HDV fraction measured at I-710 based on our traffic counts during this study period. The reconstructed EFs normalized to TC (in ng of organic species per μg of TC) are compared with those of normalized measurements from the I-710.

Figure 5.5a shows the normalized chemical profile of hopanes and steranes at the CA-110 freeway against those measured inside the pure LDV bore of the Caldecott tunnel. The normalized mass concentrations of these molecular markers have virtually identical chemical profiles in these two different environments. The normalized tunnel concentrations are slightly lower than the corresponding normalized levels at the CA-110, possibly because of the higher TC levels due to some positive artifacts in the ultrafine size mode at the tunnel compared to the freeway. This is because higher concentrations of gas-phase organics in the tunnel would result in overestimation of TC due to increased adsorption of these species on the PM –collecting filters and therefore might be responsible for the somewhat observed lower hopane-sterane/TC ratios in the Caldecott tunnel compared to the CA-110 measurement. Similarly, Figure 5.5b, demonstrates generally very similar chemical profiles measured at the I-710 freeway compared to the reconstructed normalized concentrations from the Caldecott tunnel measurements.

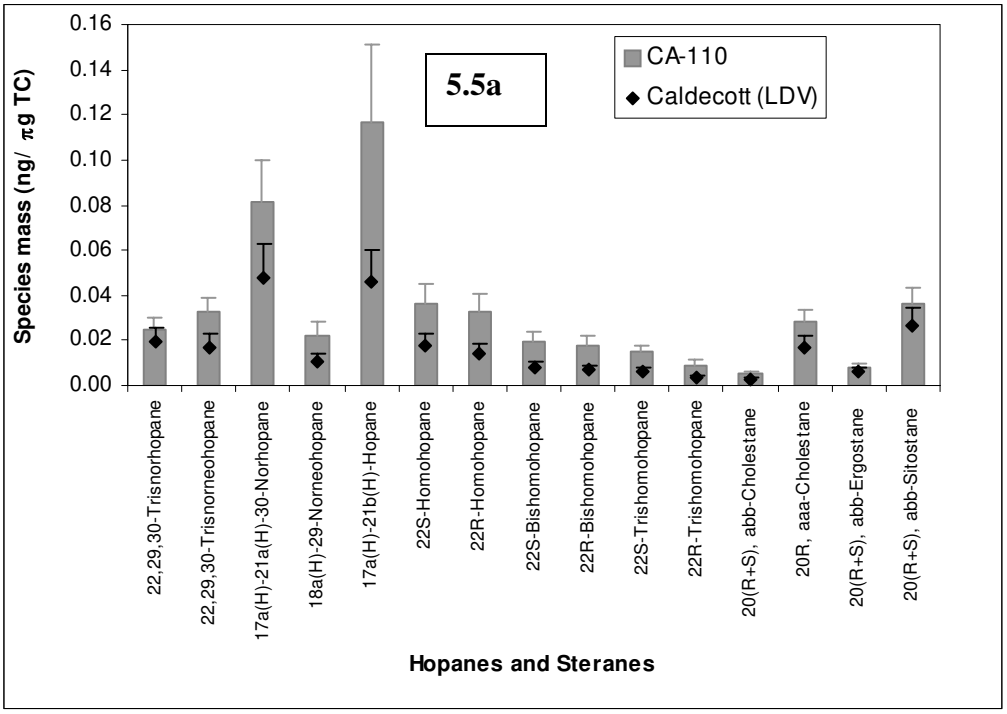

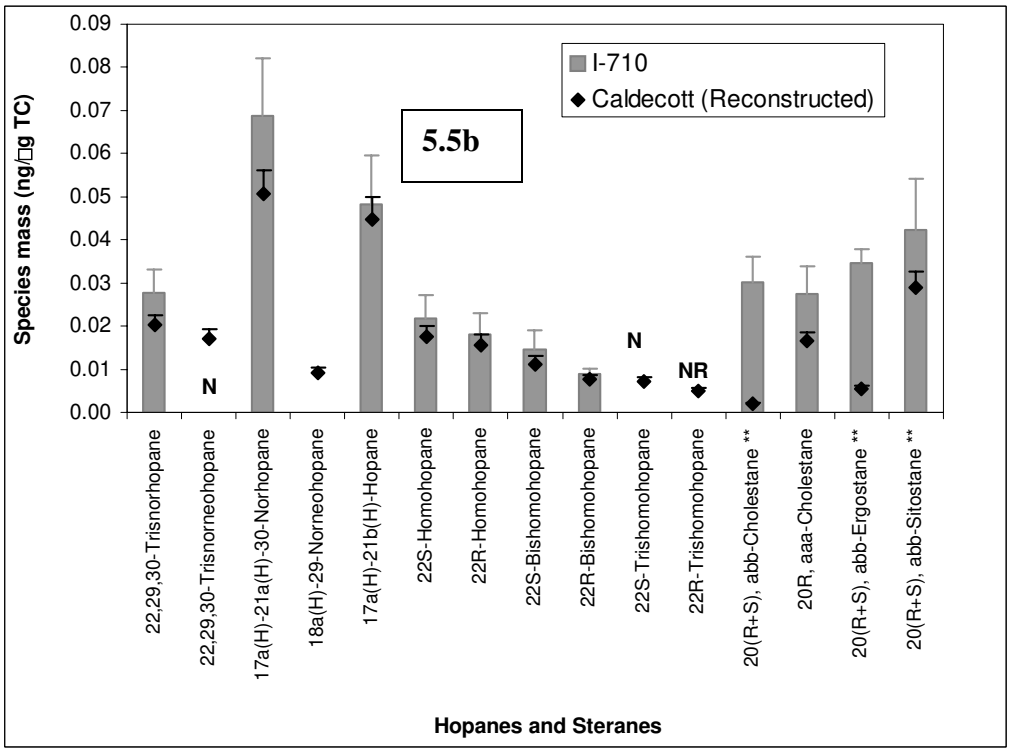

Figure 5.5. Chemical profile of hopanes and steranes (normalized to TC) in a) CA-110 and Caldecott (LDV) study and b) I-710 study and Reconstructed Caldecott study.

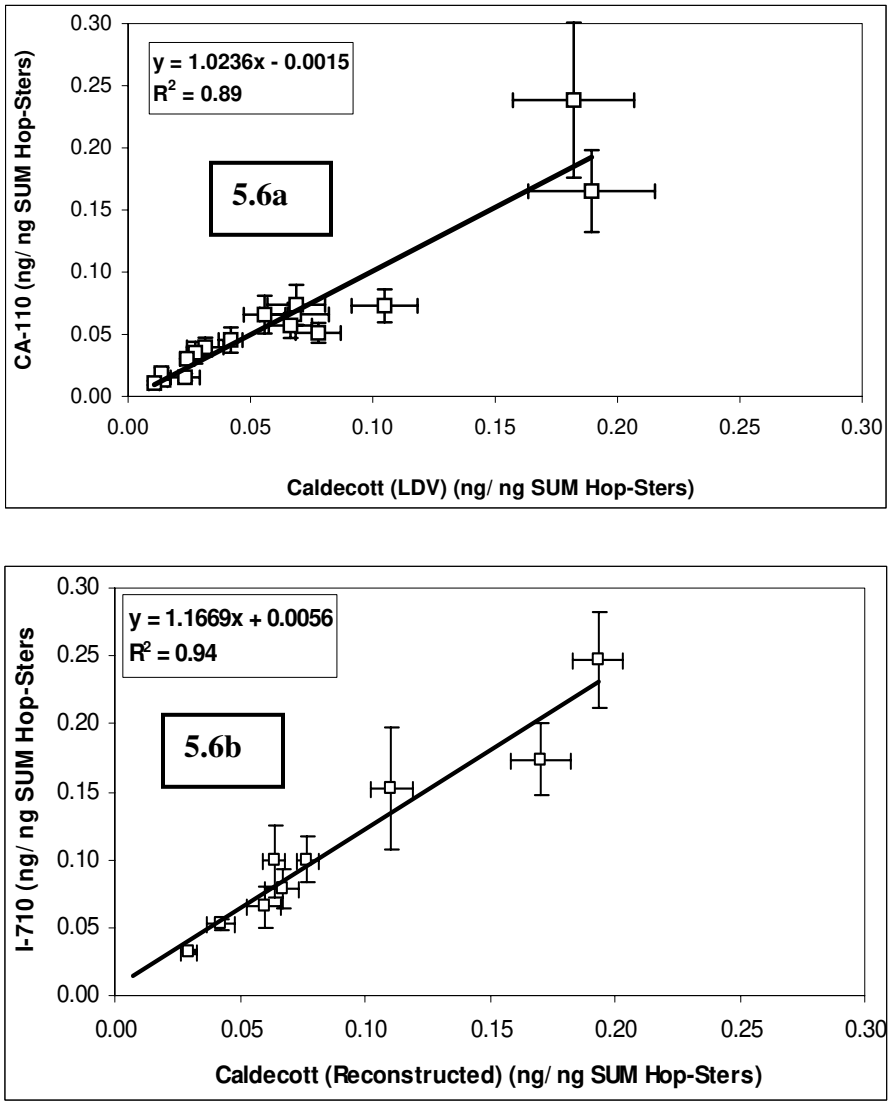

Figure 5.6. Correlation of hopanes and steranes (normalized to Sum of hopanes and steranes) in $PM_{2.5}$ size mode between a) CA-110 study and Caldecott (LDV) study; and b) b) I-710 study and Reconstructed Caldecott study. Error bars represent SE.

Several studies have shown similar source profile of hopanes and steranes between gasoline and diesel engines tested on dynamometer facilities (Cadle et al., 1999; Zielinska et al., 2004) as well as between on road LDV and HDV fleet in tunnel environment (Phuleria et al., 2006). Fraser et al. (1999) have also shown consistent

agreement between relative chemical distribution of hopanes and steranes measured in ambient air vis-à-vis tunnel emission rate measurements. In order to illustrate the internal consistency among individual hopane and steranes species, a correlation between the CA-110 measurements (normalized to sum of hopanes and steranes) and LDV emission factors (normalized to sum of hopanes and steranes) from the Caldecott tunnel study is given in Figure 5.6a. Correlation between normalized I-710 measurements and normalized reconstructed emission factors obtained from the Caldecott tunnel are shown in Figure 5.6b. The very high correlations and slopes ~1 illustrate the conservative nature of these organic markers and reaffirm their use as reliable markers of vehicular emissions.

This correlation is reflective of the natural distribution of hopanes-steranes found in the crude oil stock used to make lubricating oil. It should be noted that the lower number of data points in Figure 5b is due the fact that few hopanes are not reported and correlations are only obtained for the available data. The data plotted in Figures 5.6a and 5.6b show that the relative concentrations (normalized to sum of hopanes and steranes) of these individual species is similar in vehicles powered by either gasoline or diesel engines, consistent with the notion that that these species originate from lubricating oil (Fine et al., 2004, Fraser et al., 1998). Zielinska et al (2004) have studied the fuel and oil properties used in gasoline and diesel engines and showed that hopane and steranes are only present in lubricating oil and not in the fuel.

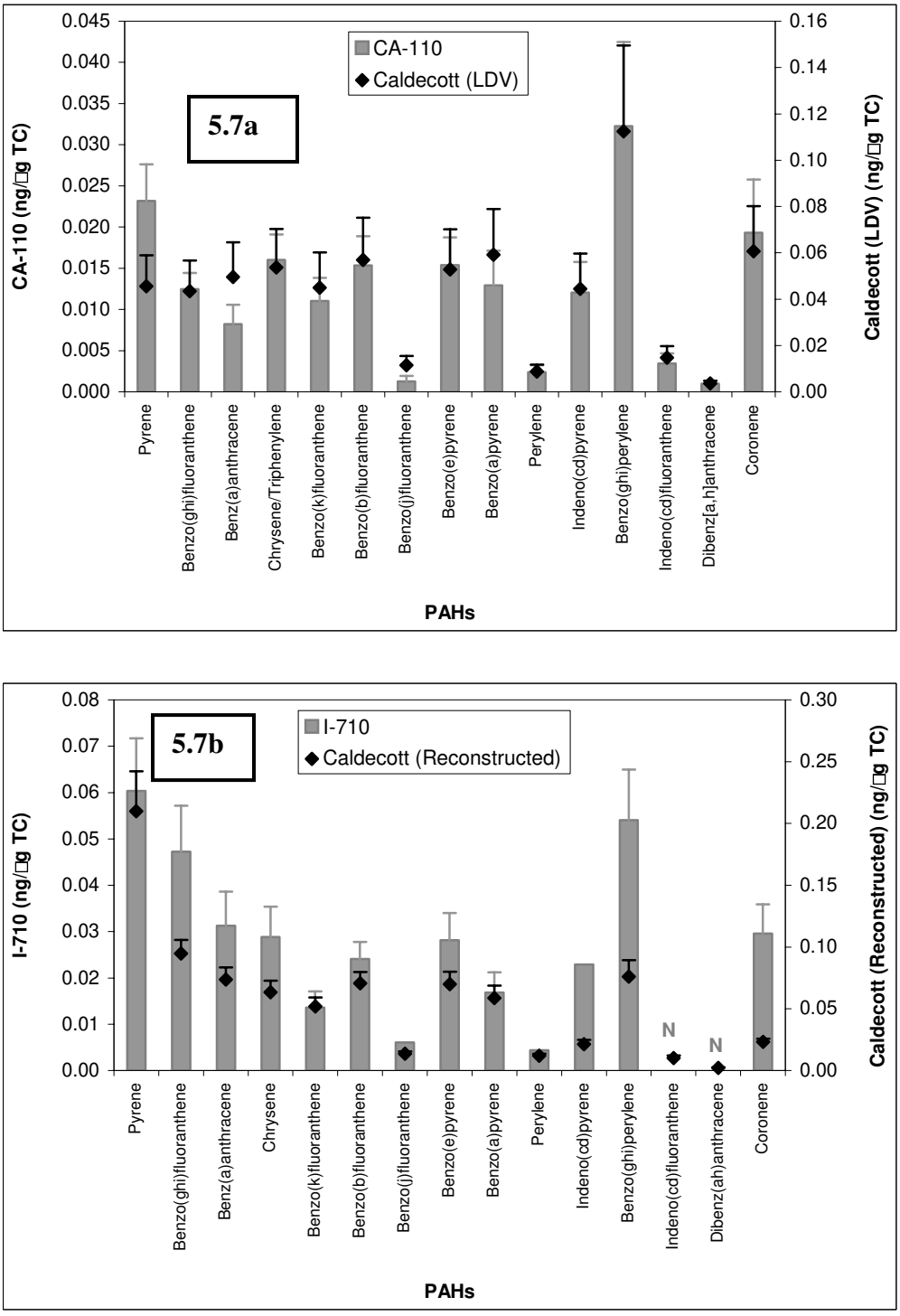

Figure 5.7. Chemical profile of PAHs (normalized to TC) in $PM_{2.5}$ size mode in a) CA-110 study and Caldecott (LDV) study; and b) I-710 study and Reconstructed Caldecott study. Error bars represent SE.

Similar to the hopanes and steranes data, Figures 5.7a and 5.7b present the normalized chemical profile of the measured PAHs at the CA-110 and I-710 against normalized EFs measured for LDVs and HDVs from the Caldecott tunnel, respectively. (The concentrations are normalized to TC measured in the respective studies). The normalized PAH concentrations are about 2-3 times lower in the freeways than the corresponding normalized concentrations of the tunnel for lighter PAHs, while for heavier PAHs the chemical profiles become more comparable, especially for the I-710 data. Part of these differences may arise from different vehicle operating conditions, such as engine load and speed (considering that the Caldecott tunnel has a 4% grade), ambient temperature and atmospheric dilution (affecting the ambient sites but not the tunnel measurements) as

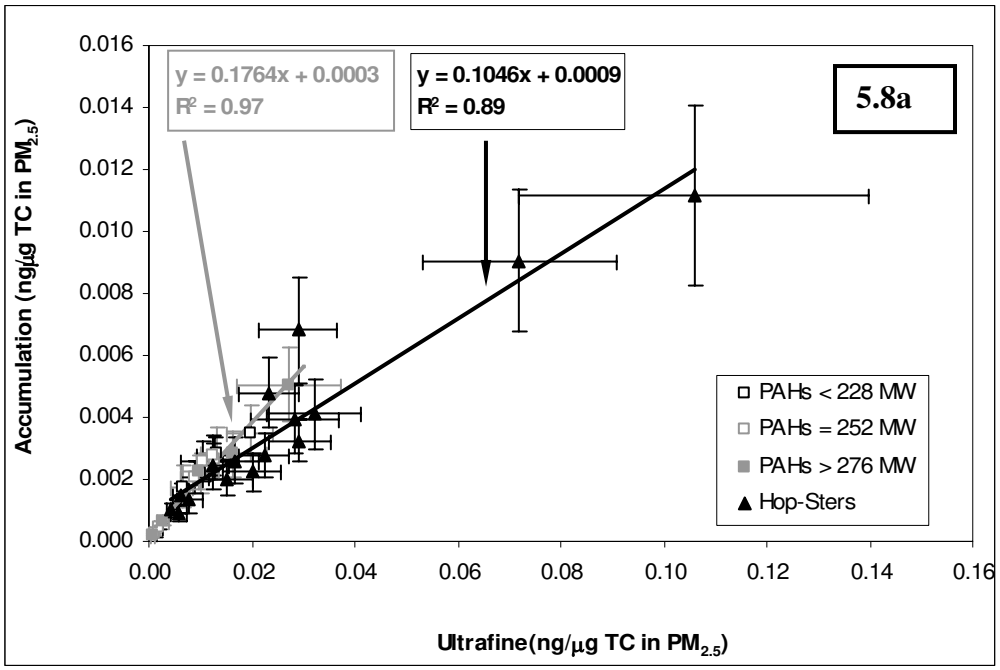

Figure 5.8. Correlation of measured organic species (normalized to TC in $PM_{2.5}$) between ultrafine and accumulation size modes in a) CA-110 study; and b) Caldecott (LDV) study. Error bars represent SE.

Figure 5.8 Continued…

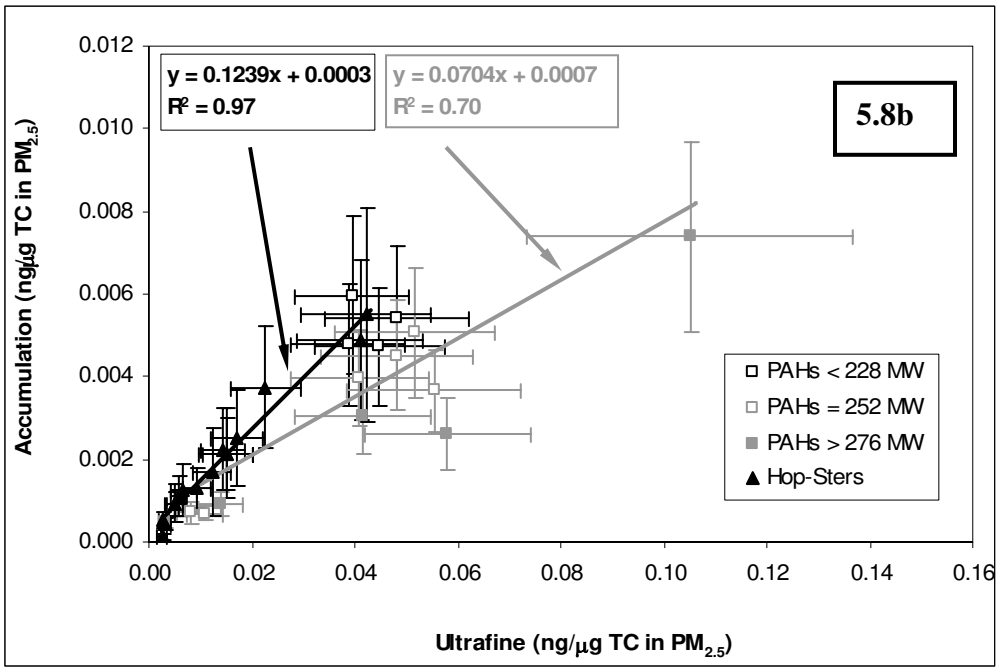

well as catalytic converter efficiency in these two different environments (Schauer et al., 2003). Since PAHs result from fuel combustion in the engines, they strongly depend on the factors influencing combustion, including engine-load and ambient air temperature (Kean et al., 1999). Furthermore, the gas-particle partitioning of semi-volatile PAHs can be strongly influenced by ambient temperature (Mader and Pankow, 2000; Finlayson-Pitts and Pitts, 2000), particularly for low molecular weight PAHs whose vapor pressures are higher than heavier PAHs and the hopanes and steranes (Schauer et al., 2003). It should be also noted that the plotted data in these figures reflect concentrations normalized to TC, which themselves are also affected by engine operating parameters, thus influence the fraction of carbon emitted as these organic markers. Photochemical degradation of PAHs on the filter (Schauer C. et al., 2003) as well as in the atmosphere

(Zielinska, 2005; Finlayson-Pitts and Pitts, 2000) affect both the total carbon as well as particulate phase PAHs concentrations measured near the roadway environments. In tunnel studies, these phenomena are expected to be minimal. All of these factors may compromise the use of PAHs as tracers of vehicular emissions.

The relationship between PAHs and hopanes- steranes (normalized to TC in $PM_{2.5}$ size mode) in the ultrafine and accumulation size modes at the CA-110 and the corresponding levels for the LDVs measured in Caldecott tunnel is shown in Figures 5.8a and 5.8b, respectively. The normalization to TC is done in order to bring the units to same scales between the freeway and reconstructed Caldecott studies, and does not affect the slope and correlation coefficients of the linear regressions between these species. The high correlations in the CA-110 as well as for LDVs at the Caldecott tunnel show that high emissions of a PAHs and hopanes and steranes in one mode are accompanied by high emissions in the other mode, thus indicating similar particle size distributions for these species, consistently with results shown earlier (Figure 5.5a). Hopanes and steranes appear to be distributed similarly in both tunnel and freeway environments (slope ~ 0.1 and $R^2 \geq 0.9$) between accumulation and ultrafine PM modes. In contrast, there appears to be a shift towards the accumulation mode for PAHs at the CA-110 compared to the Caldecott data, particularly for lighter PAHs. There may be several reasons for these changes in size distribution observed between the two environments. Earlier studies have reported that more volatile PAHs tend to partition into larger particle size fractions (Marr et al., 1999; Miguel et al., 1998). Moreover, since the presence of poorly maintained

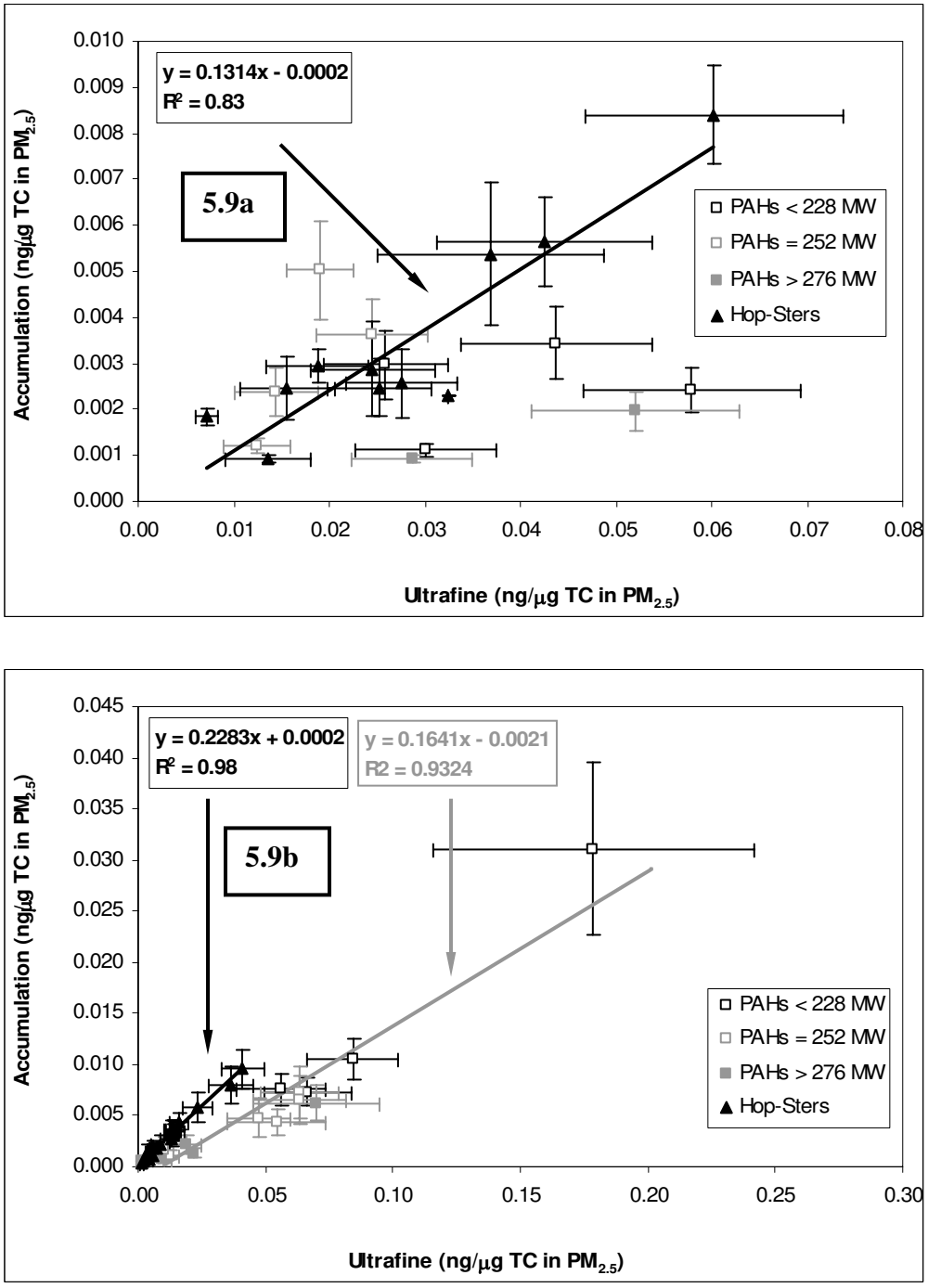

Figure 5.9. Correlation of measured organic species (normalized to TC in $PM_{2.5}$) between ultrafine and accumulation size modes in a) I-710 study; and b) Reconstructed Caldecott study. Error bars represent SE. Reconstructed Caldecott EFs are obtained using equation (2) in the text.

gasoline vehicles (gross emitters such as white and black smokers) significantly affects the total PAHs levels (Schauer et al., 2002; Zielinska et al., 2004), different fraction of these high emitters in these studies might be partially responsible for the observed differences.

The relationship between the ultrafine and accumulation size modes of PAHs, hopanes and steranes (normalized to TC in $PM_{2.5}$ size mode) at the I-710 and their corresponding reconstructed emissions factors from the tunnel measurements is shown in Figures 5.9a and 5.9b, respectively. Unlike the CA-110 and Caldecott LDV measurements, some differences in the size distribution of hopanes and steranes can be observed between I-710 and reconstructed tunnel measurements. Hopanes and steranes are shifted more towards the accumulation mode in the reconstructed emissions from the Caldecott study (slope = 0.23) compared to those of the I-710 (slope = 0.13). Based on CO_2 measurements, the dilution factor ratio between the I-710 study and the Bore 1 of the Caldecott tunnel (corresponding to HDV measurements) is on the order of 8-10 (Ntziachristos et al., 2006), which implies a stronger background influence at the I-710 site. Since hopanes and steranes come from both vehicle types, the more prevalent LDVs in the background as well as the high number of LDVs on the I-710 tend to bring the size distributions closer to those of LDVs. The fact that the freeway site measurements in the accumulation mode are relatively similar to background concentrations in I-710 study (Figure 5.3b, Table 5.1b), suggests that, while hopane and steranes in ultrafine mode are

primarily from fresh emissions in the I-710, the accumulation mode concentrations may be also influenced by background emissions of LDVs in the surrounding urban area.

Comparing the PAHs distribution in two size modes (Figures 5.9a and 5.9b), the influence of the urban background as well as the larger number of LDV cars (60% more than on CA-110) at the I-710 is even more pronounced. The accumulation mode PAH concentrations are affected significantly by local combustion sources, including LDVs (in addition to the large number of cars already on I-710), which are more regional in nature and likely influence the measurements near freeway site. In addition to the impact of background sources, the higher dilution at the I-710 compared to the tunnel measurements affects the gas-particle phase partitioning of semi volatile PAHs, and may be responsible for the observed scatter in the distribution of PAHs in these size modes. Compared to the CA-110 data, hopanes and steranes are partitioned more in the accumulation mode, although in lower fractions compared to the Caldecott data, as noted earlier. This reflects the influence of HDVs at the I-710 and is consistent with previous studies showing higher emission rates in the accumulation mode by HDVs for these species (Phuleria et al., 2006).

5.5. Chapter 5: SUMMARY AND CONCLUSIONS

The main objective of this study was to compare the concentrations of vehicular organic markers measured near freeway environments to those based on emission factors measured for LDVs and HDVs inside the Caldecott tunnel. Very good agreement is

observed between CA-110 measurements and tunnel-based LDV EFs for hopanes and steranes as well as heavier PAHs. The reconstructed profiles from the Caldecott tunnel also agree quite well with the I-710 measurements. The comparisons between the chemical profiles of these organic species in environments affected by different atmospheric dilution, meteorological conditions, and different fleet composition, validates the emission factors measured in our earlier study in the Caldecott tunnel. PAH concentrations are affected by various factors such as fuel type, engine-operating parameters as well as meteorological conditions. However, high MW PAHs seem to be less influenced and hence show better agreement between roadside and tunnel measurements as compared to lighter PAHs. A potential limitation of roadway measurements is their inability to capture cold-start emissions, which are significantly higher than the prevailing cruise or transient mode emissions of this study as well as those in roadway tunnels, and which affect the average emission profiles significantly, especially in the winter season (Manchester-Neesvig et al., 2003; Shah et al., 2005). Recognizing this limitation, our results suggest that in general, the emission factors for hopanes and steranes obtained in tunnel environments, where emissions are averaged over a large vehicle-fleet, enable reliable source apportionment of ambient PM, given the overall agreement between the roadway vs tunnel concentrations of these species.

5.6 Chapter 5: REFERENCES

Allen, J.O.; Mayo, P.R.; Hughes, L.S.; Salmon, L.G.; Cass, G.R. **2001**. Emissions of size-segregated aerosols from on-road vehicles in the Caldecott tunnel. Environmental Science and Technology 35, 4189-4197.

Biswas, S.; Ntziachristos, L.; Moore, K.F.; Sioutas, C. **2006**. Particle volatility in the vicinity of a freeway with heavy-duty diesel traffic. Submitted to Journal of Aerosol Science, June 2006.

Brunekreef, B.; Janssen, N.A.; de Hartog J.; Harssema, H.; Knape, M.; van Vliet, P. **1997**. Air pollution from truck traffic and lung function in children living near motorways. Epidemiology 8(3), 298-303.

Cadle, S.H.; Mulawa, P.A.; Hunsanger, E.C.; Nelson, K.; Ragazzi, R.A.; Barrett, R.; Gallagher, G.L.; Lawson, D.R.; Knapp, K.T.; Snow, R. **1999** Composition of light-duty motor vehicle exhaust particulate matter in the Denver, Colorado area. Environmental Science and Technology 33, 2328-2339.

Canagaratna, A.; Jayne, J.; Ghertner, D.; Herndon, S.; Shi, Q.; Jimenez, J.; Silva, P.; Williams, P.; Lanni, T.; Drewnick, F.; Demerjian, K.; Kolb, C.; Worsnop D. **2004**. Chase studies of particulate emissions from in-use New York city vehicle. Aerosol Science and Technology 38, 555-573.

Cass, G.R. **1998**. Organic molecular tracers for particulate air pollution sources. Trends in Analytical Chemistry 17(6), 356-366.

Chellam, S.; Kulkarni, P.; Fraser, M.P. **2005**. Emissions of organic compounds and trace metals in fine particulate matter from motor vehicles: A tunnel study in Houston, Texas. Journal of the Air and Waste Management Association 55, 60-72.

Diaz-Sanchez, D.; Proietti, L.; Polosa, R. **2003.** Diesel Fumes and the Rising Prevalence of Atopy: An Urban Legend? Current Allergy and Asthma Reports 3:146-152.

Finlayson-Pitts, B.J.; Pitts, J.N. **2000.** Chemistry of the Upper and Lower Atmosphere: Theory, Experiments, and Applications. Academic Press, San Diego, CA, pp. 453-509

Fine, P.M.; Chakrabarti, B.; Krudysz, M.; Schauer, J.J.; Sioutas, C. **2004.** Diurnal variations of individual organic compound constituents of ultrafine and accumulation mode particulate matter in the Los Angeles Basin. Environmental Science and Technology 2004, 38, 1296-1304.

Fraser, M.P.; Buzcu, B.; Yue, Z.W.; McGaughey, G.R.; Desai, N.R.; Allen, D.T.; Seila, R.L.; Lonneman, W.A.; Harley, R.A. **2003a**. Separation of fine particulate matter emitted from gasoline and diesel vehicles using chemical mass balancing techniques. Environmental Science and Technology 37, 3904-3909.

Fraser, M.P.; Cass, G.R.; Simoneit, B.R.T. **1998**. Gas-phase and particle-phase organic compounds emitted from motor vehicle traffic in a Los Angeles roadway tunnel. Environmental Science and Technology 32, 2051-2060.

Fraser, M.P.; Cass, G.R.; Simoneit, B.R.T. **1999**. Particulate organic compounds emitted from motor vehicle traffic and in the urban atmosphere. Atmospheric Environment 33, 2715-2724.

Fraser, M.P., Yue, Z.W.; Buzcu, B. **2002.** Source apportionment of fine particulate matter in Houston, TX, using organic molecular markers. 2003b. Atmospheric Environment 37, 2117-2123.

Geller, M.D., Sardar, S.B., Phuleria, H.C., Fine P.M.; Sioutas, C. **2005**. Measurement of particle number and mass concentrations and size distributions in a tunnel environment. Environmental Science and Technology 39, 8653-8663.

Gertler, A.W. **2005**. Diesel vs. gasoline emissions: Does PM from diesel and gasoline dominate in the US? Atmospheric Environment 39, 2349-2355.

Hitchins, J., Morawska, L., Wolff, R., and Gilbert, D. **2000**. Concentrations of submicrometre particles from vehicle emissions near a major road. Atmospheric Environment 34(1), 51–59.

Kean, A.J.; Harley, R.A.; Kendall, G.R. **2003.** Effects of vehicle speed and engine load on motor vehicle emissions. Environmental Science and Technology 37, 3739-3746.

Kirchstetter, T.W.; Singer, B.C.; Harley, R.A.; Kendall, G.R.; Traverse, M. **1999.** Impact of California reformulated gasoline on motor vehicle emissions. I. Mass emission rates. Environmental Science and Technology 33, 318-328.

Kittelson, D.B., Engines and nanoparticles: A review. **1998.** Journal of Aerosol Science 29, 575-588.

Kleinman, M.T.; Hamade, A.; Meacher, D.; Oldham, M.; Sioutas, C.; Chakrabarti, L.; Stram, D.; Froines, J.R.; Cho, A.K. **2005**. Inhalation of concentrated ambient particulate matter near a heavily trafficked road stimulates antigen-induced airway responses in mice. Journal of the Air and Waste Management Association 55(9), 1277-1288.

Kuhn, T.; Biswas, S.; Fine, P.M.; Geller, M.D.; Sioutas, C. **2005a**. Physical and chemical characteristics and volatility of PM in the proximity of a light-duty vehicle freeway. Aerosol Science and Technology 39(4), 347 – 357.

Kuhn, T.; Biswas, S.; Fine, P.M.; Geller, M.D.; Sioutas, C. **2005b**. Diurnal and seasonal characteristics of particle volatility and chemical composition in the vicinity ofa light-duty vehicle freeway. Atmospheric Environmment 39, 7154-7166.

Mader, B.T., Pankow, J.F. **2001**. Gas/Solid Partitioning of semivolatile organic compounds (SOCs) to air filters. 3. An analysis of gas adsorption artifacts in measurements of atmospheric SOCs and organic carbon (OC) when using teflon membrane filters and quartz fiber filters. Environmental Science and Technology 35(17), 3422–3432.

Manchester-Neesvig, J.B.; Schauer, J.J.; Cass, G. R. **2003.** The Distribution of particle-phase organic compounds in the atmosphere and their use for source apportionment during the Southern California Children's Health Study. Journal of the Air and Waste Management Association. 53, 1065-1079.

Marr, L.C.; Kirchstetter, T.W.; Harley, R.A.; Miguel, A.H.; Hering, S.V.; Hammond, S.K. **1999**. Characterization of polycyclic aromatic hydrocarbons in motor vehicle fuels and exhaust emissions. Environmental Science and Technology 33, 3091-3099.

Mauderly, J.L. **1994**. Toxicological and epidemiological evidence for health risks from inhaled engine emissions. Environmental Health Perspectives 102, 165-171.

McDonald, J.D.; Eide, I.; Seagrave, J.; Zielinska, B.; Whitney, K.; Lawson, D.R.; Mauderly, J.L. **2004.** Relationship between composition and toxicity of motor vehicle emission samples. Environmental Health Perspectives 12, 1527–1538.

Miguel, A.H.; Kirchstetter, T.W.; Harley, R.A.; Hering, S.V. **1998.** On-road emissions of particulate polycyclic aromatic hydrocarbons and Black Carbon from gasoline and diesel vehicles. Environmental Science and Technology 32, 450-455.

Misra, C.; Kim, S.; Shen, S.; Sioutas, C. **2002.** A high flow rate, very low pressure drop impactor for inertial separation of ultrafine from accumulation mode particles. Journal of Aerosol Science 33, 735-752.

Nel, A.; Xia, T.; Maumldler L.; Li, N. **2006.** Toxic Potential of Materials at the Nanolevel. Science 311(5761), 622-627.

Ntziachristos, L., Zhi, N., Geller, M.D., Sioutas C. **2006.** Particle concentration and characteristics near a major freeway with heavy-duty diesel traffic, Submitted to Environmental Science and Technology, June 2006.

Peters, A.; Wichmann, H.E.; Tuch, T.; Heinrich, J.; Heyder, J. **1997.** Respiratory effects are associated with the number of ultrafine particles. American Journal of Respiratory and Critical Care Medicine, 155, 1376-1383.

Phuleria, H.C.; Geller, M.D.; Fine, P.M.; Sioutas, C. **2006**. Size-resolved emissions of organic tracers from light- and heavy-duty vehicles measured in a California roadway tunnel. Environmental Science and Technology 40, 4109-4118.

Pope (III), C.A.; Dockery, D.W. **2006**. Health effects of fine particulate air pollution: lines that connect. Journal of the Air and Waste Management Association 56, 709-742.

Rogge W.F.; Hildemann, L.M.; Mazurek, M.A.; Cass, G.R.; Simoneit B.R.T. **1993**. Sources of fine organic aerosol. 2. Noncatalyst and catalyst-equipped automobiles and heavy-duty diesel trucks. Environmental Science and Technology 27, 636-651.

Schauer, C.; Niessner, R.; Poschl, U. **2003**. Polycyclic aromatic hydrocarbons in urban air particulate matter: Decadal and seasonal trends, chemical degradation, and sampling artifacts. Environmental Science and Technology 37, 2861-2868.

Schauer, J.J. **2003.** Evaluation of elemental carbon as a marker for diesel particulate matter. Journal of Exposure Science and Environmental Epidemiology 13, 443-453.

Schauer, J.J.; Cass, G.R. **2000**. Source apportionment of wintertime gas-phase and particle-phase air pollutants using organic compounds as tracers. Environmental Science and Technology 34, 1821-1832.

Schauer, J.J.; Kleeman, M.J.; Cass, G.R.; Simoneit, B.R.T. **1999.** Measurement of emissions from air pollution sources. 2. C_1 through C_{30} organic compounds from medium duty diesel trucks. Environmental Science and Technology 33, 1578-1587.

Schauer, J.J.; Kleeman, M.J.; Cass, G.R.; Simoneit, B.R.T. **2002**. Measurement of emissions from air pollution sources. 5. C_1-C_{32} organic compounds from gasoline-powered motor vehicles. Environmental Science and Technology 36, 1169-1180.

Schauer, J.J.; Rogge, W.F.; Hildemann, L.M.; Mazurek, M.A.; Cass, G.R.; Simoneit, B.R.T. **1996**. Source apportionment of airborne particulate matter using organic compounds as tracers. Atmospheric Environment 30, 3837-3855.

Schauer, J.J.; Shafer, M.; Christensen, C.; Kittelson, D.B.; Johnson, J.; Watts, W. **2003**. Impact of cold-start temperature on the chemical composition of PM emissions from SI vehicles. 13th CRC On-Road Vehicle Emissions Workshop, San Diego, CA, April 7-9.

Schwartz, J.; Laden, F.; Zanobetti, A. **2002.** The concentration-response relation between $PM_{2.5}$ and daily deaths. Environmental Health Perspectives 110(10), 1025-1029.

Shah, S.D., Cocker, D.R., Miller, J.W., and Norbeck, J.M. **2004.** Emission rates of particulate matter and elemental and organic carbon from in-use diesel engines. Environmental Science and Technology 38(9), 2544–2550.

Sheesley, R.J.; Schauer, J.J.; Chowdhury, Z.; Cass, G.R.; Simoneit, B.R.T. **2003**. Characterization of organic aerosols emitted from the combustion of biomass indigenous to South Asia. Journal of Geophysical Research - Atmosphere 108, No. 4285.

Simoneit, B.R.T. **2002**. Chemical characterization of sub-micron organic aerosols in the tropical trade winds of the Caribbean using gas chromatography-mass spectrometry. Atmospheric Environment 36, 5259-5263.

Sternbeck, J., Sjodin, A., Andreasson, K. **2002.** Metal Emissions from Road Traffic and the Influence of Resuspension—Results from Two Tunnel Studies. Atmospheric Environment 36(30), 4735–4744.

Venkataraman, C.; Lyons, J.M.; Friedlander, S.K. **1994**. Size distributions of polycyclic aromatic hydrocarbons and elemental carbon. 1. Sampling, measurement methods, and source characterization. Environmental Science and Technology 28, 555-562.

Weingartner, E.; Keller, C.; Stahel, W.A.; Burtscher, H.; Baltensperger, U. **1997**. Aerosol emission in a road tunnel. Atmospheric Environment 31(3), 451-462.

Zhang, M.Z., Wexler, A.S.; Niemeier, D.; Zhu, Y.F.; Hinds, W.; Sioutas, C. **2005.** Evolution of particle number distribution near roadways. Part III. Traffic analysis and on-road size resolved particulate emission factors. Atmospheric Environment 39, 4155-4166.

Zheng, M.; Cass, G.R.; Schauer, J.J.; Edgerton, E.S. **2002**. Source apportionment of $PM_{2.5}$ in the Southeastern United States using solvent-extractable organic compounds as tracers. Environmental Science and Technology 36, 2361-2371.

Zhu, Y., Hinds, W.C.; Kim, S.; Sioutas, C. **2002a**. Concentration and size distribution of ultrafine particles near a major highway. Journal of the Air and Waste Management Association 52, 1032-1042.

Zhu, Y., Hinds, W.C.; Kim, S.; Sioutas, C. **2002b.** Study of ultrafine particles near a major highway with heavy-duty diesel traffic. Atmospheric Environment 36(27), 4323-4335.

Zhu, Y., Hinds, W.C.; Shen, S.; Sioutas, C. 2004. Seasonal trends of concentration and size distribution of ultrafine particles near major highways in Los Angeles. Aerosol Science and Technology 38, 5-13.

Zielinska, B. **2005.** Atmospheric transformation of diesel emissions 57, 31-42.

Zielinska, B.; Sagebiel, J.; McDonald, J.D.; Whitney, K.; Lawson, D.R. **2004**. Emission rates and comparative chemical composition from selected in-use diesel and gasoline-fueled vehicles. Journal of the Air and Waste Management Association 54, 1138-1150.

Chapter 6: Conclusions and future research directions

6.1 SUMMARY

Recent focus of studies on health effects of ambient particulate matter (PM) have suggested particle chemical composition in addition to particle size, shape and number concentration responsible for observed health outcomes. Chemical composition of the atmospheric particles, however, can have seasonal, temporal, spatial and size-dependent variability. In addition, differences in ambient temperature, relative humidity, and photochemical activity and source contributions affect the concentration and size distribution of particular chemical species.

There are very significant differences in urban versus rural location; source versus receptor sites in terms of PM exposure, which invite for characterizing the sources, and develop methods of assessing their impact on air quality. Two of the events where we studied the impact of specific sources were Long Beach harbor strike in October 2002 and Southern California wildfires in late October 2003. In the former case the airborne PM contribution originating from cargo trucks was reduced while resulted simultaneously in elevated idling ship emissions. In later case, however, there was high level of PM emissions originating from wildfires during the fire episode. As against uncontrolled wildfires, which produce particles in lower accumulation size ranges and have more regional impact on air quality, emissions from gasoline and diesel driven vehicles impact the air quality locally and more so in ultrafine and nano particle size ranges.

Size fractionated speciated organic chemical analysis was attempted for emission characterization from averaged PM emission sampled from gasoline and diesel vehicles inside Caldecott tunnel. The tunnel off limits one bore to only light duty gasoline vehicles and hence provided the opportunity to segregate and study the emission from LDVs and HDVs. While the LDVs are shown to emit high molecular weight PAHs, the relative emissions is dominated by light molecular weight PAHs and EC in the case HDVs. Hopanes and steranes emissions, which emanate from lubricating oil, are found to have similar chemical profile from both type of vehicles. HDVs. To understand vehicle contribution to ambient PM near freeway environments where people spend a lot of time in commute, measurements were carried out near CA-110 and I-710 freeways.

CA-110 measurements, which provided the pure LDV emissions, were compared against mix-fleet (20% HD fraction) of vehicles on I-710 for the measured organic tracers near these freeways. Successively the chemical profiles of the organic tracers obtained from these freeway measurement were compared with the earlier obtained chemical profiles from Caldecott tunnel measurements. Very good agreement is obtained between these different studies, conducted in different environments, and hence provides the potential use of these molecular marker EFs in CMB model calculations for source apportionment over to single vehicle laboratory dynamometer measurements.

6.2 CONCLUSIONS

Preventing people from the deleterious and carcinogenic health effects of ambient air pollution is the desired goal and motivation of any kind of air quality study. In order to

relate public health with ambient air pollution, mechanistic pathways of PM induced health effects need to be established (Dockery and Pope, 2006). Since there is huge variability in sources, exposed population, population sensitivity, meteorology as well as measurement methods, extensive physicochemical characterization of airborne PM is necessary to develop future emission control technologies as well as in focusing on more specific PM component than mass.

Within the uncertainty in the measurements as stated in relevant sections of this thesis, the research work presented here successfully demonstrate the association between ambient PM, sources and the temporal, seasonal and spatial variability linked with these measurements. The measured emission factors for vehicular organic tracers from on-road fleet of gasoline and diesel vehicles using GCMS methods proved very useful and presents the potential use of these molecular source profiles in CMB model calculations for ultrafine and fine PM source apportionment. To date no single source profiles are available for different ultrafine PM sources other than obtained in this work here and it just presents a small step forward towards achieving these goals. The PM measurements and data obtained in this study provides an increased understanding of the relationship between sources and the ambient concentrations of their PM emissions and how physical and chemical characteristics of the fine and ultrafine particles changes in different environments, which is necessary in order to understand the exposure outcomes.

6.3 FUTURE WORK DIRECTIONS

Major research effort is underway to improve scientific understanding of airborne PM and its effects on human health. The research effort is directed at reducing scientific and technical uncertainties in the evidence related to regulation of airborne PM. For effective emission-management strategies, and regulatory decision making processes, development of measurement methods to characterize size distribution, chemical composition and emission rates from different sources is essential. The required data includes chemically speciated and size-resolved emission factors/ ratios for a sufficient number of geographic locations and source types (NRC, 1999).

Similar to the study of spatial, seasonal and temporal differences in PM levels in Southern California, different locations having different mix of sources, and progressively evolving pollution control technologies would continue to be the focus of air quality evaluation studies in future. The focus of the research work presented here is on PM of primary source origin, however, secondary particle formation from precursor gaseous species would be another potent area of future studies in perspective to the organic gaseous emissions from different combustion sources including mobile vehicular emissions. We studied the impact of wildfire emissions on local air quality in Los Angeles Basin, however, as the particle originating from these fire episodes are in 100-200 nm size ranges, they have higher residence time in atmosphere and would affect the visibility and regional air quality, in general. How these particles of fire origin would change characteristics in the atmosphere on a longer time scale would be another area of future study.

EFs calculated in Caldecott tunnel are specific to the tunnel grade and vehicle operating conditions. In different load and smooth/congested driving conditions the emission factors would change (since catalytic converter efficiency is a strong function of catalyst operating temperature) and one needs to be cautious before their use in CMB applications and in data assimilation with other studies. On similar lines, the traffic was observed very smooth in the Caldecott tunnel and steady state driving pattern was observed. Since idling and transient operation of vehicle as well as cold-start emissions from engines are significantly different, the relative contribution of these must be included before applying tunnel based EFs in CMB models.

We observed strong impact of ambient dilution on the ambient levels of deferent species, which suggest that it may not be appropriate to compare the strength of two sources without accounting the difference in atmospheric dilution. The source profiles of LDVs as well as HDVs (adjusted for dilution using CO_2 measurements), with respect to hopanes and steranes, were observed similar in tunnel and freeway environments despite high differences in atmospheric dilution. This important finding further invites the comparison and assimilation of these data with other laboratory dynamometer measurements involving limited vehicles. As stated earlier, LDV/HDV split for 6tire-2axle trucks is assumed to remain same as observed in 1997 (Kirchstetter et al, 1999). This must be accounted before attributing PM concentration to HD diesel vehicles and invites an updated comprehensives mobile emission inventory. The uncertainty in few of the organic marker measurements (especially lighter molecular weight PAHs) was about

50% and hence one must be cautious to attribute the impact of LDV and HDV on source apportionment studies using these molecular markers with high uncertainties.

Most of our knowledge of the detailed chemical composition of PM emissions from gasoline vehicles comes from the standard cold and hot start chassis dynamometer tests. Standard cold start testing, however, does not truly represent the cold start conditions in many locations during the winter. The accurate assessment of the impact of the vehicular sources on ambient PM concentrations requires knowledge of the emission rates and composition of the true vehicle fleet in a region (Schauer et al., 2003). The emission factors derived for the diesel and gasoline vehicles from tunnel studies are representative of the true on-road vehicle fleet but does not incorporate the cold-start emissions. The nature of the organic carbon emissions for the cold start, steady state and hot UDC cycles are different based on organic tracer analysis (Schauer et al., 2003; Shah et al., 2005). Hence a potential area of research would be to incorporate LDV emission measurements near multi-complex parking structure for cold-start conditions.

Studies that use organic molecular markers to trace emissions from both gasoline and diesel powered vehicles suggests that diesel contribution attributable to ambient PM is greater than that of the gasoline vehicles (Schauer et al., 1996; Zheng et al., 2002). Other studies which incorporate cold-start emissions and poorly maintained gasoline vehicles estimate that the gasoline contribution more than the diesel powered vehicles (Watson et al., 2002; Fraser et al., 2003). However, reconciliation in these opposite findings can be achieved by measuring average fleet emission profiles from the on-road vehicles. More

studies of similar nature but different fleet composition and driving characteristics would be necessary for the development of comprehensive source profiles for different exposure environments.

Despite the consistent wind patterns in Los Angeles, it is conceivable that variations in wind speed and direction will inevitably occur during sampling, and additional sources, other than the one under study, will contribute to the samples at each site. Merely locating the samplers and concentrators near a source may not ensure that the sample will be influenced by that source alone at all times. Therefore, the actual contribution of the source of interest and other PM sources to each sample or exposure atmosphere should be quantified using source apportionment techniques. Two approaches can be employed to evaluate source contributions from source emissions data and ambient monitoring data: source-oriented models and receptor-oriented models. The source-oriented models rely profoundly on inventory estimates, which are often based on rough emission factors (Fine, 2002). Receptor-oriented models, on the other hand provide an alternative to source-oriented models and use the best combination of source contributions needed to reconstruct the chemical composition of an ambient sample (Watson, 1984).

One useful method for assigning ambient particulate matter concentration increments to the sources from which they originate, which has been already referenced many times earlier in the text, is the chemical mass balance (CMB) technique. CMB methods using individual organic compounds and trace elements have been successfully used to apportion the mass of a given $PM_{2.5}$ sample to different PM sources (Schauer and Cass,

2000; Schauer et al., 1996; Zheng et al., 2002). In the CMB method, a mass balance is constructed in which the concentration of specific chemical constituents in a given ambient sample is described as arising from a linear combination of the relative chemical compositions of the contributing sources.

The dominant sources of airborne fine organic particulate matter in Los Angeles were found to be diesel engine exhaust, gasoline-powered vehicle exhaust, the effluent from meat cooking operations, and wood smoke. Paved road dust was the next largest contributor, followed by four smaller sources: tire wears debris, vegetative detritus, natural gas combustion aerosol, and cigarette smoke. The remaining contributions to fine particle mass concentrations in Los Angeles are due to sulfate, nitrate, and secondary organic aerosols that are formed from gas phase precursors by atmospheric chemical reactions and that cannot be attributed to specific primary particle emissions sources by the organic chemical tracer techniques (Schauer et al., 1996; Cass, 1998; Schauer and Cass, 2000).

As technology changes over time (e.g. as cleaner diesel engines; cleaner fuel and better control technologies are introduced) source test data will need to be updated and the hence the need for the assessment of revised source contributions arises. In addition, there are no source profiles available today for ultrafine particle composition form different sources. As understanding of PM characteristics has improved and hence the promulgation of newer air quality standards, $PM_{2.5}$ mass standards would no longer be enough to protect human health from increased ultrafine nano-size particle emissions

from vehicles and other stationary combustion sources and necessitate the need for generation of ultrafine PM source profiles.

Accurate emission factors are the critical starting point for any atmospheric models. Understanding the factors that influence particle emission factors from motor vehicles will also help in future emissions control efforts. The information generated through this study would add to existing source-exposure knowledge and shall serve as the basis for linking emissions to local air quality and ultimately to health effects. Knowing the relative toxicity of different PM sources will allow for more targeted and effective regulatory strategies. Furthermore, these data on which PM sources are the most toxic, combined with detailed chemical and physical characterization of PM from these sources will allow for a narrower, more focused effort in identifying the biological mechanisms of PM health effects.

6.4 Chapter 6: REFERENCES

Fine, P.M., Chakrabarti, B., Krudysz, M., Schauer, J.J. and Sioutas, C., 2**004**. Diurnal variations of individual organic compound constituents of ultrafine and accumulation mode particulate matter in the Los Angeles basin. *Environmental Science & Technology,* 38(5): 1296-1304.

Geller M.D., Sardar S.B., Phuleria H.C., Fine P.M and Sioutas C. **2005**. Measurement of particle number and mass concentrations and size distribution in tunnel environments, Submitted to *Environmental Science and Technology*.

NRC (National Research Council) 1999. Research priorities for airborne particulate matter. II. Evaluating the research progress and updating the portfolio. Washington, D.C. National Academic Press.

Schauer, J.J. and Cass, G.R., **2000**. Source apportionment of wintertime gas-phase and particle-phase air pollutants using organic compounds as tracers. *Environmental Science & Technology*, 34(9): 1821-1832.

Schauer, J. J.; Shafer, M.; Christensen, C.; Kittelson, D. B.; Johnson, J.; Watts, W. Impact of Cold-Cold Start Temperature on the Chemical Composition of PM Emissions from SI Vehicles. *13th CRC On-Road Vehicle Emissions Workshop*, San Diego, CA, April 7-9, **2003.**

Schauer, J. J.; Cass, G. R. Source apportionment of wintertime gas-phase and particle-phase air pollutants using organic compounds as tracers. *Environ. Sci. Technol.* **2000**, *34*, 1821-1832.

Cass, G. R. Organic molecular tracers for particulate air pollution sources. *Trends in Anal. Chem.* **1998**, *17*(6), 356-366.

Fraser, M. P.; Buzcu, B.; Yue, Z. W.; McGaughey, G. R.; Desai, N. R.; Allen, D. T.; Seila, R. L.; Lonneman, W. A.; Harley, R. A. Separation of fine particulate matter emitted from gasoline and diesel vehicles using chemical mass balancing techniques. *Environ. Sci. Technol.* **2003,** *37*, 3904-3909.

Schauer, J. J.; Rogge, W. F.; Hildemann, L. M.; Mazurek, M. A.; Cass, G. R.; Simoneit, B. R. T. Source apportionment of airborne particulate matter using organic compounds as tracers. *Atmos. Environ.* **1996**, *30*, 3837-3855.

Zhu, Y.F., Hinds, W.C., Kim, S., Shen, S. and Sioutas, C., **2002a**. Study of ultrafine particles near a major highway with heavy-duty diesel traffic. *Atmospheric Environment,* 36(27): 4323-4335.

Bibliography

Abu-Allaban, M.; Coulomb, W.; Gertler, A. W.; Gillies, Pierson, J. W. R.; Rogers, C. F.; Sagebiel, J. C.; Tarnay, L. Exhaust particle size distribution measurements at the Tuscarora mountain tunnel. *Aerosol Sci. Technol*. **2002**, *36*, 771 – 789.

Allen, J. O.; Dookeran, N. M.; Taghizadeh, K.; Lafleur, A. L.; Smith, K. A.; Sarofim, A. F. Measurement of oxygenated polycyclic aromatic hydrocarbons associated with a size-segregated urban aerosol. *Environ. Sci. Technol.* **1997**, *31*, 2064-2070.

Allen, J. O.; Durant, J. L.; Dookeran, N. M.; Taghizadeh, K.; Plummer, E. F.; Lafleur, A. L.; Sarofim, A. F.; Smith, K. A. Measurement of $C_{24}H_{14}$ polycyclic aromatic hydrocarbons associated with a size-segregated urban aerosol. *Environ. Sci. Technol.* **1998**, *32*, 1928-1932.

Allen, J. O.; Mayo, P. R.; Hughes, L. S.; Salmon, L. G.; Cass, G. R. Emissions of size-segregated aerosols from on-road vehicles in the Caldecott tunnel. *Environ. Sci. Technol.* **2001**, *35*, 4189-4197.

Allen, J.O.; Dookeran, K. M.; Smith, K. A.; Sarofim, A. F.; Taghizadeh, K.; Lafleur, A. L. Measurement of polycyclic aromatic hydrocarbons associated with size-segregated atmospheric aerosols in Massachusetts. *Environ. Sci. Technol.* **1996**, *30*, 1023-1031.

Allen, R., T. Larson, L. Sheppard, L. Wallace, and L.J.S. Liu (**2003**), Use of real-time light scattering data to estimate the contribution of infiltrated and indoor-generated particles to indoor air, *Environmental Science & Technology*, *37* (16), 3484-3492.

Baltensperger U., Streit N., Weingartner E., Nyeki S., Prevot A.S.H., Van Dingenen R., Virkkula A., Putaud J.P., Even A., ten Brink H., Blatter A., Neftel A., Gaggeler H.W. Urban and rural aerosol characterization of summer smog events during the PIPAPO field campaigne in Milan, Italy. *J Geophys Res.* **2002**.: 107 (D22): 8193-8204.

Barbosa, P.M., D. Stroppiana, J.M. Gregoire, and J.M.C. Pereira (**1999**), An assessment of vegetation fire in Africa (1981-1991): Burned areas, burned biomass, and atmospheric emissions, *Global Biogeochemical Cycles*, *13* (4), 933-950.

Baumgardner D., Raga G.B., and Muhlia A. Evidence for the formation of CCN by photochemical processes in Mexico City. *Atmos Environ* **2004**: 38(3): 357-367.

Birmili W., Wiedensolher A., Heintzenber J. and Lehmann K. Atmospheric particle number size distribution in central Europe: statistical relations to air masses and meteorology. *J Geophys Res* **2001**:106 (D23): 32005-32018.

Biswas P. and Wu Y. (**2005**) Nanoparticles and the environment. *Journal of the Air & Waste Management Association*, (6), 708-746.

Biswas, S.; Ntziachristos, L.; Moore, K.F.; Sioutas, C. **2006**. Particle volatility in the vicinity of a freeway with heavy-duty diesel traffic. Submitted to Journal of Aerosol Science, June 2006.

Bravo, A.H., E.R. Sosa, A.P. Sanchez, P.M. Jaimes, and R.M.I. Saavedra (**2002**), Impact of wildfires on the air quality of Mexico City, 1992-1999, *Environmental Pollution*, *117* (2), 243-253.

Brunekreef, B.; Janssen, N.A.; de Hartog J.; Harssema, H.; Knape, M.; van Vliet, P. **1997**. Air pollution from truck traffic and lung function in children living near motorways. Epidemiology 8(3), 298-303.

Brunke, E.G., C. Labuschagne, and H.E. Scheel (**2001**), Trace gas variations at Cape Point, South Africa, during May 1997 following a regional biomass burning episode, *Atmospheric Environment*, *35* (4), 777-786.

Buzorius G., Hameri K., Pekkanen J. and Kulmala M. Spatial variation of Aerosol Number Concentration in Helinski City. *Atmos Environ* **1999**: 33: 553-565.

Cadle, S.H., P. Mulawa, P. Groblicki, C. Laroo, R.A. Ragazzi, K. Nelson, G. Gallagher, and B. Zielinska (**2001**), In-use light-duty gasoline vehicle particulate matter emissions on three driving cycles, *Environmental Science & Technology*, *35* (1), 26-32.

Cadle, S.H.; Mulawa, P.A.; Hunsanger, E.C.; Nelson, K.; Ragazzi, R.A.; Barrett, R.; Gallagher, G.L.; Lawson, D.R.; Knapp, K.T.; Snow, R. **1999** Composition of light-duty motor vehicle exhaust particulate matter in the Denver, Colorado area. *Environmental Science and Technology* 33, 2328-2339.

Canagaratna, A.; Jayne, J.; Ghertner, D.; Herndon, S.; Shi, Q.; Jimenez, J.; Silva, P.; Williams, P.; Lanni, T.; Drewnick, F.; Demerjian, K.; Kolb, C.; Worsnop D. Chase studies of particulate emissions from in-use New York city vehicle. *Aerosol Sci. Technol.* **2004**, *38*, 555-573.

Cass, G. R. Organic molecular tracers for particulate air pollution sources. *Trends in Anal. Chem.* **1998**, *17*(6), 356-366.

Cass, G.R., L.A. Hughes, P. Bhave, M.J. Kleeman, J.O. Allen, and L.G. Salmon, (**2000**). The chemical composition of atmospheric ultrafine particles, *Philosophical Transactions of the Royal Society of London Series a-Mathematical Physical and Engineering Sciences*, 358 (1775), 2581-2592.

Chakrabarti, B.; Singh, M.; Sioutas, C. Development of a near-continuous monitor for measurement of the sub-150 nm PM mass concentration. *Aerosol Sci. Tech.* **2004**, *38*, 239-252.

Chase, R.E., G.J. Duszkiewicz, T.E. Jensen, D. Lewis, E.J. Schlaps, A.T. Weibel, S. Cadle, and P. Mulawa (**2000**), Particle mass emission rates from current-technology, light-duty gasoline vehicles, *Journal of the Air & Waste Management Association*, *50* (6), 930-935.

Chellam, S.; Kulkarni, P.; Fraser, M. P. Emissions of organic compounds and trace metals in fine particulate matter from motor vehicles: A tunnel study in Houston, Texas. *J. Air Waste Mange. Assoc.* **2005**, *55*, 60-72.

Cheng M.D. and Tanner R.L. Characterization of ultrafine and fine particles at a site near the Great Smoky Mountains. *Atmos Environ* **2002**: 36: 5795-5806.

Cheng, L., K.M. McDonald, R.P. Angle, and H.S. Sandhu (**1998**), Forest fire enhanced photochemical air pollution. A case study, *Atmospheric Environment*, *32* (4), 673-681.

Chow J.C., Watson J.G., Fujita E.M., Lu Z., Lawson D.R. and Ashbaugh L.L. Temporal and spatial variations of $PM_{2.5}$ and PM_{10} aerosol in the Southern California air quality study. *Atmos Environ* **1994**: 28 (12): 2061-2080.

Christoforou, C.S., L.G. Salmon, M.P. Hannigan, P.A. Solomon, and G.R. Cass (**2000**), Trends in fine particle concentration and chemical composition in Southern California, *Journal of the Air & Waste Management Association*, *50* (1), 43-53.

Chung, A., D. P. Y. Chang, M. J. Kleeman, K. D. Perry, T. A. Cahill, D. Dutcher, E. M. McDougall and K. Stroud (**2001**), Comparison of real time instruments used to monitor airborne particulate matter, *Journal of the Air & Waste Management Association*, *51* (1), 109-120.

CNN, Long Beach harbor strike, Internet, accessed August 24, **2004**, http://money.cnn.com/2002/10/08/news/ports_longshoremen

Cooper D.A. Exhaust emissions from ships at berth. *Atmos Environ* **2003**: 37: 3817-3830.

Corbett J.J. and Fischbeck P. Emissions from ships. *Science* **1997**: 278 (5339): 823-824.

Crutzen, P.J., and M.O. Andreae (**1990**), Biomass Burning in the Tropics - Impact on Atmospheric Chemistry and Biogeochemical Cycles, *Science*, *250* (4988), 1669-1678.

Crutzen, P.J., L.E. Heidt, J.P. Krasnec, W.H. Pollock, and W. Seiler (**1979**), Biomass Burning as a Source of Atmospheric Gases CO, H_2, N_2O, NO, CH_3Cl and COS, *Nature*, *282* (5736), 253-256.

Cyrys J., Stolzel M., Heinrich J., Kreyling W.G., Menzel N., Wittmaack K., Tuch T. and Wichmann H.E. Elemental composition and sources of fine and ultrafine ambient particles in Erfurt, Germany. *Sc Total Env* **2003**: 305: 143-156.

Dennis, A., M. Fraser, S. Anderson, and D. Allen (**2002**), Air pollutant emissions associated with forest, grassland, and agricultural burning in Texas, *Atmospheric Environment*, *36* (23), 3779-3792.

Derwent R.G., Davies T.J., Delaney M., Dollard G.J., Field R.A., Dumitrean P., Nason P.D., Jones B.M.R. and Pepler S.A. Analysis and interpretation of the continuous hourly monitoring data for 26 C_2–C_8 hydrocarbons at 12 United Kingdom sites during 1996. *Atmos Environ* **2000**: 34 (2): 297-312.

Diaz-Sanchez, D.; Proietti, L.; Polosa, R. **2003.** Diesel Fumes and the Rising Prevalence of Atopy: An Urban Legend? Current Allergy and Asthma Reports 3:146-152.

Dockery, D. W.; Pope, C. A.; Xu, X. P.; Spengler, J. D.; Ware, J. H.; Fay, M. E.; Ferris, B. G.; Speizer, F. E. An association between air-pollution and mortality in 6 United-States cities. *New England J. Med.* **1993**, *329*, 1753-1759.

Dockery, D.W. and Pope, C.A. (**1994**). Acute Respiratory Effects of Particulate Air-Pollution. *Annual Review of Public Health*.15: 107-132.

Donaldson, K. and MacNee, W. (**1998**). The Mechanism of Lung Injury Caused by PM_{10} *in Issues in Environmental Science and Technology*, Ed. R.E. Hester and R.M.Harrison, the Royal Society of Chemistry. 10:21-32.

Einfeld, W., D.E. Ward, and C.C. Hardy (**1991**), Effects of Fire Behaviour on Prescribed Fire Smoke Characteristics: A Case Study, *Global Biomass Burning: Atmospheric, Climatic, and Biospheric Implications*, edited by J. S. Levine, pp. 412-419, MIT Press, Cambridge, Mass.

EPA (**2003**). National Ambient Air Quality Standards (NAAQS). *http://www.epa.gov/air/criteria.html*

Ferin, J., Oberdorster, G., Soderholm, S.C. Gelein, R. (**1991**). Pulmonary Tissue Access of Ultrafine Particles. *Journal of Aerosol Medicine-Deposition Clearance and Effects in the Lung*.4(1):57-68.

Fine P.M., Shen S. and Sioutas C. Inferring the sources of fine and ultrafine particulate matter at downwind receptor sites in the Los Angeles Basin using multiple continuous measurements. *Aerosol Sci Technol* **2004**: 18: 182-195.

Fine, P. M.; Cass, G. R.; Simoneit, B. R. T. Chemical characterization of fine particle emissions from fireplace combustion of woods grown in the Northeastern United States. *Environ. Sci. Technol.* **2001**, *35*, 2665-2675.

Fine, P. M.; Chakrabarti, B.; Krudysz, M.; Schauer, J. J.; Sioutas, C. Diurnal variations of individual organic compound constituents of ultrafine and accumulation mode particulate matter in the Los Angeles Basin. *Environ. Sci. Technol.* **2004**, *38*, 1296-1304.

Finlayson-Pitts, B.J.; Pitts, J.N. **2000.** Chemistry of the Upper and Lower Atmosphere: Theory, Experiments, and Applications. Academic Press, San Diego, CA, pp. 453-509

Formenti, P., W. Elbert, W. Maenhaut, J. Haywood, S. Osborne, and M.O. Andreae (**2003**), Inorganic and carbonaceous aerosols during the Southern African Regional Science Initiative (SAFARI 2000) experiment: Chemical characteristics, physical properties, and emission data for smoke from African biomass burning, *Journal of Geophysical Research-Atmospheres*, *108* (D13), 8576.

Fraser, M. P.; Cass, G. R.; Simoneit, B. R. T. Air quality model evaluation data for organics. 6. C_3–C_{24} organic acids. *Environ. Sci. Technol.* **2003**, *37*, 446-453.

Fraser, M. P.; Cass, G. R.; Simoneit, B. R. T. Gas-phase and particle-phase organic compounds emitted from motor vehicle traffic in a Los Angeles roadway tunnel. *Environ. Sci. Technol.* **1998**, *32*, 2051-2060.

Fraser, M. P.; Yue, Z. W.; Buzcu, B. Source apportionment of fine particulate matter in Houston, TX, using organic molecular markers. *Atmos. Environ* **2003b**, *37*(15), 2117-2123.

Fraser, M.P.; Buzcu, B.; Yue, Z.W.; McGaughey, G.R.; Desai, N.R.; Allen, D.T.; Seila, R.L.; Lonneman, W.A.; Harley, R.A. **2003a**. Separation of fine particulate matter emitted from gasoline and diesel vehicles using chemical mass balancing techniques. Environmental Science and Technology 37, 3904-3909.

Fraser, M.P.; Cass, G.R.; Simoneit, B.R.T. **1999**. Particulate organic compounds emitted from motor vehicle traffic and in the urban atmosphere. Atmospheric Environment 33, 2715-2724.

Fujita, E.M., D.E. Campbell, B. Zielinska, J.C. Sagebiel, J.L. Bowen, W.S. Goliff, W.R. Stockwell, and D.R. Lawson (**2003**), Diurnal and weekday variations in the source contributions of ozone precursors in California's South Coast Air Basin, *Journal of the Air & Waste Management Association*, *53* (7), 844-863.

Garnes, L. A.; Allen, D. T. Size distributions of organonitrates in ambient aerosol collected in Houston, Texas. *Aerosol Sci. Technol.* **2002**, *36*(10), 983-992.

Geller M.D., P.M. Fine, and C. Sioutas (**2003**), The relationship between real-time and time-integrated coarse (2.5-10 mm) intermodal (1.0-2.5 mm) and fine particulate matter (<2.5 mm) in the Los Angeles basin, *Journal of the Air & Waste Management Association*, in press.

Geller, M.D., Sardar, S.B., Phuleria, H.C., Fine P.M.; Sioutas, C. **2005**. Measurement of particle number and mass concentrations and size distributions in a tunnel environment. Environmental Science and Technology 39, 8653-8663.

Gertler, A.W. **2005**. Diesel vs. gasoline emissions: Does PM from diesel and gasoline dominate in the US? Atmospheric Environment 39, 2349-2355.

Goode, J.G., R.J. Yokelson, D.E. Ward, R.A. Susott, R.E. Babbitt, M.A. Davies, and W.M. Hao (**2000**), Measurements of excess O_3, CO_2, CO, CH_4, C_2H_4, C_2H_2, HCN, NO, NH_3, HCOOH, CH_3COOH, HCHO, and CH_3OH in 1997 Alaskan biomass burning plumes by airborne fourier transform infrared spectroscopy (AFTIR), *Journal of Geophysical Research-Atmospheres*, *105* (D17), 22147-22166.

Gross, D. S.; Galli, M. E.; Silva, P. J.; Wood, S. H.; Liu, D.Y.; Prather, K. A. Single particle characterization of automobile and diesel truck emissions in the Caldecott tunnel *Aerosol Sci. Technol.* **2000**, *32*(2), 152-163.

Gross, D.S.; Barron, A. R.; Sukovich, E. M.; Warren, B. S.; Jarvis, J. C.; Suess, D. T.; Prather, K. A. Stability of single particle tracers for differentiating between heavy- and light-duty vehicle emissions. *Atmos. Environ.* **2005**, *39*(16), 2889-2901.

Harrison R.M., Shi J.P., Xi S., Khan A., Mark D., Kinnersley R. and Yin J. Measurement of number mass and size distribution of particles in the atmosphere. *Phil Tran. R Soc Lond* 2000: 358: 2567-2580.Isakson J., Persson T.A. and Lindgren E.S. Identification and assessment of ship emissions and their effects in the harbor of Goteborg Sweden. *Atmos Environ* **2003**: 35: 3659-3666.

Hays, M. D.; Smith, N. D.; Dong, Y. Nature of unresolved complex mixture in size-distributed emissions from residential wood combustion as measured by thermal desorption-gas chromatography-mass spectrometry. *J. Geophys. Res.*, **2004**, *109* (D16S04).

Hays, M.D., C.D. Geron, K.J. Linna, N.D. Smith, and J.J. Schauer (**2002**), Speciation of gas-phase and fine particle emissions from burning of foliar fuels, *Environmental Science & Technology*, *36* (11), 2281-2295.

Hinds, W.C. (**1999**). Properties, Behavior, and Measurement of Airborne Particles. Aerosol Technology, 2nd Ed. John Wiley & Sons Inc., New York.

Hitchins, J., Morawska, L., Wolff, R., and Gilbert, D. **2000**. Concentrations of submicrometre particles from vehicle emissions near a major road. Atmospheric Environment 34(1), 51–59.

Ibald-Mulli A, Wichmann HE, Kreyling W, Peters A. (**2002**). Epidemiological Evidence on Health Effects of Ultrafine Particles. *Journal of Aerosol Medicine.* 15 (2): 189-201.

Jacques P.A., Ambs J.L., Grant W.L. and Sioutas C. Field evaluation of the differential TEOM monitor for continuous $PM_{2.5}$ mass concentrations. *Aerosol Sci Technol* **2004** (Suppl. 1): 38: 49-59.

Janhall, S.; Jonsson, A. M.; Molnar, P.; Svensson, E. A.; Hallquist, M. Size resolved traffic emission factors of submicrometer particles. *Atmos. Environ.* **2004**, *26*, 4331-4340.

Johnston, C. J.; Finkelstein, J. N.; Mercer, P.; Corson, N.; Gelein, R.; Oberdorster, G. Pulmonary Effects Induced by Ultrafine PTFE Particles. *Toxicol. Applied Pharmacol.* **2000**, *168*, 208-215.

Kean, A. J.; Harley, R. A.; Kendall, G. R. Effects of vehicle speed and engine load on motor vehicle emissions. *Environ. Sci. Technol.* **2003**, *37*, 3739-3746.

Kim S., Shen S., Sioutas C., Zhu Y. F. and Hinds W. C. Size distribution and diurnal and seasonal trends of ultrafine particles in source and receptor sites of the Los Angeles Basin. *J Air Waste Manage Assoc* **2002**: 52: 297-307.

Kirchstetter, T. W.; Harley, R. A.; Kreisberg, N. M.; Stolzenburg, M. R.; Hering, S. V. On-road measurement of fine particle and nitrogen oxide emissions from light- and heavy-duty motor vehicles. *Atmos. Environ.* **1999a**, *33*, 2955-2968.

Kirchstetter, T. W.; Singer, B. C.; Harley, R. A.; Kendall, G. R.; Traverse, M. Impact of California reformulated gasoline on motor vehicle emissions. I. Mass emission rates. *Environ. Sci. Technol.* **1999b**, *33*, 318-328.

Kittelson, D. B., Engines and nanoparticles: A review. *J. Aerosol Sci*., **1998**, *29*, 575-588.

Kleeman, M. J.; Schauer, J. J.; Cass, G. R. Size and composition distribution of fine particulate matter emitted from motor vehicles. *Environ. Sci. Technol.* **2000**, *34*, 1132-11

Kleinman, M. T.; Hamade, A.; Meacher, D.; Oldham, M.; Sioutas, C.; Chakrabarti, L.; Stram, D.; Froines, J. R.; Cho, A. K. Inhalation of concentrated ambient particulate matter near a heavily trafficked road stimulates antigen-induced airway responses in mice. *J. Air Waste Manage. Assoc.* **2005**, *55*(9), 1277-1288.

Kleinman, M. T.; Sioutas, C.; Chang, M. C.; Boere, A. J. F.; Cassee, F. R. Ambient fine and coarse particle suppression of alveolar macrophage functions *Toxicol. Letters*, **2003**, *137*, 151-158.Kikas U., Mirma A., Tamm E. and Raunemaa T. Statistical characteristics of aerosol in Baltic sea region. *J Geophys Res* **1996**: 101 (D14): 19319-19327.

Kotzick, R. and Niessner, R. (**1997**). The Effects of Aging Processes on Critical Supersaturation Ratios of Ultrafine Carbon Aerosols. *Atmos. Environ.* 33:2669-2677.

Kuhn, T.; Biswas, S.; Fine, P.M.; Geller, M.D.; Sioutas, C. **2005a**. Physical and chemical characteristics and volatility of PM in the proximity of a light-duty vehicle freeway. Aerosol Science and Technology 39(4), 347 – 357.

Kuhn, T.; Biswas, S.; Fine, P.M.; Geller, M.D.; Sioutas, C. **2005b**. Diurnal and seasonal characteristics of particle volatility and chemical composition in the vicinity ofa light-duty vehicle freeway. Atmospheric Environmment 39, 7154-7166

Kulmala M. How particles nucleate and grow. *Science.* **2002**: 302: 1000-1001

Kulmala M., Vehkamäki H., Petäjä T., Dal Maso M., Lauri A., Kerminen V.M., Birmili W. and McMurry P.H. Formation and growth rates of ultrafine atmospheric particles: a review of observations. *J Aerosol Sci* **2004**: 35: 143-176.

Künzli N., McConnell R., Bates D., Bastain T., Hricko A., Lurmann F., Avol E., Gilliland F. and Peters J. Breathless in Los Angeles: The exhausting search for clean air. *Am J Pub Hlth* **2003**: 93(9): 1494-1499.

Lawless P.A., Rodes C.E. and Evans G. Aerosol concentration during the 1999 Fresno exposure studies as functions of size season and meteorology. *Aerosol Sci Technol* **2001**: 34: 66-74.

LeCanut, P., M.O. Andreae, G.W. Harris, F.G. Wienhold, and T. Zenker (**1996**), Airborne studies of emissions from savanna fires in southern Africa .1. Aerosol emissions measured with a laser optical particle counter, *Journal of Geophysical Research-Atmospheres*, *101* (D19), 23615-23630.

Li N., Alam J., Eiguren A., Slaughter N., Wang X., Huang A., Wang M., Sioutas C. and Nel, A.E. Nrf2 is a Key Transcription Factor in Antioxidant Defense in Macrophages and Epithelial Cells: Protecting Against the Injurious Effects of Pro-oxidative Air Pollutants. *J Immunol* **2004**: 173 (5): 3467-3481.

Li N., Sioutas C., Froines J.R., Cho A., Misra C and Nel A., Ultrafine Particulate Pollutants Induce Oxidative Stress and Mitochondrial Damage. *Environ Health Persp* **2003**: 111 (4): 455-460.

Lighty, J.B.; Veranth, J.M.; Sarofim, A.F. Combustion aerosols: Factors governing their size and composition and implications to human health. *J. Air Waste Manage. Assoc.* **2000**, *50*, 1565-1618.

Liu P.S.K. and Deshler T. Causes of concentration differences between a Scanning Mobility Particle Sizer and a Condensation Particle Counter. *Aerosol Sci Technol* **2003**: 37: 917-923.Kavouras, I., Mihalopoulos, N., and Stephanou, E. (**1998**). Formulation of Atmospheric Particles from Organic Acids Produced by Forests. *Nature.* 395:683-686.

Long, C.M., H.H. Suh, L. Kobzik, P.J. Catalano, Y.Y. Ning, and P. Koutrakis (**2001**), A pilot investigation of the relative toxicity of indoor and outdoor fine particles: In vitro effects of endotoxin and other particulate properties, *Environmental Health Perspectives*, *109* (10), 1019-1026.

Lu, R., and R.P. Turco (**1996**), Ozone distributions over the Los Angeles basin: Three-dimensional simulations with the SMOG model, *Atmospheric Environment*, *30* (24), 4155-4176.

Mader, B.T., Pankow, J.F. **2001**. Gas/Solid Partitioning of semivolatile organic compounds (SOCs) to air filters. 3. An analysis of gas adsorption artifacts in measurements of atmospheric SOCs and organic carbon (OC) when using teflon membrane filters and quartz fiber filters. Environmental Science and Technology 35(17), 3422–3432.

Mäkelä J.M., Aalto P., Jokinen P., Pohja T., Nissinen A., Palmroth S., Markkanen T., Seitsonen K., Lihavainen H. and Kulmala M. Observations of ultrafine aerosol particle formation and growth in boreal forest. *Geophys Res Lett* **1997**: 24: 1219-1222.

Manchester-Neesvig, J.B.; Schauer, J.J.; Cass, G. R. **2003.** The Distribution of particle-phase organic compounds in the atmosphere and their use for source apportionment during the Southern California Children's Health Study. Journal of the Air and Waste Management Association. 53, 1065-1079.

Marr, L. C.; Kirchstetter, T. W.; Harley, R. A.; Miguel, A. H.; Hering, S. V.; Hammond, S. K. Characterization of polycyclic aromatic hydrocarbons in motor vehicle fuels and exhaust emissions. *Environ. Sci. Technol.* **1999**, *33*, 3091-3099.

Mathis, U.; Ristimäki, J.; Mohr, M.; Keskinen, J.; Ntziachristos, L.; Samaras, Z.; Mikkanen, P. Sampling conditions for the measurement of nucleation mode particles in the exhaust of a diesel vehicle. *Aerosol Sci. Technol.* **2004**, *38*(12), 1149 – 1160.

Mauderly, J. L. Toxicological and epidemiological evidence for health risks from inhaled engine emissions. *Environ. Health Perspect.* **1994**, *102*, 165-171.

Mauderly, J. L. Toxicological approaches to complex mixtures. *Environ. Health Perspect.* **1993**, *101*, 155-165.Misra, C.; Kim, S.; Shen, S.; Sioutas, C. (**2002**). A High Flow Rate, Very Low Pressure Drop Impactor for Inertial Separation of Ultrafine from Accumulation Mode Particles. *Journal of Aerosol Science.* 33:735-752.

Mazurek, M. A.; Simoneit, B. R. T.; Cass, G. R.; Gray, H. A. Quantitative high-resolution gas-chromatography and high-resolution gas-chromatography mass-spectrometry analyses of carbonaceous fine aerosol-particles. *Int. J. Environ. Anal. Chem.* **1987**, *29*, 119-139.

Mazzoleni, C.; Kuhns, H. D.; Moosmuller, H.; Keislar, R. E.; Barber, P. W.; Robinson, N. F.; Watson, J. G. On-road vehicle particulate matter and gaseous emission distributions in Las Vegas, Nevada, compared with other areas. *J. Air Waste Mange. Assoc.* **2004**, *54*(6), 711-726.

McDonald, J.D.; Eide, I.; Seagrave, J.; Zielinska, B.; Whitney, K.; Lawson, D.R.; Mauderly, J.L. **2004.** Relationship between composition and toxicity of motor vehicle emission samples. Environmental Health Perspectives 12, 1527–1538.

McGaughey, G. R.; Desai, N. R.; Allen, D. T.; Seila, R. L.; Lonneman, W. A.; Fraser, M. P.; Harley, R. A.; Pollack, A. K.; Ivy, J. M.; Price, J. H. Analysis of motor vehicle emissions in a Houston tunnel during the Texas Air Quality Study 2000. *Atmos. Environ.* **2004**, *38*(20), 3363-3372.

Miguel, A. H.; Kirchstetter, T. W.; Harley, R. A.; Hering, S. V. On-road emissions of particulate polycyclic aromatic hydrocarbons and Black Carbon from gasoline and diesel vehicles. *Environ. Sci. Technol.* **1998**, *32*, 450-455.

Misra, C.; Kim, S.; Shen, S.; Sioutas, C. A high flow rate, very low pressure drop impactor for inertial separation of ultrafine from accumulation mode particles. *J. Aerosol Sc.* **2002**, *33*, 735-752.

Morawska L., Bofinger N.D., Kocis L. and Nwankwoala A. Comprehensive characterization of aerosols in a subtropical urban atmosphere: particle size distribution and correlation with gaseous pollutants. *Atmos Environ* **1998**: 32 (14-15): 2467-2478.

Morawska L., Jayarantne E.R., Mengersen K. and Thomas S. Differences in airborne particle and gaseous concentrations in urban air between weekdays and weekends. *Atmos Environ* **2002**: 36: 4375-4383.

Na K.S., Sawant A.A., Song C. and Cocker D.R. Primary and secondary carbonaceous species in the atmosphere of Western Riverside County, California. *Atmos Environ* **2004**: 38 (9): 1345-1355.

Nel, A.; Xia, T.; Maumldler L.; Li, N. **2006.** Toxic Potential of Materials at the Nanolevel. Science 311(5761), 622-627.

Neususs, C., H. Wex, W. Birmili, A. Wiedensohler, C. Koziar, B. Busch, E. Bruggemann, T. Gnauk, M. Ebert, and D.S. Covert, (**2002**). Characterization and parameterization of atmospheric particle number-, mass-, and chemical-size distributions in central Europe during LACE 98 and MINT, *Journal of Geophysical Research-Atmospheres*, 107 (D21).

Noble C.A., Mukerjee S., Gonzales M., Rodes C.E., Lawless P.A., Natarajan S., Myers E.A., Norris G.A., Smith L., Ozkaynak H. and Neas L.M. Continuous measurement of fine and ultrafine particulate matter criteria pollutants and meteorological conditions in urban El Paso, Texas. *Atmos Environ* **2003**: 37: 827-840.

Ntziachristos, L., Zhi, N., Geller, M.D., Sioutas C. **2006.** Particle concentration and characteristics near a major freeway with heavy-duty diesel traffic, Submitted to Environmental Science and Technology, June 2006.

Oberdörster G. and Utell M.J. Ultrafine particles in the urban air: To the respiratory tract-and beyond? *Environ Health Persp* **2002**: 110 (8): A440-A441.

Oberdorster, G. Pulmonary effects of inhaled ultrafine particles. *Int. Archives Occupat. Environ. Health.* **2001**, *74*, 1-8.

Oberdorster, G., Ferin, J., Gelein, R., Soderholm, S.C., Finkelstein, J. (**1992**). Role of the Alveolar Macrophage in Lung Injury - Studies with Ultrafine Particles. *Environmental Health Perspectives*. 97:193-199.

Oberdorster, G.; Sharp, Z.; Atudorei, V.; Elder, A.; Gelein, R.; Lunts, A.; Kreyling, W.; Cox, C. Extrapulmonary translocation of ultrafine carbon particles following whole-body inhalation exposure of rats. *J. Toxicol. Environ. Health-Part A.* **2002**, *65*, 1531-1543.

O'Dowd C., McFiggans G., Creasey D.J., Pirjola L., Hoell C., Smith M.H., Allan B.J., Plane J.M.C., Heard D.E., Lee J.D., Pilling M.J. and Kulmala M. On the photochemical production of new particles in the coastal boundary layer. *Geophys Res Lett* **1999**: 26 (12): 1707-1710.

Pereira, J.M.C., B.S. Pereira, P. Barbosa, D. Stroppiana, M.J.P. Vasconcelos, and J.M. Gregoire (**1999**), Satellite monitoring of fire in the EXPRESSO study area during the 1996 dry season experiment: Active fires, burnt area, and atmospheric emissions, *Journal of Geophysical Research-Atmospheres*, *104* (D23), 30701-30712.

Peters A., Wichmann H.E., Tuch T. and Heinrich J. Respiratory effects are associated with the number of ultrafine particles. *Amer J Resp Crit Care Med* **1997**: 155: 1376-1383.

Peters, A., Frohlich, M., Doring, A. (**2001**). Particulate Air Pollution is Associated with an Acute Phase Response in Men-Results from the MONICA-Augsburg Study. *Eur. Heart J.* 22 (14):1198-1204

Peters, A., Varrier, R.L., Schwartz, J., Gold, D.R., Mittleman, M., Baliff, J., Oh, J.A., Allen, G., Monahan, K. and Dockery, D.W. (**2000**). Air Pollution and Incidence of Cardiac Arrythmia. *Epidemiol.* 11:11-17.

Phuleria H.C., Fine P.M., Zhu Y. and Sioutas C. Characterization of Particulate Matter and co-pollutants during the fall 2003 Southern California fires. *J Geophy Res-Atmos* **2004** *(in press)*

Phuleria, H.C.; Geller, M.D.; Fine, P.M.; Sioutas, C. **2006**. Size-resolved emissions of organic tracers from light- and heavy-duty vehicles measured in a California roadway tunnel. Environmental Science and Technology 40, 4109-4118.

Pope (III), C.A.; Dockery, D.W. **2006**. Health effects of fine particulate air pollution: lines that connect. Journal of the Air and Waste Management Association 56, 709-742.

Pope C.A. Review: epidemiological basis for particulate air pollution health standards. *Aerosol Sci Technol* **2000**: 32 (1): 4-14.

Pope, C.A., Dockery, D.W. and Schwartz, J. (**1995**). Review of Epidemiological Evidence of Health Effects of Particulate Air Pollution. *Inhalation Toxicology*. 7:1-18.

Pope, C.A., Verrier, R.L., Lovett, E.G., Larson, A.C., Raizenne, M.E., Kanner, R.E., Schwartz, J., Villegas, M., Gold, D.R. and Dockery, D.W. (**1999**). Heart Rate Variability Associated with Particulate Air Pollution. Amer. Heart. J. 138:890-899.

Radke, L.F., D.A. Hegg, P.V. Hobbs, J.D. Nance, J.H. Lyons, K.K. Laursen, R.E. Weiss, P.J. Riggan, and D.E. Ward (**1991**), Particulate and Trace gas emissions from Large Biomass Fires in North America, *Global Biomass Burning: Atmospheric, Climatic, and Biospheric Implications*, edited by J. S Levine, pp. 209-224, MIT Press, Cambridge, Mass.

Rogge W. F.; Hildemann, L. M.; Mazurek, M. A.; Cass, G. R.; Simoneit B. R. T. Sources of fine organic aerosol. 2. Noncatalyst and catalyst-equipped automobiles and heavy-duty diesel trucks. *Environ. Sci. Technol.* **1993**, *27*, 636-651.

Ruuskanen J., Tuch. Th., Ten Brink H., Peters A., Khystov A., Mirme A., Kos G.P.A., Brunekreef B., Wichmann H.E., Buzorius G., Vallius M., Kreyling W.G. and Pekkanen J. Concentrations of ultrafine, fine and $PM_{2.5}$ particles in three European cities. *Atmos Environ* **2001**: 35: 3729-3738.

Sakurai, H., K. Park, P.H. McMurry, D.D. Zarling, D.B. Kittelson, and P.J. Ziemann (**2003**), Size-dependent mixing characteristics of volatile and nonvolatile components in diesel exhaust aerosols, *Environmental Science & Technology*, *37* (24), 5487-5495.

Sardar, S.B.; Fine, P. M.; Yoon, H.; Sioutas, C. Associations between particle number and gaseous co-pollutant concentrations in the Los Angeles Basin. *J. Air Waste Manage. Assoc.* **2004**, *54*, 992-1005.

Saxe H. and Larsen T. Air pollution from ships in three Danish ports. *Atmos Environ* **2004**: 38: 4057-4067.Schwartz J.and Dockery, D.W. (**1992**).Increased Mortality in Philadelphia Associated with Daily Air-Pollution Concentrations. *American Review of Respiratory Disease.*145 (3): 600-604.

Schauer, C.; Niessner, R.; Poschl, U. **2003**. Polycyclic aromatic hydrocarbons in urban air particulate matter: Decadal and seasonal trends, chemical degradation, and sampling artifacts. Environmental Science and Technology 37, 2861-2868.

Schauer, J. J. Evaluation of elemental carbon as a marker for diesel particulate matter. *J. Exposure Anal. Environ. Epidem.* **2003**, *13*, 443-453.

Schauer, J. J.; Cass, G. R. Source apportionment of wintertime gas-phase and particle-phase air pollutants using organic compounds as tracers. *Environ. Sci. Technol.* **2000**, *34*, 1821-1832.

Schauer, J. J.; Kleeman, M. J.; Cass, G. R.; Simoneit, B. R. T. Measurement of emissions from air pollution sources. 2. C_1 through C_{30} organic compounds from medium duty diesel trucks. *Environ. Sci. Technol.* **1999**, *33*, 1578-1587.

Schauer, J. J.; Kleeman, M. J.; Cass, G. R.; Simoneit, B. R. T. Measurement of emissions from air pollution sources. 5. C_1-C_{32} organic compounds from gasoline-powered motor vehicles. *Environ. Sci. Technol.* **2002**, *36*, 1169-1180.

Schauer, J. J.; Rogge, W. F.; Hildemann, L. M.; Mazurek, M. A.; Cass, G. R.; Simoneit, B. R. T. Source apportionment of airborne particulate matter using organic compounds as tracers. *Atmos. Environ.* **1996**, *30*, 3837-3855.

Schauer, J. J.; Shafer, M.; Christensen, C.; Kittelson, D. B.; Johnson, J.; Watts, W. Impact of Cold-Cold Start Temperature on the Chemical Composition of PM Emissions from SI Vehicles. *13th CRC On-Road Vehicle Emissions Workshop*, San Diego, CA, April 7-9, **2003.**

Schauer, J.J. **2003.** Evaluation of elemental carbon as a marker for diesel particulate matter. *Journal of Exposure Science and Environmental Epidemiology* 13, 443-453.

Schauer, J.J.; Cass, G.R. **2000**. Source apportionment of wintertime gas-phase and particle-phase air pollutants using organic compounds as tracers. Environmental Science and Technology 34, 1821-1832.

Scholes, R.J., D.E. Ward, and C.O. Justice (**1996**), Emissions of trace gases and aerosol particles due to vegetation burning in southern hemisphere Africa, *Journal of Geophysical Research-Atmospheres*, *101* (D19), 23677-23682.

Schwartz, J.; Laden, F.; Zanobetti, A. **2002.** The concentration-response relation between $PM_{2.5}$ and daily deaths. Environmental Health Perspectives 110(10), 1025-1029.

Seinfeld, C. and Pandis, S. (**1998**). Atmospheric Chemistry and Physics. John Wiley & Sons Inc., New York.

Shah, S.D., Cocker, D.R., Miller, J.W., and Norbeck, J.M. **2004.** Emission rates of particulate matter and elemental and organic carbon from in-use diesel engines. Environmental Science and Technology 38(9), 2544–2550.

Sheesley, R. J.; Schauer, J. J.; Chowdhury, Z.; Cass, G. R.; Simoneit, B. R. T. Characterization of organic aerosols emitted from the combustion of biomass indigenous to South Asia. *J. Geophys. Res. - Atmos.* **2003**, *108*, No. 4285.

Shi J.P. and Qian Y. Aerosol size distributions (3 nm to 3 um) measured at St. Louis Supersite (4/1/01-4/30/02) *M. S. Thesis Department of Mechanical Engineering University of Minnesota Minneapolis MN, 55455.* **2003**.

Shi J.P., Evans D.E., Khan A.A. and Harrison R.M. Sources and concentration of nanoparticles (<10 nm diameter) in the urban atmosphere. *Atmos Environ* **2001**: 35:1193-1202.

Shi J.P.; Khan A.A. and Harrison R.M. Measurements of ultrafine particle concentration and size distribution in the urban atmosphere. *Sci Total Environ* **1999**: 235: 51-64

Simoneit, B. R. T. Chemical characterization of sub-micron organic aerosols in the tropical trade winds of the Caribbean using gas chromatography-mass spectrometry. A*tmos. Environ.* **2002**, *36*, 5259-5263.

Simoneit, B. R. T. Organic-matter of the troposphere. 3. Characterization and sources of petroleum and pyrogenic residues in aerosols over the Western United States *Atmos. Environ.* **1984**, *18*(1), 51-67.

Sinha P., Hobbs P.V., Yokelson R.J., Christian T.J., Kirchstetter T.W. and Bruintjes R. Emissions of trace gases and particles from two ships in the southern Atlantic Ocean. *Atmos Environ.* **2003**: 37: 2139-2148.

Sioutas, C., Delfino, R. J.; Singh M. Exposure assessment for atmospheric ultrafine particles (UFPs) and implications in epidemiologic research. *Environ. Health Perspec*. **2005,** *113*, 947-955

Stanier C.O., Khlystov A.Y. and Pandis S.N. Ambient aerosol size distributions and number concentrations measured during the Pittsburgh Air Quality Study (PAQS). *Atmos Environ.* **2004**: 38: 3275-3284.

Sternbeck, J., Sjodin, A., Andreasson, K. **2002.** Metal Emissions from Road Traffic and the Influence of Resuspension—Results from Two Tunnel Studies. Atmospheric Environment 36(30), 4735–4744.

Strom J., Umegard J., Torseth K., Tunved P., Hansson H.-C., Holmen K., Wismann V., Herber A. and Langlo G.K. One-year particle size distribution and aerosol chemical composition measurements at the Zeppelin Station, Svalbard, March 2000-March 2001. *Atmos Environ.* **2003**: 28: 1181-1190.

Tobias, H.J., D.E. Beving, P.J. Ziemann, H. Sakurai, M. Zuk, P.H. McMurry, D. Zarling, R. Waytulonis, and D.B. Kittelson (**2001**), Chemical analysis of diesel engine nanoparticles using a nano-DMA/thermal desorption particle beam mass spectrometer, *Environmental Science & Technology*, *35* (11), 2233-2243.

Venkataraman, C.; Lyons, J.M.; Friedlander, S.K. **1994**. Size distributions of polycyclic aromatic hydrocarbons and elemental carbon. 1. Sampling, measurement methods, and source characterization. Environmental Science and Technology 28, 555-562.

Wallace, L., and C. Howard-Reed (**2002**), Continuous monitoring of ultrafine, fine, and coarse particles in a residence for 18 months in 1999-2000, *Journal of the Air & Waste Management Association*, *52* (7), 828-844.

Weber R.J., Marti J.J., McMurry P.H., Eisle, F.L., Tanner D.J. and Jefferson A. Measurement of new particle formation and ultrafine particle growth rates at a clean continental site. *J Geophys Res* **1997**: 102 (D4): 4375-4385.

Wehner B., Wiedensohler A. A long-term measurement of submicrometer urban aerosols: statistical analysis for correlations with meteorological conditions and trace gases. *Atmos Chem Phys* **2003**: 3: 867-879.

Weingartner, E.; Keller, C.; Stahel, W.A.; Burtscher, H.; Baltensperger, U. Aerosol emission in a road tunnel. *Atmos. Environ.* **1997**, *31*(3), 451-462.

Whitby, K.T. and Svendrup, G.M. (**1980**). California Aerosols: Their Physical and Chemical Characteristics. *Env. Health Perspectives*.10: 477.

Woo K.S., Chen D.R., Pui D.Y.H. and McMurry P.H. Measurement of Atlanta aerosol size distributions: observations of ultrafine particle events. *Aerosol Sci Technol* **2001**: 34: 75-87.

Woods, D.C., R.L. Chaun, W.R. Cofer III, and J.S. Levine (**1991**), Aerosol Characterization in Smoke Plumes from a Wetland fire, *Global Biomass Burning: Atmospheric, Climatic, and Biospheric Implications*, *edited by J. S. Levine*, pp. 240-244, MIT Press, Cambridge, Mass.

Wotawa, G., and M. Trainer (**2000**), The influence of Canadian forest fires on pollutant concentrations in the United States, *Science*, *288* (5464), 324-328.

Xia, T.; Korge, P.; Weiss, J. N.; Li, N.; Venkatesen, I. M.; Sioutas, C.; Nel A. Quinones and aromatic chemical compounds in particulate matter induce mitochondrial dysfunction: Implications for ultrafine particle toxicity. *Environ. Health Perspect.* **2004**, *112*(14), 1347 –1358.

Yu F. and Turco R.P. From molecular clusters to nanoparticles: Role of ambient ionization in tropospheric aerosol formation. *J Geophys Res* **2001**: 106 (D5): 4797-4814.

Zanobetti A., Schwartz J. and Dockery D.W. Airborne particles are a risk factor for hospital admissions for heart and lung disease. *Environ. Health Persp.* **2000**: 108(11): 1071-1077.

Zhang K.M. and Wexler A.S. A hypothesis for growth of fresh atmospheric nuclei. *J Geophys Res-Atmos* **2002**:107 (D21): 4577.

Zhang R., Suh I., Zhao J., Fortner E.C., Tie X., Molina L.T., and Molina M.J. Atmospheric new particle formation enhanced by organic acids. *Science* **2004**: 304: 1487-1490.

Zhang, M.Z., Wexler, A.S.; Niemeier, D.; Zhu, Y.F.; Hinds, W.; Sioutas, C. **2005.** Evolution of particle number distribution near roadways. Part III. Traffic analysis and on-road size resolved particulate emission factors. Atmospheric Environment 39, 4155-4166.

Zheng, M.; Cass, G. R.; Schauer, J. J.; Edgerton, E. S. Source apportionment of $PM_{2.5}$ in the Southeastern United States using solvent-extractable organic compounds as tracers. *Environ. Sci. Technol.* **2002**, *36*, 2361-2371.

Zhu Y.F., Hinds W.C., Kim S. and Sioutas C. Concentration and size distribution of ultrafine particles near a major highway. *J. Air Waste Manage. Assoc.* **2002b**: 52: 1032-1042.

Zhu Y.F., Hinds W.C., Kim S., Shen S. and Sioutas C. Study of ultrafine particles near a major highway with heavy-duty diesel traffic. *Atmos Environ* **2002a**: 36: 4323-4335.

Zhu, Y., Hinds, W.C.; Shen, S.; Sioutas, C**. 2004.** Seasonal trends of concentration and size distribution of ultrafine particles near major highways in Los Angeles. Aerosol Science and Technology 38, 5-13.

Zhu, Y.F., Hinds, W.C., Kim, S., Shen, S. and Sioutas, C., **2002a**. Study of ultrafine particles near a major highway with heavy-duty diesel traffic. *Atmospheric Environment,* 36(27): 4323-4335.

Zhu, Y.F., W.C. Hinds, S. Kim, and C. Sioutas (**2002b**), Concentration and size distribution of ultrafine particles near a major highway, *Journal of the Air & Waste Management Association*, *52* (9), 1032-1042

Zielinska, B. **2005.** Atmospheric transformation of diesel emissions 57, 31-42.

Zielinska, B.; Sagebiel, J.; McDonald, J. D.; Whitney, K.; Lawson, D. R. Emission rates and comparative chemical composition from selected in-use diesel and gasoline-fueled vehicles. *J. Air Waste Manage. Assoc.* **2004**, *54*, 1138-1150.

Ziemann P., Tobias H.J., Beving D.E., Sakurai H., Zuk M., McMurry P.H., Zarling D., Waytulonis R., Kittelson D.B. Chemical analysis of diesel engine nanoparticles using a nano-DMA/thermal desorption particle beam mass spectrometer. *Env. Sc. Technol.* **2001**: 35: 2233-2243